Assessment of climate change impacts on water resources and agriculture in data-scarce Kabul basin, Afghanistan

Masoud Ghulami

Thèse de doctorat

En cotutelle internationale
Présentée en vue de l'obtention du grade

UNIVERSITÉ CÔTE D'AZUR
et
ASIAN INSTITUTE OF TECHNOLOGY

Discipline
Sciences de l'ingénieur

par

Masoud Ghulami

Evaluation des impacts du changement climatique sur la ressource en eau et l'agriculture dans le bassin à faibles données disponibles, Kabul, Afghanistan

Dirigée par Philippe Audra
et codirigée par Mukand S Babel

Soutenue le 18 décembre 2017

Devant le jury composé de :

Shie-Yui Liong, Professeur, National University of Singapore	**Rapporteur**
Manuel Gómez Valentín, Professeur, Universitat Politècnica de Catalunya	**Rapporteur**
Philippe Gourbesville, Professeur, Université de Nice Sophia Antipolis	**Examinateur**
Sangam Shrestha, Professeur, Université de Nice Sophia Antipolis	**Examinateur**
Akiyuki Kawasaki, Professeur, Université de Nice Sophia Antipolis	**Examinateur**
Damien Jourdain, Professeur, Université de Nice Sophia Antipolis	**Examinateur**
Philippe Audra, Professeur, Université Nice-Sophia Antipolis	**Directeur de these**
Mukand S Babel, Professeur, Asian Institute of Technology	**Co-directeur**

ACKNOWLEDGEMENT

I would like to express my deepest gratitude to my advisors Pr Philippe Audra and Pr Mukand S. Babel as well as committee members Pr Philippe Gourbesville, Pr Jourdain Damien, Pr Akiyuki Kawasaki, and Pr Sangam Shrestha for their kind and continuous support and guidance. They have never failed to support me from the very beginning and provided me with plenty of academic opportunities to accomplish my PhD research work.

I would like to thank my scholarship donor, Norwegian Ministry of Foreign Affairs, which provided me full financial support throughout the entire PhD program. I am also thankful to all coordinators in Erasmus Mundus EMMA 4 program for providing me a scholarship to spend a year as exchange doctoral student in France.

My deepest thanks to Dr. Mandira Shrestha, Dr. Arun Shrestha, Dr. Aditi Mukherji, and Dr. Santosh Nepal from International Centre for Integrated Mountain Development (ICIMOD) for providing me lots of support and guidance during my stay in Nepal as a young ICIMOD professional officer.

I am grateful for my past and present members of research groups, friends and colleagues from AIT, UNICE, ICIMOD, and Afghanistan Ministry of Energy and Water for helping me with the ideas and making my PhD life a wonderful learning experience. I would like to express our sincere gratitude to the various regional and international agencies for providing the data required for this study.

I would like to acknowledge AIT administration especially Ms. Pajee and Ms. Emelyn for their always kind follow up on my work. More thanks to all administration people at UNS.

Special thanks to Dr. Solmaz Heydarifard, my best friend, for being always morally supportive to me even from a long distance.

Finally, I am really grateful to my family from the bottom of my heart. I owe a lot to my mom and my sisters. I cannot find words to express my gratitude to them. Their constant love, support and encouragement have always been there for me. I want to thank my late father who motivated me a lot to go for PhD and I am sad that he cannot see me graduate.

ABSTRACT

Afghanistan is a semi-arid and mountainous country which faced three decades of conflict. It is one of the most vulnerable countries in the world to climate change as it has very limited capacity to address the impacts of climate change. It has been also considered as a data-scarce region both temporally and spatially with limited capability to measure hydro-meteorological parameters with in situ gauges. The current study focuses on Kabul basin which lies in the northeast quarter of Afghanistan. It accounts for thirty-five percent of the population's water supply, and has the fastest population growth rate in the country. The main objective of this study is to understand the impacts of climate change on water resources and agriculture. To understand the impact on water resource, first of all, the performance evaluation of global datasets/remote sensed products is investigated in order to generate precipitation and temperature datasets for baseline period of climate change studies and developing hydrological model. Then a hydrological model is selected to understand hydrologic response of the Kabul basin and future projections of water availability using future climate projections. To understand the impact on agriculture, a study on farmers' perception about climate change and its impacts on their agriculture is undertaken. Secondly, a crop model is used to evaluate the impacts of climate change on wheat yield.

The gridded satellite/global precipitation time series data of CPC-RFE, GSMaP_MVK, TMPA, and APHRODITE are validated using the data from recently established precipitation gauge locations over the Kabul basin from 2004 to 2007, the common years of availability of all used datasets. These products are evaluated at different spatial and temporal resolutions (daily, monthly, and annual). The validation approach used here includes continuous (mean absolute error [MAE], root mean square error [RMSE], correlation [r], and multiplicative bias [Mbias]) and categorical (probability of detection [POD] and false alarm ratio [FAR]) verification statistics. Furthermore, the spatial performance is evaluated by visual inspection as well as mapping the data and analyzing the distribution of precipitation as a function of elevation. The future predictions of precipitation and temperature under different RCP (Representative Concentration Pathways) scenarios are investigated from a set of recent CMIP5-GCMs (Coupled Model Inter-comparison Project Phase 5-Genral Circulation Models) after bias correction and downscaling. The GCMs' output is downscaled and bias corrected to the stations using the linear downscaling method. The values of all stations then are averaged over Kabul basin for each month and the changes are calculated for future periods of 2020s, 2050s, and 2080s compared to the baseline of 1971-2000. The values also are averaged over the season, winter and summer. The winter starts in November and ends by April. The summer is also a period of six months from May to October. For the assessment of future climate predictions on water resources, the bias-corrected precipitation and temperature are used as input to the J2000 hydrological model, which is a physically distributed model with separate modules for snow and glacier contributions.

Two field surveys using questionnaire are done to understand the farmers' perception about climate change and their adaptation measures. The descriptive statistics is then used to summarize the results of the surveys. AquaCrop model is used to determine the impacts of climate change on wheat yield, which is the most dominant crop in the study area and accounts for 80% of planted areas of cereals in Afghanistan. The impact of shifting the planting date and using full or deficit irrigation as agro-adaptation measures is then investigated.

For hydrological applications, it is essential to quantify precipitation. The availability of satellite-based precipitation products and gridded interpolated datasets provides a great

opportunity for those regions suffering from poor spatial and temporal sampling of precipitation. The estimates from four tested products showed a relatively good detection of precipitation distribution and precipitation amounts for most cases. The results of continuous and categorical verification statistics suggest that the APHRODITE dataset performs better than other gridded datasets for the study basin. APHRODITE temperature data is also found very suitable for the study area after comparison with the surface observations.

The results of trend analysis suggest that the temperature has been increased over last five decades while such a clear trend for precipitation is not detected. The median of the results from all 8 GCMs suggests an increasing trend in maximum and minimum temperature in the future, as compared to the baseline. The increases for maximum temperature range from +1.7°C to +4.1°C under RCP 4.5 and +1.7°C to +6.3°C under RCP 8.5. The increases for minimum temperature range from +1.5°C to +3.8°C under RCP 4.5 and +1.4°C to +6.0°C under RCP 8.5. The projections for precipitation mainly show a decreasing trend under both RCPs, with variations ranging from -19% to -6% under RCP 4.5 and -18% to 3% under RCP 8.5.

The results of J2000 hydrological model show that the model performed well and can be used to reproduce the hydrological response of the basin. As per the predictions, future runoff ranges between -14% and +49% under RCP 4.5 and between -16% and +100% under RCP 8.5 during the 21st century. The median values varying between -9% and +22%.

Based on the results of field surveys, climate change is already perceived by many farmers in the selected districts of the study area. As it was expected from climate trend analysis, most of the farmers agreed on increasing temperature, but there was no clear trend for precipitation. While the amount of precipitation might not change significantly, water resources have decreased. This might be due to the changes in precipitation and runoff distribution. Broadly, the changes in the water resources in the study areas might be due to climate change or/and increase of water usage as a result of increased population. The main adaptation measures taken by farmers include planting trees and changing the crop type and crop calendar.

AquaCrop modeling results for winter wheat show that under future climate change scenarios, the yield will increase. The main reason for this increase is the decrease in the stress related to cold temperature. Shifting the planting date and applying different levels of irrigation were examined by the AquaCrop model and the results show that these measures can be effective in maximizing the yield.

This study recommends that the future projections of temperature and precipitation are highly uncertain and policy makers should include a range of projections while making the decisions for development plans and adaptation strategies. Temperature is projected to increase in future for the study area but the results suggest that it might create further opportunities due to increase in the water availability and decrease in the cold temperature stress for the crops. However, lack of infrastructure might lead to further problems due to the possibility of more frequent and extreme floods and droughts. This study can be used as an outline for other river basins in Afghanistan.

TABLE OF CONTENTS

LIST OF FIGURES

LIST OF TABLES

LIST OF ABBREVIATIONS

APHRODITE	Asian Precipitation - Highly-Resolved Observation Data Integration Towards Evaluatioion
AR4	Fourth assessment report of IPCC
AR5	Fifth assessment report of IPCC
CC	Climate Change
CMCC	Centro Euro-Mediterraneo per I Cambiamenti Climatici
CMIP5	Coupled Model Intercomparison Project 5
CNRM	Centre National de Recherches Meteorologiques
CPC-RFE	Climate Prediction Center-Rainfall Estimates
DEM	Digital Elevation Model
ESGF	Earth System Grid Federation
ET	Evapotranspiration
FAO	Food and Agriculture Organization of the United Nations
FAR	False alarm ratio
G-G	Grid to grid
GIS	Geographical Information System
GSMaP	Global Satellite Mapping of Precipitation
HRU	Hydrological response unit
INM	Institute for Numerical Mathematics
IPCC	Intergovernmental Panel of Climate Change
IPSL	Institut Pierre-Simon Laplace
MAE	Mean absolute error
Mbias	Multiplicative bias
MIROC	Model for Interdisciplinary Research on Climate
MPI-M	Max Planck Institute for Meteorology
NSE	Nash–Sutcliffe model efficiency
P_{bias}	Percentage error
POID	Probability of detection
P-P	Point to point
QM	Quantile mapping
r	Correlation
RCM	Regional climate model
RCP	Representative Concentration Pathways
RD1	Overland Flow
RD2	Interflow 1
RG1	Interflow 2
RG2	Baseflow
rhum	Relative humidity
RMSE	Root mean square error
RS	Remote Sensing
RSA	Regional Sensitivity Analysis
Std	Standard deviation
sunh	Sunshine hours
T_{max}	Maximum Temperature
T_{mean}	Mean Temperature
T_{min}	Minimum Temperature
TRMM	Tropical Rainfall Measuring Mission

CHAPTER 1
INTRODUCTION

1.1 Background

Climate change affects the patterns of precipitation and evapotranspiration (Tsanis et al., 2011). As a result, other variables, such as water availability and its spatial and temporal distribution, also get affected (Arnell et al., 2011). Climate change is also likely to intensify the global hydrological cycle, which can increase the risk of floods and droughts. Climate change also affects the function, operation, and management practices of existing water infrastructure. Adverse impacts of climate change on water resources systems intensify the effects of other factors such as increased population, heightened economic activities, and land use changes. Globally, due to population growth and increasing affluence, the demand for water is projected to increase in the coming decades and regionally, changes in the demands for irrigation water (as an example of the results of climate change) are also expected (Bates et al., 2008).

Precipitation is one of the most important input variables for land surface hydrological models but it is a challenging task to prepare precipitation data since precipitation is characterized by high spatial and temporal variability (Zhang and Srinivasan, 2010). The traditional approach is to measure precipitation with rain gauges, but a sparse spatial distribution of gauges makes it difficult to capture the spatial variability of precipitation, especially in mountainous regions where heterogeneity is very high and data collection would require an even greater density of rain gauges. The global availability of satellite data provides an effective and economical approach to estimate areal precipitation in poorly gauged basins (Artan et al., 2007). These satellite-based estimates of precipitation can provide crucial information about the occurrence, amount, and distribution of precipitation (Bajracharya et al., 2014). Observed hydrological data are the basic requirements for effective water management. However, as data records are usually inadequate in length, completeness, quality, and spatial coverage, models are exploited to generate synthetic time series. Some aspects of hydrological systems are still not understood and some of these aspects are even unknown. Such things are only revealed by adopting a perennially questioning attitude towards what we hear and see and are able to measure and analyse (Walker et al., 2003).

Potential impacts of climate change on the production of food have been widely studied in many regions. The results suggest that the changes in production, which are dependent on the location, may be improved or worsened. This may lead to changes in agricultural production zones around the world. The impacts would also be different for various crops. So, all this suggests that there is a need for adaptation strategies to help farmers and agriculture (e.g., Parry et al. (2004)).

1.2 Problem statement

Afghanistan is a mountainous and dry country which faces the threat of global climate change on a large scale. UNEP (2007) identified the country as one of the most vulnerable to climate change due to the potential impacts of climate change in this region and the very limited capacity of the country to address those impacts. While the averaged nationwide water availability is 2775 m^3/cap.yr (Favre and Kamal, 2004), the country is considered water insecure because of mismanaged land and water resources, which have caused a decline in water quality and availability (Beekma and Fiddes, 2011). According to Mcsweeney et al.

(2007), in Afghanistan, mean annual temperature has increased by 0.6˚C with an average rate of 0.13˚C per decade since 1960. The precipitation values over the country have decreased slightly at an average rate of 0.5 mm per month per decade since 1960. The projections of mean annual temperature for the future suggest an increase by 1.4 to 4.0˚C by the 2060s, and 2.0 to 6.2˚C by the 2090s. The projections of mean annual rainfall in the future, under different scenarios, from a multi-model approach, show a decreasing trend of precipitation for Afghanistan. Projections vary between -31 and +28% by the 2090s, with ensemble median values of -5 to - 8% in annual rainfall, and -51 to +9% with median values -7 to -19%. Based on this information, combined with the data and trends from neighboring countries, it seems that Afghanistan will likely be impacted by a range of new and increased climatic hazards in the near future.

Most hydrological and climatic data collection activities in Afghanistan were interrupted in the early 1980s as a fall out of the war and did not restart until 2003 or later. Thus, given the limited data or ungauged basin conditions, which constrain a modeling approach, a physically based coherent methodological approach is required (Candela et al., 2012). To address the problem of scarce and missing data, one approach that could be of use is global datasets or remotely sensed products. Research on a suite of models and methods which can be used in data scarce regions for hydrological modeling and hydrological predictions is the main focus of a decadal initiative by the International Association of Hydrological Sciences (IAHS) in "Predictions in Ungauged Basins," which started in 2003 (Sivapalan et al., 2003). The validation of precipitation estimates from different products with ground data has been done extensively around the world, including in the Hindu Kush-Himalayan (HKH) region (Bajracharya et al., 2014), but there is a lack of such studies for Afghanistan per se.

Understanding the impacts of climate variability/changes on different sectors (such as hydropower, irrigation and agriculture, water supply, and sanitation) may lead to more flexible development plans to adapt to these changes and mitigate their impacts. It is an important step which needs to be investigated. Thus, for a country like Afghanistan, in which a majority of its population is engaged in agricultural activities, a lack of understanding about climate change impacts is a very significant problem and needs to be addressed.

The present research was conducted in the Kabul basin, which is the most important river basin in Afghanistan. The Kabul basin drains a quarter of the total annual water flow of Afghanistan (Favre and Kamal, 2004) and has a population higher than any other river basin in the country. The capital city of Kabul and some other main cities are located in this river basin (CSO, 2014).

1.3 Research questions

In this study, the following questions were answered:

1. What is the performance of different global datasets/remote sensed products to estimate the precipitation and temperature values for the Kabul basin?

2. What are the trends and variations in climate or weather within the Kabul basin over the recent historical period (1971-2000)? And, what are the projected precipitation and temperature patterns and values for the future under different RCP scenarios (till 2100)?

3. Which landscape features control hydrological system dynamics in the Kabul basin and what are the projected impacts of future climate scenarios on its water resources, considering the uncertainty from different sources (e.g., input data, different GCMs' outputs, and model parameters)?

4. How is agriculture, the most important economic sector in Afghanistan, affected by the impacts of climate change/variability? What is the perception of Afghan farmers about climate change and what are their problems and potentials in the context of adaptation measures?

5. How will the yield of the main crops be affected by climate change in the study area?

1.4 Objectives of the research

The overall objective of the research was to analyze the impacts of climate change on water resources and agriculture in the data-scarce Kabul basin. The specific objectives of this study are as follows:

1. To evaluate the performance of global precipitation and temperature datasets/remotely sensed products for the Kabul basin

2. To translate global scale climate projections of precipitation and temperature to the basin scale

3. To analyze the hydrological response of the Kabul basin and the impacts of climate change on its water resources

4. To understand farmers' perceptions about climate change and their adaptation measures in selected areas of the Kabul basin

5. To investigate the impacts of climate change on wheat yield and potential adaptation measures/opportunities

1.5 Scope of the study

1. Historical hydro-meteorological data, including precipitation, temperature, and discharge, were collected from Afghanistan's hydro-meteorological stations and global datasets/RS products.

2. Performance evaluation of global datasets/RS precipitation and temperature products was done for the study area using continuous and categorical verification statistics.

3. Trend analysis of historical climate data (precipitation and temperature) was done through various methods (regression method, Mann-Kendall test, and Sen's slope).

4. Eight CMIP5 GCMs were selected to follow a multi-model approach for identifying uncertainty in the projections of maximum and minimum temperature and precipitation under climatic scenarios RCP 4.5 and RCP 8.5.

5. The delta method (linear downscaling) was used to downscale the GCMs' outputs to the stations to make the former suitable for hydrological modeling.

6. The J2000 hydrological model was developed for the study area.

7. The impacts of climate change on water resources in the Kabul basin, in terms of water availability, were estimated under different climate change scenarios based on the results of a calibrated hydrological model.

8. Two field surveys were done to understand the farmers' perceptions about climate change and its impacts on their agriculture.

9. The AquaCrop model was used to simulate the impacts of climate change on wheat yield and to investigate the potential adaptation measures/opportunities for further improvement.

1.6 Limitations of the study

1. Climate change impacts on the water resources of the basin were only investigated based on changes in climatic parameters (precipitation and temperature), so future land use scenarios and water resources development were not considered.

2. During the field survey, the impacts of climate change cannot be separated from socio-economic factors but it is assumed that the changes are due to only climate change.

1.7 Structure of the dissertation

The dissertation contains 10 chapters covering the scope of the study. A brief description of each chapter is as follows:

Chapter 1 includes the background of the study, the problem statement, objectives, scope of the work, and its limitations.

Chapter 2 provides a literature review of the application of satellite datasets in meteorology, climate change and water resources, GCMs and downscaling techniques, hydrological modeling, adaptation studies, and crop modeling.

Chapter 3 gives the necessary information about the study area such as its location, and hydro-climatic and landscape features.

Chapter 4 provides the details of the methods which were used to achieve the various objectives of the study.

Chapter 5 presents the results of the performance evaluation of global datasets/remote sensed products for the Kabul basin.

Chapter 6 includes the trend analysis of historical data, results of linear downscaling, and the future projections of precipitation and temperature temporally and spatially.

Chapter 7 summarizes the model's parameters for calibration and validation and presents the uncertainty in future changes in water availability under different climatic scenarios.

Chapter 8 summarizes the results of field surveys regarding the farmers' perceptions of climate change and their adaptation measures.

Chapter 9 provides the results of crop modeling and links the previous chapters (hydrology, climate change, and field surveys).

Chapter 10 highlights the main results for each objective of the study, concludes the findings, and makes recommendation for further studies.

References and Appendices are included at the end of the dissertation.

CHAPTER 2
LITERATURE REVIEW

2.1 Predictions in data-scarce regions

In 2003, the International Association of Hydrological Sciences (IAHS) launched an initiative to investigate solutions for Prediction in Ungauged Basins (PUB). This initiative was to mainly focus on a better understanding of climatic and landscape features which control hydrological processes occurring at all scales, to improve the ability to predict fluxes of water in ungauged/data-scarce basins, and also to be able to better predict their uncertainties.

An ungauged basin is broadly defined as a basin without adequate records of hydrological observations. This creates a problem: the inability to compute the hydrological variables of water quantity and water quality at appropriate spatial and temporal scales. Some of these variab1es are precipitation, runoff, and erosion rates.

The approaches to PUB are listed as follows (Hrachowitz et al., 2013):

1. Observe on site: this method is expensive and is also not really related to the PUB concept.

2. Extrapolate from gauged basins (regionalization): some of the limitations of this method are the inconsistences created because of the heterogeneity of land surface, and the lack of the availability of similar basins nearby which are gauged (e.g., De Lavenne et al. (2015)).

3. Observe by remote sensing: there are many satellites and their products which can be used for this aim. These include TRMM, GPM, IGOS-Water, NOAA, JERS, and SAR. The problem with this method is the coarse resolution of some of those products and the lack of surface observations to validate the data.

4. Hydrological model simulation: lack of climatic input and lack of basin data for validation are some examples of the constraints of this method (e.g., Cibin et al. (2013)).

5. Integrated meteorological and hydrological model: this method also has some limitations such as parameter identifiability.

Predicting future flow variability and changes in ungauged basins is still a big challenge due to a lack of data. Besides, this process also involves various sources of uncertainty. It is very crucial for any future water resources development project to have a reliable estimation of temporal and spatial variations in future water availability (Samuel et al., 2012).

2.2 Global datasets/remote sensed products

The estimation of temperature and precipitation and their spatial distribution are important for hydrological modeling and water resources assessment. The estimates of near surface temperature (Ta) are important for a variety of applications in agriculture, water resources, and climate change studies. However, estimating near surface air temperature, measured at 2m above the ground surface, from the land surface temperature (Ts) derived from a satellite

is still a challenging task (Vancutsem, Ceccato, Dinku, & Connor, 2010). Some of the publicly available gridded datasets for surface temperature are listed in Table 2.1.

Table 1.1 Attributes of gridded temperature datasets
Source: http://www.esrl.noaa.gov/psd/data/gridded/tables/temperature.html

Name of Dataset	Areal Coverage	Spatial Resolution	Temporal Resolution	Time Coverage
CRU Air Temperature and Combined Air Temperature/Marine Anomalies V3	Global	5.0°x5.0°	Monthly	1850-present
CRU Air Temperature and Combined Air Temperature/Marine Anomalies V4	Global	5.0°x5.0°	Monthly	1850-2013
GFS Model Output	Global	2.5°x2.5°	2X Daily	1979-present
GHCN Version 3 Land Temperature Dataset	Global	5.0°x5.0°	Monthly	1900-present
NOAA GHCN_CAMS Land Temperature Analysis	Global	0.5°x0.5°	Monthly	1948-present
GISS surface temperature analysis	Global	1.0°x1.0°	Monthly	1880-present
NCEP GODAS ocean analysis	Global	0.3°x0.3°	Monthly	1980-present
ICOADS	Global	2.0°x2.0° 1.0°x1.0°	Monthly	1800-present
Livneh daily CONUS near-surface gridded meteorological and derived hydrometeorological data.new!	CONUS	0.06°x0.06°	Daily, Monthly	1915-2011
MSU	Global	2.5°x2.5°	Daily, Monthly	1979-1996
NCEP Operational Analysis	Global	2.5°x2.5°	Daily	1979-present
NCEP Marine	Global	2.0°x2.0°	Monthly	1991-present
NCEP/NCAR Reanalysis	Global	2.5°x2.5°	4X Daily, Daily, Monthly	1948-present
NCEP/NCAR Reanalysis Products Derived at PSD	Global	2.5°x2.5°	Daily, Monthly	1948-present
NCEP/DOE Reanalysis II	Global	2.5°x2.5°	4X Daily, Daily, Monthly	1979-Dec 2012
NOAA Extended Reconstructed SST V4 new!	Global	1.0°x1.0°	Monthly	1854-present
NOAA Global Surface Temperature (NOAA Global Temp)	Global	5.0°x5.0°	Daily	1880-present
NOAA Optimum Interpolation (OI) SST V2	Global	1.0°x1.0°	Monthly, Weekly	1981-present
North American Regional Reanalysis (NARR)	Northern Hemisphere	0.25°x0.25° (32 km)	8X Daily, Daily, Monthly	1979-Dec 2012
NOAA-CIRES 20th Century Reanalysis (V2)	Global	2.5°x2.5°	4X Daily	1871-2012
NOAA-CIRES 20th Century Reanalysis (V2c) new!	Global	2.5°x2.5°	4X Daily	1851-2014
U. of Delaware Precipitation and Air Temperature	Global Land	0.5°x0.5°	Monthly	1901-2014

Given the lack of data or an inadequate number of ground rain gauge locations in mountainous areas like the Himalayan region, satellite-based rainfall estimation is used to provide information on rainfall occurrence, amount, and distribution. To achieve this, many high-resolution global satellite-based precipitation products were created by various agencies

and institutions and can be found publically and used free of cost. Some of these are listed in Table 2.2.

Table 2.2 Attributes of gridded precipitation datasets
Source: http://www.esrl.noaa.gov/psd/data/gridded/tables/precipitation.html

Name of Dataset	Areal Coverage	Spatial Resolution	Temporal Resolution	Time Coverage
CMAP Precipitation	Global	2.5°x2.5°	Monthly	1979-
CPC .25x.25 Daily US Unified Precipitation	U.S.	0.25°x0.25°	Daily	1948-2006
CPC Hourly Precipitation	U.S.	2.0°x2.5°	Hourly	1948-2002
GFS Model Output	Global	2.5°x2.5°	2X Daily	1979-present
GHCN version 2 Land Precipitation Dataset	Global	5.0°x5.0°	Monthly	1900-present
Global Precipitation Climatology Centre (GPCC)	Global	0.5°x0.5°	Monthly	1901-present
		1.0°x1.0°		
		2.5°x2.5°		
		2.5°x2.5°		
Livneh daily CONUS near-surface gridded meteorological and derived hydrometeorological data.new!	CONUS	0.06°x0.06°	Daily, Monthly	1915-2011
MSU	Global	2.5°x2.5°	Daily, Monthly	1979-1996
NCEP Operational Analysis	Global	2.5°x2.5°	Daily	1979-present
NCEP/NCAR Reanalysis	Global	2.5°x2.5°	4X Daily, Daily, Monthly	1948-present
NCEP/NCAR Reanalysis Products Derived at PSD	Global	2.5°x2.5°	Daily, Monthly	1948-present
NCEP/DOE Reanalysis II	Global	2.5°x2.5°	4X Daily, Daily, Monthly	1979-Dec 2012
NOAA's Precipitation Reconstruction (PREC)	Global	2.5°x2.5°	Monthly	1979-present
NOAA's Precipitation Reconstruction over Land (PREC/L)	Global	2.5°x2.5°	Monthly	1948-present
North American Regional Reanalysis (NARR)	Northern Hemisphere	0.25°x0.25° (32 km)	8X Daily, Daily, Monthly	1979-Dec 2012
NOAA-CIRES 20th Century Reanalysis (V2)	Global	2.5°x2.5°	4X Daily	1871-2012
NOAA-CIRES 20th Century Reanalysis (V2c) new!	Global	2.5°x2.5°	4X Daily	1851-2014
U. of Delaware Precipitation and Air Temperature	Global Land	0.5°x0.5°	Monthly	1901-2014

There are several global datasets which are based on the interpolation of observed data or outputs of reanalysed data modeling, which commonly have been used by researchers; two examples of such datasets are APHRODITE and Princeton.

2.3 Climate change

The Fifth Assessment Report (AR5) of the Intergovernmental Panel on Climate Change (IPCC) is the most comprehensive assessment of all scientific knowledge on climate change since 2007, the year the Fourth Assessment Report (AR4) was released. AR5 was released in four parts between September 2013 and November 2014. It is made up of the full reports prepared by several Working Groups (I contributes to the physical science basis of climate change, II contributes to adaptation and vulnerability, and III contributes to mitigation of climate change effects). Evaluating the socio-economic aspects of climate change, along with their implications, in order to have more sustainable development, has been greatly emphasized in this new report.

AR4 and AR5 also provide a "Summary for Policymakers" from each working group's report. According to the AR4 Working Group 2's report, "Observational evidence from all continents and most oceans shows that many natural systems are being affected by regional climate changes, particularly temperature increases".

Climate change is expected to affect precipitation and evapotranspiration patterns (Tsanis et al., 2011), and consequently variables such as local water availability, river discharge, and the seasonal availability of water supply (Arnell et al., 2011). Globally, the demand for freshwater has increased due to several factors such as population growth, water pollution, economic progress, land use and climate changes, all of which reduce water availability under uncertain future conditions (Davies and Simonovic, 2011). Socio-environmental aspects including agriculture, tourism, and biodiversity conservation are in line with the quality and quantity of water resources, so the adaptation measures for the water sector are unavoidably linked with policies across a wide range of fields (Iglesias et al., 2011).

Climate change is also expected to intensify the global hydrological cycle, resulting in direct impacts on the overall availability of water resources for both domestic and agricultural uses (Huntington, 2006). On the local scale, rainfall intensities will be affected, which will lead to changes in the propensity of rivers to flood and will create other problems as well (Wilby et al., 2008). Climate also plays an important role in determining the capability of an area's land with respect to different purposes, especially intensive agricultural production (Brown et al., 2008).

Changes in the global energy budget have resulted in changes in climate. The energy budgets are as follows: surface and atmospheric energy exchanges, internal variability, and external forcings outside the climate system. The concentration of greenhouse gases (GHGs), aerosols, volcanic activity, and solar radiation are the most dominant drivers of change over the past 2,000 years (NRC, 2006). The main GHGs related to climate change are carbon dioxide (CO_2), methane (CH_4), and nitrous oxide (N_2O). These GHGs originate from both natural sources (e.g., volcanic emissions and wildfires) and human-influenced sources (e.g., burning of fossil fuels and deforestation). According to Solomon (2007), GHGs provide a sound explanation for most of the global and local warming trends over the past few decades.

2.4 Climate change and water resources

The hydrological cycle is intimately linked with changes in atmospheric temperature and radiation balance. That the climate system is changing in recent decades is very clear. Some of the evidence consists of observations of increases in global average air temperatures, extensive melting of snow and glaciers, and rising sea level (Abadzadesahraei and Sui, 2016).

To assess hydrological changes resulting from climate change or other factors, long-term observations are necessary to form baseline conditions and to detect any changes over time. These observations from monitoring networks are also important to fully understand the hydrological response of a basin and to calibrate and validate models used to project future conditions. The information obtained from such studies regarding possible changes in future hydro-climatic conditions is necessary for planning and implementing development studies and projects that incorporate reasonable strategies for adapting to changing climate (Brekke, 2009).

Trend detection of hydro-climatic parameters is a challenging task as many other factors might be involved such as land use changes, changes in water infrastructure etc. (Cohn and Lins, 2005).

2.4.1 The main water- and agriculture-related projected impacts in Asia

The following questions were answered by WGIIAR5 (Chapter 24, Regional Aspects: Asia):

- What will the projected impact of future climate change be on freshwater resources in Asia?

"The intensity of climate change and its impact on freshwater resources vary for different locations in Asia, but overall, due to high population and the importance of agriculture in the region, adequate water resources are particularly important. The uncertainty about sub-regional precipitation projections is high and thus, the impact of climate change on the availability of water resources in the future is not very clear. However, water scarcity is expected to be a big challenge in many Asian regions because of increasing water demand from population growth and consumption per capita with higher standards of living. Shrinkage of glaciers in central Asia is expected to increase as a result of climate warming, which will influence downstream river runoff in these regions. Better water management strategies could help ease water scarcity. Examples include developing water saving technologies in irrigation, building reservoirs, increasing water productivity, changing cropping systems and water reuse."

- How will climate change affect food production and food security in Asia?

"Climate change impacts on temperature and precipitation will affect food production and food security in various ways in specific areas throughout this diverse region. Climate change will have a generally negative impact on crop production in Asia, but with diverse possible outcomes (medium confidence). For example, most simulation models show that higher temperatures will lead to lower rice yields as a result of a shorter growing period. But some studies indicate that increased atmospheric CO_2 that leads to those higher temperatures could enhance photosynthesis and increase rice yields. This uncertainty on the overall effects of climate change and CO_2 fertilization is generally true for other important food crops such as wheat, sorghum, barley, and maize, among others. Yields of some crops will increase in some

areas (e.g., cereal production in north and east Kazakhstan) and decrease in others (e.g., wheat in the Indo-Gangetic Plain of South Asia). A diverse mix of potential adaptation strategies, such as crop breeding, changing crop varieties, adjusting planting time, water management, diversification of crops, and a host of indigenous practices will all be applicable within local contexts."

- Who is most at risk from climate change in Asia?

"People living in low-lying coastal zones and flood plains are probably most at risk from climate change impacts in Asia. Half of Asia's urban population lives in these areas. Compounding the risk for coastal communities, Asia has more than 90% of the global population exposed to tropical cyclones. The impact of such storms, even if their frequency or severity remains the same, is magnified for low-lying and coastal zone communities because of rising sea level (medium confidence). Settlements on unstable slopes or landslide-prone areas, common in some parts of Asia, face increased likelihood of rainfall-induced landslides. Asia is predominantly agrarian, with 58% of its population living in rural areas, of which 81% are dependent on agriculture for their livelihoods. Rural poverty in parts of Asia could be exacerbated due to negative impacts from climate change on rice production, and a general increase in food prices and the cost of living (high confidence)."

2.5 Global climate models and downscaling

Climate projections are typically available at coarse resolution but the decisions made for water resources management are done at much smaller spatial scales. So, in order to assess management options, downscaling approaches must be applied to better translate climate data for the future for hydrological models (Kour et al., 2016).

GCM outputs are based on the fundamental laws of physics and assumptions about the concentration of GHGs in the atmosphere. GCM outputs vary depending on how they simplify the climate system and aggregate the process in space and time (Prudhomme and Davies, 2008). Therefore, a range of uncertainty should be defined by applying a multi-model approach to use GCMs for better understanding of projections for water resources in the future.

To summarize, there are two main challenges in the application of GCMs for hydrological purposes:

- Inconsistency between spatial scales of GCMs and the hydrological model: GCMs' output cannot be directly used as input for hydrological models

- The low accuracy of precipitation simulations from GCMs

To resolve these issues, dynamic downscaling and statistical downscaling are the most common approaches for making GCM output suitable for hydrological models (e.g. Pinto et al. (2010)). Dynamic downscaling models (e.g., regional climate models or RCMs) might be a better option as they have clear physical meanings but they are computationally expensive. Statistical downscaling models are merely based on a statistical relationship and need less computational time.

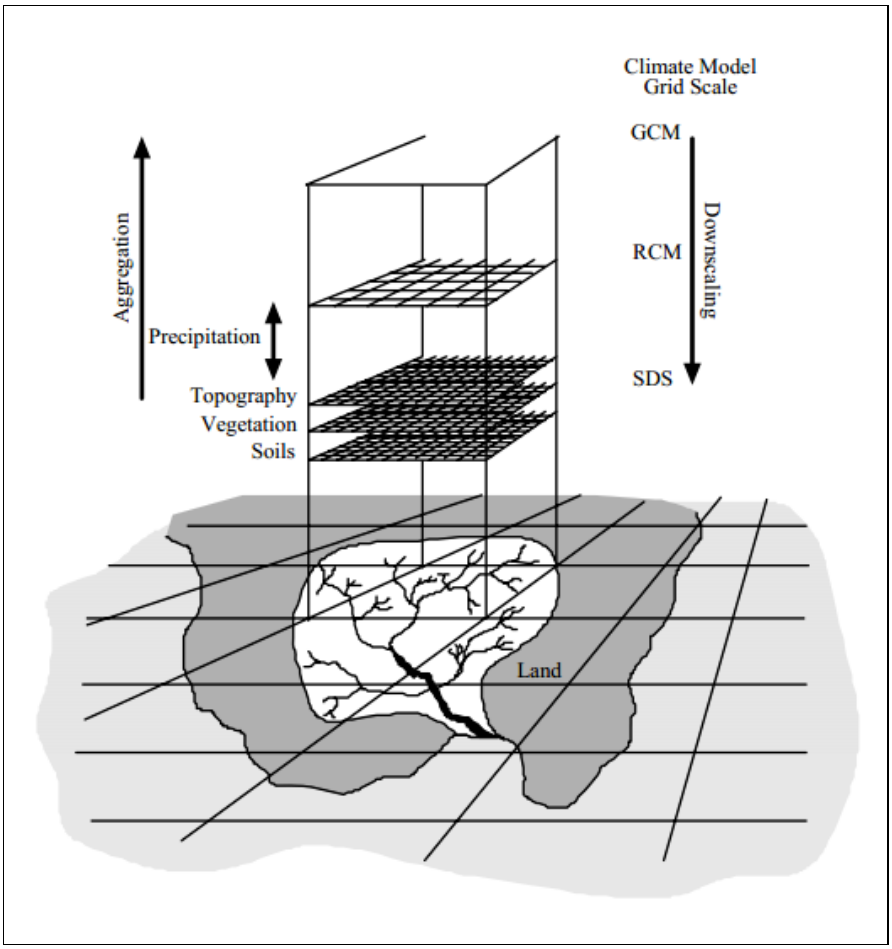

Figure 2.1 Downscaling method for hydrological modeling
Source: (SDSM, 2004)

2.5.1 RCP greenhouse gas concentrations

According to Meinshausen et al. (2011), "A set of scenarios known as Representative Concentration Pathways (RCPs) has been adopted by climate researchers to provide a range of possible futures for the evolution of atmospheric composition. These RCPs complement and, for some purposes, are meant to replace earlier scenario-based projections of atmospheric composition, such as those from the Special Report on Emissions Scenarios (SRES). The RCPs are being used to drive climate model simulations planned as part of the World Climate Research Programme's Fifth Coupled Model Intercomparison Project (CMIP5) and other comparison exercises".

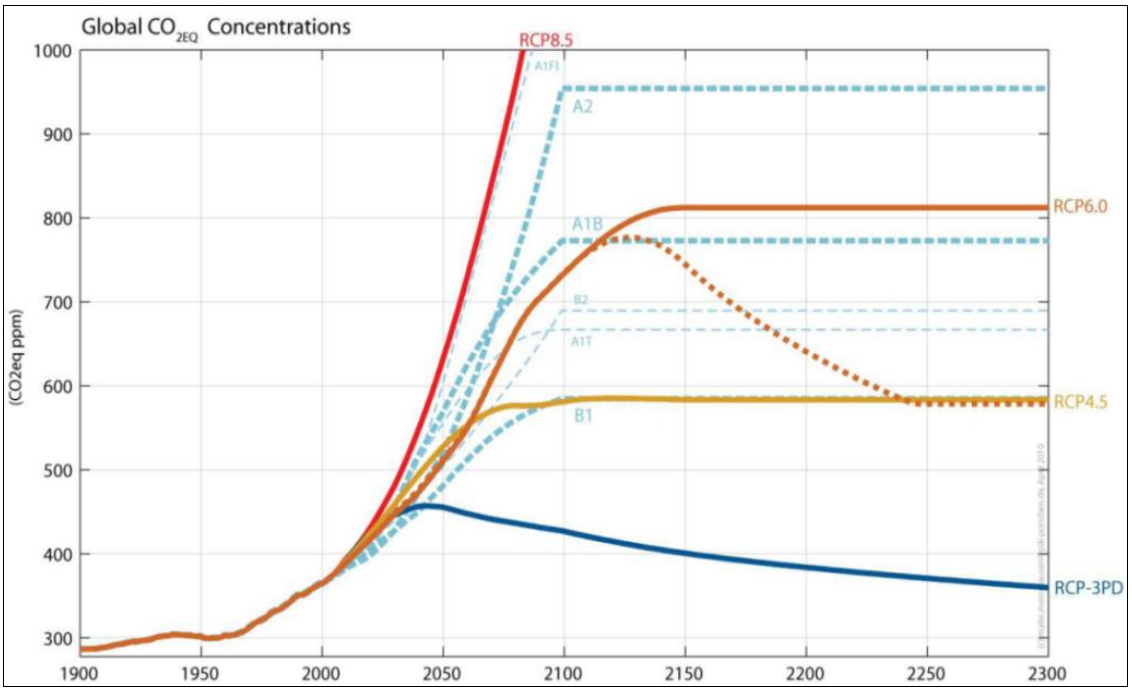

Figure 2.2 RCPs vs SRES emission scenarios

Figure 2.2 shows the comparison, in terms of equivalent global CO_2 concentrations, of SRES emission scenarios (B1, B2, A1T, A1B, A1F1, A2) used in CMIP3 simulations and RCPs (RCP-3PD, RCP4.5, RCP6.0, and RCP8.5) used as forcings for CMIP5 simulations (Lee, 2011).

2.5.2 CMIP5 GCMs

The CMIP5 archive includes the latest GCM simulations available and they are analyzed in IPCC-AR5.

Table 2.3 shows a list of some of the available CMIP5 GCMs used in this study. A complete list of all available CMIP5 GCMs can be found from their official portal (http://cmip-pcmdi.llnl.gov/cmip5/availability.html).

Table 2.3 Available CMIP5-GCMs' output

Modeling Center	Model	Institution	Terms of use
BCC	BCC-CSM1.1	Beijing Climate Center, China Meteorological Administration	unrestricted
	BCC-CSM1.1(m)		
CCCma	CanAM4	Canadian Centre for Climate Modelling and Analysis	unrestricted
	CanCM4		
	CanESM2		
CMCC	CMCC-CESM	Centro Euro-Mediterraneo per I Cambiamenti Climatici	unrestricted
	CMCC-CM		
	CMCC-CMS		
CNRM-CERFACS	CNRM-CM5	Centre National de Recherches Meteorologiques / Centre Europeen de Recherche et Formation Avancees en Calcul Scientifique	unrestricted
CNRM-CERFACS	CNRM-CM5-2	Centre National de Recherches Meteorologiques / Centre Europeen de Recherche et Formation Avancees en Calcul Scientifique	unrestricted
COLA and NCEP	CFSv2-2011	Center for Ocean-Land-Atmosphere Studies and National Centers for Environmental Prediction	unrestricted
CSIRO-BOM	ACCESS1.0	CSIRO (Commonwealth Scientific and Industrial Research	unrestricted
	ACCESS1.3		
CSIRO-QCCCE	CSIRO-Mk3.6.0	Commonwealth Scientific and Industrial Research Organisation in collaboration with the Queensland Climate Change Centre of Excellence	unrestricted
EC-EARTH	EC-EARTH	EC-EARTH consortium	unrestricted
FIO	FIO-ESM	The First Institute of Oceanography, SOA, China	unrestricted
GCESS	BNU-ESM	College of Global Change and Earth System Science, Beijing Normal University	unrestricted
INM	INM-CM4	Institute for Numerical Mathematics	unrestricted
IPSL	IPSL-CM5A-LR	Institut Pierre-Simon Laplace	unrestricted
	IPSL-CM5A-MR		
	IPSL-CM5B-LR		
LASG-CESS	FGOALS-g2	LASG, Institute of Atmospheric Physics, Chinese Academy of Sciences; and CESS, Tsinghua University	unrestricted
LASG-IAP	FGOALS-gl	LASG, Institute of Atmospheric Physics, Chinese Academy of	unrestricted
	FGOALS-s2		
MIROC	MIROC4h	Atmosphere and Ocean Research Institute (The University of Tokyo),	non-commercial only
	MIROC5		
MIROC	MIROC-ESM	Japan Agency for Marine-Earth Science and Technology,	non-commercial only
	MIROC-ESM-CHEM		
MOHC (additional realizations by INPE)	HadCM3	Met Office Hadley Centre (additional HadGEM2-ES realizations contributed by Instituto Nacional de Pesquisas Espaciais)	unrestricted
	HadCM3Q		
	HadGEM2-A		
	HadGEM2-CC		
	HadGEM2-ES		

MPI-M	MPI-ESM-LR	Max Planck Institute for Meteorology (MPI-M)	unrestricted
	MPI-ESM-MR		
	MPI-ESM-P		
MRI	MRI-AGCM3.2H	Meteorological Research Institute	non-commercial only
	MRI-AGCM3.2S		
	MRI-CGCM3		
	MRI-ESM1		
NASA GISS	GISS-E2-H	NASA Goddard Institute for Space Studies	unrestricted
	GISS-E2-H-CC		
	GISS-E2-R		
	GISS-E2-R-CC		
NASA GMAO	GEOS-5	NASA Global Modeling and Assimilation Office	unrestricted
NCAR	CCSM4	National Center for Atmospheric Research	unrestricted
NCC	NorESM1-M	Norwegian Climate Centre	unrestricted
	NorESM1-ME		
NICAM	NICAM.09	Nonhydrostatic Icosahedral Atmospheric Model Group	non-commercial only
NIMR/KMA	HadGEM2-AO	National Institute of Meteorological Research/Korea Meteorological Administration	unrestricted
NOAA GFDL	GFDL-CM2.1	Geophysical Fluid Dynamics Laboratory	unrestricted
	GFDL-CM3		
	GFDL-ESM2G		
	GFDL-ESM2M		
	GFDL-HIRAM-C180		
	GFDL-HIRAM-C360		
NSF-DOE-NCAR	CESM1(BGC)	National Science Foundation, Department of Energy, National Center for Atmospheric Research	unrestricted
	CESM1(CAM5)		
	CESM1(CAM5.1, FV2)		
	CESM1(FASTCHEM)		
	CESM1(WACCM)		

2.5.3 Evaluation of GCMs

The evaluation methods of recent GCMs range from single variable to multi-variables, multi-processes, multi-phenomena quantitative evaluations in five layers (spheres) of the Earth system, from climatic mean assessment to climate change (such as trends, periodicity, interdecadal variability), extreme values, abnormal characters and quantitative evaluations of phenomena, from qualitative assessment to quantitative calculation of reliability and uncertainty for model simulations. Researchers started considering independence and similarity between models in multi-model use, as well as the quantitative evaluation of climate prediction and projection effect and the quantitative uncertainty contribution analysis (Zong-ci et al., 2013).

The CMIP5 highlights the quantitative test method, and emphasizes the model performance metrics (quantitative measures) for the model simulations and projections of climate change (Taylor et al., 2012; Gleckler et al., 2008).

Systematic evaluation of models through comparisons with observations is a prerequisite to applying them confidently. Flato et al. (2013) described several significant developments in model evaluation including: evaluating the overall model results, isolating processes, instrument simulators, initial value techniques, and ensemble approaches for model evaluation.

2.5.4 Statistical downscaling of GCMs' output

Different methods have been developed for downscaling climate models to use them for precipitation and discharge calculations (Te Linde et al., 2010). Here, two commonly used methods are described:

- Quantile Mapping

Statistical transformations attempt to find a function h that maps a modelled variable Pm such that its new distribution equals the distribution of the observed variable Po. Statistical transformations are an application of the probability integral transform (Angus, 1994) and if the distribution of the variable of interest is known, the transformation is defined as:

$$P_o = F_o^{-1}(F_m(P_m)) \qquad \text{Eq. 2.1}$$

where F_m is the CDF of P_m and F_o^{-1} is the inverse CDF (or quantile function) corresponding to P_o.

A common approach is to solve the above equation using the empirical CDF of observed and modelled values. An R Package developed by Gudmundsson et al., (2012) is used to apply this method wherein, following the procedure of Boé et al. (2007), the empirical CDFs are approximated using tables of empirical percentiles. Values in between the percentiles are approximated using linear interpolation. If new model values (e.g. from climate projections) are larger than the training values used to estimate the empirical CDF, the correction found for the highest quantile of the training period is used.

- Delta Method (linear downscaling approach)

The delta change approach is a method to downscale global climate model data so that this data may be used as an input for hydrological models and even flood risk assessment for the future.

GCM outputs have inadequacies and a common approach to deal with that issue is the delta change method. This method computes differences between current and future GCM simulations and adds these changes to the observed time series. The delta change method is the primary future scenario generation technique suggested for use in the U.S. National Assessment. Applying the delta change method assumes that GCMs more reliably simulate relative changes rather than absolute values (Hay et al., 2000). Except for a little difference, linear downscaling is the same as the delta change approach; however, the changes are calculated for the baseline period and are applied on future time series in the case of the latter.

2.6 Hydrological modeling

For both damage mitigation and the efficient use of scarce water, the effective management of available water is necessary. Managing recharge or storing flood water, for instance, can be used to mitigate threats and maximize available resources. Observed hydrological data are the basic requirements for effective water management. However, as data records are usually inadequate in length, completeness, quality and spatial coverage, models are exploited to generate synthetic time series.

A large number of hydrological models are available for different purposes (such as flood forecasting, water supply and demand analysis, and evaluation of water quality) regarding

water resources engineering and management. These models are categorized using different classifications. One classification which is based on the conception and complexity of these models divide them into: physically based and conceptual models.

In previous years, many studies have tested various approaches to improve the applicability of hydrological models in data-scarce basins. These approaches include regionalization of model parameters (e.g., Gitau and Chaubey (2010)), the application of satellite remote sensing (e.g., Sun et al. (2012)), and the use of process-based, distributed hydrologic models (e.g., Moretti and Montanari (2008)). One approach in terms of using hydrological models in ungauged and data-scarce basins is to develop a physically based model. These models use physically based parameters spatially and temporally.

However, a conceptual model might seem a better option for data-scarce subbasins but using these models would have the problem of "equifinality," the condition whereby different combinations of the model's parameters generate the same output; thus, this becomes a primary source of uncertainty. Moreover, a conceptual model developed for a specific time and location cannot be transferable in space or time (Frenierre and Mark, 2014).

According to Gleick (1986), selecting a model for a particular case study depends on many factors such as: the purpose of the study, the model and data availability, and the compatibility of the model with existing GCMs.

Based on the above facts, it can be concluded that a physically based model which will be able to consider the contribution of glaciers and snow for the study area would be most apt for this study. A summary of the hydrological models which were made to quantify the contribution of glaciers to watershed discharge are listed in Table 2.4 (Frenierre and Mark, 2014).

2.6.1 Hydrological modeling with J2000

For this study, the J2000 hydrological model was used. J2000 is a physically based and distributed hydrological model. This model is process oriented and can be used for simulating the hydrology of meso- and macro-scale basins. The model was implemented in the Jena Adaptable Modeling System (JAMS) framework, which is a software framework for component based development and application of environmental models. To describe the hydrological processes, the model has several modules which encapsulate the process. JAMS is a modular structured environmental modeling framework and the purpose behind developing it was to address current issues in sustainable management of water resources. The JAMS framework can simulate environmental processes at discrete points in time and space, the approach which nowadays is commonly used by many distributed hydrological models (Krause et al., 2009).

Table 2.4 Hydrological models used for quantifying the contribution of glacier meltwater to watershed discharge

Model	**Model class for glacier module**	**Spatial discretization**	**Time-step**	**Standard input data**
HBV	Conceptual	HRU	Daily	Air temperature; precipitation; runoff; topography; land cover; glacier area
GSM-SOCONT	Conceptual	HRU	Daily	Air temperature; precipitation; potential evapotranspiration; runoff; glacier area; glacier mass balance
J-2000	Conceptual	HRU	Daily	Air temperature; precipitation; sunshine hours; soil characteristics; glacier area
SNOWMOD	Conceptual	HRU	Daily	Air temperature; precipitation; runoff; glacier area
SRM (Snowmelt Runoff Model)	Conceptual	HRU	Daily	Air temperature; precipitation; snow cover; glacier area
WATFLOOD	Conceptual	HRU	Daily	Air temperature; runoff; topography; land cover; glacier area

The J2000 model generates four different runoff components based on their origins. Figure 2.3 shows the model's configuration for these components, which are as follows:

1. RD1 - The fast direct runoff: This part includes runoff from sealed areas, saturation or infiltration access runoff, and snow- and ice-melt from glaciers which directly reach a stream.

2. RD2 - The slow direct runoff: This part is similar to the lateral subsurface flow within the soil zone which reacts slightly more slowly.

3. RG1 - The relatively fast baseflow: The runoff from the upper part of an aquifer. Compared to the lower zone of the aquifer, the upper part has more permeability due to weathering.

4. RG2 - The slow baseflow: The flow within fractures of solid rocks or matrices flow into homogeneous loose rock aquifers.

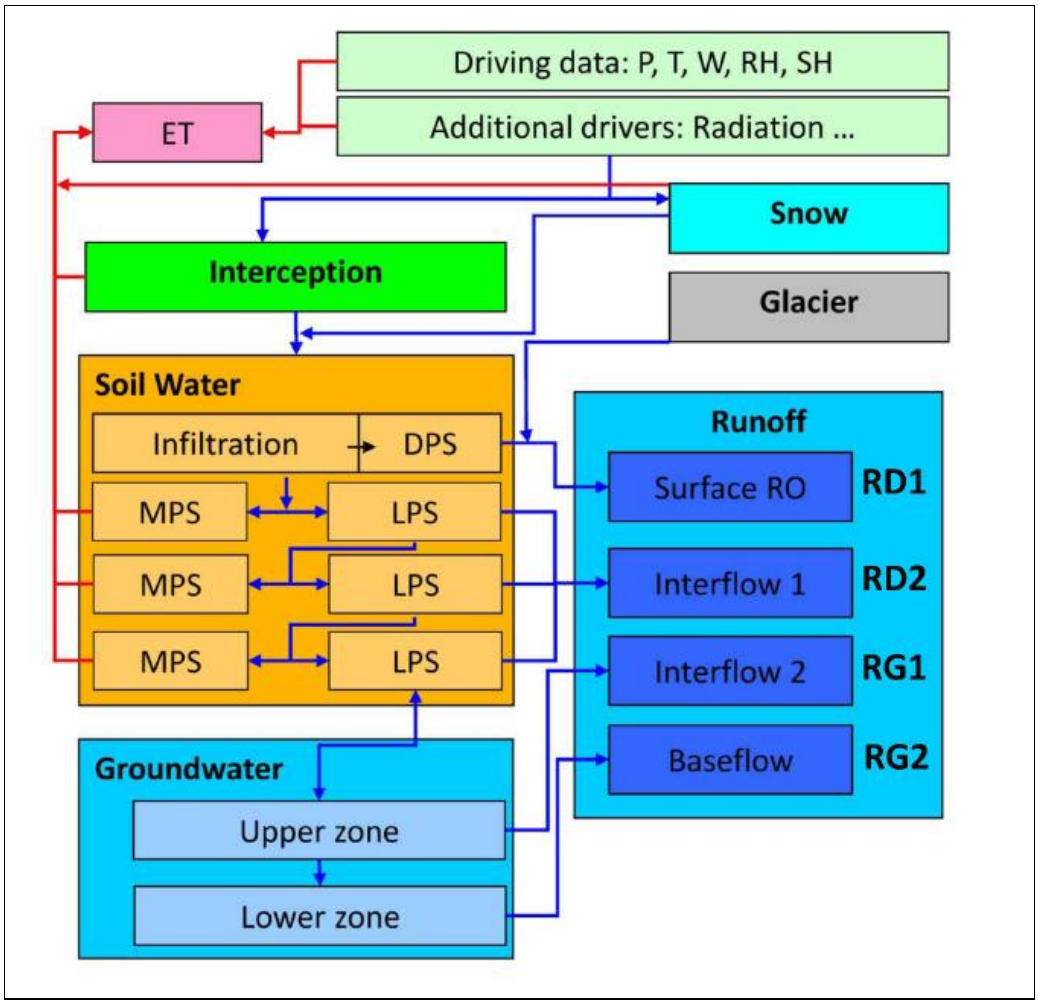

Figure 2.3 Conceptual framework of the J2000 hydrological model
Source: adapted from Krause et al. (2009)

2.7 Uncertainty analysis

Uncertainty in predictions of hydrological variables occurs at two different levels (Sivapalan et al., 2003):

- Model parameters: This uncertainty is associated with any model due to the uncertainties inherent in the estimations of parameters and input data. These uncertainties arise due to data scarcity, measurement errors, etc. and contribute to the overall uncertainty of the final result through the model. Predictive uncertainty increases if there are more parameters which need to be estimated and if their estimates are more uncertain.

- Model structure: Another kind of uncertainty results from the imperfectness in the model which is used to make predictions for a specific basin. If the results of different models are widely divergent for the same basin, it shows that the model structure's uncertainty must be high. To better understand which model can make more accurate predictions in an ungauged or data-scarce basin, the model structure's uncertainty should be assessed by validation against observed data in the basin or any other similar basin with the same the hydro-climatic conditions.

In another classification of possible sources of uncertainty in hydrological modeling, the following items have been introduced (Renard et al., 2010):

1. Uncertainty due to input data (such as measurement errors in precipitation)

2. Uncertainty due to output data (rating curve errors affect runoff estimates)

3. Model's own uncertainty (any model will be a simplified representation of the hydrological processes in the basin of interest)

4. Parametric uncertainty (it is not possible to specify the exact values of the model's parameters because of uncertainties in the calibration data, imperfect processes of understanding, etc.)

There are several approaches to estimate uncertainty in hydrological predictions such as the Generalized Likelihood Uncertainty Estimation (GLUE) (e.g., Beven and Binley (1992)).

2.7.1 Current approaches for reducing uncertainty

According to Wagener and Montanari (2011), current watershed models depend on rainfall-runoff observations to carry out the calibration process and to understand how a specific watershed functions. The calibration process is needed because it is not optimal to reach the reliable reproduction of the hydrological response of a basin by using merely the physical characteristics of that basin. This is because it is not possible to observe all the aspects of a system in adequate detail, such as the geology of an area. Another issue is how to translate such information into actual model parameters as scales can be different from measurements.

Therefore, the main focus of researchers working on ungauged basins is on how to reduce uncertainty due to model parameters. They are not looking to define the parameters of a specific model but to understand an ungauged basin and its expected behavior, what should or should not occur in a specific ungauged basin.

Usually, a single model structure is selected at the beginning and later on, the focus shifts to reduce the uncertainty in the model parameters by defining, implicitly or explicitly, a prior probability of how well the system might be represented by a given parameter, based mostly on the modeler's experience with a particular model at similar locations. Then, the defined parameter space can be explored. In the absence of long term hydrological observations to validate the model, local information from the study basin can be used. For instance, Montanari and Toth (2007) showed how to calibrate hydrological models with short and fragmented hydrological time series using spectral techniques.

2.8 Adapting to the impacts of climate change

2.8.1 Vulnerability of water resources and agriculture sectors in the face of climate change

According to Burton et al. (2006), climate change will affect water supplies as well as water quality all over the world. It might cause long-lasting shortages. In many areas, stream flow is shifting from spring to winter peaks and glacial retreat is widely accelerated. These shifts affect the availability of water for different purposes such as agriculture. Due to rising sea levels, saltwater intrusion into coastal freshwater aquifers is likely to take place, which will reduce the availability of freshwater resource. More floods and droughts can be expected;

demand for water for irrigation will increase due to the changes in quantity and intensity of precipitation. For water management infrastructure, costly investment is usually required while the adaptive responses are generally slower in water management than in agriculture.

Crop production is the most climate-dependent economic activity. Climate change through changes in temperature and moisture can lead to significant impacts on crop yields. Shifts in climate patterns may also lead to changes in the distribution of plant diseases and pests, which are likely to have negative impacts on agriculture. However, agriculture is one of the most adaptable human activities and can rapidly adapt to changing climatic conditions. The investments are usually for a short term and if it needed, the crops and cultivars can be quickly replaced to adapt to new conditions. Farming practices, the application of water for irrigation, as well as other inputs are flexible; hence, adapting to climate change is highly possible for the agriculture sector but for only a moderate amount of global warming (perhaps up to 2.5°C increase in current temperature but with no dramatic change in climate variability). Conditions might be different regionally: for example, crops in low altitudes are already close to their limit of heat tolerance. However, for higher altitudes, growth conditions might become better.

2.8.2 Afghanistan's agricultural context

According to Kawasaki et al. (2012), the most dominant sector for development in Afghanistan is agriculture. 80% of the population lives in rural areas and 58% of the GDP is generated by agriculture and rural development. Due to three decades of conflict, the agricultural production and rural infrastructure have been drastically damaged. Agricultural production is the key sector for improving the livelihood of people in the country and for the revival of its economy. Under current conditions, the country is far from achieving food self-sufficiency and being able to export agricultural products due to many issues such as limited irrigated area and very low-efficiency irrigation methods.

The Afghanistan National Development Strategy (ANDS) was prepared in May 2008 and agriculture was recognized as the most important pillar for the promotion of economic development. The sector faces many challenges including the restoration of infrastructure as irrigation facilities, the development of alternative crops to replace poppy cultivation etc. As two-thirds of the labor population is involved in agricultural activities, providing a stable life for them by developing agriculture is very crucial for the country.

Key challenges

According to the World Bank's last measurement in 2012, irrigated land in Afghanistan is 5.47% of the total agricultural land. Due to prolonged political conflicts and unstable snowfall, even the irrigated areas are not fully farmed, which affects crop yields and prevents the stable growth of the agricultural industry for the country. So, a major challenge now is to rebuild the irrigation areas which are the main crop-growing lands for Afghanistan. As a solution, the government should put efforts to repair or construct and effectively manage irrigation facilities. Water saving methods for the efficient use of water should also be proposed.

Priorities for agriculture and rural development

According to the World Bank's 2012 report, priority areas for agriculture and rural development in Afghanistan are as follows:

- Increasing agriculture productivity and growth:
    - Tackling the opium economy
    - Improving water resources and irrigation management
    - Expanding access to technology: key priorities include adaptive rather than basic research, farmer participation in setting priorities, implementation, and evaluation of research programs
    - Strengthening marketing systems
- Increasing access to assets and sustainable use of natural resources
    - Enhancing land tenure security
    - Improving access to credit
- Institutions for the poor and service delivery
    - Community driven development

2.8.3 Adaptation measures

Specific to the water sector, the IPCC Technical Paper on Water (Bates et al., 2008) suggested three approaches which can be used to address climate change adaptation planning under uncertain future hydrological conditions:

- Scenario-based: to develop probable future scenarios to help decision makers in the context of uncertainty
- Adaptive management: to increase use of robust measures of water management to withstand uncertainty
- Integrated Water Resources Management (IWRM): to resolve conflicts between competing water uses and to facilitate adaptation in the water sector

Adaptation measures will garner more tangible responses to predicted impacts of climate change if they are driven by local capacities and meet immediate needs.

In the water sector, planned measures consist of both supply and demand sides. Adaptation options from the supply side aim to increase the storage capacity or abstraction of water while the demand side measures target increasing the value per volume used and ensuring that quality is maintained through use in higher-value sectors.

It is also important to know that adapting to climate change is a dynamic, development-orientated process which needs to be considered under a broader socio-political context. To

reach this aim, an area-based adaptation approach needs to be more actively applied in conjunction with the dominant sector-based approaches (Keskinen et al., 2010).

According to Lioubimtseva and Henebry (2009), the analysis and development of adaptation measures for addressing the socio-economic impacts of climate change are connected to vulnerability analysis at all geographic scales. A sector or region's capacity to adapt to climate change depends on the level of economic development and investments, access to markets and insurance, social and economic strategies, cultural and political concerns, the private and public properties' legislation regarding natural resources, and so on. The adverse impacts of climate change can be reduced by appropriate adaptations or taking advantage of the new opportunities presented by changing climate conditions; therefore, analysis of adaptation measures is a very important element of any policy which is a response to climate change. This fact has already been recognized by most governments across the globe.

The rationale for taking the adaptation measures into account has been discussed a lot among scientists and many reasons have been offered to encourage early consideration of adaptations (Burton, 1996):

1. Climate change cannot be completely escaped.

2. Precautionary adaptations have more efficiency and less cost than forced and emergency adaptations.

3. Climate change may be more rapid and more pronounced than current estimates suggest. Unexpected events are possible.

4. Immediate benefits also can be obtained by adapting to climate variability and extreme atmospheric events as well as removing maladaptive policies and practices.

5. Climate change brings both opportunities and threats. So by better adaptation, benefits can be accrued in the future from climate change.

2.8.4 Selection and evaluation of adaptation measures

Many adaptation measures are able to reduce human vulnerability to climate change but the capacity to implement them has many constraints in line with geographic, historical, political, and economic factors. Vulnerability to climate change can be reduced by sustainable development (Solomon, 2007).

To reduce the inter-connected and unintended effects among the sectors, an area-based or context-based approach for climate change adaptation should be applied. In this approach, the potential sectoral and cross-sectoral responses are assessed under future climate risks and related adaptation policies are based on a holistic framework to integrate the specific context of each area and the various stakeholders' opinions (Keskinen et al., 2010).

To cope with increasing multiple regional stresses due to climate change as well as non-climatic factors such as land use, political, and socio-economic changes of the past decades, Afghanistan needs to develop and implement sustainable adaptive strategies. Sustainable adaptation to climate change can be achieved only by considering many environmental and socio-economic criteria. To be effective, the adaptation measures should be (a) environmentally appropriate, (b) economically cost-effective, and (c) socially and culturally acceptable (Lioubimtseva and Henebry, 2009).

According to Iglesias et al. (2007), the study titled "Adaptation to Climate Change in the Agricultural Sector" consists of several tasks, including the assessment of climate change impacts, the analysis of risks and opportunities, the identification of potential adaptation measures, and the integration of those measures into the Common Agricultural Policy (CAP).

The process for identifying potential adaptation measures consists of three main stages:

1. Analysis of relevant literature and ongoing studies to characterize adaptation measures related to the risks and opportunities identified in the assessment of impacts.

2. A review of national adaptation frameworks to highlight ongoing work to prepare national adaptation strategies.

3. A stakeholder consultation exercise to obtain practical information on adaptation measures; this took the form of a questionnaire in this study.

2.9 Crop modeling

Potential impacts of climate change on the production of food have been widely studied in many regions. The results suggest that production changes, depending on the location, may improve or worsen, leading to changes in agricultural production zones around the world. The impacts would be different for various crops. All this cumulatively suggests that there is a need for adaptation measures to help farmers and agriculture (e.g., Parry et al. (2004)).

The modeling approach has been used widely to identify the impacts of climate change on crop yield and the suitability of potential adaptation measures (e.g., Bird et al. (2015), Qin et al. (2015), and Deb et al. (2015)). The main reasons for applying the model are as follows:

- Understanding the interactions between water, food, and climate change.

- Investigating the possible options to improve crop production under current and future climatic conditions.

There are many models which can be used to achieve these aims and some of these are AquaCrop, CropWat, CropSyst, CERES, DSSAT, and EPIC.

All these models can be used to simulate crop production for a variety of crops. However, the representation of physical processes and the main focus of the model make them somehow different. Some of these models might be more suitable to analyze the impact of fertilizer use, while others are better for simulating different crop varieties and farming practices.

For those studies in which the focus is on crop-water-climate interactions, CropWat, AquaCrop, and SWAP/WOFOST, which specifically emphasize the interactions among water availability, crop growth, and climate change, are more suitable. These three models are free and publicly available on the web and have been used widely around the globe. AquaCrop has several advantages which make it a good candidate for this study. These advantages are:

- Fewer data requirements

- A user-friendly interface enabling non-specialists also to develop scenarios

- Focusing on climate change, CO_2, water, and crop yields

CHAPTER 3
STUDY AREA AND DATA

3.1 Afghanistan

Afghanistan is a landlocked country. A part of the country lies within the Hindu-Kush Himalayan region. About ten percent of this territory is arable. One quarter of the country has elevation higher than 2500 masl. Rain and snow fall are the main sources of river flow in Afghanistan. The high altitudes of the Pamir and Hindu-Kush mountains are the original potential for several river basins in Afghanistan (Habib, 2014). Water flow in Afghanistan is divided among five main river basins (Figure 3.1):

1. The Amu Darya basin
2. The Helmand basin
3. The Kabul (Indus) basin
4. The Harirod -Morghab basin
5. The Northern basin

According to the sources of irrigation water, the Government of Afghanistan has divided irrigation water into four classes; they are:

- River and Streams: 84.6%
- Springs: 7.9%
- Karezes (kanats): 7%
- Shallow and deep wells: 0.5%

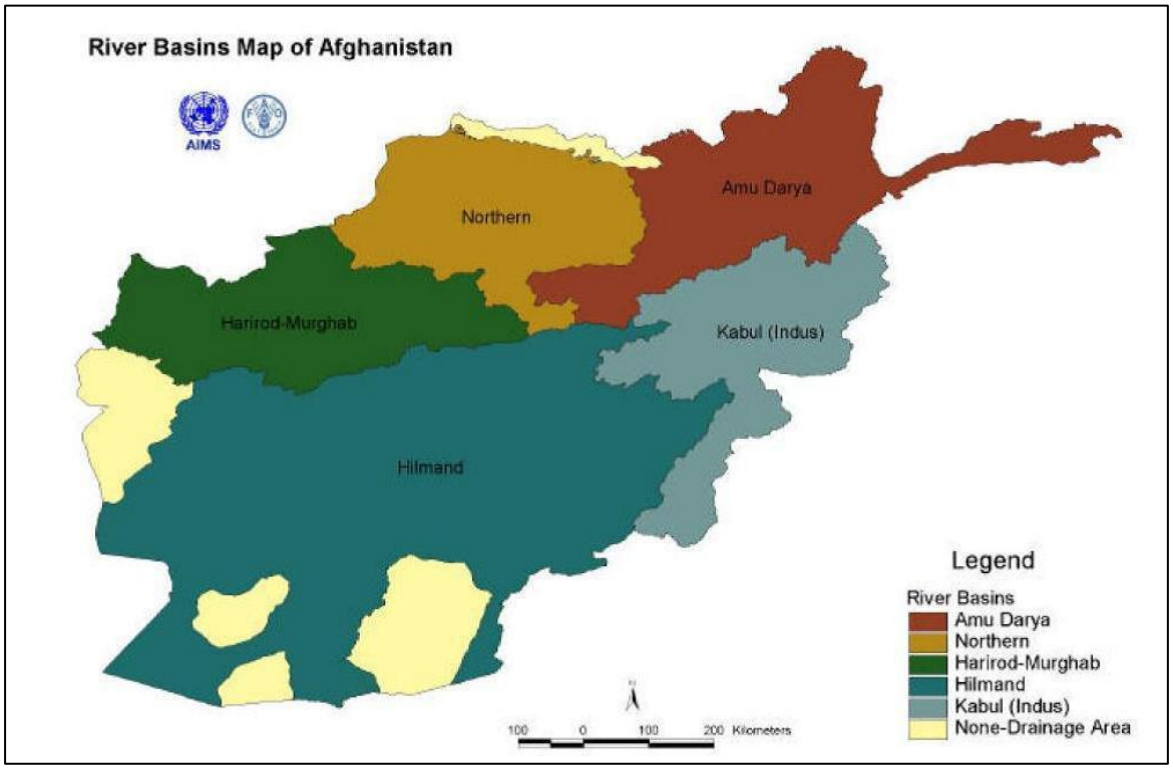

Figure 3.1 Location map of Afghanistan's river basins

Afghanistan also features extremes of temperature, ranging from -50°C on mountain peaks during winter and +50°C across its deserts during summer (Azizi, 2002). Among the reasons for this extreme temperature range is the absence of large water bodies that could have ensured a more constant temperature through heat exchange and these extreme temperatures are amplified by the correlation between the decline in temperature and the incline in elevation (Pedersen, 2009).

3.2 Kabul basin

The Kabul basin is surrounded by mountains located in the eastern and central part of the country. The Afghan capital is located in this basin and the main river here is called the Kabul River, which is the most important (although not the largest) river in Afghanistan. Much of the discharge of the Kabul River results from the melting snow accumulating during the winter season in the mountains. However, winter rains, which are common in late winter and early spring, falling on a ripe snow pack in the highlands can greatly augment the flow of the main streams (Lashkaripour and Hussaini, 2007).

The Kabul River includes all Afghan rivers that join the Indus River in Pakistan. The Indus empties into the Arabian Sea of the Indian Ocean. The Kabul basin covers twelve percent of the national territory of Afghanistan, but alone it drains one-fourth (twenty six percent) of the total annual water flow of the country. As per the information obtained from the Afghanistan Central Statistics Organization (CSO), provinces in the Kabul basin account for thirty five percent of the nation's population, and this region has the fastest population growth rate in the country.

In this study, the Kabul basin has been divided into nine main subbasins, which are shown in Figure 3.2. The total area of the basin is almost 69,269 km^2 and the main subbasins and outlets are described in Table 3.1.

Table 3.1 Characteristics of the subbasins of the Kabul basin

	Subbasin				**Outlet**			
ID	**Area (km^2)**	**Elevation (m)**			**Name**	**Lat (°N)**	**Long (°E)**	**Drainage Area (km^2)**
		Mean	**Min**	**Max**				
1	3538.1	3642	1616	5718	Gulbahar_Panjshir	35.17	69.29	3538.1
2	4032.8	3069	1613	4809	Pul-i-Ashawa	35.08	69.13	4032.8
3	7177.5	2190	978	4828	Naghlu	34.62	69.73	27837.6
4	6206.2	2820	646	5420	Pul-i-Qarghai	34.55	70.23	6206.2
5	25913.5	3433	553	7603	Pul-i-Kama	34.47	70.55	25913.5
6	1635.8	2857	1886	4506	Tang-i-Saidan	34.40	69.08	1635.8
7	9311.8	1591	401	4697	Dakah	34.23	71.04	69269.1
8	6546.9	3097	2043	4736	Shekhabad	34.08	68.76	6546.9
9	4906.5	2398	1801	4260	Sang-i-Naweshta	34.43	69.20	11453.4

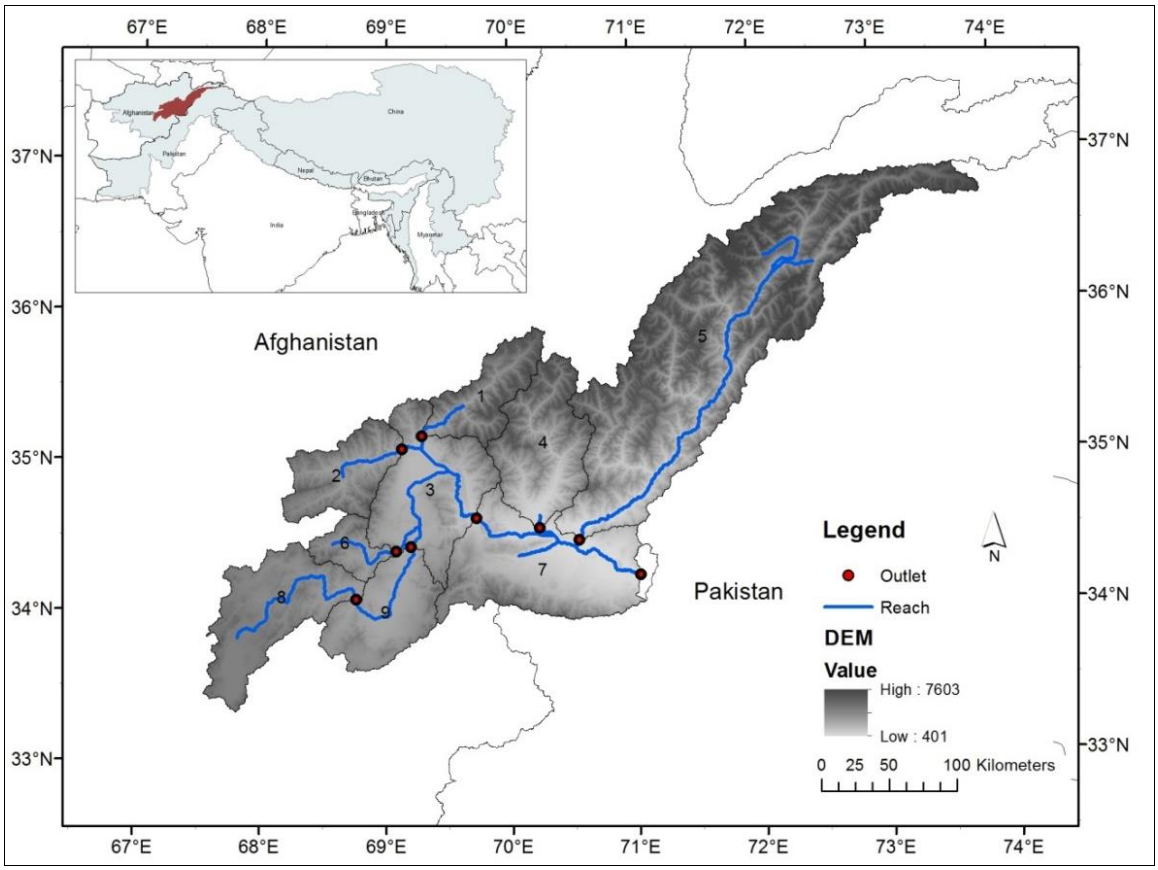

Figure 3.2 Location map of the Kabul basin, Afghanistan
(blue areas on the smaller map shows Kabul basin in Hindu-Kush Himalayas)

3.3 Hydrological data

River discharge measurements in Afghanistan were started in the mid-1940s across a few sites. The number of stations increased steadily over the years until the late 1970s. Measurements were interrupted after the Soviet Union invasion of Afghanistan. No records had been kept from September 1980 till recent years when The World Bank, in collaboration with FAO, began to reestablish the hydrometric network of Afghanistan. Until 1978, Afghanistan had a network of approximately 160 river gauging stations. Figure 3.2 shows the locations of some of the hydrometric stations on the main rivers inside the Kabul basin which have been used in this study to delineate the subbasins. The mean annual discharge of these stations was calculated from the available daily data and is shown in Table 3.2.

Table 3.2 Mean annual runoff of gauging stations in the Kabul basin

ID	Name	Runoff (m^3/s)	
		1960-1979	2008-2011
1	Gulbahar_Panjshir	54.9	46.2
2	Pul-i-Ashawa	23.1	20.5
3	Naghlu	113.0	86.3
4	Pul-i-Qarghai	59.0	50.8
5	Pul-i-Kama	482.2	443.0
6	Tang-i-Saidan	3.9	2.9
7	Dakah	633.1	522.5
8	Shekhabad	8.0	--
9	Sang-i-Naweshta	9.6	7.6

3.4 Meteorological data

While Afghanistan's meteorological stations were established during the 1950s, once the war started, data recording stopped everywhere except for the Kabul airport, which has long-term data available. As is shown in Figure 3.3, the long term average precipitation for the Kabul airport station was 330 mm/yr and the average temperature for the same period was 10.8°C. Figure 3.4 shows long term seasonal average precipitation and evapotranspiration for the Kabul airport station.

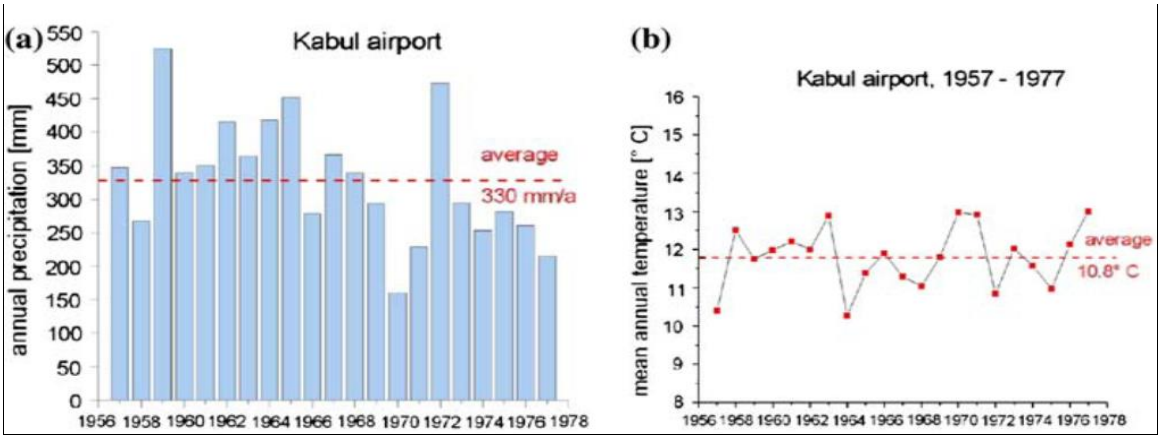

Figure 3.3 Mean annual precipitation (a) and temperature (b) at the Kabul airport station
Source: (Tunnemeier & Houben, 2005)

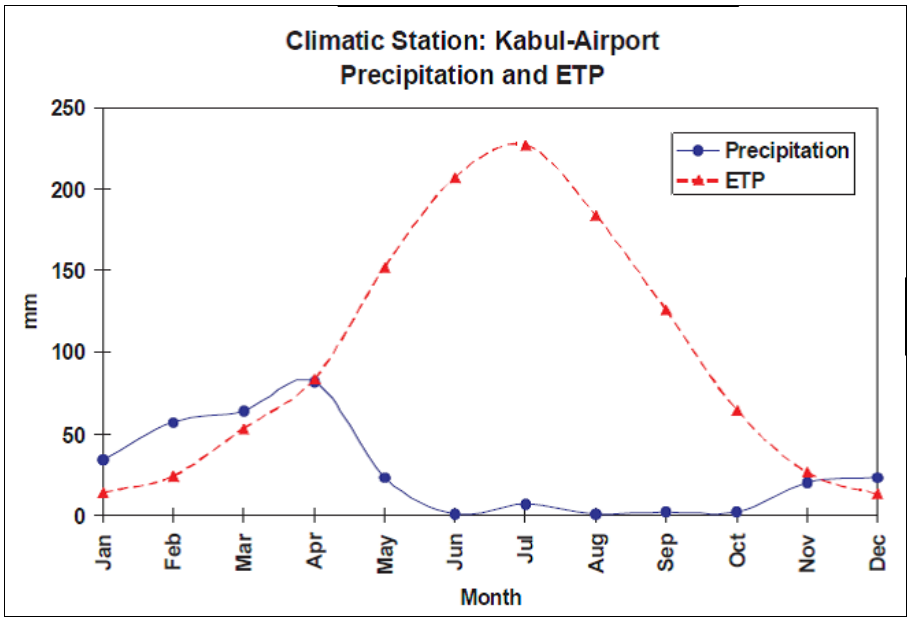

Figure 3.4 Long-term averages of precipitation and evapotranspiration at the Kabul airport station
Source: (Favre and Kamal, 2004)

Data collection activities gradually restarted after 2003. For this study, the available data for recent years (since 2003) were acquired from relevant ministries and organizations in Afghanistan. Figure 3.5 shows the reestablished meteorological stations for the Kabul basin which were used to develop the hydrological model in this study.

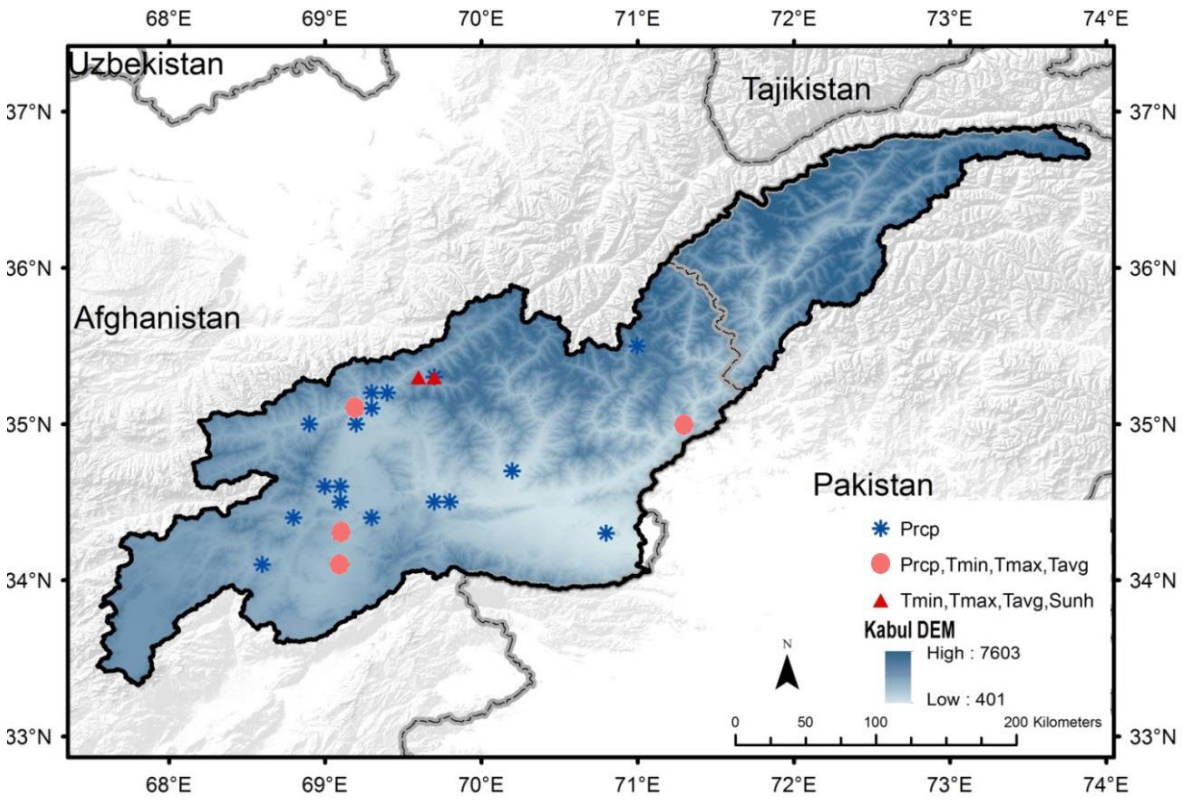

Figure 3.5 Location map of weather stations for the Kabul basin used in this study

3.5 Global datasets/RS products

Four gridded precipitation datasets were used in this study: CPC-RFE 2.0, GSMaP MVK V5, TRMM 3B42 V7, and APHRODITE V1101. They were selected from different sources based on their high resolution—temporally and spatially—for the domain of Afghanistan (Table 3.3).

Table 3.3 List of RS/global dataset precipitation products used in this study

Name of the Product	Spatial Resolution (H×V) (Degree)	Temporal Resolution	Domain	Data Source	Agency/ Academic Institution	Coverage
CPC-RFE 2.0 (Satellite Rainfall Estimation)	0.1×0.1	daily	Afghanistan 20°E-95°E,10°N-60°N	Satellite + Gauge	Climate Prediction Centre (CPC), NOAA	2001 – Present
GSMaP MVK V5	0.1×0.1	hourly	Global (60°N-60°S)	Satellite	Japan Aerospace Exploration Agency	2003 – 2010
TRMM 3B42 V7 (Tropical Rainfall Measuring Mission)	0.25×0.25	3-hourly	Global 50°S-50°N	Satellite + Gauge	National Aeronautics and Space Administration (NASA)	1998 – present
APHRODITE Precipitation V1101	0.25×0.25	daily	Monsoon Asia 60°E-150°E, 15°S-55°N	Gauge	Research Institute for Humanity and Nature (RIHN), Meteorological Research Institute of Japan Meteorological Agency (MRI/JMA)	1951 – 2007

CPC-RFE 2.0 (Climate Prediction Center Rainfall Estimates) is a precipitation product for the South Asian region. It provides real time daily precipitation information with a resolution of 0.1°. The version used in this study was specifically made available for Afghanistan, covering the area of 20-95°E and 10-60°N since January 2003. CPC-RFE combines four different primary products, of which one is a rain gauge network and three are remotely sensed (Xie et al., 2002). Shrestha et al. (2008) compared CPC-RFE with rain gauged

observations in the Bagamati Basin in the middle and lower Himalayas in Nepal. Their results suggest that CPC-RFE is able to capture the occurrence of rainfall events well but significantly underestimates precipitation amounts.

The GSMaP MVK V5 (The Global Satellite Mapping of Precipitation, a passive microwave radiometer) dataset was developed from satellite observations. It incorporates MWR measures from TRMM-TMI, SSM/I, Advanced Microwave Scanning Radiometer–EOS on the board of the AQUA satellite (AMSR-E), AMSU-B and IR (Andermann, Bonnet, & Gloaguen, 2011). This dataset uses the Kalman filter approach containing both forward and backward propagation processes to provide more accurate PM estimates in time and space (Veerakachen et al., 2014). It provides hourly data with the resolution of 0.1°. Tufa Dinku et al. (2010) compared GSMaP MVK with several other satellite-based products and rain gauge data over the whole of Colombia and found that it (GSMaP MVK) generally underestimates precipitation in the mountains where heterogeneity is high (Vancutsem et al., 2010). Hourly GSMaP MVK data was summed to a daily interval to match the observed rainfall product and other satellite/global precipitation products.

TRMM 3B42 (the Tropical Rainfall Measuring mission) is a satellite-based precipitation product from National Aeronautics and Space Administration (NASA). This product is available temporally at 3-hourly intervals and spatially at 0.25°. The algorithm to produce this dataset combines high quality (HQ)/infrared (IR) precipitation and root-mean-square (RMS) precipitation-error estimates (Nastos et al., 2013). Previous studies suggest that this product underestimates precipitation values, especially in mountainous regions, and more so in those places with high snowfall contribution (Kamal-Heikman et al., 2007). 3-hour TRMM 3B42 V7 data was summed to a daily interval to match the observed rainfall product and other satellite/global precipitation products.

APHRODITE (Asian Precipitation Highly Resolved Observational Data Integration Towards Evaluation of Water Resources, Monsoon Asia (V1101)) is an interpolated dataset from rain gauge locations. Depending on availability, between 5,000 and 12,000 rain gauge locations are considered for interpolation. These daily data cover a period of more than 50 years (1951-2007) with a spatial resolution of 0.25°. The interpolation algorithm incorporates orographic correction of precipitation (Xie et al., 2007). Information on the density of rain gauges in each grid for each day is also attached with the daily precipitation product, enabling users to know if a grid box has an interpolated value or is close to a rain gauge location.

3.6 Future climate data

For this study, a Multi-GCMs approach was used to identify the uncertainty in a climate change model for predictions of future precipitation and temperature for the Kabul basin (Table 3.4).

Table 3.4 List of CMIP5-GCMs used in this study

Model	Resolution	Modeling Center	Institution
CMCC-CMS	1.87° ×1.85°	CMCC	Centro Euro-Mediterraneo per I Cambiamenti Climatici
CNRM-CM5	1.4° ×1.4°	CNRM-CERFACS	Centre National de Recherches Meteorologiques / Centre Europeen de Recherche et Formation Avancees en Calcul Scientifique
FGOALS-g2	2.8° ×3°	LASG-CESS	LASG, Institute of Atmospheric Physics, Chinese Academy of Sciences; and CESS, Tsinghua University
HadGEM2-AO	1.87° ×1.2°	NIMR/KMA	National Institute of Meteorological Research/Korea Meteorological Administration
INM-CM4	2° ×1.5°	INM	Institute for Numerical Mathematics
IPSL-CM5A-LR	3.7° × 1.9°	IPSL	Institut Pierre-Simon Laplace
MIROC5	1.4° ×1.4°	MIROC	Atmosphere and Ocean Research Institute (The University of Tokyo), National Institute for Environmental Studies, and Japan Agency for Marine-Earth Science and Technology
MPI-ESM-LR	1.87° ×1.85°	MPI-M	Max Planck Institute for Meteorology (MPI-M)

3.7 Landscape features

The landscape features (Figure 3.6) for hydrological modeling were also obtained from different sources and for some of them, a combination of two sources was used:

- DEM

The 90-m resolution Digital Elevation Model (DEM) was downloaded from the CGIAR-CSI website: http:// srtm.csi.cgiar.org/SELECTION/inputCoord.asp. Based on this map, the highest elevation of the Kabul basin is 7603 masl and the lowest is 401 masl.

- Physiography and Geology

Based on DEM, a profile graph was obtained and three main classes were defined for the physiography of the basin. Moreover, based on the geological map of Afghanistan (USGS, 2006), the dominant lithology type of each of these physiography classes was determined.

- Soil

The Harmonized World Soil Database (HWSD), combined with the USDA soil map, was used to specify the soil types of the basin.

- Land use

The new Globcover 2009 Map of the European Space Agency (ESA) was applied to specify the different land use and land cover types. For the glacier extent of the basin, the map provided by ICIMOD was used.

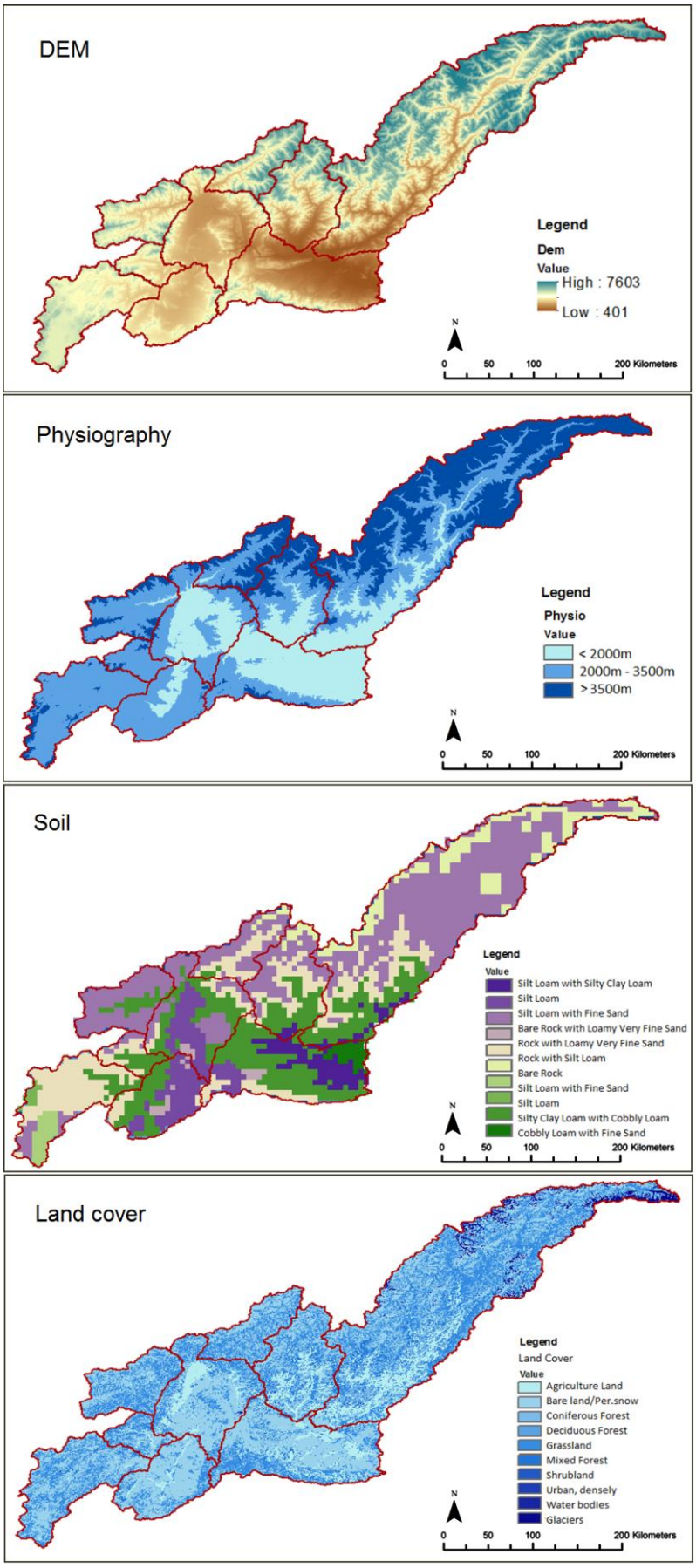

Figure 3.6 Landscape features of the Kabul basin

CHAPTER 4
METHODOLOGY

4.1 Overall methodology

This study was conducted in the Kabul basin, which is located in the northeast quarter of Afghanistan. The general procedure which was followed in this research is shown in Figure 4.1.

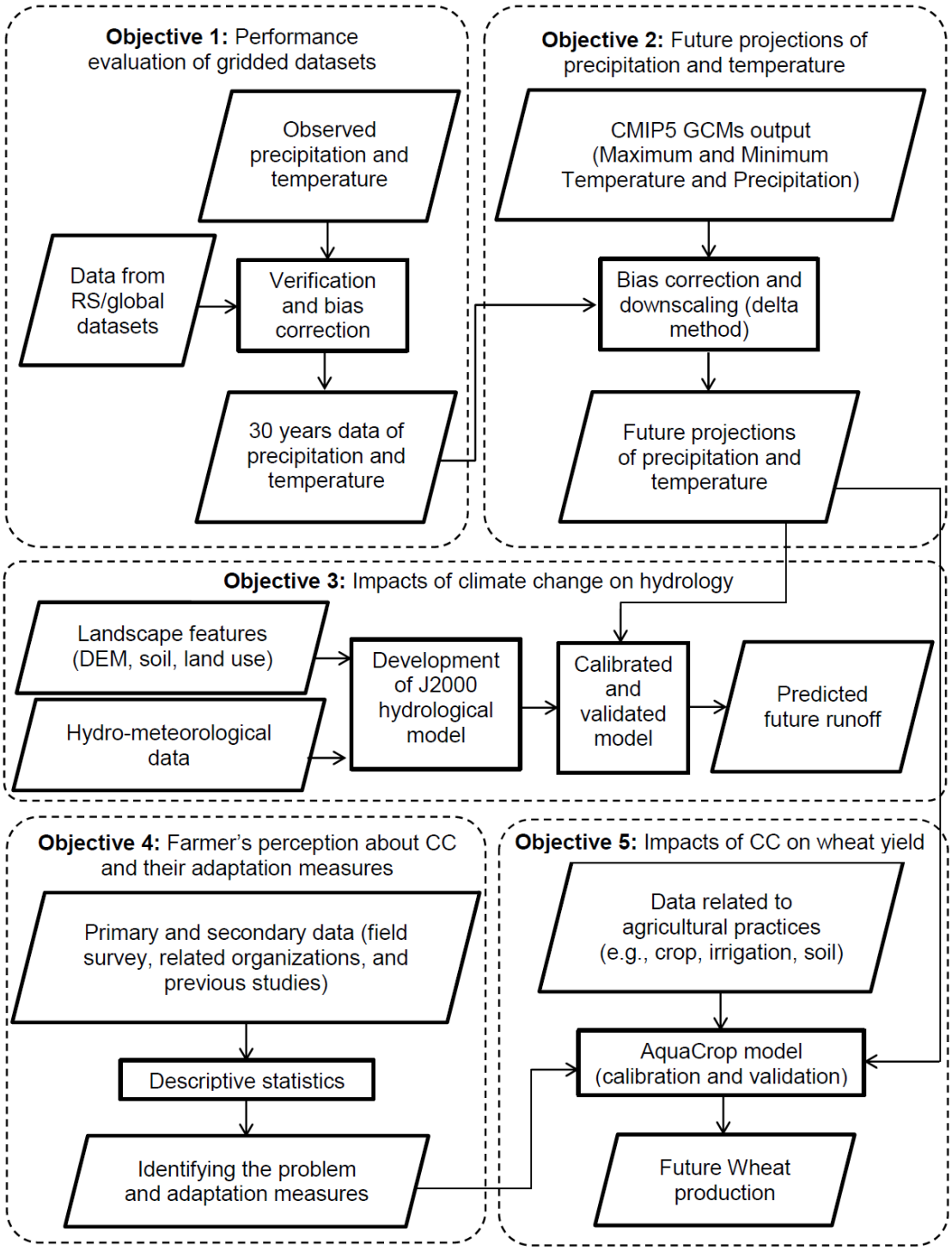

Figure 4.1 Overall methodology flowcharts

First, the required data including hydro-meteorology and landscape features (DEM, soil, land cover, and geology) were collected. The performance of global datasets/RS products was evaluated for the Kabul basin. The linear downscaling method was used to downscale the outputs of GCMs and predictions of future runoff were obtained using the calibrated and validated J2000 hydrological model for the basin. In addition to the secondary data related to agriculture and socio-economic conditions, two field surveys were done to elicit the farmers' perceptions about climate change and the adaptation measures taken by them. The AquaCrop model was then developed for estimating wheat production under future climate scenarios in order to create a link between modeling results and field surveys.

4.2 Performance evaluation of global datasets/RS products

Precipitation is one of the most important input variables for land surface hydrological models and it is characterized by high spatial and temporal variability (Zhang and Srinivasan, 2010). However, in a country like Afghanistan, which has limited capability to measure precipitation at rain gauges, the application of global datasets and remote sensed estimations has a more significant role in supplementing the data for running any hydrological model. Comparing the temporal and spatial qualities of these supplementary data, which were obtained from different sources, provides good inputs in order to better understand the data's common aspects, differences, and validity (Nasrabadi et al., 2013).

4.2.1 Data selection

For this study, the available precipitation data from stations newly established under the AgroMET-USGS project in Afghanistan were used. Based on the temporal and areal extent of the satellite/global datasets' precipitation products for Afghanistan, a period of four years (2004 to 2007) was selected for data analysis. Considering the observed data coverage, ten stations which had no missing values were selected (Figure 4.2 and Table 4.1).

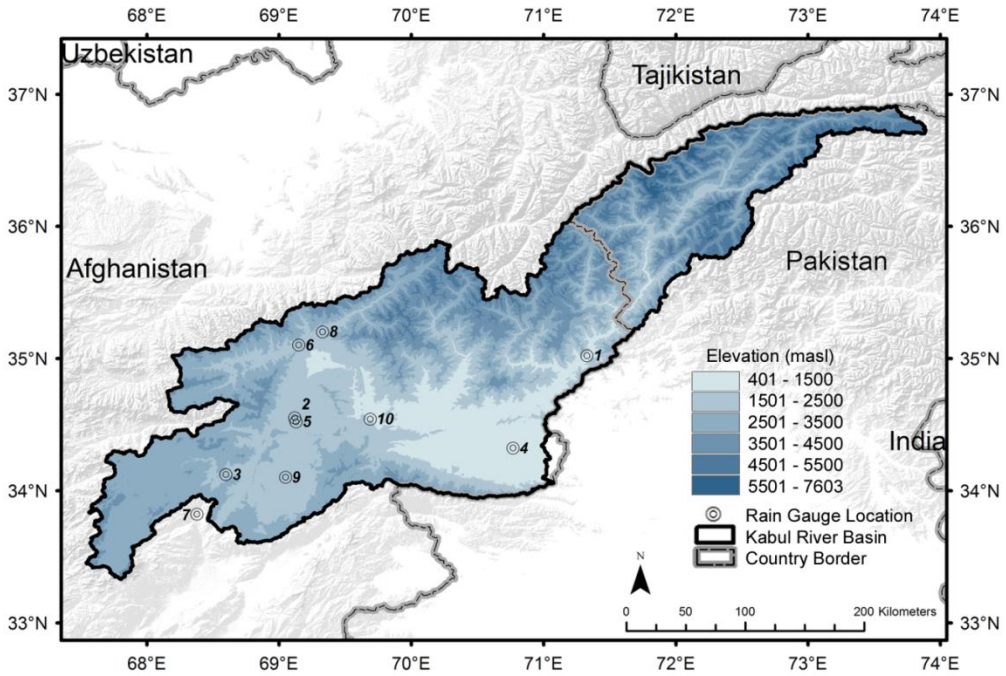

Figure 4.2 Location map of rainfall stations of AgroMET-USGS project in Afghanistan (numbers refer to the rain gauges in Table 4.1)

Table 4.1 List of rainfall stations of AgroMET-USGS project in Afghanistan

Station ID (in Figure 1)	Station Name	Long.	Lat.	Elev. (m)
1	Asmar	71.33	35.02	1088
2	Ghazi_Abad	70.77	34.32	1803
3	Jaghatoo	68.38	33.82	2168
4	Kapisa	69.33	35.20	491
5	Logar	69.05	34.10	1819
6	Badam_Bagh	69.12	34.55	1820
7	Chack	68.60	34.12	2482
8	Gul_Khana	69.13	34.52	2178
9	Jabulsaraj	69.15	35.10	1882
10	Sarobi	69.69	34.54	1396

4.2.2 Evaluation methods

Data for point-to-point analysis

To compare the data from available observed precipitation at gauge points, the gridded data for the corresponding points over the period of 2004 to 2007 were extracted and used for P-P comparison on a daily basis.

Data for grid-to-grid analysis

This method was applied to compare the observed data with all the points in the gridded precipitation products. As the spatial resolutions of the products used in this study are different, by using the spatial analyst tool in ArcGIS, all raster precipitation data were re-gridded to a resolution equal to the CPC_RFE's, whose highest resolution is 0.1°. This step was carried out to obtain the same number of cells from all the target precipitation products. The Kriging interpolation technique was used to generate raster precipitation data for the study area since this technique has been found to be the most suitable for the Indian Himalayan region (Basistha et al., 2008).

4.2.3 Verification method

The standard verification techniques described by Ebert et al. (2007) were used in this study to compare the gridded precipitation products with gauge observed precipitation. These techniques can be classified into three main categories: visual verification analysis, continuous verification statistics, and categorical verification statistics.

Visual verification compares maps of gridded precipitation estimations and observations; however, this verification is not quantitative but subjective. In addition to the comparison of the entire river basin, the precipitation datasets were also compared during the years of common availability of all datasets (2004 to 2007) with respect to elevation using the "Sample Spatial Analyst" tool in ArcGIS. Topographical information was derived from the 90m resolution Digital Elevation Model (DEM) downloaded from the CGIAR-CSI website (version 4.1, http:// srtm.csi.cgiar.org/SELECTION/inputCoord.asp).

Continuous verification statistics (MAE, RMSE, r, and Mbias represented in Equations 4.1 to 4.4) were used to measure the accuracy of a continuous variable such as rain amount or intensity. These are the most commonly used statistics in validating satellite estimates:

$$\mathrm{MAE} = \frac{1}{N}\sum_{i=1}^{N} |G_i - O_i| \qquad \text{Eq. 4.1}$$

$$\mathrm{RMSE} = \left[\frac{\sum_{i=1}^{N}(G_i - O_i)^2}{N}\right]^{1/2} \qquad \text{Eq. 4.2}$$

$$r = \frac{\sum_{i=1}^{N}(G_i - \bar{G})(O_i - \bar{O})}{\sqrt{\sum_{i=1}^{N}(G_i - \bar{G})^2}\sqrt{\sum_{i=1}^{N}(O_i - \bar{O})^2}} \qquad \text{Eq. 4.3}$$

$$\mathrm{Mbias} = \frac{\sum_{i=1}^{N} G_i}{\sum_{i=1}^{N} O_i} \qquad \text{Eq. 4.4}$$

where G_i stands for gridded precipitation data at a point or grid box i, O_i is the observation at the same grid box, and N is the number of samples.

A 2 × 2 contingency table was used to represent the number of hits, misses, false alarms, and correct negatives (Table 4.2). A threshold of 0 mm day-1 was considered to discriminate between rain and no rain. Table 4.3 was used to derive categorical statistics for the evaluation of the accuracy of estimated precipitation occurrence (Equations 4.5 and 4.6).

Table 4.2 2×2 Contingency table

		Estimated	
		No rain	**Rain**
Observed	**No rain**	correct negatives	false alarms
	Rain	misses	Hits

$$\text{Probability of detection (POD)} = \text{hits}/(\text{hits} + \text{misses}) \qquad \text{Eq. 4.5}$$

$$\text{False alarm ratio (FAR)} = \text{false alarms}/(\text{hits} + \text{false alarms}) \qquad \text{Eq. 4.6}$$

4.2.4 Verification approach

For P-P analysis, first, all the gridded data were resized to a resolution of 0.1×0.1 degrees, which was the highest available resolution for RFE precipitation. Then, the data were extracted from the grids to the corresponding locations of the rain gauges. Continuous and categorical verification statistics were then applied to validate the performance of these gridded datasets to estimate precipitation. Although APHRODITE data is based on observed precipitation, these datasets for the study area do not include the data from the stations selected for this study. Verification with our observed data was, therefore, justified and necessary.

The number of observed stations with available daily data constrains the validity of both G-G analysis on a daily basis as well as the application of categorical and statistical verification methods. Thus, to generate interpolated precipitation grids, monthly and annual observations were used by including more stations than those listed in Table 4.1, since such data are more

easily obtained from different organizations inside Afghanistan and near its border with Pakistan.

4.3 Projections of future temperature and precipitation

The methodology used for downscaling future projections of temperature and precipitation in the Kabul basin is described below.

4.3.1 Selection of GCMs

In this study, data covering a range of projections of precipitation and temperature in the future for the Kabul basin were investigated using 8 CMIP5 GCM outputs for RCP 4.5 and 8.5 scenarios till 2100.

4.3.2 Evaluation of GCMs

Model performance is usually evaluated by measuring the ability that a particular model has to reproduce current climate. However, the validation does not necessarily mean that the selected model is going to generate future projections (Reichler and Kim, 2008). The present research applied a variety of evaluation techniques ranging from visual comparison of observations and application of quantitative performance metrics. In order to assess the performance of the models, averaged monthly patterns and probability density functions (PDFs) calculated from model simulations were compared with the corresponding patterns and PDFs from observations. Standard Deviation and Correlation (using Taylor Diagrams) also were compared to check the performance of each GCM.

In order to compare actual and modelled PDFs, the skill score (s) used by (Maxino et al., 2008) can be adopted. This technique provides a simple but useful measure of similarity between two probability density functions. This skill score is a calculation of the common area under the two PDFs analysed. If the model results simulated the observed conditions perfectly, the skill score would equal 1, which is the total area under a given PDF. On the contrary, if a model simulates the observed PDF poorly, it will have a skill score close to 0, with low overlap between the observed and modelled data (Figure 4.3).

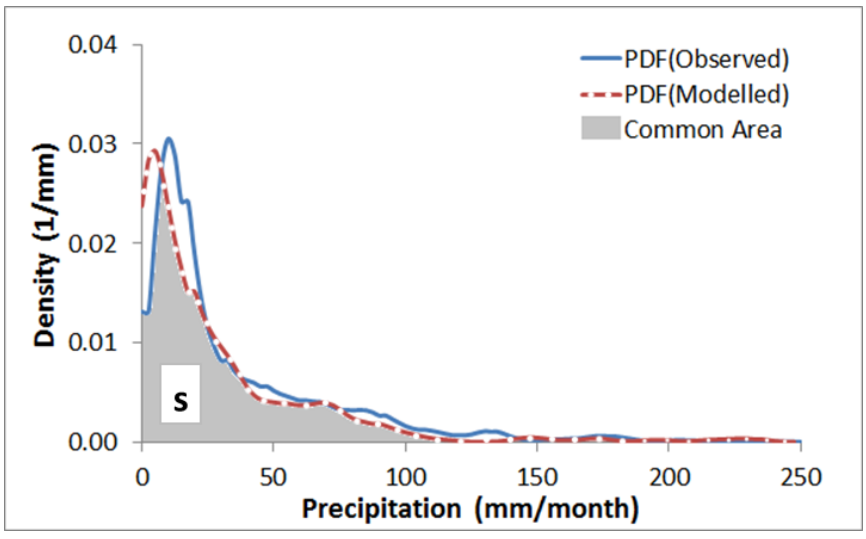

Figure 4.3 Skill score to compare PDFs of observed and modeled data

The formula for calculating the skill score is:

$$s = \sum_{m=1}^{n} \text{minimum}(Z_m, Z_0) \quad \text{Eq. 4.7}$$

where s is the numerical value of the skill score, n is the number of intervals used to discretize the PDF estimated by means of the Epanechnikov kernels, Z_m is the value of the probability density function from the model and Z_0 is the value of the probability density function from observed data.

4.3.3 Delta method: linear downscaling

A delta method (linear downscaling) approach was applied for downscaling the coarse resolution of the GCMs' outputs. The linear method is widely used in such studies, and can be applied to a single predictor-predictand pair. The constraint of this approach is that it is not suitable for non-normal distributions or for analyzing extreme events (Trzaska and Schnarr, 2014).

For this study, bias corrected APHRODITE precipitation and temperature data were used as baseline historical observations. The GCMs' output for the baseline period was compared to the observations. Changes in mean climate, calculated for each calendar month, were applied at the daily time scale as follows (Shrestha et al., 2016):

$$P_{his}(d)^* = P_{his}(d) \times [\mu_m(P_{obs}(d))/\mu_m(P_{his}(d))] \quad \text{Eq. 4.8}$$

$$P_{sim}(d)^* = P_{sim}(d) \times [\mu_m(P_{obs}(d))/\mu_m(P_{his}(d))] \quad \text{Eq. 4.9}$$

$$T_{his}(d)^* = T_{his}(d) + [\mu_m(T_{obs}(d)) - \mu_m(T_{his}(d))] \quad \text{Eq. 4.10}$$

$$T_{sim}(d)^* = T_{sim}(d) + [\mu_m(T_{obs}(d)) - \mu_m(T_{his}(d))] \quad \text{Eq. 4.11}$$

where d = daily, μ_m = long term monthly mean, * = bias corrected, his = GCM simulated 1971–2000, sim = RCM/GCM simulated 2020–2100, obs = observed 1971–2000.

4.3.4 Uncertainty analysis

Climate data for future periods were generated. Three periods, Early Future (2011 to 2040), Mid Future (2041 to 2070), and Late Future (2071 to 2100), were selected as periods to be compared with the baseline and to be used to summarize the results. Moreover, to show future variability in temperature and precipitation, the results are also shown on yearly and decadal bases. The inter-model differences of GCMs were considered to represent the uncertainty. The GCMs in this study were ranked but all of them were considered for the analysis of the results to cover a wider range of uncertainty. A range of future climate projections from different GCMs was studied on seasonal and annual scales.

4.4 Impacts of climate change on hydrology

For this study, the J2000 hydrological model was used. The J2000 model consists of several modules which represent various hydrological processes. Each module has different calibration parameters which need to be estimated during the application of the model for any specific basin.

4.4.1 Watershed delineation

Hydrological Response Units (HRUs) were used in this model to represent the spatial heterogeneity of the basin (Flugel, 1995). These HRUs are the entities for the J2000 hydrological model. HRUs are distributed, heterogeneously structured entities with similar attributes such as climate, land cover, and geological features which control their hydrological dynamics. In this study, HRUs were delineated based on the spatially distributed information of DEM (topography), land cover, soil type, and geology. These landscape features have already been described in the previous chapter of this dissertation. All these maps were reclassified at 1000-m resolution. The HRUs were delineated by overlaying the maps in a GRASS-GIS environment using a process developed by Pfennig and Wolf (2007).

4.4.2 Description of the modeling process

The modeling process is briefly described below (Nepal et al., 2012):

First, precipitation is distributed to rain and snow, based on the air temperature.

- Interception module: Maximum interception storage capacity is calculated considering the Leaf Area Index of the respective land use and calibration parameters. Precipitation values higher than storage capacity are passed on to the next module and it is assumed that the interception storage is depleted by evaporation only.

- Snow module: It accounts for different phases of snow accumulation, metamorphosis, and snowmelt. Using factors such as temperature, rainfall, and ground conditions (soil heat flux), the potential snowmelt is calculated. The snowmelt runoff from the snowpack is passed to the soil water module.

- Glacier module: This is a separate module which uses an enhanced degree-day factor by taking temperature and radiation into account and its resulted runoff directly contributes to a stream as a direct runoff (RD1).

- Soil water module: This module considers the unsaturated zone and controls the regulation and distribution of the water's movement. The inputs for this module are snowmelt and rain. Infiltration is calculated by an empirical approach based on actual soil moisture. The rest of the water is stored at the surface as depression storage up to a certain amount, and any extra water is accounted as surface runoff (RD1) and routed to the next downstream HRU.

- Groundwater module: Based on a simple storage concept of groundwater storage for each HRU, the storage in the upper groundwater zone (RG1) is considered to be the weathered layer on top of bedrock. The storage in the lower groundwater zone (RG2) represents saturated groundwater aquifers. Percolation is distributed between RG1 and RG2, based on the slope of the HRU.

The commonly applied kinematic wave approach for reach routing describes flow processes in a stream channel and the calculation of velocity is done according to Manning and Strickler method.

4.4.3 Data requirement

The hydro-climatic input data for the modeling system of J2000 are shown in Table 4.3.

Table 4.3 Input dataset requirements for the J2000 hydrological model

S.N.	Name	description	unit
1	orun.dat	observed runoff	m^3/s
2	rain.dat	measured amount of precipitation	mm
3	rhum.dat	relative humidty	%
4	sunh.dat	sunshine hour	h
5	tmax.dat	maximum temperature	^oC
6	tmean.dat	mean temperature	^oC
7	tmin.dat	minimum temperature	^oC
8	wind.dat	wind speed	m/s

4.4.4 Calibration parameters

The J2000 model has separate parameter files for each landscape feature and river network including: land use, soil, geology, HRU and reach. Here, the instructions from Nepal (2012) was followed to prepare the data for these parameter files. These parameter files are spatially distributed but temporally static descriptors and represent the spatial heterogeneity of a watershed. The second group of spatial and temporal static calibration parameters to adapt the model's response to is shown in Table 4.4.

4.4.5 Evaluation of the model's performance

The model's performance should be evaluated both visually and statistically as there might not always be an agreement between good statistical results and the model's predictions of the area's hydrological behavior and the agreement may not be done with sufficient accuracy regarding different components such as water balance. To have a more reliable understanding of a model's performance, using several efficiency criteria is necessary. In this study, four different efficiency criteria were applied: coefficient of determination (r^2), Nash-Sutcliffe (ENS), Root mean square error (RMSE), and Pbias (%)(Equations 4.12 to 4.15).

$$r^2 = \left(\frac{\sum_{i=1}^{n}(O_i - \bar{O})(P_i - \bar{P})}{\sqrt{\sum_{i=1}^{n}(O_i - \bar{O})^2}.\sqrt{\sum_{i=1}^{n}(P_i - \bar{P})^2}} \right)^2 \quad \text{Eq. 4.12}$$

$$E_{NS} = 1 - \frac{\sum_{i=1}^{n}(O_i - P_i)^2}{\sum_{i=1}^{n}(O_i - \bar{O})^2} \quad \text{Eq. 4.13}$$

$$\mathrm{RMSE} = \left[\frac{\sum_{i=1}^{n}(O_i - P_i)^2}{n} \right]^{1/2} \quad \text{Eq. 4.14}$$

$$P_{bias} = \frac{\sum_{i=1}^{n} P_i - \sum_{i=1}^{n} O_i}{\sum_{i=1}^{n} O_i} \times 100 \quad \text{Eq. 4.15}$$

where O and P are observed and predicted values respectively.

As the model used for this study is a complex model with a large number of parameters so it might suffer from "equifinality" problem which means different parameter sets performing equally good in simulation. Thus, the idea of incorporating soft data (i.e., qualitative

knowledge from the basin based on the previous studies which cannot be used directly as exact numbers) for multi-criteria model calibration (Seibert and McDonnell, 2002) was applied. Here the calibration was done by looking at low flows, high flows separately and contribution of different modules such as snow and glaciers were also considered to have more realistic results which leads to a better calibrated model in order to predict the future plausible conditions of the basin.

Table 4.4 Calibration parameters for the J2000 hydrological model

Module	Parameter	Description	Range
Precipitation distribution	Trs	Base temperature	-1 to +1
Interception module	a_rain	Interception storage for rain	0-5
	a_snow	Interception storage for snow	0-5
Snow module	snowCritDens	Critical density of snowpack	0-1
	snowColdContent	Cold content of snowpack	0-1
	baseTemp	**Threshold temperature for snowmelt**	-5 to +5
	t_factor	**Melt factor by sensible heat**	0-5
	r_factor	Melt factor by liquid precipitation	0-5
	g_factor	Melt factor by soil heat flow	0-5
Glacier module	**meltFactorIce**	**Melt factor for ice melt**	0-5
	alphaIce	Radiation melt factor for ice	0-5
	kIce	Routing coefficient for ice melt	0-50
	kSnow	Routing coefficient for snowmelt	0-50
	kRain	Routing coefficient for rain runoff	0-50
	debrisFactor	Debris factor for ice melt	0-10
	Tbase	**Threshold temperature for melt**	-5 to +5
Soil module	soilMaxDPS	Maximum depression storage	0-10
	soilLinRed	**Linear reduction coefficient for actual evapotranspiration**	0-10
	soilMaxInfSummer	**Maximum infiltration in summer**	0-200
	soilMaxInfWinter	**Maximum infiltration in winter**	0-200
	soilMaxInfSnow	Maximum infiltration in snow cover areas	0-200
	soilImpLT80	Infiltration for areas lesser than 80% sealing	0-1
	SoilDistMPSLPS	MPS–LPS distribution coefficient	0-10
	SoilDiffMPSLPS	MPS–LPS diffusion coefficient	0-10
	soilOutLPS	Outflow coefficient for LPS	0-10
	soilLatVertLPS	**Lateral vertical distribution coefficient**	0-10
	soilMaxPerc	**Maximum percolation rate to**	0-100
	soilConcRD1Flood	**Recession coefficient for flood event**	0-10
	soilConcRD1Floodthreshold	Threshold value for soilConcRD1Flood	0-500
	soilConcRD1	**Recession coefficient for overland flow**	0-10
	soilConcRD2	**Recession coefficient for interflow**	0-10
Groundwater module	**gwRG1RG2dist**	**RG1–RG2 distribution coefficient**	0-5
	gwRG1Fact	**Adaptation for RG1 flow**	0-10
	gwRG2Fact	**Adaptation for RG2 flow**	0-10
	gwCapRise	Capillary rise coefficient	0-10
Reach routing	**flowRouteTA**	**Flood routing coefficient**	0-10

4.4.6 Analysis of the impacts of climate change on water resources

The calibrated and validated J2000 hydrological model for the baseline period was used to predict the impacts of climate change in the future on the hydrology of the Kabul basin. Minimum and maximum temperature and precipitation were downscaled using the linear method and were used as input for the hydrological model. Other climatic variables (relative humidity, wind speed, and sunshine hours) were assumed to be same as they were in the baseline period. 8 GCMs and two scenarios (RCP 4.5 and RCP 8.5) were selected for uncertainty analysis of predictions for the future. Different parameters were considered to assess the impacts of climate change on hydrology including:

- Yearly and decadal changes in runoff
- Monthly and seasonal changes

4.5 Farmers' perception about climate change and their adaptation measures

4.5.1 Data collection

The first step for this part of the study was to collect primary data through field surveys and secondary data from related ministries and organizations and published studies:

- Primary Data
    - Household questionnaire survey
    - Field observations
- Secondary Data
    - Hydro-climatic data
    - Demographic data
    - Data related to agriculture (irrigation, crops, etc.)

To understand the current situation and previous work done on the subject in Afghanistan, a literature review was done and available socio-economic and agricultural profiles of the Kabul basin were collected. These included data on such diverse aspects as population density, population growth, level of education, key livelihood items, cropping patterns, etc. However, the problem that arose was these data are not available on a long term basis, especially at the provincial or district levels.

4.5.2 Selection of the study area and sample size for field surveys

Two field surveys were conducted in the Shakar Dara district, close to Kabul city, and in the Watapoor district in the Kunar province (Figure 4.4). These areas were selected based on the importance of their agriculture and because they belong to different agro-climatic zones. A random sampling approach was used.

Table 4.5 Number of households and the sample size in sample districts

District	Characteristic			Number of Households	Selected Sample Size
	Land use pattern	Dominant Crop	Dominant Fruit Trees		
Watapoor	low land	Wheat and Maize	Mulberry and Walnuts	4000	60
Shakar Dara	Hilly	Rice and Wheat	Grape and Apple	10000	60

Source: Based on the surveys done in 2004 (socio-demographic) and 2008 (agricultural profile)

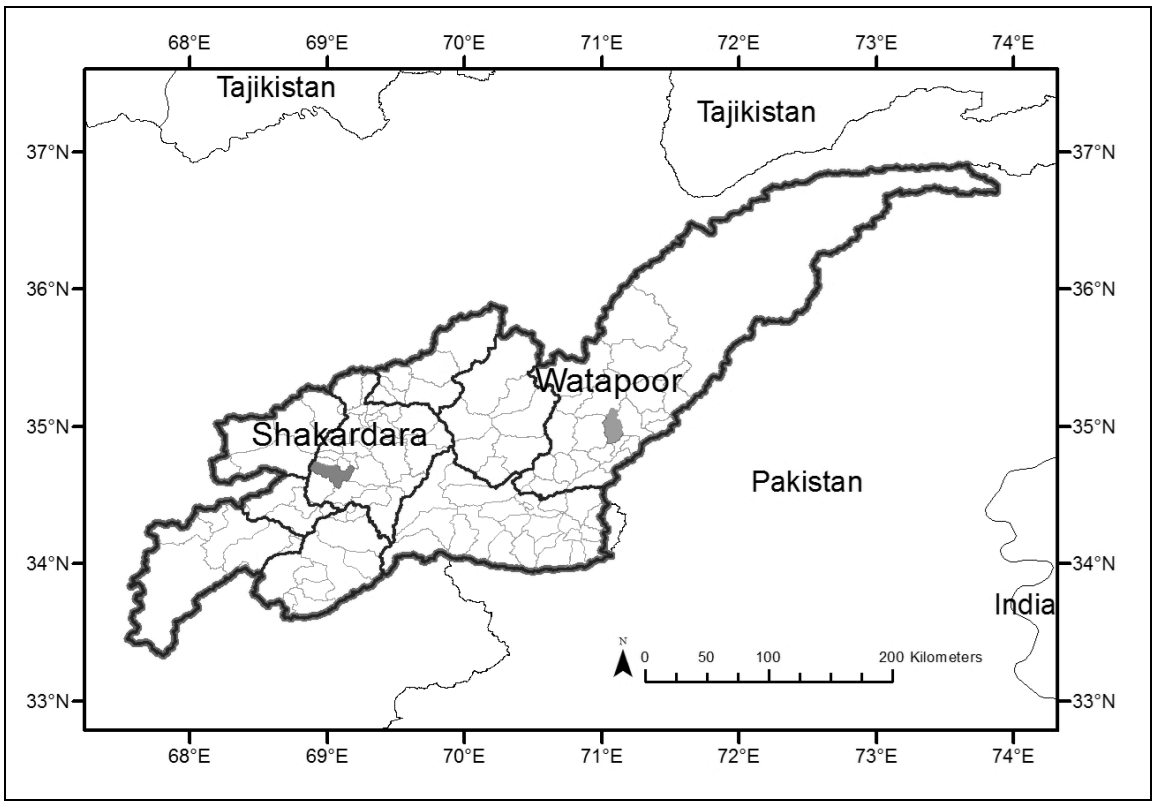

Figure 4.4 Location map of the two districts selected for field surveys

4.5.3 Detailed questionnaire and data analysis approach

The main information which was obtained based on the field survey results, are listed below:

- Understanding how the issue of climate change is understood by farmers in the study area
- Identifying the impact of climate change on their agriculture
- Identifying the type of livelihood practices and agricultural practices that the farmers are adopting at the local level to minimize the impact of climate change

To elicit the farmers' responses to climate change and their adaptations measures, an in-depth interview using a questionnaire was designed (Annex 2). A Descriptive Statistic approach was then used to summarize the collected data in a clear and comprehensible way. There are two basic methods to accomplish this: numerical and graphical. Under the numerical approach, the percentage of different answers was computed for each question and then to better identify the patterns in the data, the graphical approach was jointly used with the tables.

4.6 AquaCrop for simulating Wheat production

4.6.1 The AquaCrop Model

The FAO crop model, AquaCrop, simulates attainable yields of major herbaceous crops as a function of water consumption under rainfed, supplemental, deficit, and full irrigation conditions. The growth engine of AquaCrop is water-driven, in that transpiration is calculated first and translated into biomass using a conservative, crop-specific parameter (Geerts et al., 2009). In this model, the biomass water productivity is normalized for the atmospheric evaporative demand and air CO_2 concentration. The normalization is to make AquaCrop applicable to diverse locations and seasons. Simulations are performed on thermal time, but can be on calendar time as well, in daily time-steps. The model uses canopy ground cover instead of the Leaf Area Index (LAI) as the basis to calculate transpiration and to separate soil evaporation from transpiration. Crop yield is calculated as the product of above-ground dry biomass and the Harvest Index (HI). Starting with flowering, HI increases linearly with time after a lag phase, until near physiological maturity of the crop. Other than for the yield, there is no biomass partitioned into various organs. Crop responses to water deficits are simulated with four modifiers that are functions of fractional available soil and water modulated by evaporative demands, based on differential sensitivity to water stress of four key plant processes: canopy expansion, stomatal control of transpiration, canopy senescence, and HI. HI can be modified negatively or positively, depending on stress level, timing, and stress duration. AquaCrop uses a relatively small number of parameters (explicit and mostly intuitive) and attempts to balance simplicity, accuracy, and robustness. The model is aimed mainly at practitioner-type end-users such as those working for extension services, consulting engineers, governmental agencies, nongovernmental organizations, and various kinds of farmers associations. It is also designed to fit the need of economists and policy specialists who use simple models for planning and scenario analysis (Steduto et al., 2009).

Figure 4.5 for AquaCrop shows the main components of the soil–plant–atmosphere continuum and the parameters driving phenology, canopy cover, transpiration, biomass production, and final yield. Continuous lines indicate direct links between variables and processes. Dotted lines indicate feedbacks. The symbols are: I = irrigation; Tn = minimum air temperature; Tx = maximum air temperature; ETo = reference evapotranspiration; E = soil evaporation; Tr = canopy transpiration; gs = stomatal conductance; WP = water productivity; HI = harvest index; and CO_2 = atmospheric carbon dioxide concentration; (1), (2), (3), (4) = water stress response functions for leaf expansion, senescence, stomatal conductance, and harvest index respectively.

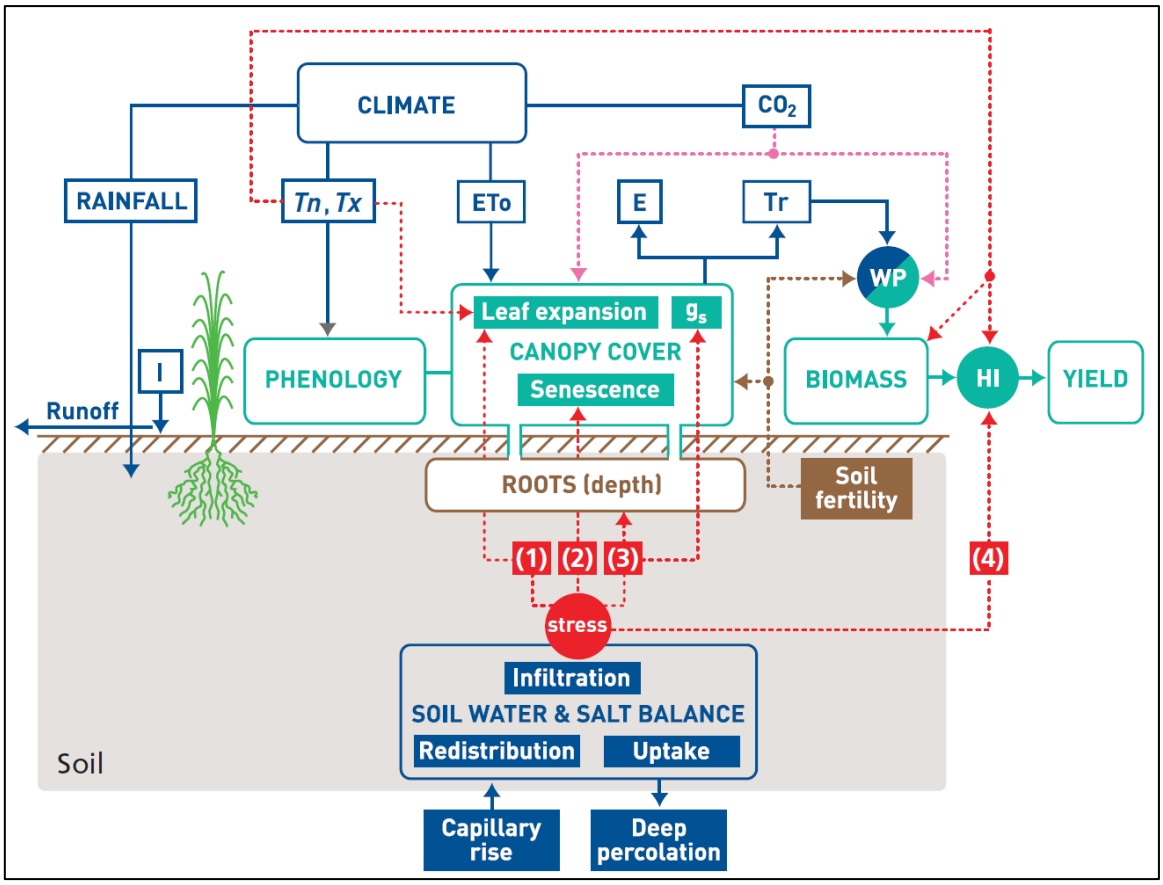

Figure 4.5 The AquaCrop modeling framework
Source: (Steduto et al., 2012)

4.6.2 Study area and data collection

The same areas selected for field surveys were also chosen for crop modeling.

The main input data and parameters for AquaCrop are shown in Figure 4.6. The climatic parameters include precipitation, maximum temperature, and minimum temperature. These variables were available for both stations in both study areas. The ET_o was estimated by an ET_o calculator (Version 3) using the Penman-Monteith Equation. The management- and cultivar-specific parameters were obtained from previous studies and reports and also from the information that was gathered through field observations during the field surveys.

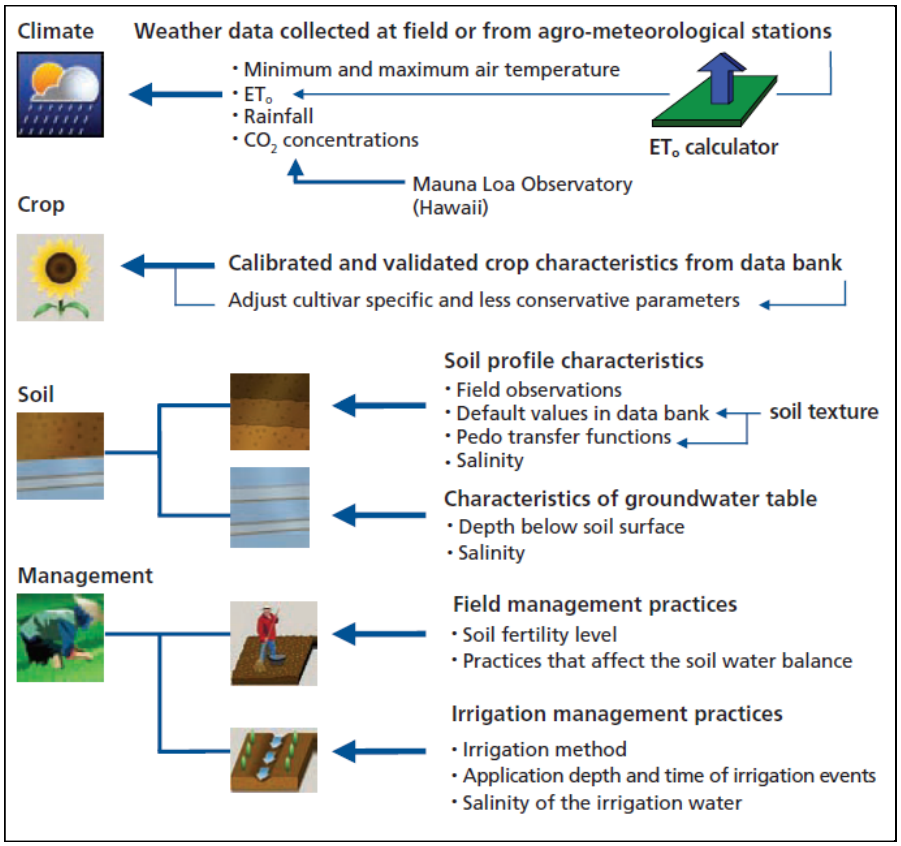

Figure 4.6 Input data for the AquaCrop model
Source: (Steduto et al., 2012)

4.6.3 The model's calibration

Model simulated yield were tested as desired output for the calibration process. Irrigation treatment was used for the calibration of the model. For each of the simulation runs, weather data, soil characteristics, canopy cover development, sowing date, and planting density were entered as input. The cultivars' data, local plant density, estimated maximum rooting depth, and time of crop development were used for the model's calibration. Assuming and/or changing conservative parameters during crop growth in the simulation of the winter wheat for study sites in Kabul basin was carried out with respect to the AquaCrop reference manual and the experience from field surveys.

4.6.4 The model's evaluation

The AquaCrop model was evaluated against the experimental data mentioned in the reports of the Afghanistan Central Statistics Organization (ACSO) for a four year period. Yield, was simulated for winter wheat in both study areas. To evaluate the performance of the crop model in estimating these values, as compared to the observations, statistical indicators such as coefficient of determination (R^2) and root mean squared error (RMSE) were used (similar to Equations 4.12 and 4.14).

4.6.5 Investigation of the impacts of future climatic scenarios and corresponding adaptation measures

Future projections of precipitation and temperature, based on the median values of 8 GCMs, were obtained for three future time slices (2020s, 2050s, and 2080s) under RCP 4.5 and RCP 8.5.

In order to overcome the projected impact of climate change/better use of future opportunities, two adaptation measures were tested: shifting transplanting dates and providing supplementary irrigation to wheat yield under future climate conditions. These methods were selected based on the results of field surveys and the suitability of the AquaCrop model for the evaluation of these methods. Simulations were carried out for winter wheat in Shakar Dara at different transplanting dates, ranging from 17 September to 12 November, at an interval of 7 days in all three future time slices. The current transplanting date is around 15 October for winter wheat in Shakar Dara while for Watapoor district, the planting date is around 15 November. Additionally, simulations were also done for future climate with supplementary irrigation of 3 applications of 40, 60, and 80 mm at an interval of 70 days starting from the transplanting date.

CHAPTER 5
PERFORMANCE EVALUATION OF GRIDDED TEMPERATURE AND PRECIPITATION DATASETS

Here in this chapter, the performance of the mean temperature of APHRODITE and the derived maximum and minimum temperatures of PRINCETON was evaluated. Gridded precipitation products were then evaluated to be used as supplementary data/replacement of observed data for the Kabul basin.

5.1 Evaluation of temperature datasets of the Kabul basin

For the selected period of evaluation (1973 to 1980), the only station with available observed temperature data on a daily basis in the Kabul basin was the Kabul airport (Figure 5.1). This data was used to remove the bias from APHRODITE data by using a simple correction factor. The approach was as follows:

- Extracting the daily mean temperature data from APHRODITE for each grid shown in Figure 5.2.

- Applying the maximum and minimum temperature diurnal from the PRINCETON data to the mean temperature values to create datasets of minimum and maximum temperature for each grid.

- Calculating the average elevation of each grid and the elevation of the center point of the same grid from DEM.

- Calculating the lapse rate based on monthly observations for the entire Kabul basin for two different seasons: winter (Nov-Apr) and summer (May-Oct).

- Applying the lapse rate and simple correction factor to remove the bias between APHRODITE and the observed data.

The final products and their coefficient of determination, in comparison to the observed data, are shown in Figure 5.3.

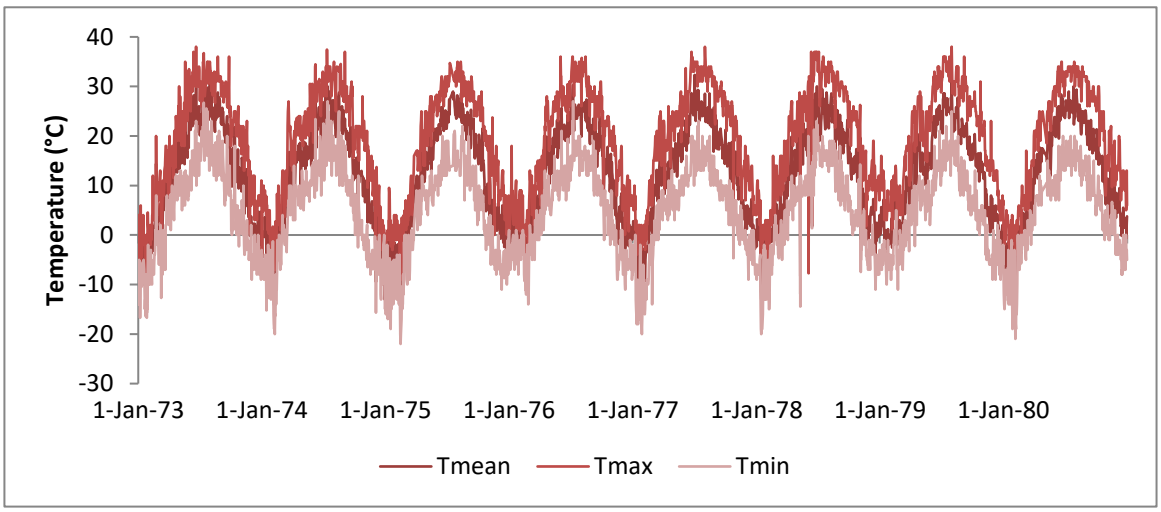

Figure 5.1 Observed temperature data at the Kabul airport station

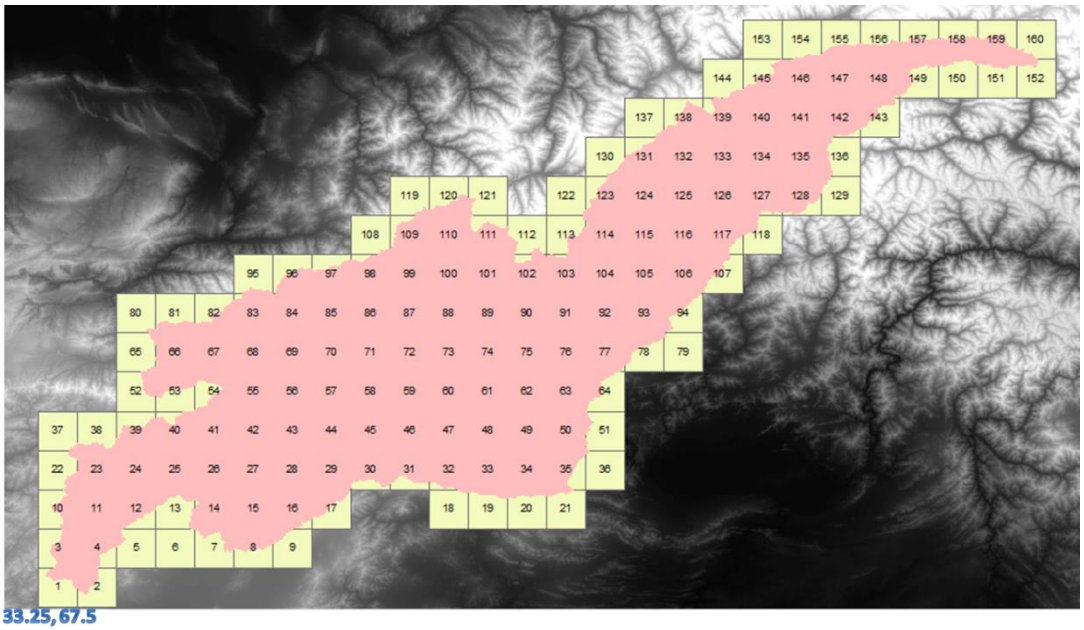

Figure 5.2 Mesh net with 0.25 resolution grids for extracting data from APHRODITE and DEM

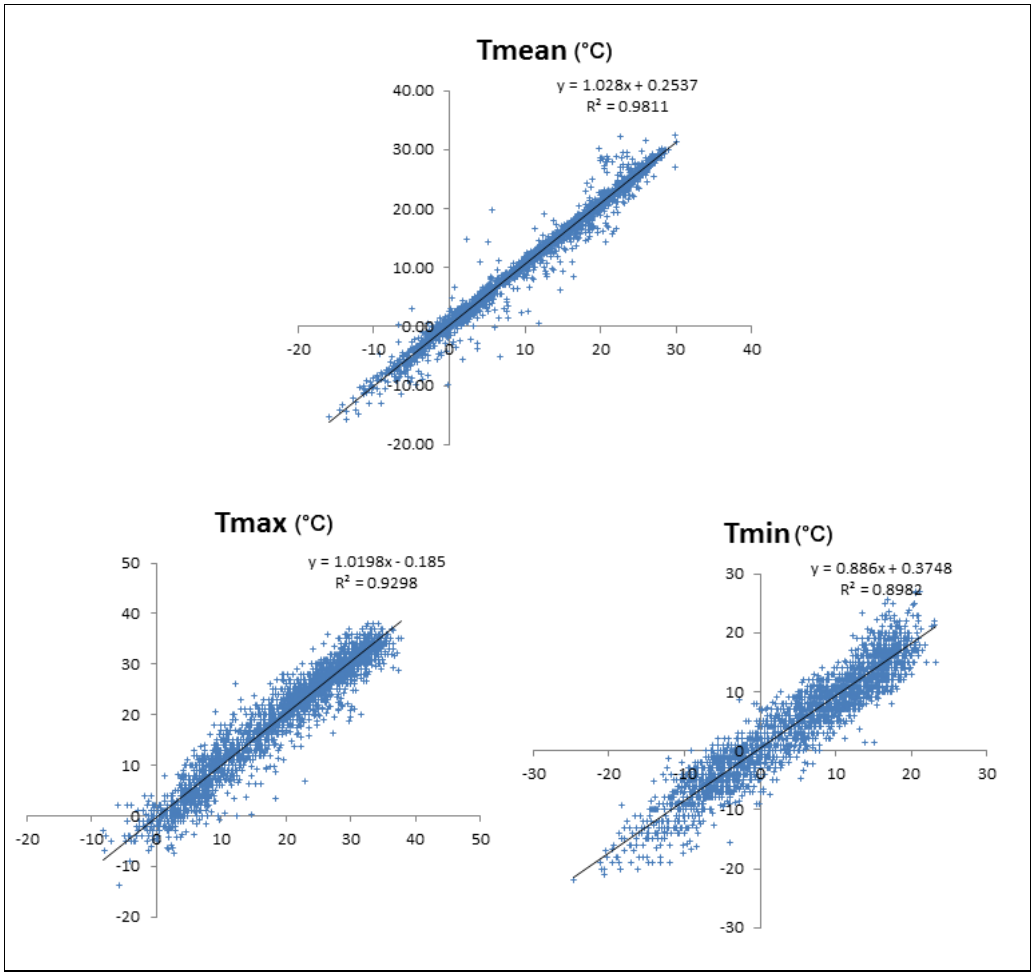

Figure 5.3 Observed temperature (y axis) vs. APHRODITE temperature data (x axis) for the Kabul airport station
(1973 to 1980)

5.2 Evaluation of precipitation datasets over the Kabul basin

In this part of the study, four precipitation datasets (CPC-RFE and TRMM 3B42, GSMaP MVK and APHRODITE) were selected to be evaluated against the observed data of the Kabul basin. The details of these datasets are mentioned in Chapter 3 of this dissertation.

5.2.1 Qualitative verification

The qualitative verification method is subjective in nature but it is considered to be one of the most effective verification methods to compare the distribution of different gridded precipitations and interpolated observations. In general, the spatial distribution of annual precipitation was investigated for four tested gridded precipitation products and interpolated observations for the period of 2004 to 2007. Due to a lack of rain gauges at higher altitudes and interpolation uncertainty caused by low gauge density, it is difficult to capture precipitation patterns influenced by orography in the study area (Bajracharya et al., 2014). In this study, two precipitation systems were detected, one over the central and southwestern parts of the Kabul basin, which has lower altitudes and some rain gauges; and the other one over the northeastern parts of the basin with higher altitudes and no rain gauges (Figure 5.4). Accordingly, studied comments can be made mainly for the first precipitation system. The annual mean precipitation values for each subbasin were also derived and are shown in Table 5.1 in order to make the comparison easier to understand. In terms of distribution, all the gridded precipitation products captured the precipitation system in the central and southwestern parts of the Kabul basin. Overall, GSMaP MVK and APHRODITE showed an overestimation while CPC-RFE and TRMM 3B42 underestimated the precipitation values. One of the possible reasons for this underestimation of precipitation by satellite-based products could be the failure of microwave sensors to discriminate between frozen hydrometers and surface snow and ice (Dinku et al., 2008).

Table 5.1 Mean annual precipitation for the Kabul subbasins
(Calculated from mapped data shown in Figure 5.4)

Subbasin ID	Outlet Name	Station ID (from Table 4.1)	Area (km^2)	Elevation (m)			Mean annual precipitation (2004-2007) (mm)				
				Mean	Min	Max	CPC-RFE	GSMaP MVK	TRMM 3B42	APHRODITE	Observed-interpolated
1	Gulbahar_ Panjshir	8	3,538	3,642	1,616	5,718	470	785	486	580	418
2	Pul-i-Ashawa	--	4,033	3,069	1,613	4,809	327	467	327	362	363
3	Naghlu	2,5,6	7,178	2,190	978	4,828	297	389	299	354	395
4	Pul-i-Qarghai	--	6,206	2,820	646	5,420	435	661	371	614	415
5	Pul-i-Kama	1	25,913	3,433	553	7,603	596	817	448	542	523
6	Tang-i-Saidan	--	1,636	2,857	1,886	4,506	270	286	199	325	312
7	Dakah	4,10	9,312	1,591	401	4,697	375	464	361	458	508
8	Shekhabad	3	6,547	3,097	2,043	4,736	222	406	162	308	375
9	Sang-i-Naweshta	9	4,906	2,398	1,801	4,260	232	271	197	308	303

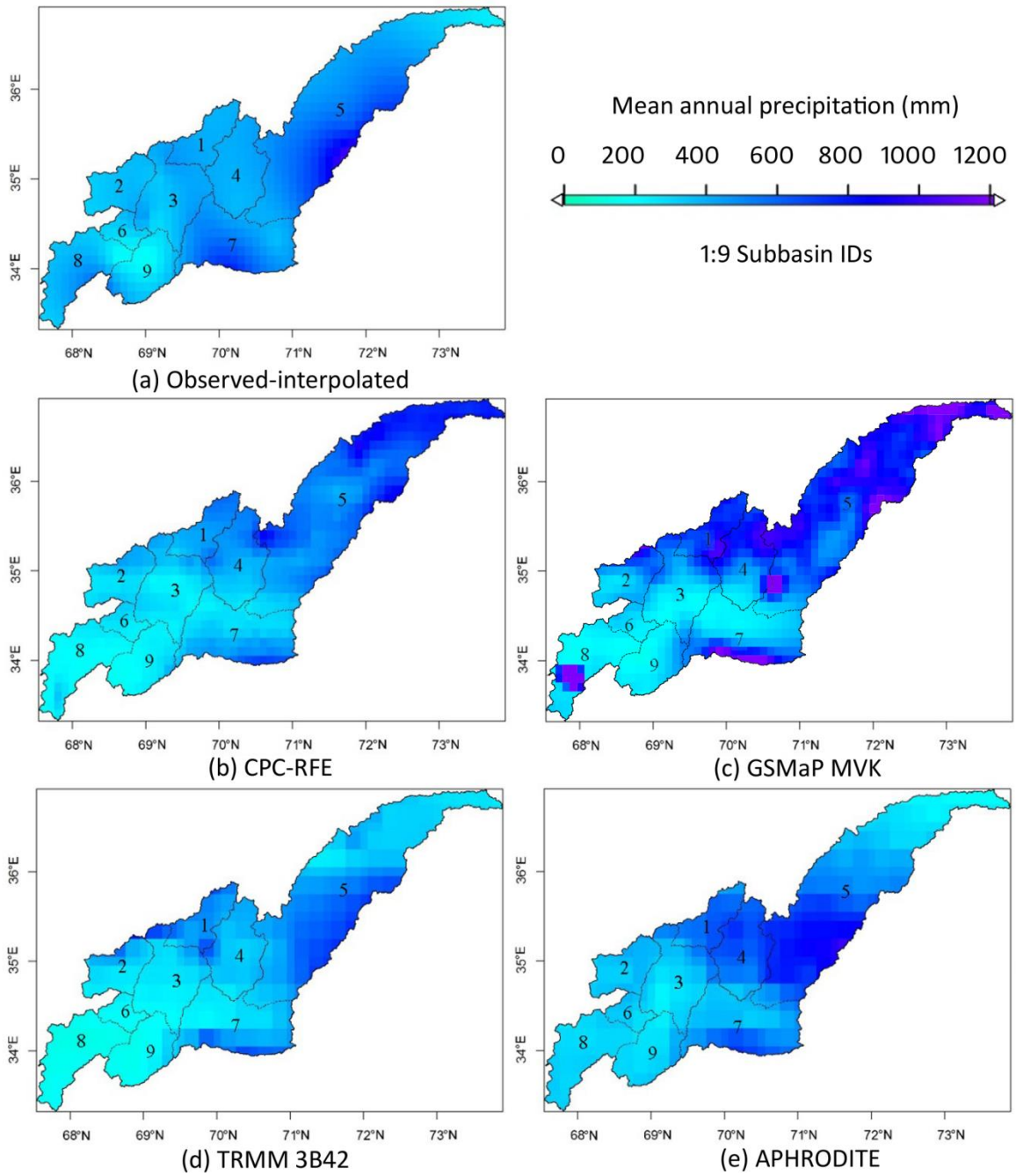

Figure 5.4 Mean annual precipitation distribution for the period of 2004 to 2007

5.2.2 Continuous verification statistics

The daily error in gridded precipitation series for each rain gauge location over the period of 2004 to 2007 was calculated and averaged over a month. Again, the results of the same month of each year were averaged. The monthly average of daily precipitation error statistics is shown in Figure 5.5. The results suggest that the APHRODITE data has the lowest mean absolute error (1.4 mm day^{-1}) and the lowest root mean square error (3.2 mm day^{-1}) through the whole year. CPC-RFE and TRMM 3B42 show slightly higher errors compared to APHRODITE, but much less than GSMaP MVK, especially during the winter season.

The monthly average correlation coefficient of the tested precipitation products is shown in the lower left panel of Figure 5.5. Again, APHRODITE proved to be the best product and showed a better performance, with a correlation coefficient of 0.3 for the whole year. The lower right panel of Figure 5.5 shows the multiplicative bias. As the values were averaged for all ten rain gauge locations and their corresponding grids so as to better understand Mbias, it was helpful to simultaneously consider the monthly time-series, as is shown in Figure 5.8. High Mbias values during the dry season (May to October)—except for GSMaP MVK which shows a reverse trend—suggest that the tested precipitation products were overestimated as compared to the observed values. On the other hand, during winter, most of the tested products were underestimated but GSMaP MVK generally overestimated the values. This is discussed again in Section 5.8 below.

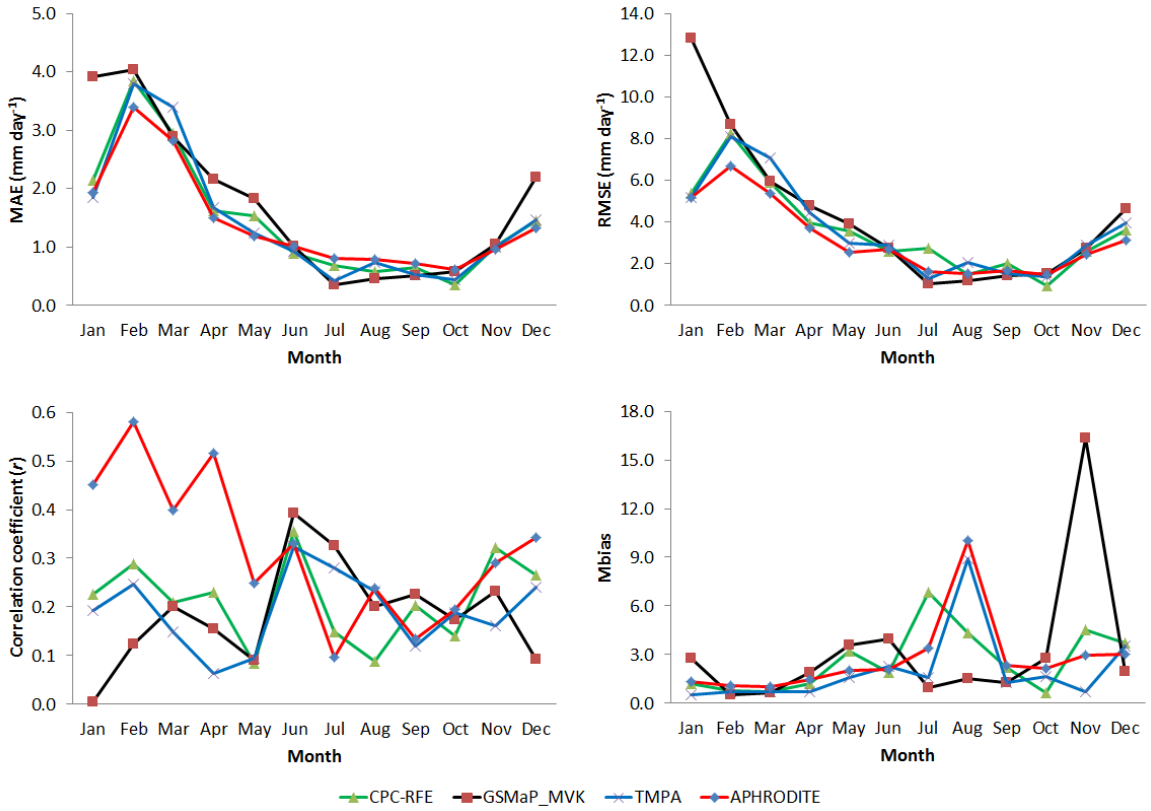

Figure 5.5 Monthly average of daily error statistics of different gridded precipitation products for the period of 2004 to 2007

5.2.3 Categorical statistics

The monthly average of daily error categorical statistics for the period of 2004 to 2007 is shown in Figure 5.6. POD is sensitive to hits but ignores false alarms. FAR is sensitive to false alarms, but ignores misses. So, the perfect score of POD is 1 while FAR should be tending to zero in the best cases. APHRODITE, with an average POD value of 0.8, was the best, followed by GSMaP MVK, which showed a better performance while the other two products gave somewhat similar results (less than 0.4). TRMM 3B42 had a relatively better FAR value of 0.7. All the other tested precipitation products had high values of FAR. One possible reason could be that they miss the very small rain amounts in rain gauges. FAR was lowest during winter and it could be due to greater volume and higher frequency of precipitation during winter.

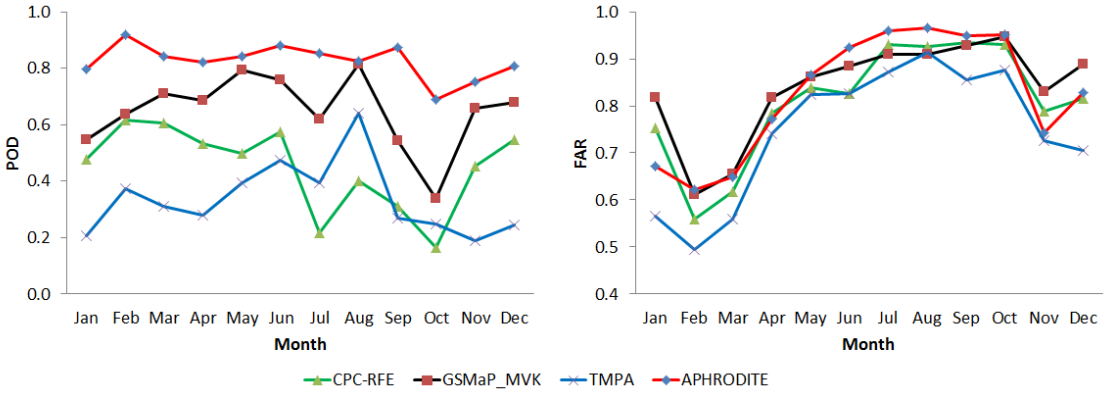

Figure 5.6 Monthly average of daily error categorical statistics of different gridded precipitation products for the period of 2004 to 2007

5.2.4 Precipitation vs. elevation

The precipitation datasets were also compared, for the years of common availability of all datasets (2004 to 2007), with respect to elevation using the "Sample Spatial Analyst" tool in ArcGIS. This evaluation had the advantage of investigating precipitation distribution as a function of elevation. It must be noted that there are no rain gauges in the mountains. In the High Himalayas, considering the low density of rain gauges, it is difficult to represent the surroundings with the elevation of a gauge (Bhatt and Nakamura, 2005).

The results of this evaluation are shown in Figure 5.7. All the rain gauges are located in low and medium altitude areas. By increasing elevation, the satellite-based precipitation products (except TRMM 3B42) showed the same increasing trend for precipitation. However, GSMaP MVK showed higher values at higher altitudes than the other products did.

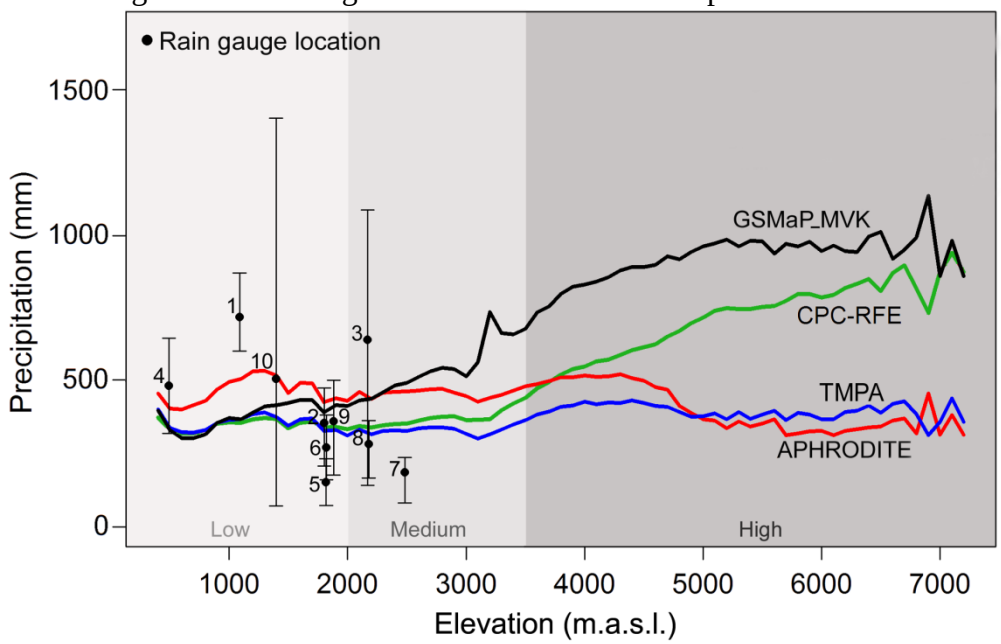

Figure 5.7 Precipitation vs. elevation.
(Mean annual precipitation for each tested dataset plotted against elevation all over the Kabul basin. The gridded precipitation data are for the years of common availability (2004 to 2007). Rain gauge data are plotted as mean values for the same period and error bars show the maxima and minima.)

As there are not enough rain gauges at higher altitudes in this region, it was difficult to make a conclusive report about this part of the study. However, based on previous studies (e.g., Winiger et al. (2005)), more precipitation in the higher altitudes of the Kabul basin is to be expected. This precipitation will occur mainly in the form of snow.

5.2.5 Monthly time-series comparison

Figure 5.8 shows the average monthly precipitation series of the ten rain gauge locations and their respective gridded data from 2004 to 2007. There is almost a general agreement in the pattern of precipitation among all the tested precipitation products and the observations (except GSMaP MVK), especially during winter. All the products generally underestimated the values during winter and overestimated them during the dry period. Statistical analysis shows that APHRODITE provided a better estimation of monthly values—as compared to the point observations—with a coefficient of determination (r^2) of 0.87. The r^2 values for CPC-RFE, TRMM 3B42, and GSMaP MVK are 0.70, 0.65, and 0.22 respectively.

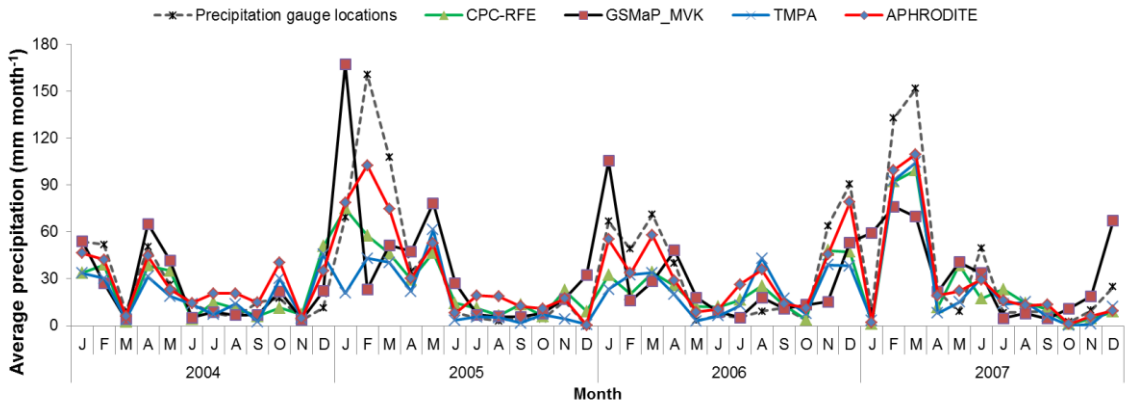

Figure 5.8 Monthly average precipitation series for the ten rain gauge locations and their respective gridded data from 2004 to 2007

5.2.6 Selection of the bias correction method for precipitation datasets

Based on the evaluation results, APHRODITE precipitation datasets were selected to be used as observations for the Kabul basin. To select the most suitable bias correction method for precipitation data over the Kabul basin, two approaches were tested and the results are shown in Figures 5.9 and 5.10. The delta method (linear downscaling) performed better to correct the bias. The evaluation was done for monthly values of precipitation over the period of four years (2004 to 2007). The details of the methods are described in Chapter 4 of this dissertation.

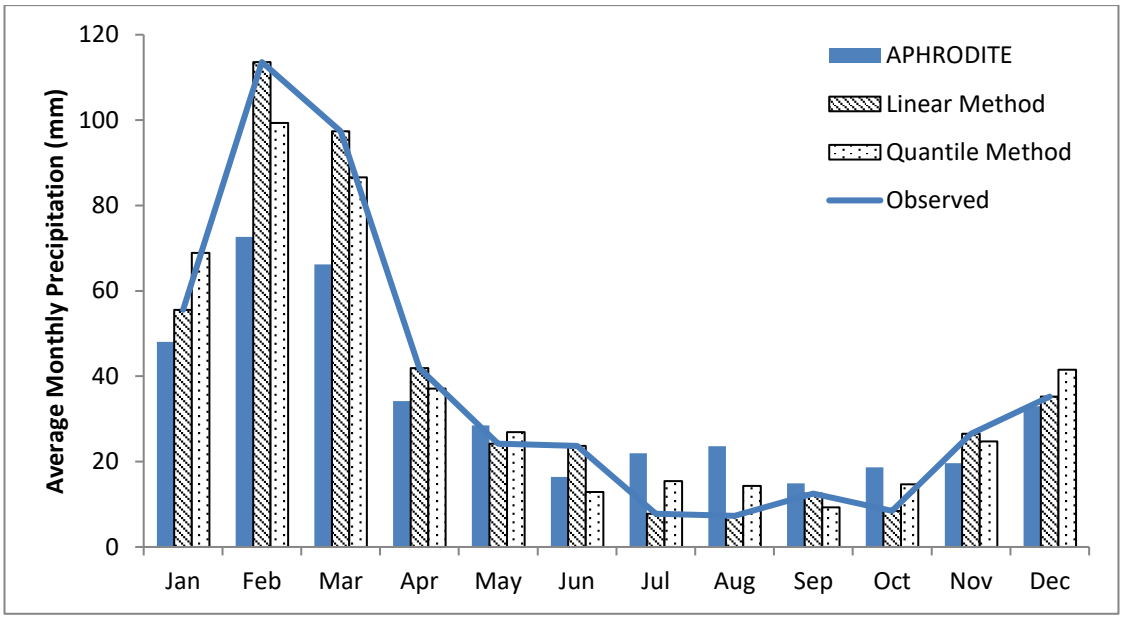

Figure 5.9 Comparison of the monthly precipitation data in APHRODITE with surface observations before and after bias correction

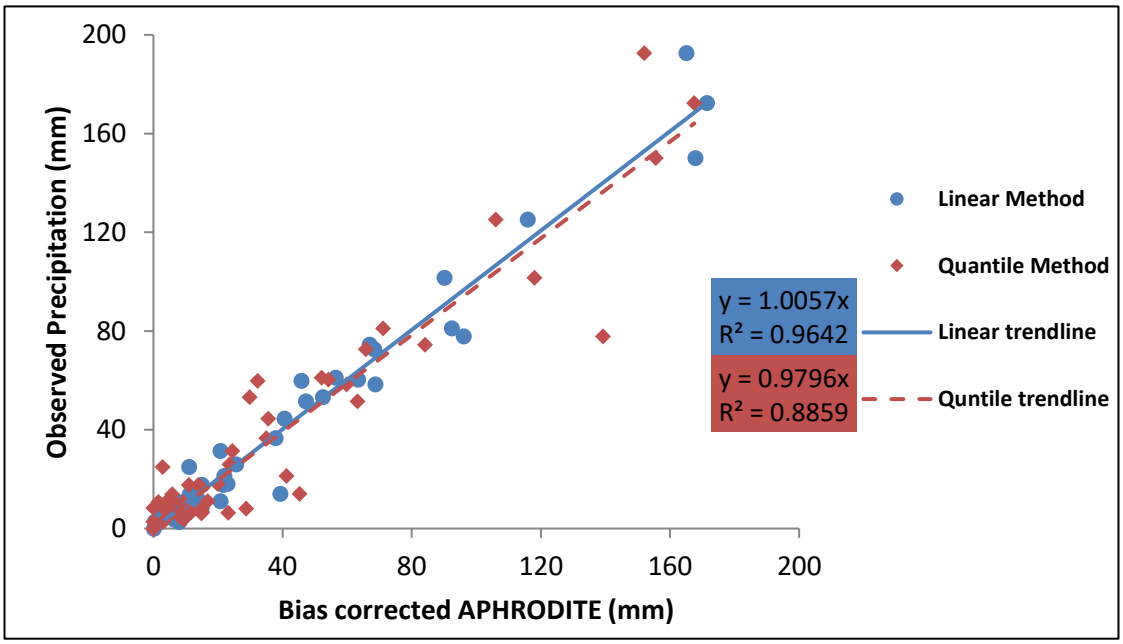

Figure 5.10 Correlation of monthly precipitation data in APHRODITE with surface observations

5.3 Summary of the results

For hydrological applications, it is essential to quantify precipitation. The availability of satellite-based precipitation products and gridded interpolated datasets provides a great opportunity for those regions suffering from poor spatial and temporal sampling of precipitation. The data-scarce Kabul basin is the most important and populated basin in Afghanistan. The newly available measured precipitation data for the period of 2004 to 2007 was the basis, in this study, to evaluate the gridded precipitation products for the basin. The evaluation was carried out at daily, monthly, and yearly levels, with values averaged using

G-G and P-P approaches. Various methods, including continuous and categorical verification statistics, visual comparison, and extracting precipitation vs. elevation were used.

The estimates from the four tested products showed a relatively good detection of precipitation distribution and precipitation amounts for most cases; however, in the G-G approach, at higher altitudes where there are no rain gauges, it was difficult to validate the values.

The results of continuous verification statistics suggest that APHRODITE is the best product and had the lowest error, while CPC-RFE and TRMM 3B42 showed slightly higher errors, but these still performed much better than GSMaP MVK, especially during winter. As for categorical verification statistics, APHRODITE was again the best, with an average POD value of 0.8. Here, GSMaP MVK gave a better performance while the other two tested products gave somewhat similar results at less than 0.4. The values of FAR were too large for all the products.

The time-series comparison of P-P monthly averaged precipitation showed a good agreement between APHRODITE and the observed data, with a coefficient of determination of 0.87. All the tested precipitation products generally showed underestimations during winter and overestimations during the dry period. GSMaP MVK's performance was the worst, with a correlation of determination of 0.22.

By investigating precipitation as a function of elevation, it was realized that by increasing elevation, the satellite-based precipitation products (except TRMM 3B42) follow the same increasing trend for precipitation. However, GSMaP MVK showed higher values at higher altitudes. Overall, this study suggests that APHRODITE is the best while considering lower altitudes but more investigations using satellite-based products should be done when observations for higher altitudes of this region become available.

APHRODITE temperature data was also found to be very suitable for the study area after comparisons with the observed data.

Temperature and precipitation data for the Kabul basin have been provided after carrying out bias correction from APHRODITE datasets which cover 1961 to 2007. These data can be used—with a high level of confidence—as observations for hydrological modeling and climate change studies in the Kabul basin.

CHAPTER 6
ANALYSIS OF HISTORICAL AND FUTURE CLIMATE

In this chapter, the trends of historical temperature and precipitation have been analyzed and discussed. Future projections of temperature and precipitation were derived and downscaled from the 8 GCMs, as discussed in Chapter 3 of this dissertation. The uncertainty arising due to the selection of different GCMs and future RCP scenarios has also been identified.

6.1 Trend analysis

6.1.1 Regression method

Trend analysis was performed to identify significant changes in climatic variables over a long period of time. The results from the regression method for the trend analysis of the Kabul airport station's data are shown in Figures 6.1 and 6.2. The results suggest that temperature has been increasing over the last five decades but an equally clear trend for precipitation was not detected.

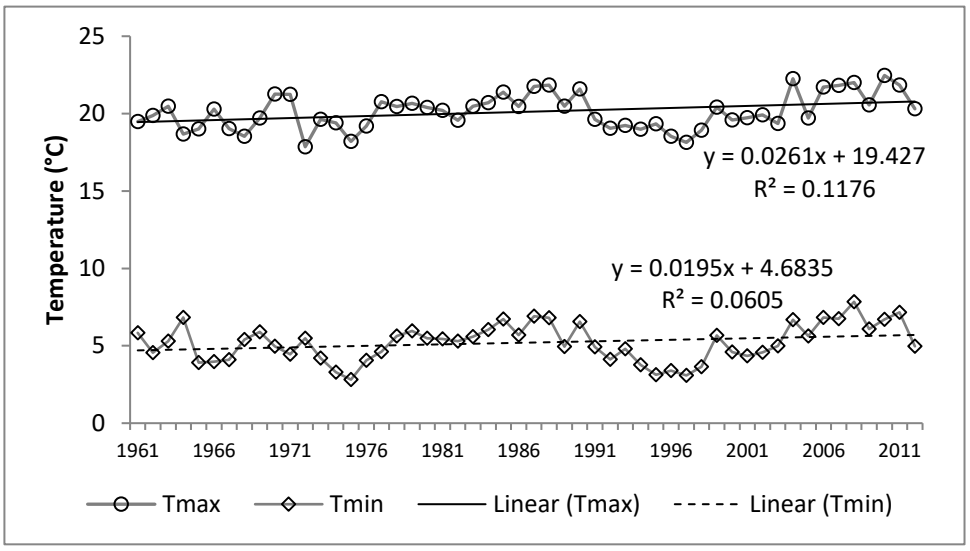

Figure 6.1 Linear trend analysis of maximum/minimum temperature for the Kabul Airport Station

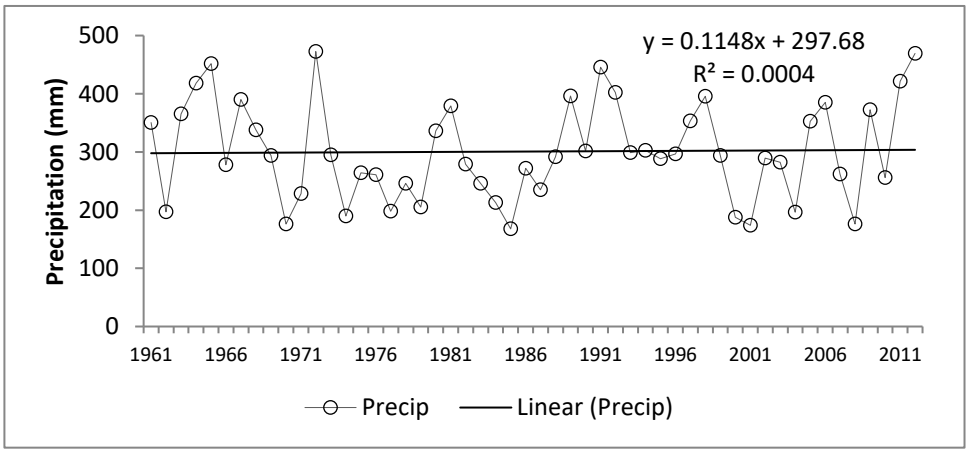

Figure 6.2 Linear trend analysis of precipitation for the Kabul Airport Station

6.1.2 Measures of shape

A histogram can give a general idea of the shape, but two numerical measures of the shape provide a more precise evaluation: skewness indicates the amount and direction of the skew (departure from horizontal symmetry), and kurtosis indicates how tall and sharp the central peak is, relative to a standard bell curve. One application is testing for normality. Many statistical inferences require that a distribution be normal or nearly normal. A normal distribution has skewness and excess kurtosis of 0, so if the distribution is close to those values, then it is probably close to normal(Table 6.1).

Table 6.1 Coefficients of skewness and kurtosis

Parameters	Skewness	Kurtosis
Tmax	0.19	-0.71
Tmin	0.00	-0.70
Precip	0.28	-0.81

6.1.3 The Mann-Kendall test

The non-parametric Mann-Kendall test is commonly employed to detect monotonic trends in series of environmental data, climate data, or hydrological data. The null hypothesis, H0, signifies that the data come from a population with independent realizations and data are identically distributed. Rejecting H0 indicates that a trend in the time series was detected, while accepting H0 indicates no trend was detected. The data show a significant positive trend if the p-value is less than 0.05 [α (alpha): significance level]. Tau is the Kendall rank correlation (the similarity of the orderings of the data when ranked by each of the quantities) coefficient. S is the Mann-Kendall statistic and varS is the variance of S. Z is the normalized test statistic.

Table 6.2 presents the results of the univariate Mann-Kendall test. The p-value indicates that the null hypothesis was rejected only in the case of maximum temperature. It can be concluded that the trend was detected for Tmax but not for Tmin and precipitation. The results of the Nonparametric Estimate of Trend in Table 6.3 present Sen's slope for the linear rate of change and the corresponding intercept.

Table 6.2 Trend detection: The univariate Mann-Kendall test (annual values)

Total series	S	varS	Z	tau	P-value	Test Interpretation
Tmax	288	16059	2.3	0.217	0.02353	Reject H0
Tmin	226	16059	1.8	0.170	0.07582	Accept H0
Precip	28	16059	0.2	0.021	0.83128	Accept H0

Table 6.3 Magnitude of trend: Sen's slope and intercept

Sen's slope and intercept	Tmax	Tmin	Precip
Slope	0.026	0.021	0.170
Intercept	19.439	4.786	287.183
nr. of observations	52	52	52

Mukherjee et al. (2015) based on APHRODITE precipitation data reported that trends are not significant for most of the Himalayan region. A significantly decreasing trend was also found by Palazzi et al. (2013) over Himalayan region in the APHRODITE dataset for 1951–2007 period.

6.2 Evaluation of GCMs

Here, eight GCMs (CMCC-CMS, CNRM-CM5, FGOALS-g2, HadGEM2-AO, INM-CM4, IPSL-CM5A-LR, MIROC5, and MPI-ESM-LR), which have been described in detail in Chapter 3, were used. All the GCMs' precipitation data for the baseline period (1971 to 2000) against observations were drawn and the comparison is shown in Figure 6.3.

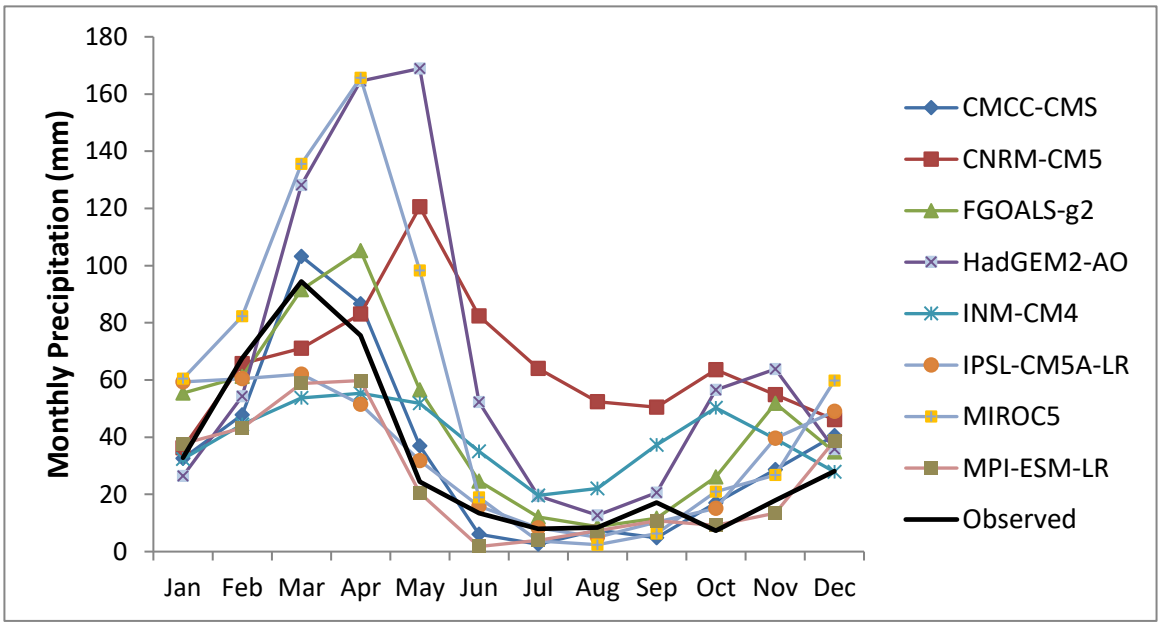

Figure 6.3 Comparison of raw GCMs' data with observed precipitation data for the baseline period

Some of the GCMs showed lower performance against observations for the baseline period; these were CNRM-CM5, HadGEM2-AO, and MIROC5. However, none of the GCMs were excluded from the analysis because after downscaling, the performance of all the GCMs improved. The delta method (linear downscaling) was applied to the GCMs' data.

As it is shown in Figure 6.4 (Taylor diagram), after applying the downscaling method, higher correlation values were obtained and the standard deviation of all the GCMs reached very close to the one obtained from the observations. So, it can be concluded that the downscaling method managed to successfully decrease the bias against observations. Onyutha et al., (2016) suggested that the differences in the results of different statistical downscaling methods indicate that the selection of a method should be done based on the aim of climate change impact study. As an example, for rainfall extremes, the more advanced quantile perturbation method (wetQP) which considers changes in both wet-day rainfall intensity and the frequency is more suitable approach rather than Delta.

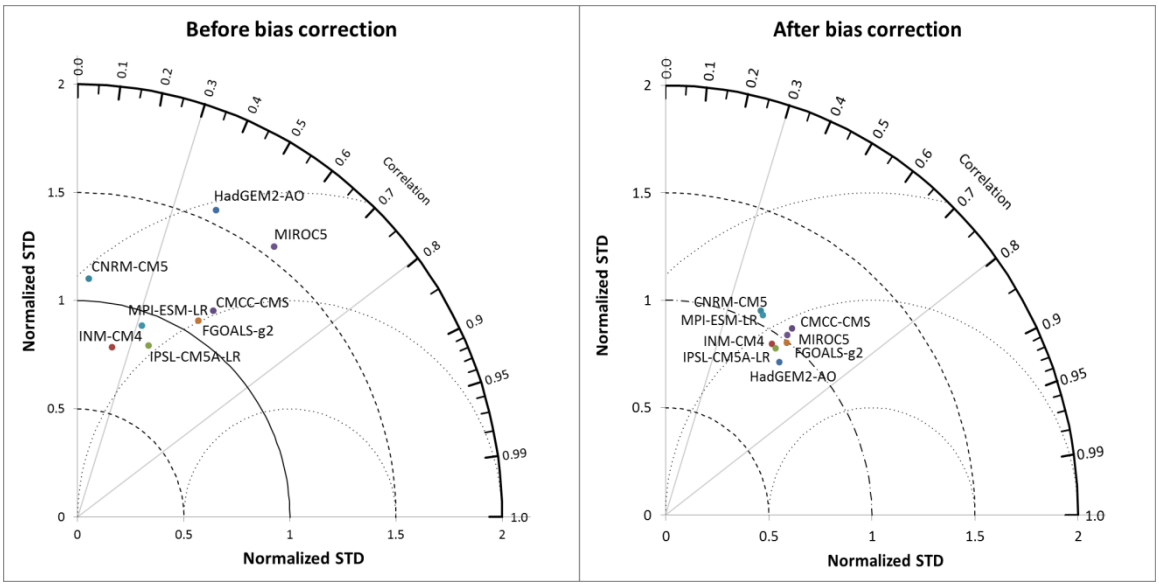

Figure 6.4 Taylor diagram for comparison of raw and downscaled GCMs' data with observed precipitation data for the baseline period

6.2.1 PDF and inverse CDF

Using the Kernel smoothing function estimate in MATLAB, which returns a probability density estimate for a sample in vector x, the following results were obtained. This function works best with continuously distributed samples.

Figures 6.5 and 6.6 show the PDFs of different GCMs used in this study compared with the observation data before and after bias correction respectively. Figures 6.7 and 6.8show the inverse CDF (empirical quantile-quantile plots) of different GCMs, before and after downscaling.

Similar to the results of the Taylor diagram, the PDF and inverse CDF graphs also show that the downscaling method performed well and all the bias corrected GCMs can be used for the study of future climate in the Kabul basin.

In general, these PDFs indicate inter-annual variability (an individual GCM's PDF) as well as probable uncertainty (PDFs of different GCMs) for average annual temperature and precipitation projections (Agarwal et al., 2015).

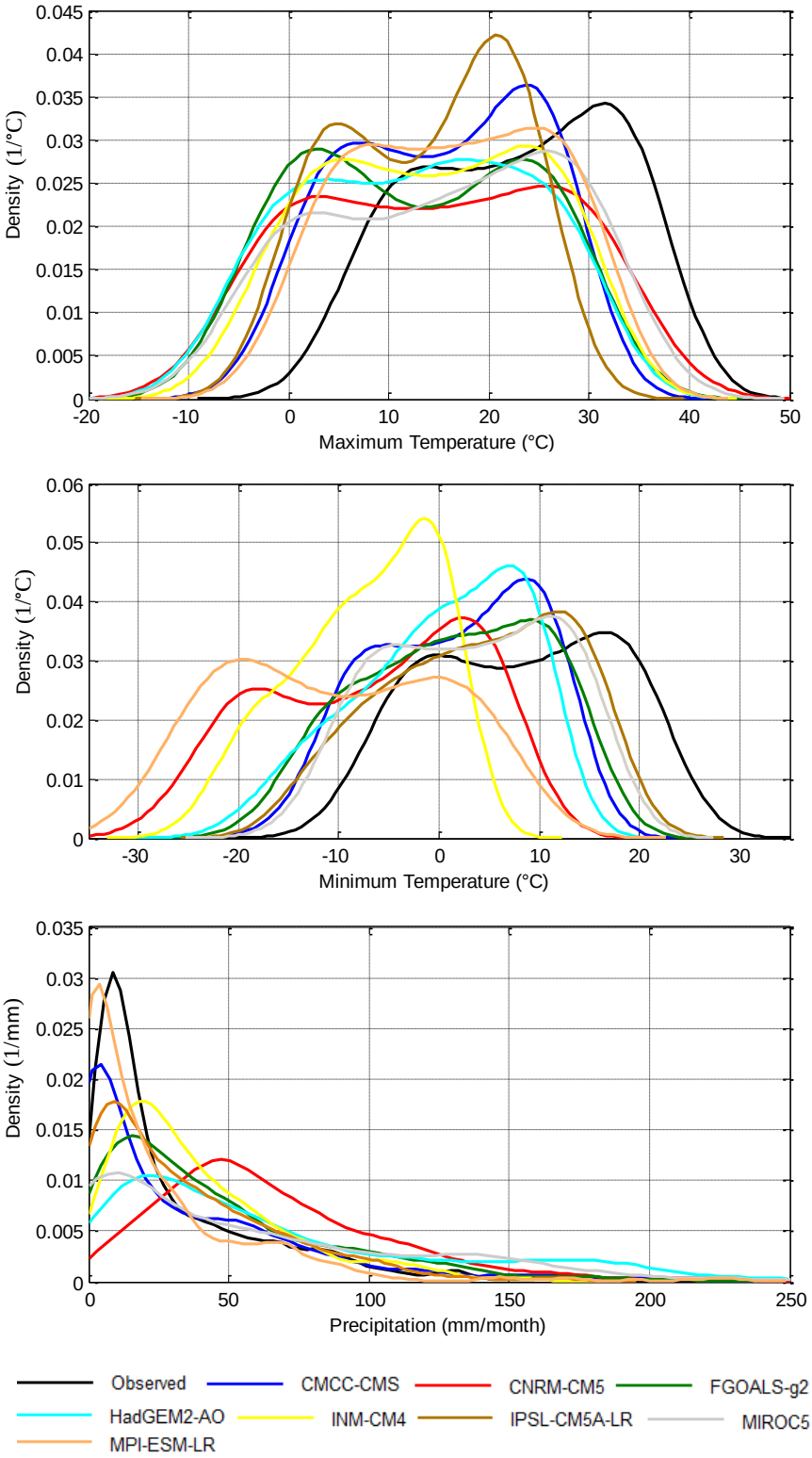

Figure 6.5 Probability density functions of maximum/minimum temperature and precipitation for raw GCMs' data

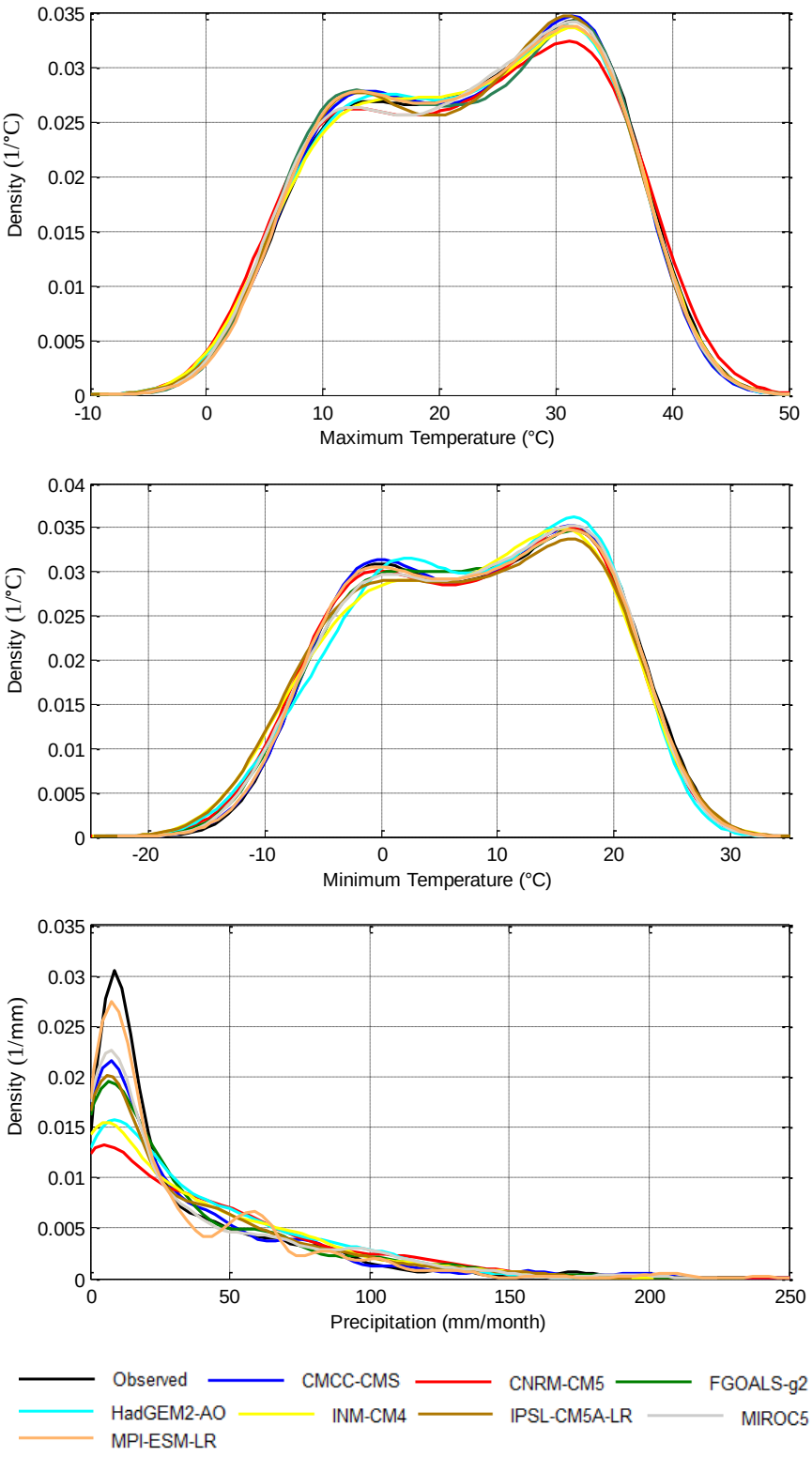

Figure 6.6 Probability density function of maximum/minimum temperature and precipitation for downscaled GCMs' data

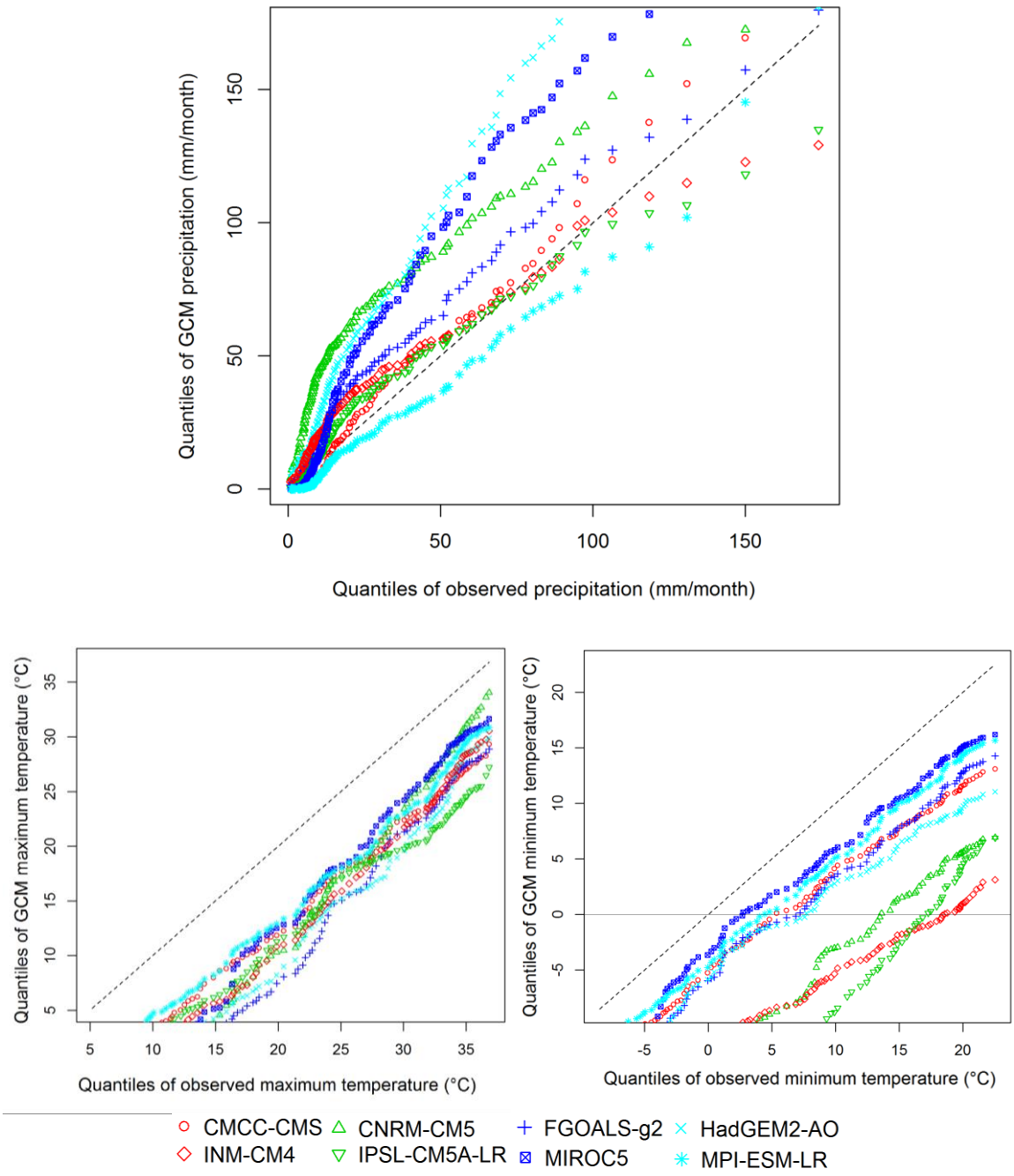

Figure 6.7 Empirical quantile-quantile plots of maximum/minimum temperature and precipitation for raw GCMs' data

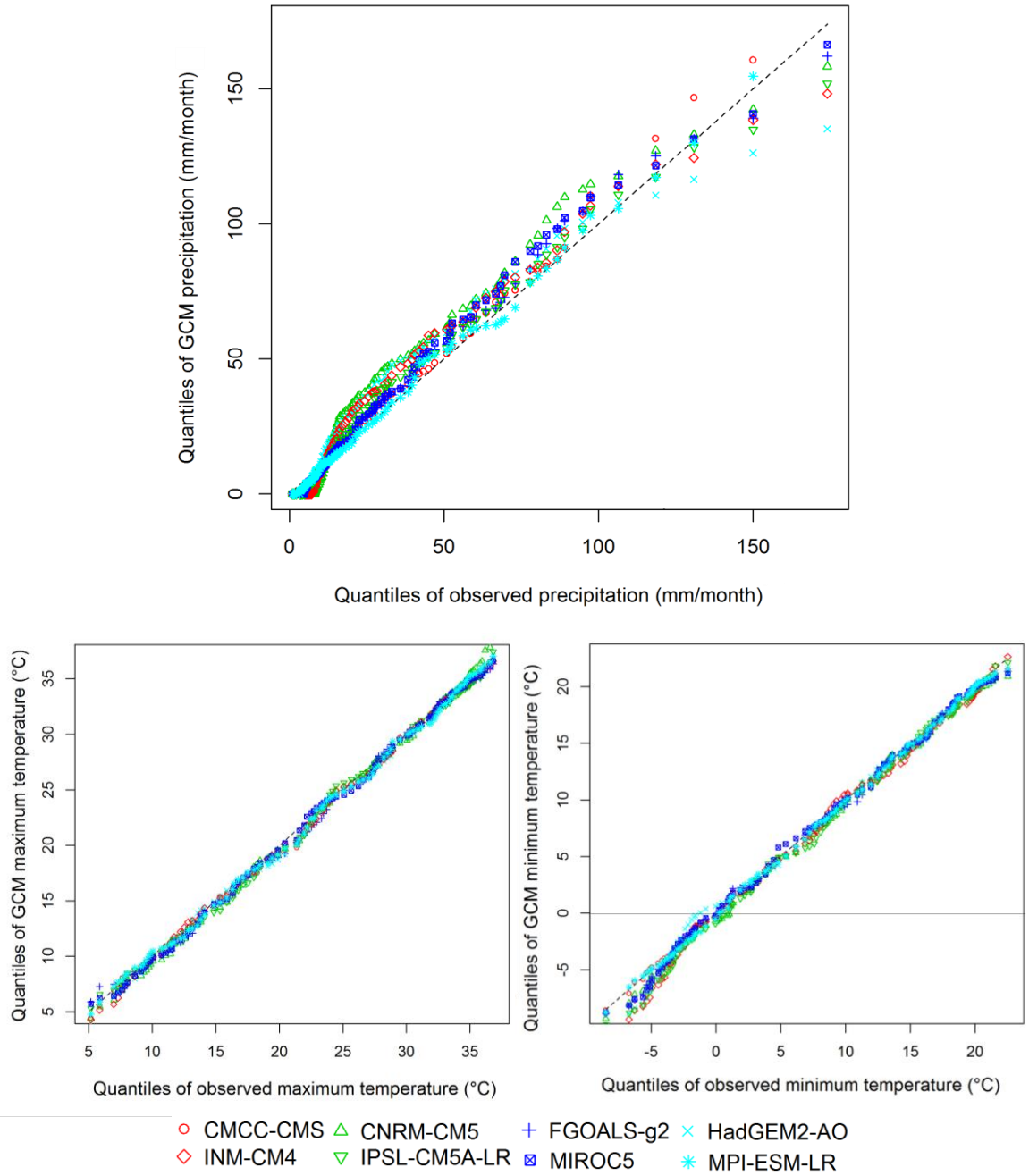

Figure 6.8 Empirical quantile-quantile plots of maximum/minimum temperature and precipitation for downscaled GCMs' data

6.2.2 Ranking of GCMs

Table 6.4 lists the skill scores calculated for all the GCMs used in this study. The results suggest that for precipitation, the best GCM is IPSL-CM5A-LR while it is the last in the ranking of GCMs for temperature. Three best GCMs for each climatic parameter were then highlighted in the table. Table 6.5 lists the skill score as well as standard deviation and correlation for precipitation outputs of all the used GCMs. Using several indicators for ranking of GCMs will be better. The weights given to each of these indicators will result different ranking orders at the end. Here the weight was considered to be equal. This time considering several indicators for precipitation, the best GCM would be MPI-ESM-LR. This GCM was also the best for temperature.

Table 6.4 Skill score (s) of maximum/minimum temperature and precipitation for GCMs' data

GCM Name	Prcp	Rank	Tmax	Rank	Tmin	Rank
CMCC-CMS	0.777	3	0.735	5	0.722	4
CNRM-CM5	0.523	8	0.746	3	0.549	6
FGOALS-g2	0.728	4	0.700	7	0.751	3
HadGEM2-AO	0.629	7	0.713	6	0.664	5
INM-CM4	0.724	5	0.745	4	0.395	8
IPSL-CM5A-LR	0.784	1	0.652	8	0.468	7
MIROC5	0.658	6	0.784	2	0.831	1
MPI-ESM-LR	0.777	2	0.786	1	0.805	2

Table 6.5 Skill score (s) of precipitation for GCMs' data compared with their respective STD and Correlation

GCM Name	s	Rank	STD (Normalized)	Rank	Correlation	Rank
CMCC-CMS	0.777	3	1.15	5	0.558	2
CNRM-CM5	0.523	8	1.10	3	0.050	8
FGOALS-g2	0.728	4	1.07	2	0.531	3
HadGEM2-AO	0.629	7	1.56	8	0.418	4
INM-CM4	0.724	5	0.80	6	0.204	7
IPSL-CM5A-LR	0.784	1	0.86	4	0.390	5
MIROC5	0.658	6	1.56	7	0.596	1
MPI-ESM-LR	0.777	2	0.93	1	0.324	6

6.3 Future projections of temperature and precipitation

The selected GCMs' output (maximum and minimum temperature and precipitation) were downscaled and bias corrected for the stations using the linear downscaling method (same stations as used to evaluate the performance of global/RS datasets mentioned in Chapter 5). The values of all the stations were then averaged over the Kabul basin for each month. The values were also averaged over the seasons, winter and summer. Winter starts in November and ends by April. Summer is also a period of six months, from May to October. First, three periods, Early Future (2020s: 2011-2040), Mid Future (2050s: 2041-2070), and Late Future (2080s: 2071-2100) were selected to be compared with the baseline period of 1971 to 2000. The annual and decadal values of temperature and precipitation over the 21st century were also analyzed.

The boxplots in Figure 6.9 show future projections of maximum and minimum temperature and precipitation. The mean values of future maximum temperature is likely to be between 24.3 to 26.5°C under RCP 4.5 and 24.3 to 28.8°C under RCP 8.5 while minimum temperature will range from 9.7 to 11.5°C under RCP 4.5 and 9.7 to 13.9°C under RCP 8.5. The mean annual values of precipitation under RCP 4.5 range from 366 to 400 mm/yr and from 378 to 412 mm/yr under RCP 8.5. The projections for maximum and minimum temperature during the 2020s are expected to be similar, irrespective of the scenario that may follow. This may be because the differences among the scenar- ios in early-century periods are relatively small (Stott et al., 2006).

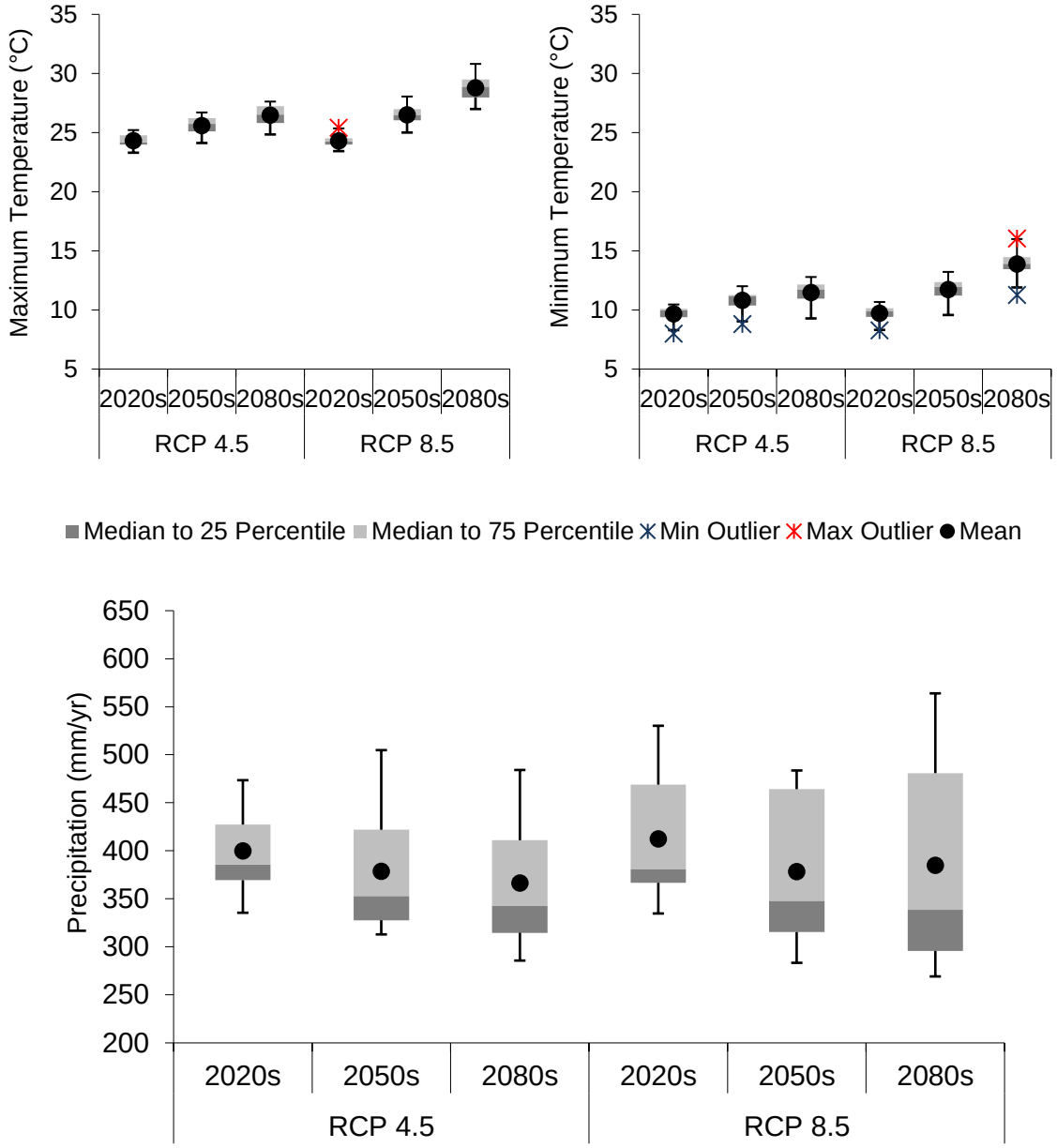

Figure 6.9 Future projections of maximum/minimum temperature and precipitation for the Kabul basin

The seasonal changes are one of the key matters that should be incorporated in climate projection studies and such analysis can also be found in several research (Helfer et al., 2012). The seasonal values of future maximum and minimum temperature and precipitation are shown in Figures 6.10 and 6.11. Maximum and minimum temperature values, under both RCP 4.5 and RCP 8.5 scenarios, show an increasing trend over the 21st century. The median values of precipitation show a decreasing trend of precipitation till the middle of the century. However, this trend changes under RCP 4.5, under which an increased amount of precipitation for the 2080s is predicted.

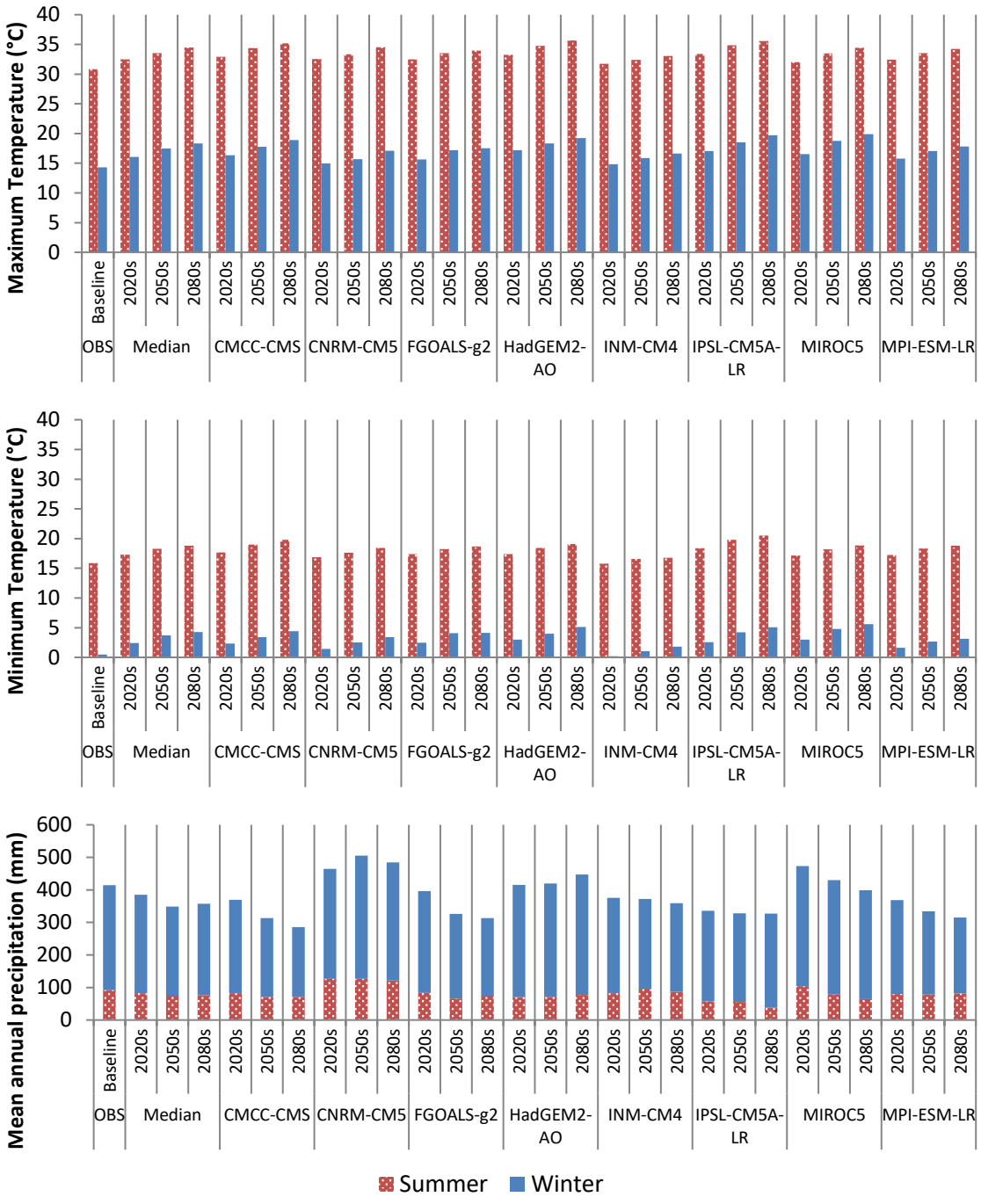

Figure 6.10 Average seasonal maximum/minimum temperature and precipitation for the Kabul basin under RCP 4.5

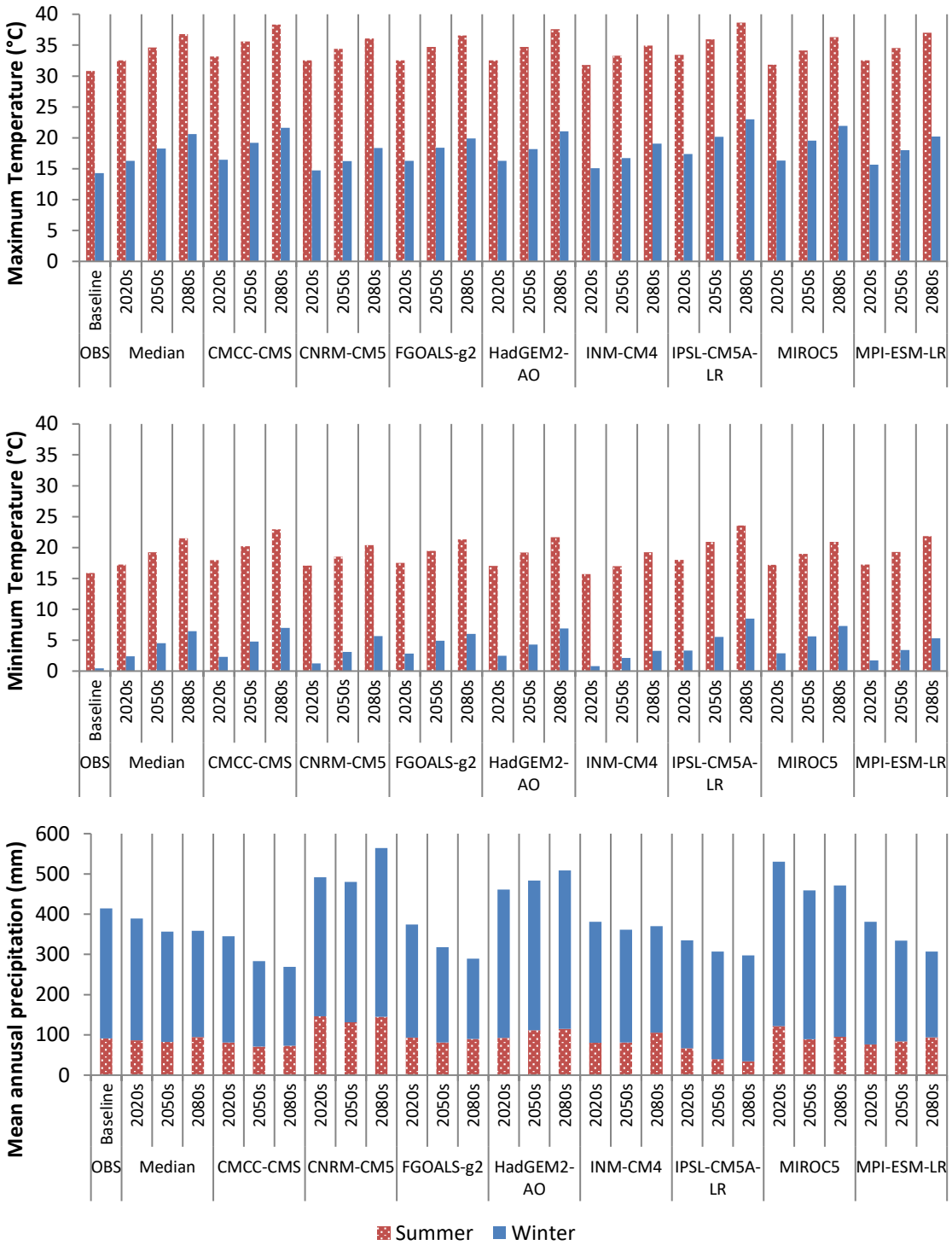

Figure 6.11 Average seasonal maximum/minimum temperature and precipitation for the Kabul basin under RCP 8.5

The boxplots in Figure 6.12 show projections of maximum temperature for the future. The annual mean values of maximum temperature under RCP 4.5 for all the decades over the 21st century range from 23.8 to 26.6°C while under RCP 8.5, the range of values is between 23.7 and 29.6°C. In general, the maximum temperature values show a steadily increasing trend towards the end of the century under both RCP scenarios.

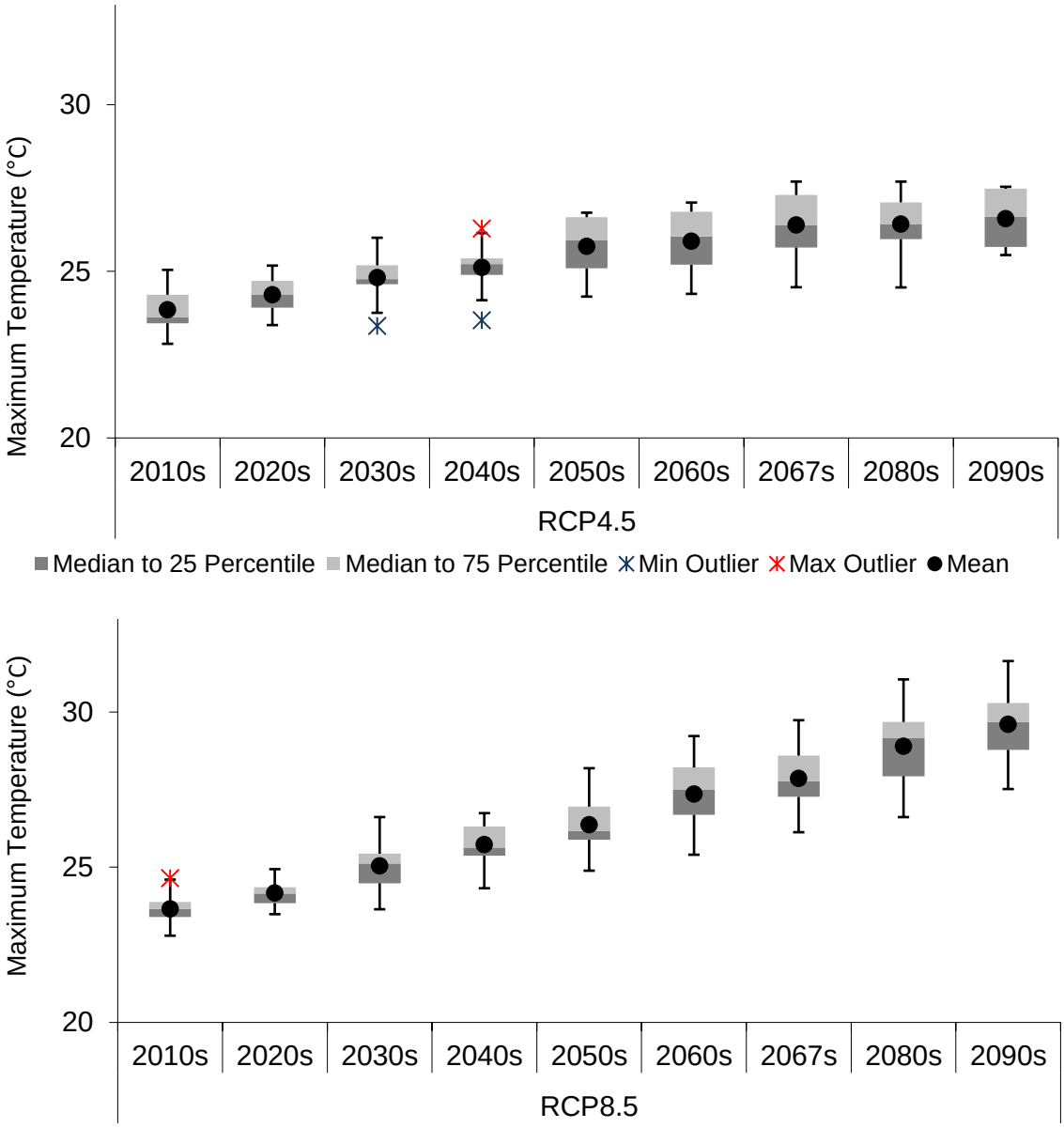

Figure 6.12 Future projections of maximum temperature for the Kabul basin

The boxplots in Figure 6.13 show projections of minimum temperature in the study area in the future. The annual mean values of minimum temperature under RCP 4.5 for all the decades over the 21st century range from 9.3 to 11.6°C while under RCP 8.5, the range of values is between 9.1 and 14.6°C. In general, the minimum temperature values show a steadily increasing trend towards the end of the century under both RCP scenarios.

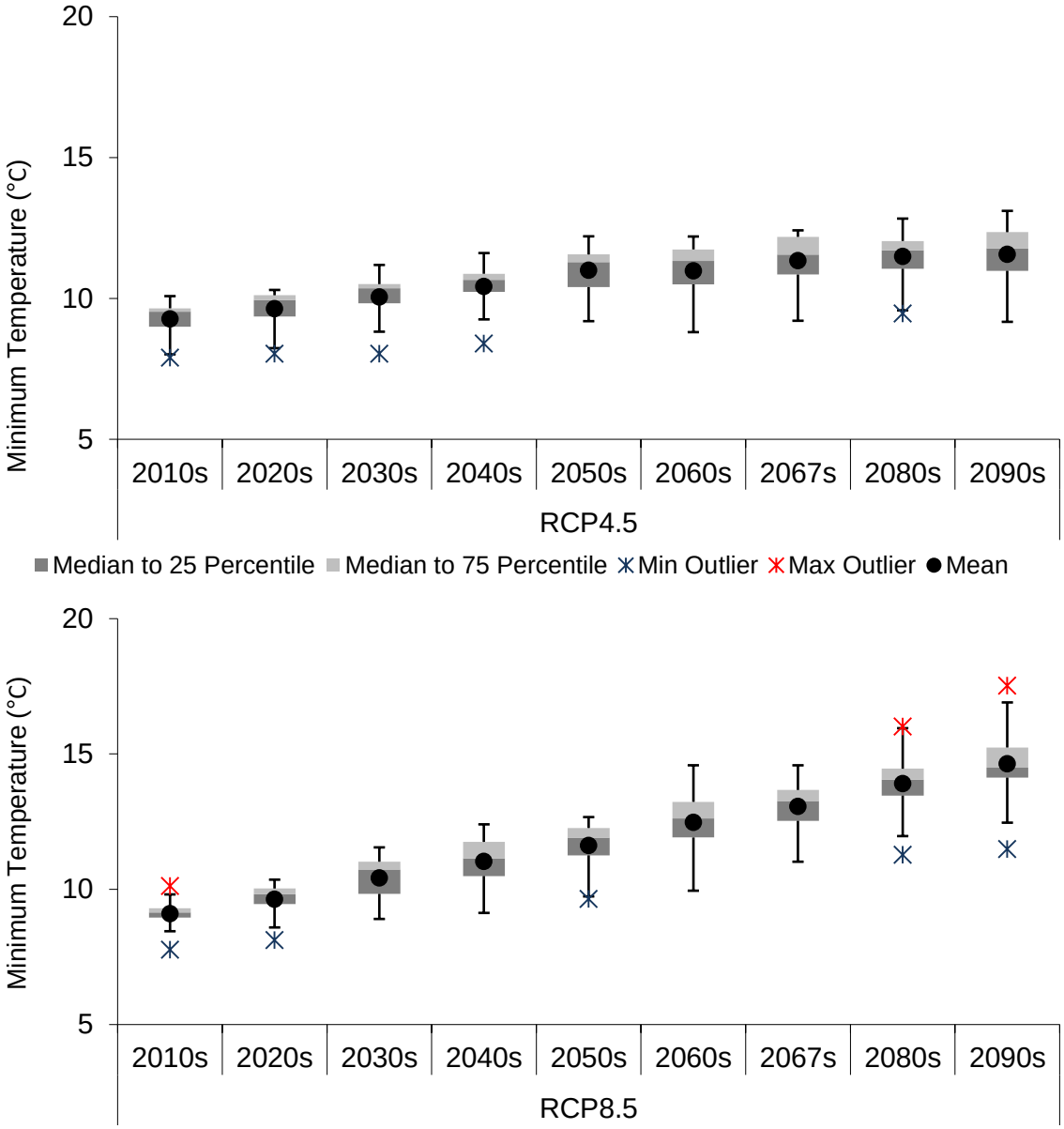

Figure 6.13 Future projections of minimum temperature for the Kabul basin

The boxplots in Figure 6.14 show projections of precipitation values for the future. The annual mean values of precipitation under RCP 4.5, for all the decades over the 21st century, range from 293 to 346 mm/yr, while under RCP 8.5 the range of values is between 298 and 362 mm/yr. In general, precipitation values show a slightly decreasing trend towards the end of the century under both RCP scenarios.

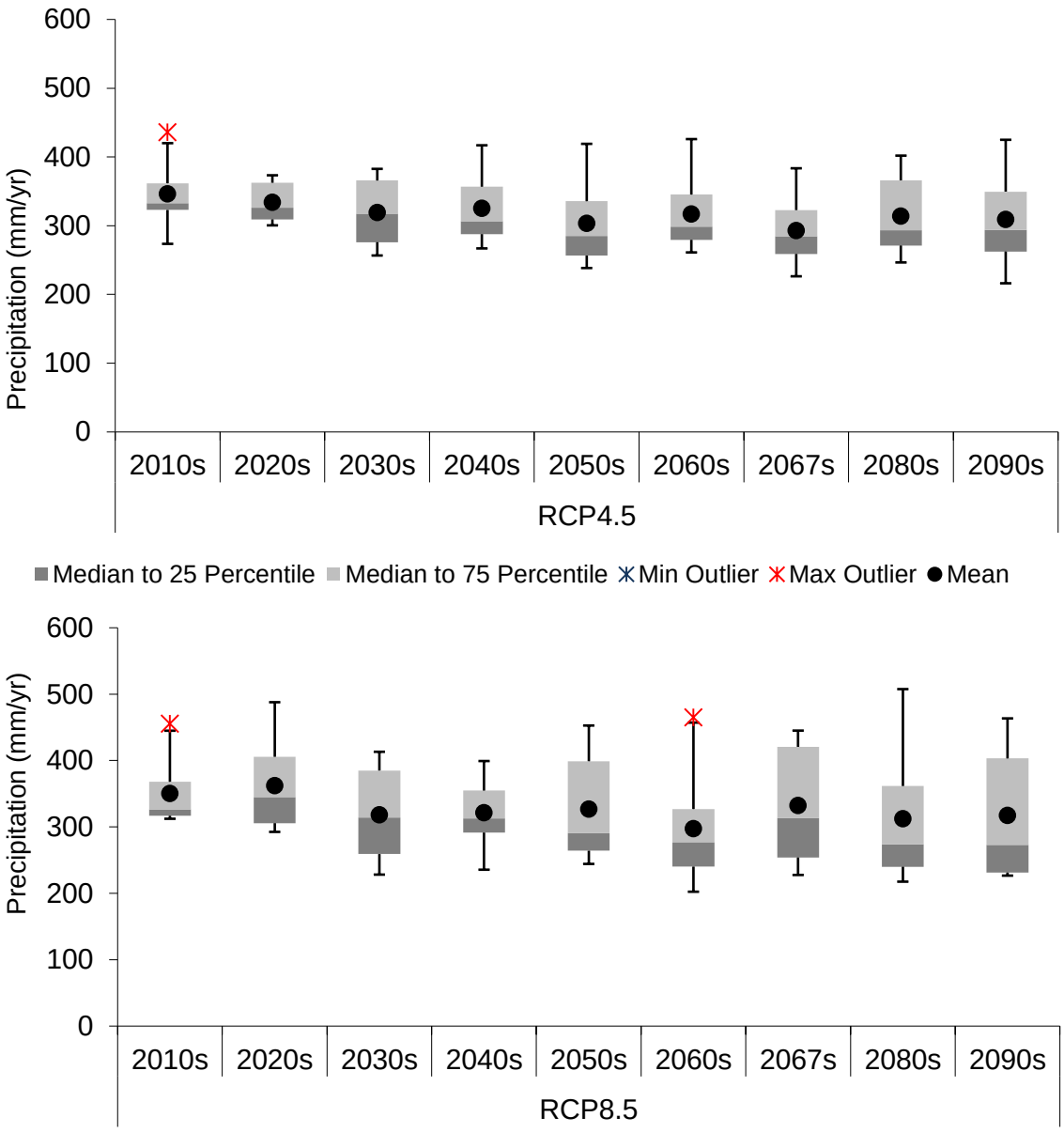

Figure 6.14 Future projections of precipitation for the Kabul basin

Figure 6.15 shows the uncertainty in future annual time series of maximum and minimum temperature and precipitation for the Kabul basin. It is difficult to identify a trend for precipitation values under both RCPs 4.5 and 8.5; however, the increasing trend of future maximum and minimum temperature is very clear.

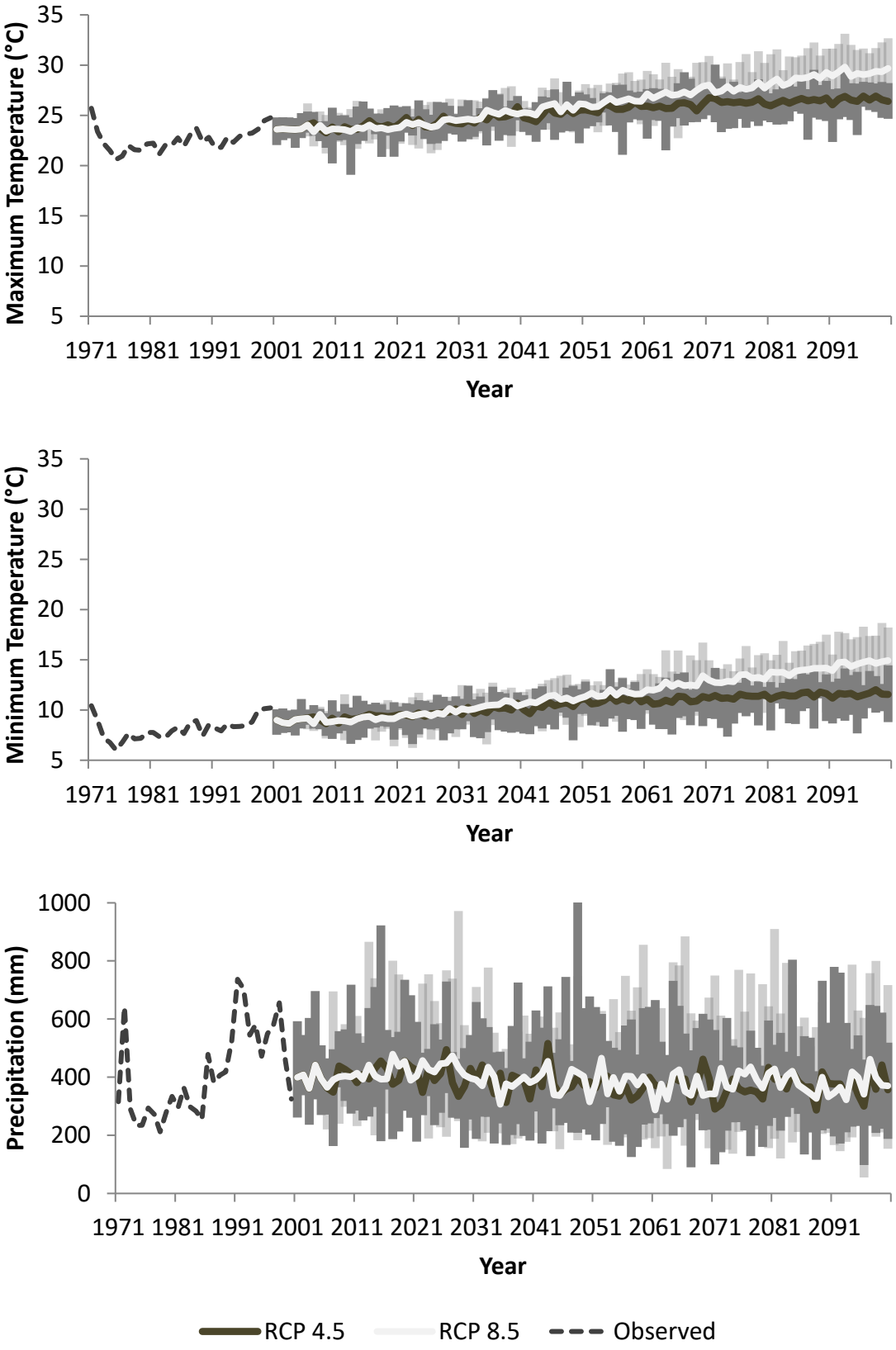

Figure 6.15 Future projections of annual maximum/minimum temperature and precipitation for the Kabul basin

6.4 Changes in temperature and precipitation in the future

The downscaled GCMs were compared with the baseline observations for each month and the changes were calculated for the whole Kabul basin. These results are presented in Tables 6.6 to 6.8.

Figure 6.16 shows the median of all 8 downscaled GCMs. The results suggest an increasing trend in maximum and minimum temperature in the future, as compared to the baseline. The increases for maximum temperature range from +1.7°C to +4.1°C under RCP 4.5 and +1.7°C to +6.3°C under RCP 8.5. The increases for minimum temperature range from +1.5°C to +3.8°C under RCP 4.5 and +1.4°C to +6.0°C under RCP 8.5. The projections for precipitation mainly show a decreasing trend under both RCPs, ranging from -19% to -6% under RCP 4.5 and -18% to 3% under RCP 8.5. Negative precipitation trends in parts of western Himalaya have been reported by others, like Singh and Sen Roy (2002) for Beas basin and Kumar and Jain (2010) for Qazigund and Kukarnag which comes in Kashmir.

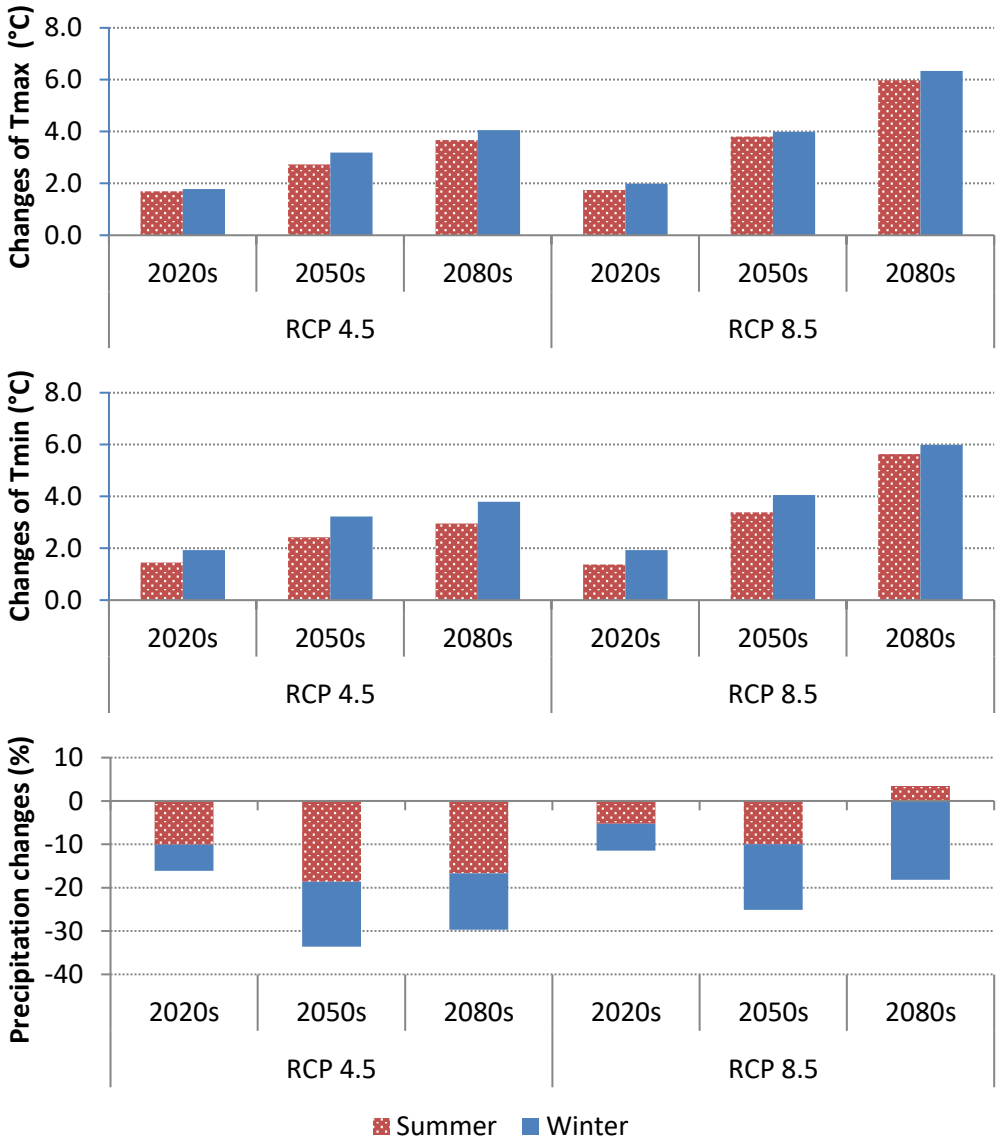

Figure 6.16 Median of seasonal changes from all downscaled GCMs' data, compared to the baseline

Table 6.6 Monthly changes in future maximum temperature (°C) for the Kabul basin using 8 GCMs under 2 RCP scenarios

	CMCC-CMS						CNRM-CM5					
	RCP 4.5			RCP 8.5			RCP 4.5			RCP 8.5		
Month	2020s	2050s	2080s	2020s	2050s	2080s	2020s	2050s	2080s	2020s	2050s	2080s
Jan	1	3	4	1	4	6	1	2	3	1	2	4
Feb	2	4	5	2	5	8	1	2	4	0	2	4
Mar	3	4	5	2	6	8	1	2	3	1	3	5
Apr	2	3	4	2	5	7	2	3	4	1	4	5
May	1	3	4	2	4	7	3	4	5	3	5	7
Jun	2	3	4	2	5	7	3	3	3	3	4	5
Jul	2	3	3	2	4	7	0	1	4	1	3	4
Aug	1	4	4	2	4	8	0	2	3	1	3	4
Sep	1	3	3	2	4	7	1	2	3	1	3	6
Oct	2	3	4	1	4	7	1	1	2	0	3	5
Nov	1	2	3	1	3	6	1	2	3	1	3	5
Dec	2	3	5	2	5	8	2	2	4	3	2	6
Winter	2	3	4	2	5	7	1	2	4	1	3	5
Summer	2	3	4	2	4	7	2	2	3	2	3	5

	FGOALS-g2						HadGEM2-AO					
	RCP 4.5			RCP 8.5			RCP 4.5			RCP 8.5		
Month	2020s	2050s	2080s	2020s	2050s	2080s	2020s	2050s	2080s	2020s	2050s	2080s
Jan	1	3	2	1	3	4	4	5	6	2	4	7
Feb	2	3	4	2	5	7	4	5	7	3	5	8
Mar	1	4	4	3	6	7	3	4	5	2	4	6
Apr	1	2	4	2	4	6	2	3	3	1	3	6
May	1	2	2	0	3	5	2	3	4	2	3	6
Jun	2	3	4	2	4	6	3	5	6	2	4	8
Jul	1	2	3	2	4	5	2	4	5	2	4	7
Aug	1	2	3	2	3	5	1	3	4	1	3	5
Sep	2	3	3	2	4	6	2	3	4	1	3	6
Oct	1	2	3	2	4	5	3	4	5	1	4	6
Nov	2	3	2	1	4	5	2	4	4	2	3	6
Dec	1	2	2	2	3	5	3	4	5	3	4	7
Winter	1	3	3	2	4	6	3	4	5	2	4	7
Summer	1	2	3	1	4	5	2	4	5	1	4	6

	INM-CM4						IPSL-CM5A-LR					
	RCP 4.5			RCP 8.5			RCP 4.5			RCP 8.5		
Month	2020s	2050s	2080s	2020s	2050s	2080s	2020s	2050s	2080s	2020s	2050s	2080s
Jan	0	1	1	0	2	5	3	3	5	3	6	8
Feb	-1	1	3	0	2	5	2	4	6	4	6	9
Mar	2	2	3	1	4	5	3	4	5	3	6	9
Apr	1	2	3	2	3	4	2	4	3	2	5	7
May	1	2	2	1	3	4	1	4	4	2	4	7
Jun	2	2	2	1	3	5	3	4	5	3	5	8
Jul	1	1	2	1	3	4	2	3	4	2	4	8
Aug	1	2	2	1	2	4	2	4	4	2	4	7
Sep	0	1	2	0	2	4	3	4	5	3	5	8
Oct	1	2	2	1	2	4	2	3	4	2	5	8
Nov	1	1	1	0	1	4	2	4	5	2	4	8
Dec	1	2	3	1	2	5	3	4	6	2	6	9
Winter	0	1	2	1	2	5	2	4	5	3	5	8
Summer	1	2	2	1	2	4	2	4	4	2	5	7

	MIROC5						MPI-ESM-LR					
	RCP 4.5			RCP 8.5			RCP 4.5			RCP 8.5		
Month	2020s	2050s	2080s	2020s	2050s	2080s	2020s	2050s	2080s	2020s	2050s	2080s
Jan	2	4	5	2	5	9	2	4	4	2	4	6
Feb	2	5	7	2	7	10	2	4	4	2	4	6
Mar	4	7	7	3	7	9	2	3	4	1	3	6
Apr	2	4	4	1	4	6	1	2	3	1	3	5
May	1	3	4	1	4	5	1	2	3	1	3	6
Jun	0	2	3	0	3	5	1	3	3	1	4	6
Jul	1	3	4	1	3	5	2	3	3	2	4	6
Aug	1	2	3	1	3	5	1	2	3	2	3	5
Sep	1	2	3	1	3	5	1	2	3	2	3	6
Oct	1	3	3	1	3	5	1	2	3	1	3	6
Nov	1	2	3	1	3	4	1	2	3	1	4	6
Dec	1	3	4	1	4	7	1	2	3	0	4	6
Winter	2	4	5	2	5	7	1	3	3	1	4	6
Summer	1	2	3	1	3	5	1	2	3	1	3	6

Table 6.7 Monthly changes in future minimum temperature (°C) for the Kabul basin using 8 GCMs under 2 RCP scenarios

	CMCC-CMS						CNRM-CM5					
	RCP 4.5			RCP 8.5			RCP 4.5			RCP 8.5		
Month	2020s	2050s	2080s	2020s	2050s	2080s	2020s	2050s	2080s	2020s	2050s	2080s
Jan	1	3	4	2	4	6	3	3	4	2	4	6
Feb	2	3	4	2	5	7	1	2	3	0	3	5
Mar	2	3	4	2	4	6	1	3	4	2	3	6
Apr	1	2	3	2	4	6	2	3	4	1	4	6
May	1	3	4	2	4	6	2	3	4	2	4	6
Jun	1	3	4	2	4	6	1	2	3	2	3	4
Jul	2	3	4	2	4	7	1	2	3	1	3	4
Aug	1	3	3	1	4	7	1	2	3	1	3	4
Sep	1	3	3	2	4	7	1	2	2	1	3	5
Oct	2	3	3	2	3	7	1	2	3	1	3	5
Nov	1	2	3	1	3	6	2	3	3	1	3	6
Dec	2	3	4	2	4	7	2	3	4	3	3	7
Winter	2	3	4	2	4	6	2	3	4	2	3	6
Summer	1	3	4	2	4	7	1	2	3	1	3	5

	FGOALS-g2						HadGEM2-AO					
	RCP 4.5			RCP 8.5			RCP 4.5			RCP 8.5		
Month	2020s	2050s	2080s	2020s	2050s	2080s	2020s	2050s	2080s	2020s	2050s	2080s
Jan	2	5	4	2	5	6	4	6	7	3	5	9
Feb	3	5	5	3	6	7	4	5	8	4	6	9
Mar	2	3	3	3	4	5	3	3	5	2	4	6
Apr	1	1	2	1	2	4	2	3	3	1	3	6
May	1	2	2	1	3	4	1	2	3	1	3	5
Jun	1	2	3	2	3	5	1	2	3	1	3	5
Jul	2	2	3	2	3	5	2	3	3	1	3	6
Aug	1	2	3	1	3	6	2	3	4	1	4	6
Sep	2	3	3	2	4	6	2	3	4	2	4	7
Oct	1	2	3	2	3	5	2	3	3	1	4	6
Nov	1	2	2	1	3	4	1	1	2	1	2	4
Dec	2	4	3	2	4	5	2	3	3	2	3	6
Winter	2	3	3	2	4	5	3	4	5	2	4	7
Summer	1	2	3	1	3	5	2	3	3	1	3	6

	INM-CM4						IPSL-CM5A-LR					
	RCP 4.5			RCP 8.5			RCP 4.5			RCP 8.5		
Month	2020s	2050s	2080s	2020s	2050s	2080s	2020s	2050s	2080s	2020s	2050s	2080s
Jan	0	1	2	0	3	5	2	3	4	3	6	7
Feb	-1	2	2	0	2	2	1	2	4	3	4	8
Mar	1	0	0	0	1	2	2	3	4	3	5	9
Apr	0	0	0	0	1	1	3	5	5	3	5	8
May	0	0	0	0	0	2	1	3	2	1	3	5
Jun	0	1	2	0	2	3	2	4	5	1	5	7
Jul	0	1	2	1	2	4	2	4	5	2	5	8
Aug	1	1	1	0	2	4	3	5	6	3	6	9
Sep	1	1	1	0	2	5	3	5	6	2	6	8
Oct	-1	1	0	0	0	3	3	4	5	3	6	9
Nov	-1	1	1	0	1	2	2	3	5	2	5	7
Dec	1	1	3	2	4	6	2	4	4	3	5	8
Winter	0	1	1	0	2	3	2	4	4	3	5	8
Summer	0	1	1	0	1	4	2	4	5	2	5	8

	MIROC5						MPI-ESM-LR					
	RCP 4.5			RCP 8.5			RCP 4.5			RCP 8.5		
Month	2020s	2050s	2080s	2020s	2050s	2080s	2020s	2050s	2080s	2020s	2050s	2080s
Jan	2	5	6	2	6	8	2	3	3	2	3	5
Feb	3	6	8	3	7	10	2	3	3	2	4	5
Mar	4	6	7	3	7	8	1	2	3	1	2	4
Apr	2	3	4	2	4	5	1	2	2	1	3	4
May	1	3	3	2	3	5	1	2	2	0	3	5
Jun	1	2	3	1	2	4	1	2	3	1	3	6
Jul	1	2	3	1	3	5	2	3	3	2	4	6
Aug	1	2	3	1	3	5	1	2	3	1	3	6
Sep	2	2	3	1	3	5	1	2	3	2	4	6
Oct	2	3	3	2	3	6	1	2	2	1	3	6
Nov	1	2	2	1	2	3	1	2	3	1	3	6
Dec	1	2	3	1	3	4	1	2	2	1	3	5
Winter	2	4	5	2	5	6	1	2	3	1	3	5
Summer	1	2	3	1	3	5	1	2	3	1	3	6

Table 6.8 Monthly changes in future precipitation (%) for the Kabul basin using 8 GCMs under 2 RCP scenarios

	CMCC-CMS						CNRM-CM5					
	RCP 4.5			RCP 8.5			RCP 4.5			RCP 8.5		
Month	2020s	2050s	2080s	2020s	2050s	2080s	2020s	2050s	2080s	2020s	2050s	2080s
Jan	12	5	3	31	-6	-13	60	-4	17	49	28	42
Feb	9	-3	-11	-4	-9	-32	-16	15	-21	-11	-3	-11
Mar	-23	-54	-49	-28	-46	-37	-6	22	12	15	-9	15
Apr	-19	-13	-44	-32	-51	-69	-4	1	28	-15	-9	39
May	6	-18	-49	-12	-25	-45	-15	-11	16	-2	51	35
Jun	-5	-20	-2	-12	-17	-20	-31	-25	24	-28	-35	11
Jul	27	0	69	17	38	14	68	23	-55	14	41	3
Aug	40	39	3	7	19	-4	15	-39	-52	35	-36	-19
Sep	18	2	-3	0	11	36	30	57	24	71	57	29
Oct	-34	-24	15	67	-39	16	9	54	22	84	-9	69
Nov	15	-26	-20	-6	-34	5	26	30	18	-11	39	73
Dec	2	-13	-32	-11	-16	-21	-24	-9	-23	-13	22	22
Winter	-1	-17	-26	-8	-27	-28	6	9	5	2	11	30
Summer	9	-3	6	11	-2	-1	13	10	-3	29	12	21

	FGOALS-g2						HadGEM2-AO					
	RCP 4.5			RCP 8.5			RCP 4.5			RCP 8.5		
Month	2020s	2050s	2080s	2020s	2050s	2080s	2020s	2050s	2080s	2020s	2050s	2080s
Jan	-27	-33	-38	-3	-44	-65	5	33	31	37	19	56
Feb	4	-27	-35	-2	-30	-43	8	22	28	19	34	36
Mar	8	-13	-28	-19	-21	-23	7	13	19	12	16	26
Apr	-6	-25	-39	-26	-38	-49	29	-2	10	33	10	11
May	-25	-67	-38	18	-34	-61	-64	-75	-60	-51	-24	-62
Jun	-10	-37	-41	0	2	-34	-38	-60	-52	-24	21	-4
Jul	-12	-10	-9	-41	-12	96	17	62	89	55	91	221
Aug	-3	-36	-23	-44	0	29	70	127	66	79	133	233
Sep	8	17	-7	25	7	21	-28	-35	-33	4	-22	-40
Oct	15	26	53	15	-2	60	-49	-44	-39	-19	-51	-18
Nov	-41	-11	9	-6	-30	-39	-32	-57	-1	-31	-15	-25
Dec	2	-8	7	-14	6	-25	-26	2	-27	-28	-1	4
Winter	-10	-20	-21	-12	-26	-41	-1	2	10	7	11	18
Summer	-5	-18	-11	-5	-7	18	-15	-4	-5	7	25	55

	INM-CM4						IPSL-CM5A-LR					
	RCP 4.5			RCP 8.5			RCP 4.5			RCP 8.5		
Month	2020s	2050s	2080s	2020s	2050s	2080s	2020s	2050s	2080s	2020s	2050s	2080s
Jan	23	20	11	12	9	-6	18	7	21	-11	18	-18
Feb	-1	-6	-13	3	-11	-22	-24	-15	-22	-17	-18	-20
Mar	-2	-21	-18	-9	-19	-13	-15	-13	-7	-5	-6	-4
Apr	-19	-19	-22	-15	-21	-30	-10	-15	-6	-12	-20	-16
May	-39	-18	-37	-25	-26	-30	-45	-53	-56	-20	-55	-72
Jun	-38	-36	-13	-40	-32	-41	-43	-65	-73	-36	-55	-72
Jul	-16	-3	-27	-44	-17	42	-53	-63	-76	-46	-62	-82
Aug	0	-54	-7	-3	-17	27	-35	-31	-12	-3	-18	-43
Sep	3	11	-13	-19	-28	2	18	-2	-30	25	-41	-29
Oct	-31	33	-8	-18	-23	33	-33	48	-74	-53	-76	-41
Nov	-36	28	-2	0	32	-14	4	-61	-18	-40	-31	-31
Dec	14	-21	17	28	18	39	-16	0	-11	-35	-43	-37
Winter	-4	-3	-4	3	1	-8	-7	-16	-7	-20	-17	-21
Summer	-20	-11	-18	-25	-24	6	-32	-28	-53	-22	-51	-57

	MIROC5						MPI-ESM-LR					
	RCP 4.5			RCP 8.5			RCP 4.5			RCP 8.5		
Month	2020s	2050s	2080s	2020s	2050s	2080s	2020s	2050s	2080s	2020s	2050s	2080s
Jan	6	-15	-4	18	24	22	-27	-35	-27	0	-33	-45
Feb	25	45	34	20	27	48	-1	-19	-28	-12	-3	-31
Mar	14	32	27	21	42	32	-15	-16	-23	-20	-24	-24
Apr	-11	-23	-30	24	-30	-15	-5	-21	-34	-1	-29	-40
May	16	-23	-53	44	-21	-50	-22	-45	-48	-26	-31	-49
Jun	65	-54	-51	20	-10	-16	17	30	20	2	17	49
Jul	15	-1	-4	11	3	26	-26	9	12	-10	-21	36
Aug	29	47	31	26	35	79	17	-18	40	0	53	62
Sep	19	23	10	35	21	61	17	2	21	-3	23	32
Oct	46	31	0	189	92	123	-13	62	18	23	6	52
Nov	92	6	-3	88	48	48	16	8	-2	2	-20	-5
Dec	7	-20	-27	21	-15	-44	-23	-34	-36	35	-27	-60
Winter	22	4	-1	32	16	15	-9	-20	-25	1	-23	-34
Summer	32	4	-11	54	20	37	-2	7	10	-2	8	30

The Radar plots in Figure 6.17 show the projections of maximum temperature in the future for winter and summer seasons separately under RCP 4.5 and RCP 8.5. The results show that maximum temperature is likely to increase from one decade to the next. However, although during the first few decades, the results under RCP 4.5 and RCP 8.5 are very close, by the end of the century, the results under RCP 8.5 predict much higher values of temperature as compared to those under RCP 4.5.

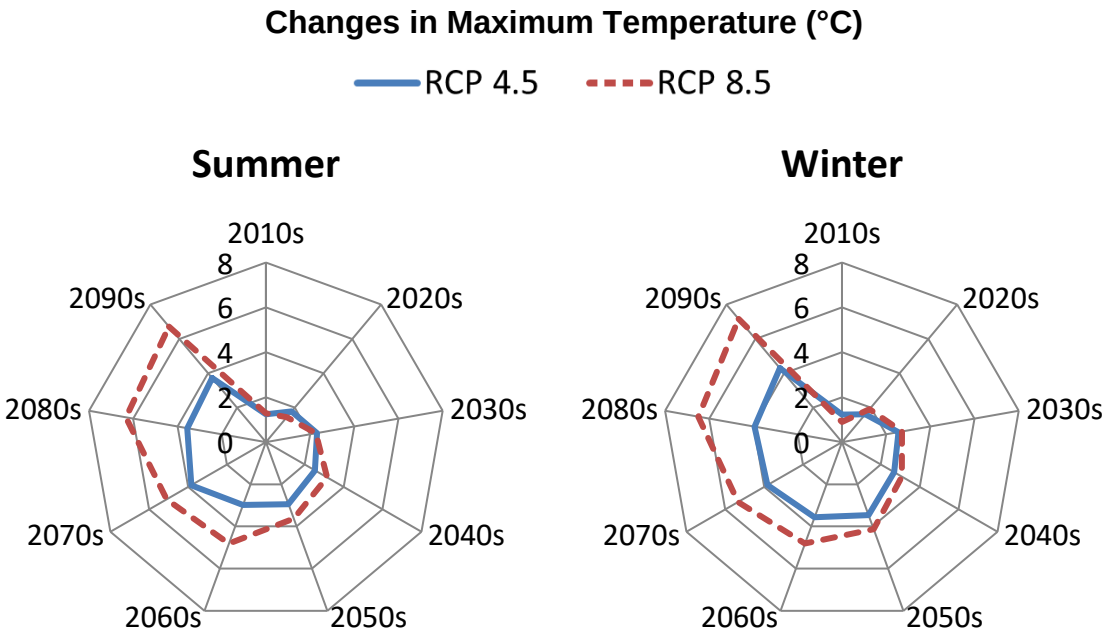

Figure 6.17 Future decadal changes in maximum temperature over the Kabul basin

The Radar plots in Figure 6.18 show the projections of minimum temperature in the future for winter and summer seasons separately under RCP 4.5 and RCP 8.5. The results show that minimum temperature is likely to increase from one decade to the next. However, although during the first few decades, the results obtained under RCP 4.5 and RCP 8.5 are very close, by the end of the century, the results under RCP 8.5 have much higher values of temperature as compared to those under RCP 4.5—a trend very similar to the results of changes in maximum temperature.

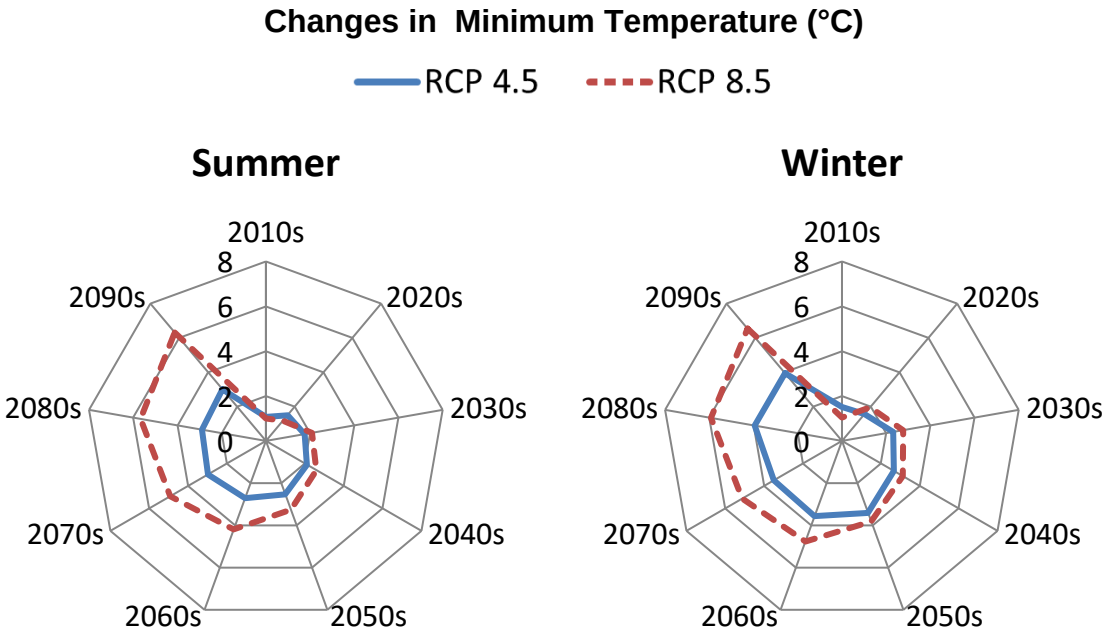

Figure 6.18 Future decadal changes in minimum temperature over the Kabul basin

The Radar plots in Figure 6.19 show the projections of precipitation values in the future for winter and summer seasons separately under RCP 4.5 and RCP 8.5. The results show that the annual mean values of precipitation under RCP 4.5 are likely to decrease in future decades, especially during summer. The results under RCP 8.5 also suggest the same decreasing trend, but this is mainly for the winter season while during summer, precipitation might increase.

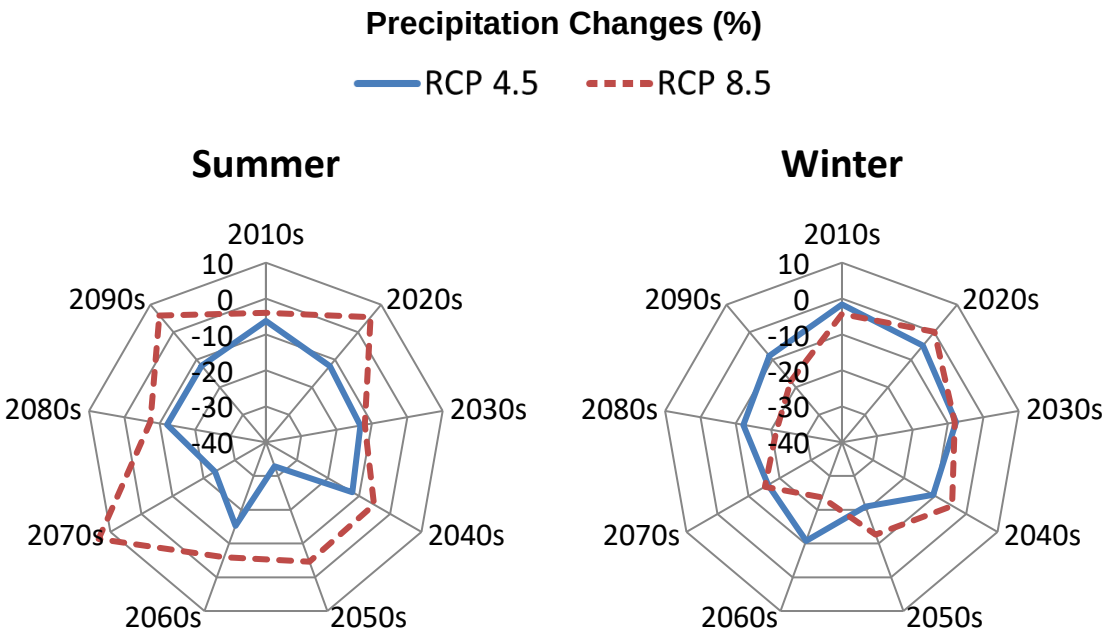

Figure 6.19 Future decadal changes in annual precipitation over the Kabul basin

To summarize, Table 6.9 lists the changes in precipitation and temperature for each future decade under RCP 4.5 and RCP 8.5, separated seasonally (winter and summer).

Table 6.9 Monthly changes in future maximum/minimum temperature and precipitation for the Kabul basin based on the median results of 8 GCMs

	Prcp (%)				Tmax (°C)				Tmin (°C)			
	Summer		Winter		Summer		Winter		Summer		Winter	
	RCP 4.5	RCP 8.5	RCP 4.5	RCP 8.5	RCP 4.5	RCP 8.5	RCP 4.5	RCP 8.5	RCP 4.5	RCP 8.5	RCP 4.5	RCP 8.5
2010s	-6	-4	-2	-4	1	1	1	1	1	1	2	1
2020s	-12	5	-5	0	2	1	2	2	2	1	2	2
2030s	-13	-12	-8	-8	2	2	3	3	2	2	2	3
2040s	-12	-5	-11	-5	3	3	3	3	2	3	3	3
2050s	-33	-5	-21	-13	3	4	3	4	3	3	3	4
2060s	-15	-6	-11	-24	3	5	4	5	3	4	4	5
2070s	-24	14	-16	-15	4	5	4	5	3	5	4	5
2080s	-12	-7	-12	-21	4	6	4	6	3	6	4	6
2090s	-12	6	-9	-18	4	7	4	7	3	6	4	7

6.5 Analysis of shifts in monthly temperature and precipitation in the future

Based on the baseline observations (of 1971 to 2000), most of the precipitation occurs during winter. March and April are the first and second wettest months. The warmest month of the year is July.

All GCM ensembles showed almost the same trend as the baseline. However, a slight decrease in precipitation is predicted for winter while there is likely to be an increase in precipitation during summer under both RCPs. These results are shown in Figure 6.20.

6.6 Spatial distribution of temperature and precipitation changes in the future

Figures 6.21 to 6.23 illustrate the spatial distribution of future maximum and minimum temperature and precipitation changes over the Kabul basin. The results of maximum and minimum temperature show a uniform increase all over the basin during the next century. Precipitation is likely to increase in the near future while it is predicted to decrease by the end of the century, especially in the central areas of the basin.

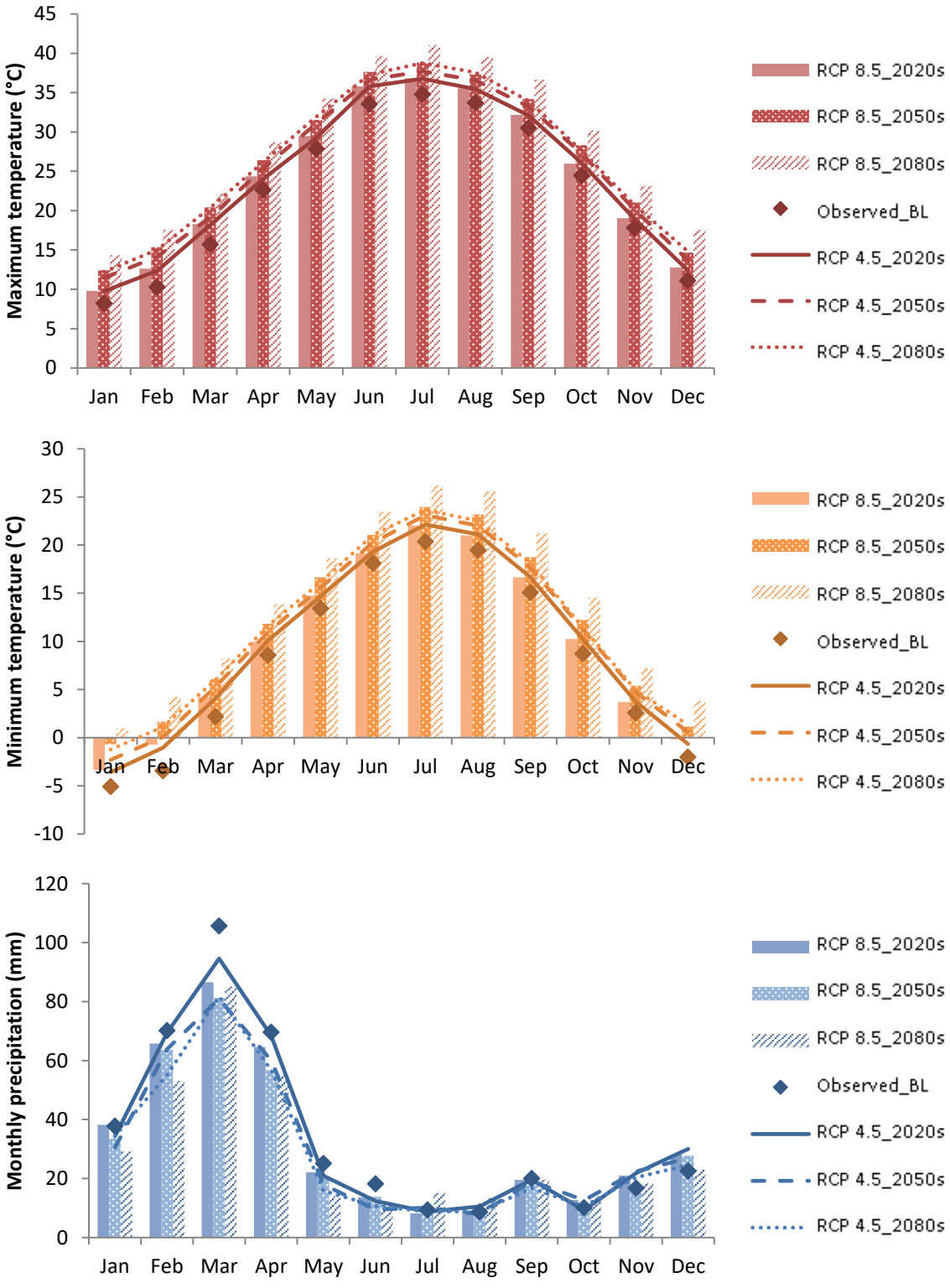

Figure 6.20 Monthly values of maximum/minimum temperature and precipitation of the GCMs' data compared to the baseline

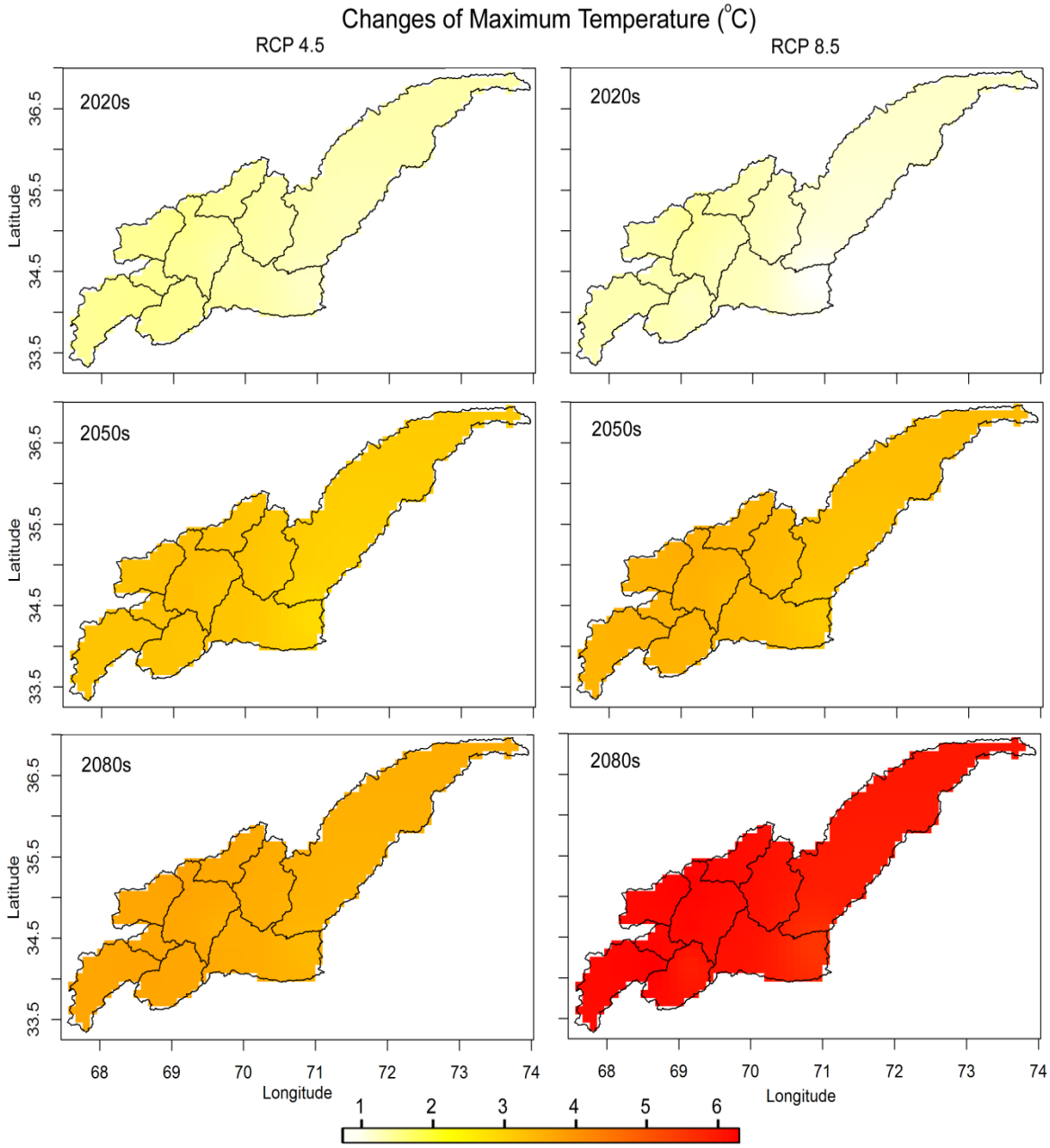

Figure 6.21 Spatial distribution of changes in maximum temperature in the future, as compared to the baseline, in the Kabul basin

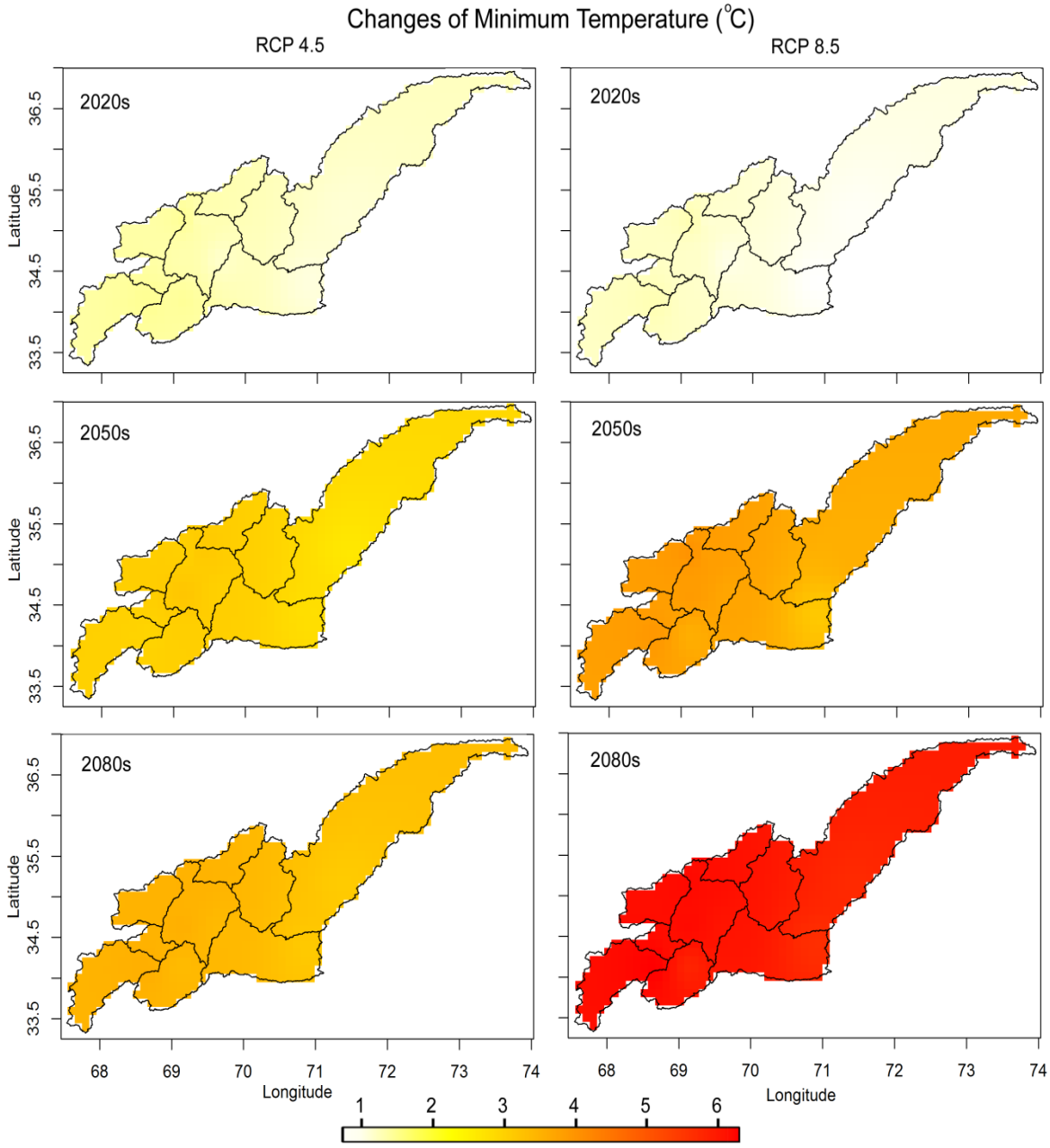

Figure 6.22 Spatial distribution of changes in minimum temperature in the future, as compared to the baseline, in the Kabul basin

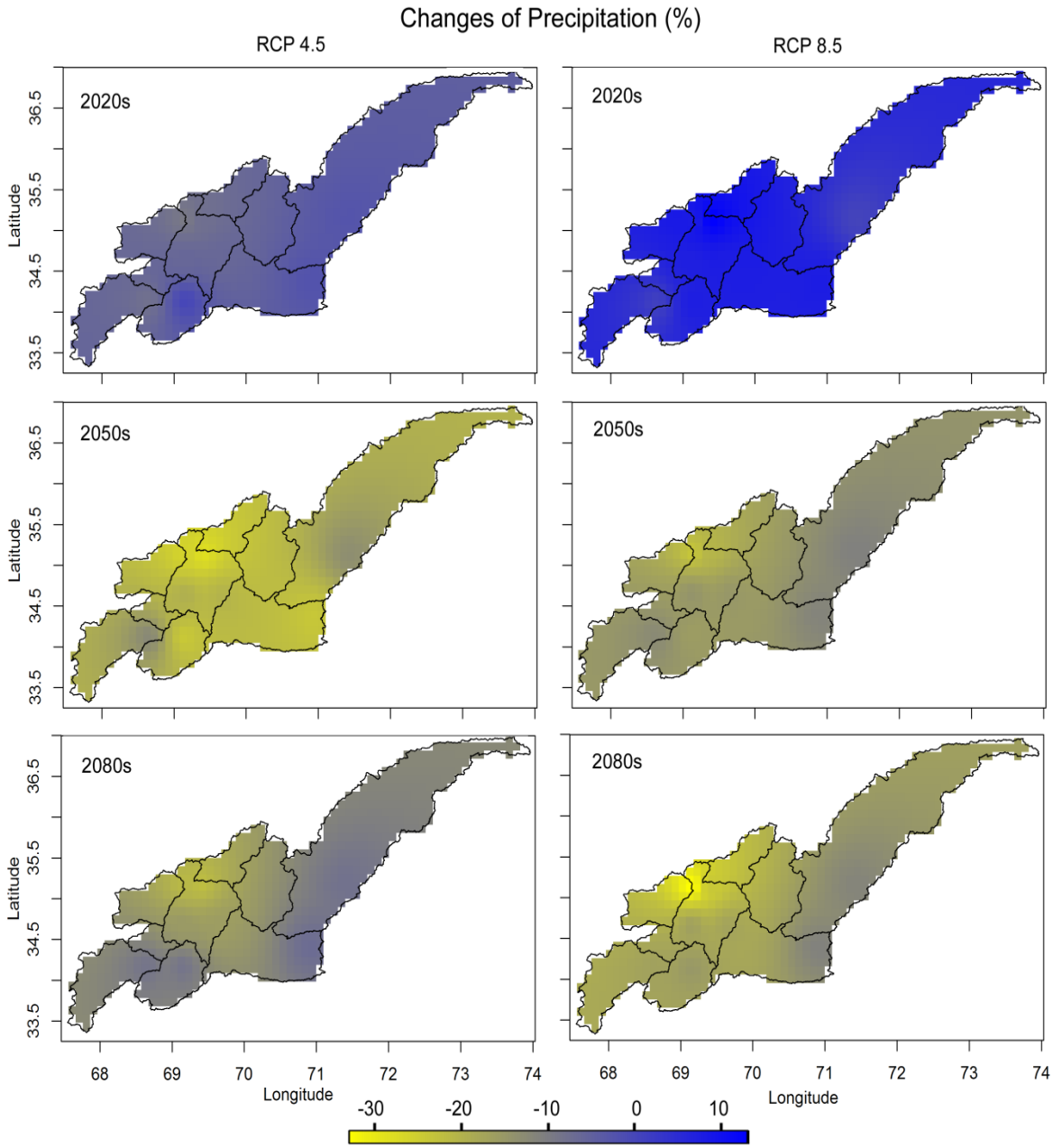

Figure 6.23 Spatial distribution of changes in precipitation in the future, as compared to the baseline, in the Kabul basin

6.7 Summary of the results

The results of the trend analysis suggest that temperature has been increasing over the last five decades while such a clear trend for precipitation could not be detected for the study area.

Predictions of precipitation and temperature for the future under different RCP (Representative Concentration Pathways) scenarios were investigated using data from 8 recent CMIP5-GCMs (Coupled Model Intercomparison Project Phase 5-General Circulation Models) after bias correction and downscaling. The GCMs' outputs were extracted from the grids based on their corresponding stations (same as those in the previous chapter). These

values were downscaled and bias corrected to the stations using the linear downscaling method. At the end, the values of all the stations were averaged over the Kabul basin for each month and the changes calculated were compared to the baseline values. The values were also averaged over the seasons, winter and summer. Winter starts in November and ends by April. Summer is also a period of six months, from May to October. Based on its better performance, the linear method was selected for bias correction. The baseline period of 1971 to 2000 was selected for this study. Three periods—Early Future (2011-2040), Mid Future (2041-2070), and Late Future (2071-2100)—were selected as future periods to be compared with the baseline values and to summarize the results. To show variability in the future, the results were also calculated on yearly and decadal bases.

The median of the results from all 8 GCMs suggests an increasing trend in maximum and minimum temperature in the future, as compared to the baseline. The increases for maximum temperature range from +1.7°C to +4.1°C under RCP 4.5 and +1.7°C to +6.3°C under RCP 8.5. The increases for minimum temperature range from +1.5°C to +3.8°C under RCP 4.5 and +1.4°C to +6.0°C under RCP 8.5. The projections for precipitation mainly show a decreasing trend under both RCPs, with variations ranging from -19% to -6% under RCP 4.5 and -18% to 3% under RCP 8.5. Results suggest that the mean annual values of precipitation under RCP 4.5 range from 366 to 400 mm/yr and from 378 to 412 mm/yr under RCP 8.5. The mean values of maximum temperature in the future are predicted to be between 24.3 to 26.5°C under RCP 4.5 and 24.3 to 28.8°C under RCP 8.5 while the minimum temperature range is predicted to vary from 9.7 to 11.5°C under RCP 4.5 and 9.7 to 13.9°C under RCP 8.5. Based on the baseline observations (of 1971 to 2000), most of the precipitation occurs during winter. March is the wettest month, followed by April. The warmest month is July. All GCM ensembles show almost the same trend as the baseline values. However, it is predicted a slight decrease in precipitation during winter and an increase in precipitation during summer under both RCPs.

The results of mapping the data to better understanding the spatial distribution of changes in the future for the subbasins of the Kabul basin suggest that maximum and minimum temperature show a uniform increase all over the basin during the next century. Precipitation is likely to increase in the near future but it will decrease by the end of the century, especially in the central areas of the basin.

The decadal results also suggest that the annual mean values of precipitation under RCP 4.5 for all the decades of the 21st century range from 293 to 346 mm/yr while under RCP 8.5, the range of values is between 298 and 362 mm/yr. Overall, precipitation values show a slightly decreasing trend towards the end of the century under both RCP scenarios.

CHAPTER 7
ASSESSMENT OF CLIMATE CHANGE IMPACTS ON HYDROLOGY

This chapter presents and discusses the following for the study basin:

- Suitability of the J2000 hydrological model to reproduce the hydrological response of the Kabul basin
- Sensitivity analysis and assessing the uncertainty arising from the model's parameters and the input data
- Assessment of the impacts of climate change on hydrology (e.g. different runoff components under future climatic scenarios)

7.1 Calibration and validation of the J2000 hydrological model

7.1.1 Calibration parameters and efficiencies

The spatial heterogeneity of the watershed was distributed into Hydrological Response Units (HRUs) as suggested by Flugel (1995). These HRUs were selected as a modeling entity. The delineated HRUs and averaged daily precipitation over the Kabul basin during the simulation period are shown in Figure 7.1.

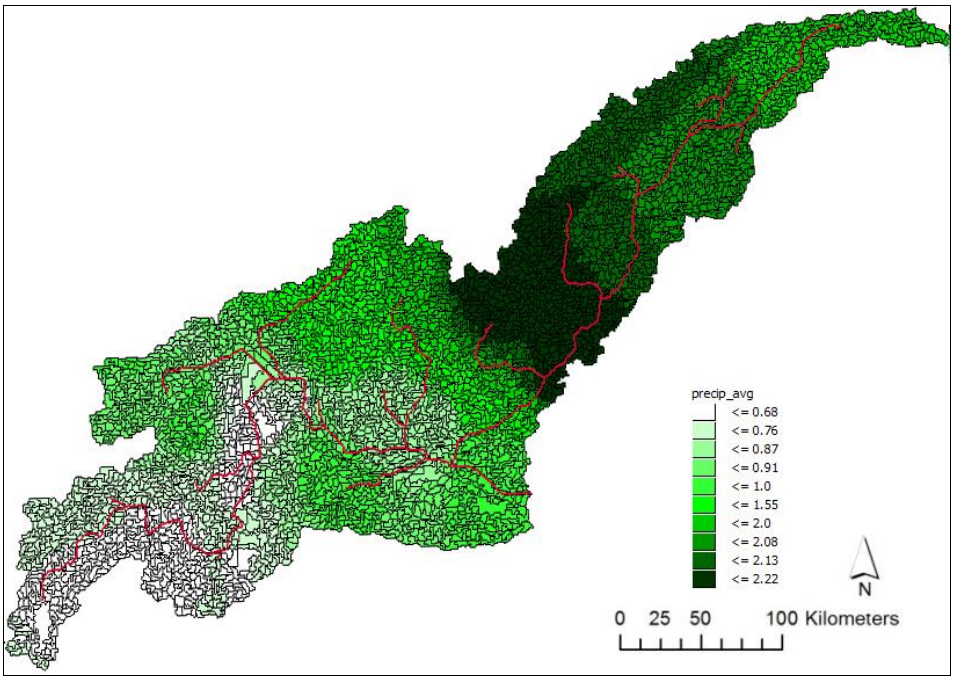

Figure 7.1 HRUs and averaged daily precipitation values (mm) for the simulation period (1969 to 1979)

The input data for the calibration and simulation periods were selected based on the availability of data, as discussed in Chapter 3, and from supplementary precipitation and temperature data from APHRODITE, which is discussed in Chapter 5.

The J2000 model comprises modules to represent the important hydrological processes. A short description of these modules is provided in the section 4.4.2. All the modules contain

a number of calibration parameters that have to be adapted during the model application. The list of the calibration parameters is provided in Table 7.1. The detailed description of these parameters and of the modules which they are related to is provided in Nepal (2012).

Table 7.1 Calibrated parameters for the J2000 hydrological model

ID	Parameter	Description	Actual value	Range
1	**flowRouteTA**	**Flood routing coefficient**	3.4	0-10
2	soilOutLPS	Outflow coefficient for LPS	2.5	0-10
3	**soilMaxPerc**	**Maximum percolation rate to groundwater**	6.0	0-100
4	**soilMaxInfWinter**	**Maximum infiltration in winter**	63.5	0-200
5	**soilMaxInfSummer**	**Maximum infiltration in summer**	141.2	0-200
6	soilMaxInfSnow	Maximum infiltration in snow cover areas	195.4	0-200
7	soilMaxDPS	Maximum depression storage	6.2	0-10
8	**soilLinRed**	**Linear reduction coefficient for actual evapotranspiration**	6.4	0-10
9	**soilLatVertLPS**	**Lateral vertical distribution coefficient**	0.7	0-10
10	soilImpLT80	Infiltration for areas lesser than 80% sealing	0.9	0-1
11	SoilDistMPSLPS	MPS–LPS distribution coefficient	9.6	0-10
12	SoilDiffMPSLPS	MPS–LPS diffusion coefficient	8.9	0-10
13	**soilConcRD2**	**Recession coefficient for interflow**	9.0	0-10
14	soilConcRD1Floodthreshold	Threshold value for soilConcRD1Flood	11.6	0-500
15	**soilConcRD1Flood**	**Recession coefficient for flood event**	8.7	0-10
16	**soilConcRD1**	**Recession coefficient for overland flow**	5.0	0-10
17	a_snow	Interception storage for snow	3.0	0-5
18	a_rain	Interception storage for rain	4.8	0-5
19	**gwRG2Fact**	**Adaptation for RG2 flow**	4.1	0-10
20	**gwRG1RG2dist**	**RG1–RG2 distribution coefficient**	2.4	0-5
21	gwCapRise	Capillary rise coefficient	0.4	0-10
22	**gwRG1Fact**	**Adaptation for RG1 flow**	2.8	0-10
23	**Tbase**	**Threshold temperature for melt**	-3.7	-5 to +5
24	**meltFactorIce**	**Melt factor for ice melt**	2.1	0-5

25	kSnow	Routing coefficient for snowmelt	6.7	0-50
26	kRain	Routing coefficient for rain runoff	26.1	0-50
27	kIce	Routing coefficient for ice melt	0.9	0-50
28	debrisFactor	Debris factor for ice melt	7.5	0-10
29	alphaIce	Radiation melt factor for ice	0.7	0-5
30	**t_factor**	**Melt factor by sensible heat**	4.1	0-5
31	snowCritDens	Critical density of snowpack	0.1	0-1
32	Trs	Base temperature	2.0	-1 to +1
33	r_factor	Melt factor by liquid precipitation	3.2	0-5
34	g_factor	Melt factor by soil heat flow	0.3	0-5
35	snowColdContent	Cold content of snowpack	0.1	0-1
36	**baseTemp**	**Threshold temperature for snowmelt**	0.3	-5 to +5

The results of daily simulations for the calibration (1969-1974) and validation (1975-1980) periods, along with the model's efficiencies, are shown in Figure 7.2 and Table 7.2 respectively. The red and blue lines represent simulated and observed streamflow discharges, respectively. The daily mean precipitation (blue bars) is given in upper panel. During the calibration and validation periods, the model is able to reproduce overall hydrological responses fairly well, on the basis of results given in the graphical and statistical evaluations.

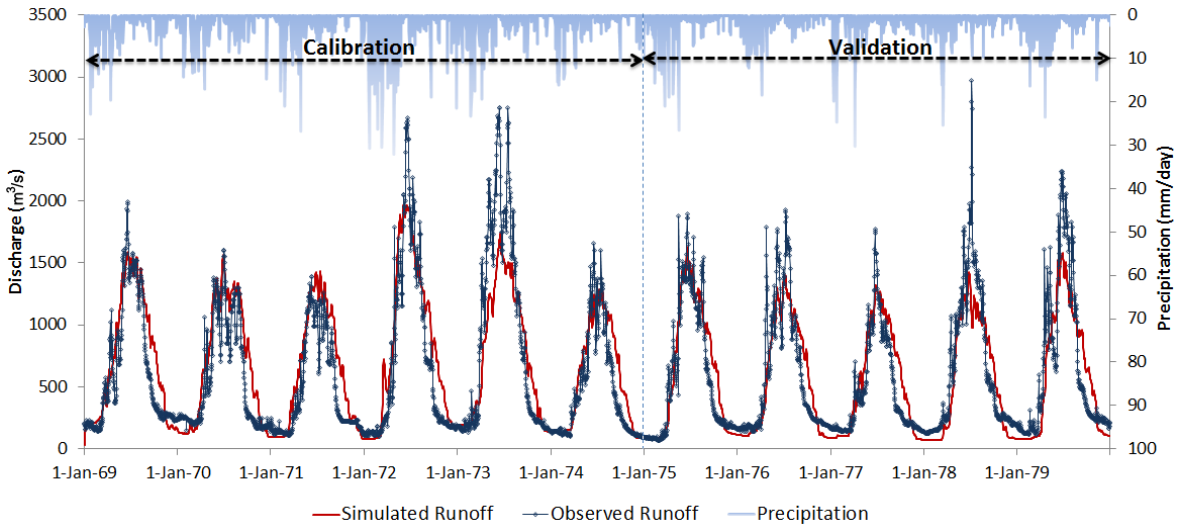

Figure 7.2 Daily simulation results for the simulation period (calibration: 1969 to 1974, validation: 1975 to 1979)

Table 7.2 Model performance indicators for daily and monthly simulations

Indicator	Daily		Monthly	
	Calibration	Validation	Calibration	Validation
Coefficient of determination (r^2)	0.79	0.79	0.84	0.86
Nash–Sutcliffe model efficiency coefficient	0.78	0.79	0.83	0.85
Root mean square error (RMSE) (m^3/s)	272	242	233	187
P_{bias} (%)	10.1	-2.6	10.1	-2.6

7.1.2 Runoff components

The main input and output components for checking the water balance are shown in Figure 7.3. The contribution of snowmelt and ice-melt to the outlet runoff is estimated to be around 85% during the simulation period (1969 to 1979).

Different components of runoff and their monthly distribution are shown in Figure 7.4. The highest portion is for surface runoff while the baseflow accounts for 8.6% of the total runoff.

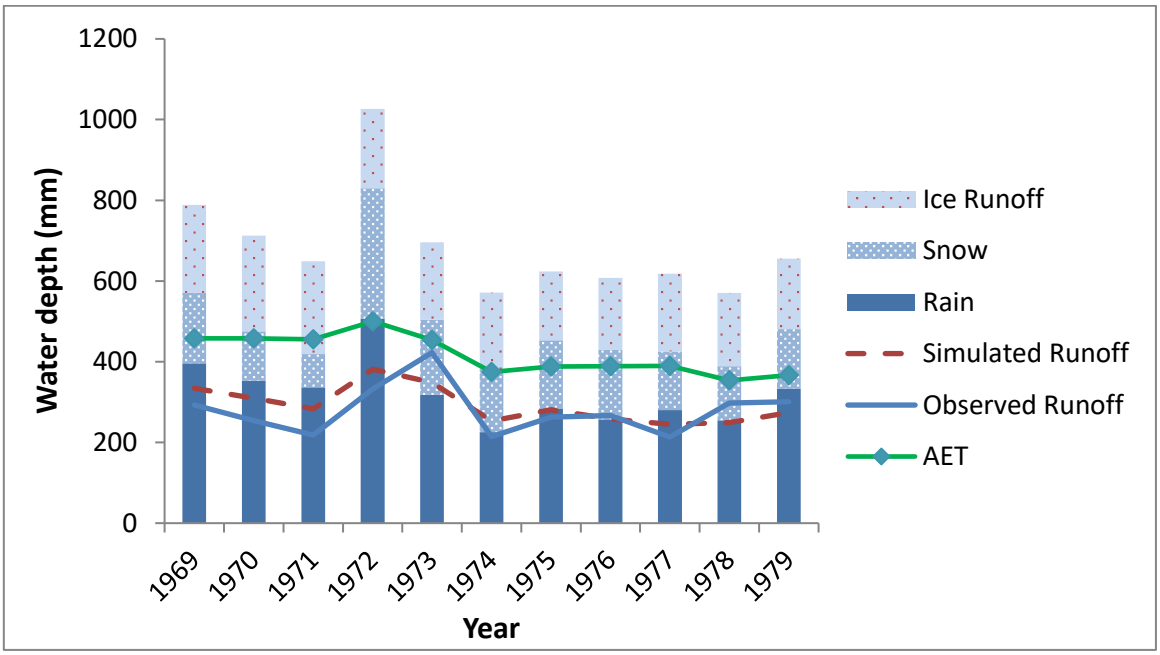

Figure 7.3 Annual distributions of hydrological system components in the Kabul basin during the simulation period (1969 to 1979)

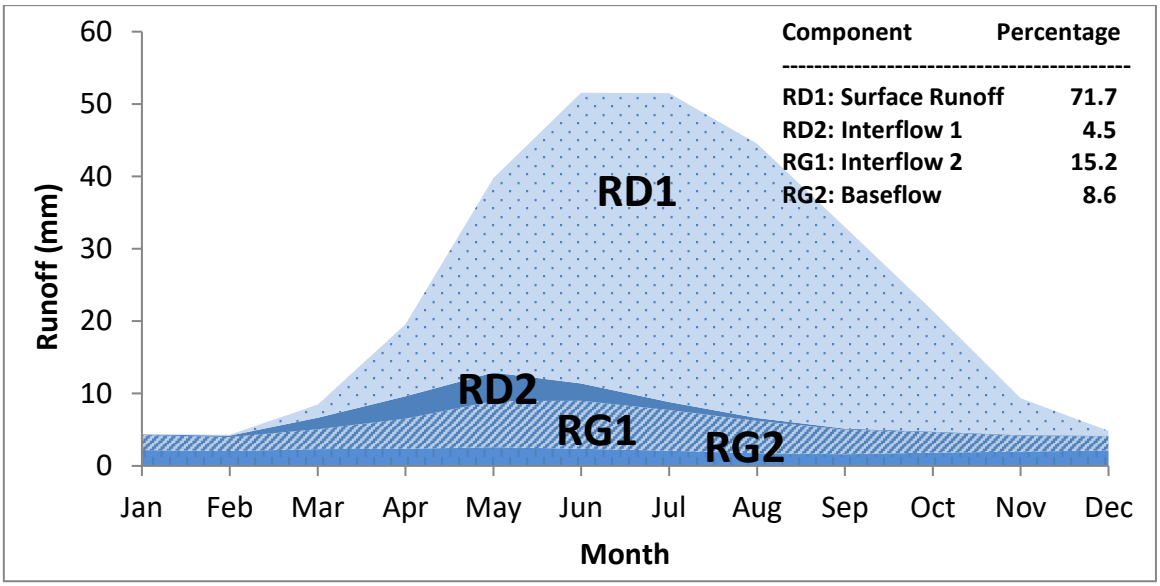

Figure 7.4 Simulated runoff components for the period of 1969 to 1979

7.1.3 Analysis of sensitivity and uncertainty

The results for the sensitivity and uncertainty analysis are shown in Figures 7.5 and 7.6. For the sensitivity analysis, based on the available literature, 16 parameters, which were found to be the most sensitive parameters, were evaluated. These parameters are in bold font in Table 7.1. The results of the sensitivity analysis suggest that the most sensitive parameter is soil maximum percolation while base temperature, which is the threshold temperature for melt, is the least sensitive parameter.

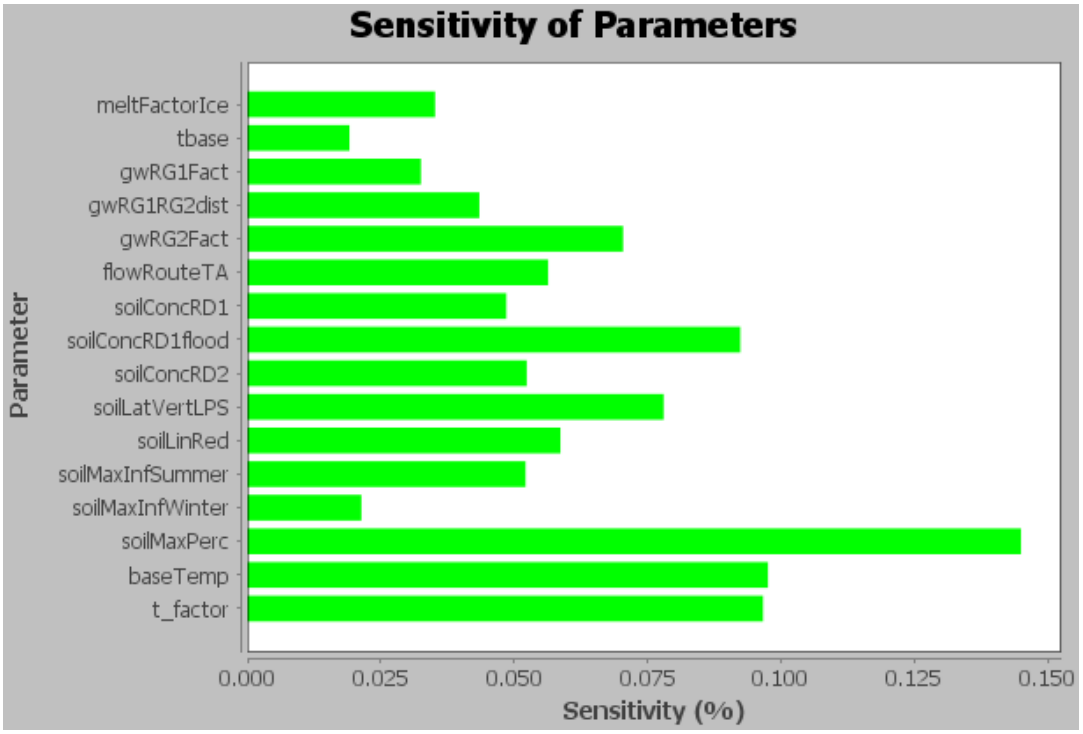

Figure 7.5 Sensitivity of the selected calibration parameters with the Nash–Sutcliffe efficiency criterion based on the results of 1000 simulations

The uncertainty analysis shown in Figure 7.6 is for a two years period. It was carried out to better understand the possibility of the model's parameters and the model's structure to capture the observed runoff. The observed runoff on some days is out of the uncertainty range generated based on different ranges of parameters. This identifies the model structure's certainty or uncertainty due to input data.

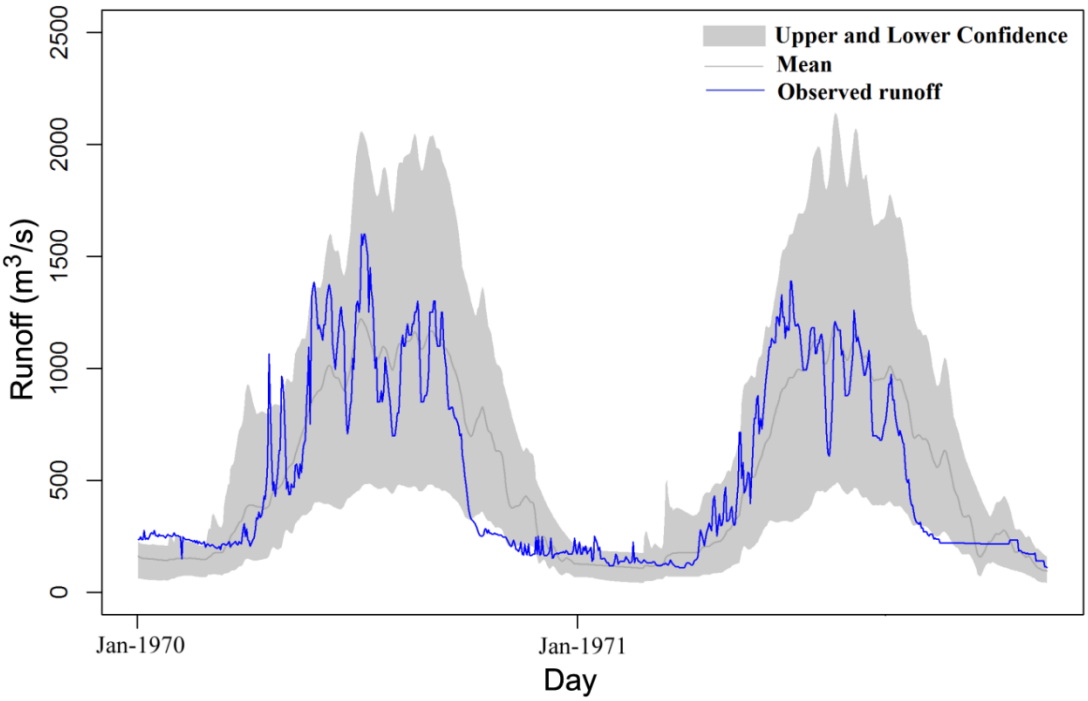

Figure 7.6 Results of the uncertainty analysis using the general likelihood uncertainty estimation method (Jan1970 to Dec1971)
(The grey band represents ensemble values from 1000 simulations)

The uncertainty due to different input precipitation data was also investigated using different precipitation inputs (same precipitation series as evaluated for Objective 1 mentioned above). The calibrated model was used for simulating the runoff for the period of 2004 to 2007. There was no observed hydrograph during this period but the aim was to compare the results of different gridded datasets with the simulated runoff generated from daily observations of precipitation. These results are shown in Figures 7.7 and 7.8. APHRODITE data showed good agreement with the observed values in generating the runoff.

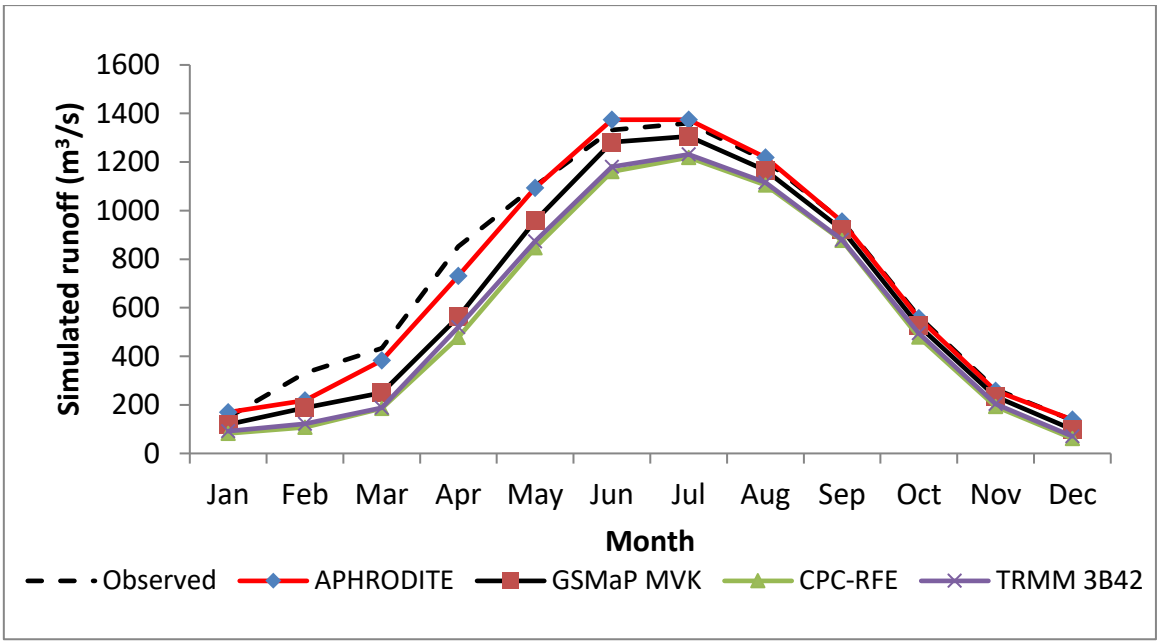

Figure 7.7 Simulated runoff from different precipitation sources for the period of 2004 to 2007

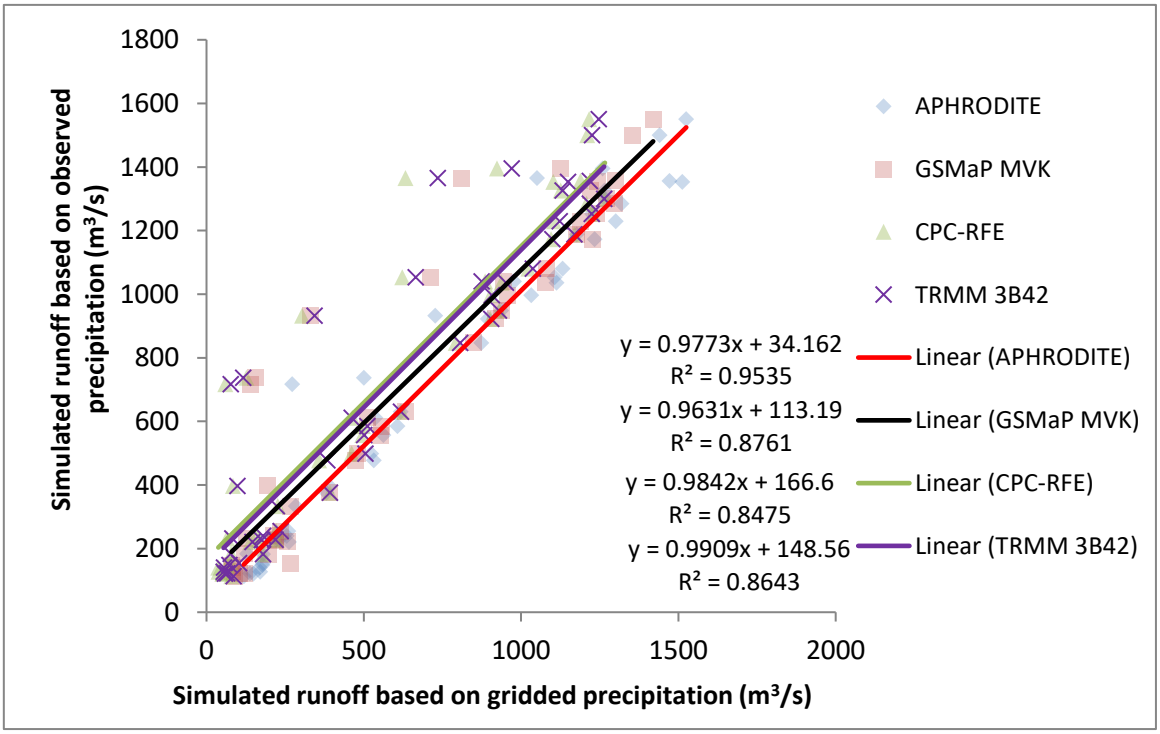

Figure 7.8 Simulated runoff from observed precipitation vs. simulated runoff from gridded precipitation datasets for the period of 2004 to 2007 (monthly values)

7.2 Simulation results for the baseline period

To understand the impacts of predicted precipitation and temperature changes in the Kabul basin (discussed in the previous section), the downscaled and bias corrected input data were used to generate future runoff under different RCP scenarios. At the outset, the calibrated and validated model was run for the baseline period of 1971 to 2000.

The main input and output components for checking the water balance are shown in Figure 7.9. The contribution of snowmelt and ice melt to the outlet runoff was estimated to be around 82% during the baseline period (1971 to 2000).

Different components of runoff and their monthly distribution are shown in Figure 7.10. The highest portion is for surface runoff while the baseflow accounts for 9.0% of the total runoff.

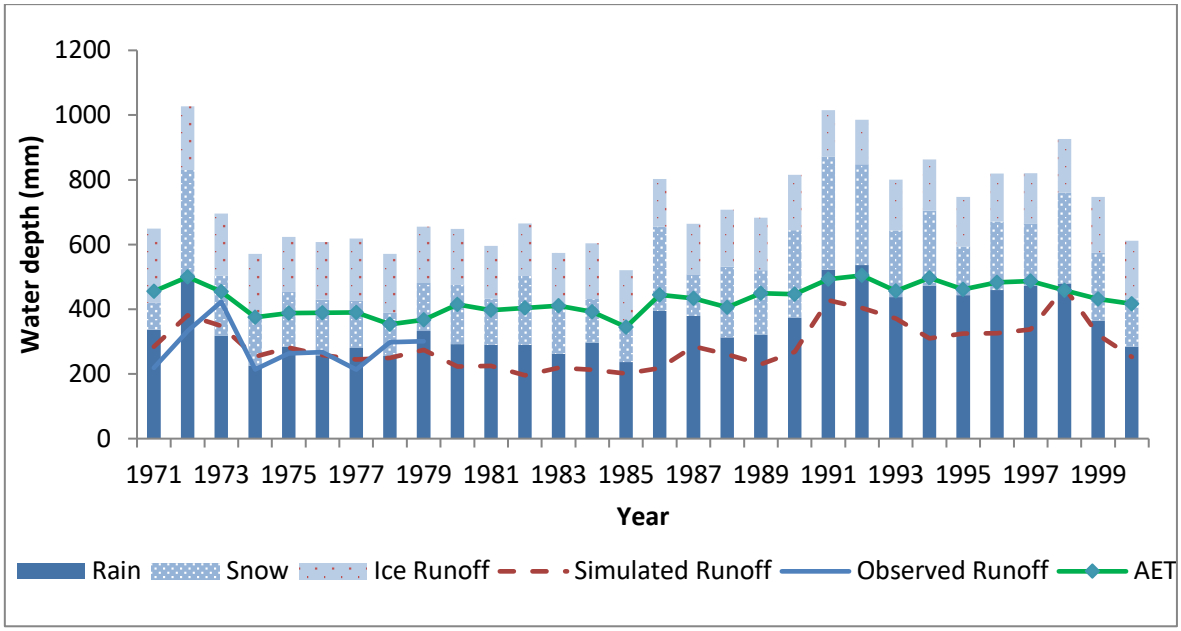

Figure 7.9 Annual distributions of the hydrological system components for the Kabul basin during the baseline period

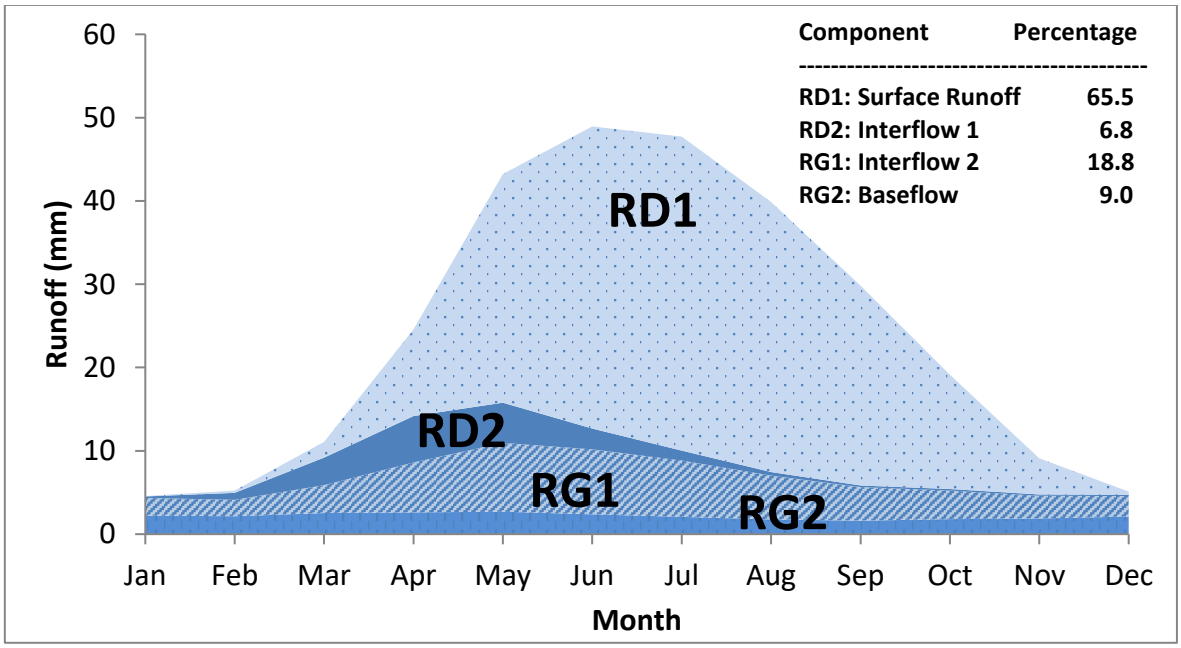

Figure 7.10 Simulated runoff components for the baseline period

7.3 Simulation results of future runoff under future climatic scenarios

The annual time series and their uncertainty ranges are shown in Figure 7.11. The median results show an increasing trend in both RCP scenarios; RCP 8.5 shows much higher values after the 2060s to the end of the century.

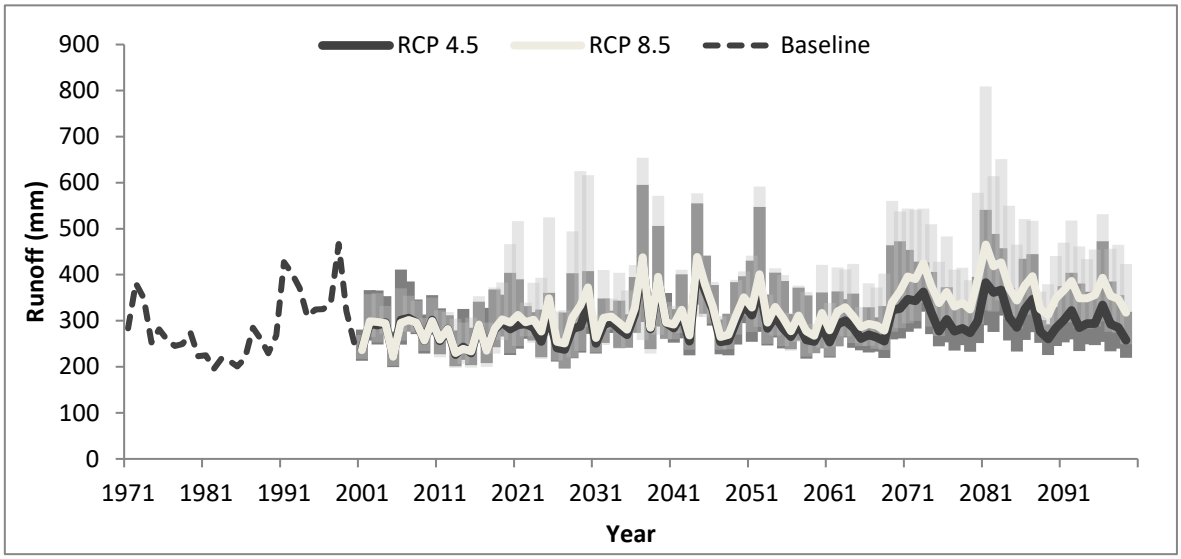

Figure 7.11 Uncertainty in future predicted annual runoff

Figure 7.12 shows the seasonal distribution of monthly future runoff under RCP 4.5 and Figure 7.13 shows the corresponding results for RCP 8.5. Broadly, it can be concluded that there is an increasing trend of runoff during the next decades under both RCP scenarios in both seasons (winter and summer). The outlier values under RCP 4.5 are for the results of CNRM-CM5 while the outlier values under RCP 8.5 refer to MIROC5.

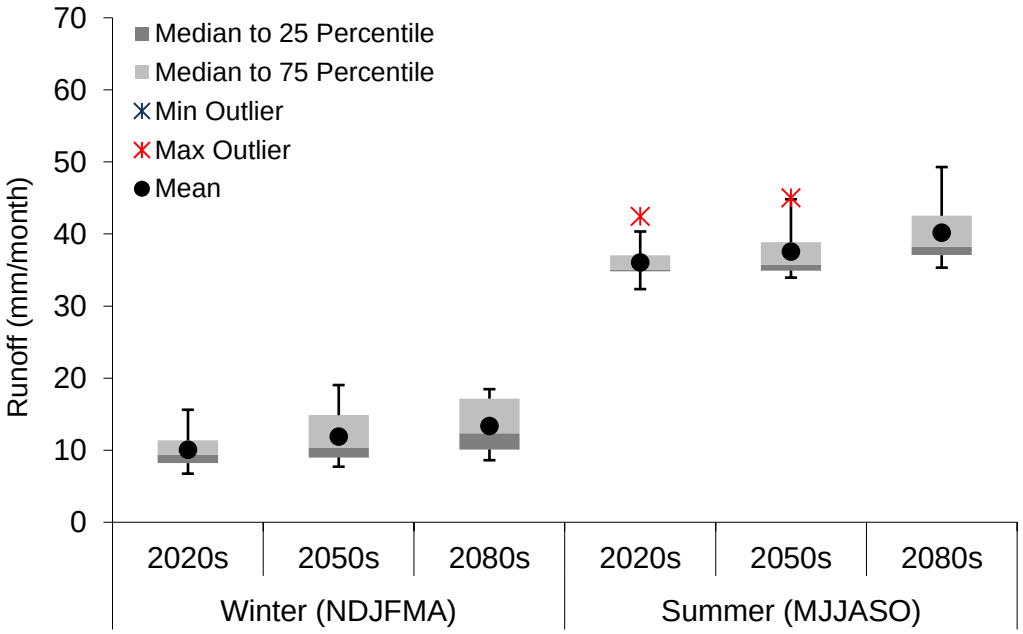

Figure 7.12 Seasonal distribution of monthly future runoff under RCP 4.5

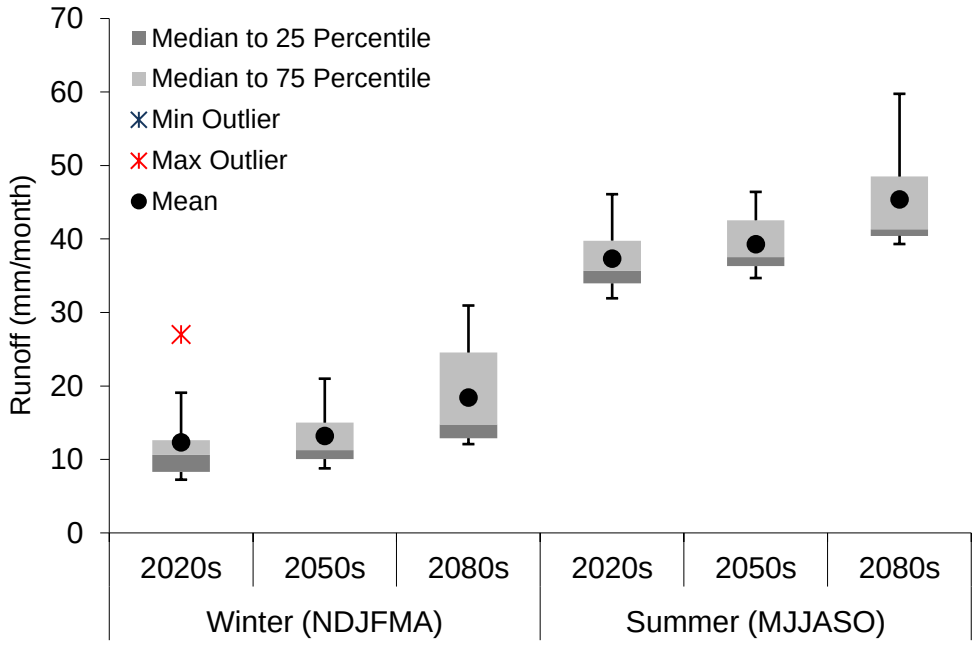

Figure 7.13 Seasonal distribution of monthly future runoff under RCP 8.5

7.4 Assessment of future changes in runoff, as compared to the baseline

The simulations' results of future runoff were compared with the results of the models for the baseline period of 1971 to 2000. Figure 7.14 shows future runoff for each decade under different RCP scenarios for all the GCMs. Overall, the results suggest that future runoffs are very likely to increase. This is mainly due to the increase in temperature which in turn causes an increase in snow- and ice-melt. To better understand the results, we have also shown the median of changes in precipitation and temperature for crosschecking with their respective generated runoff.

The predictions for future runoff range between -14% to +49% over the 21st century under RCP 4.5 while these changes are predicted to be within -16% to +100% under RCP 8.5 for the same period. However, the median values show much lesser range and vary between -9% to +22%.

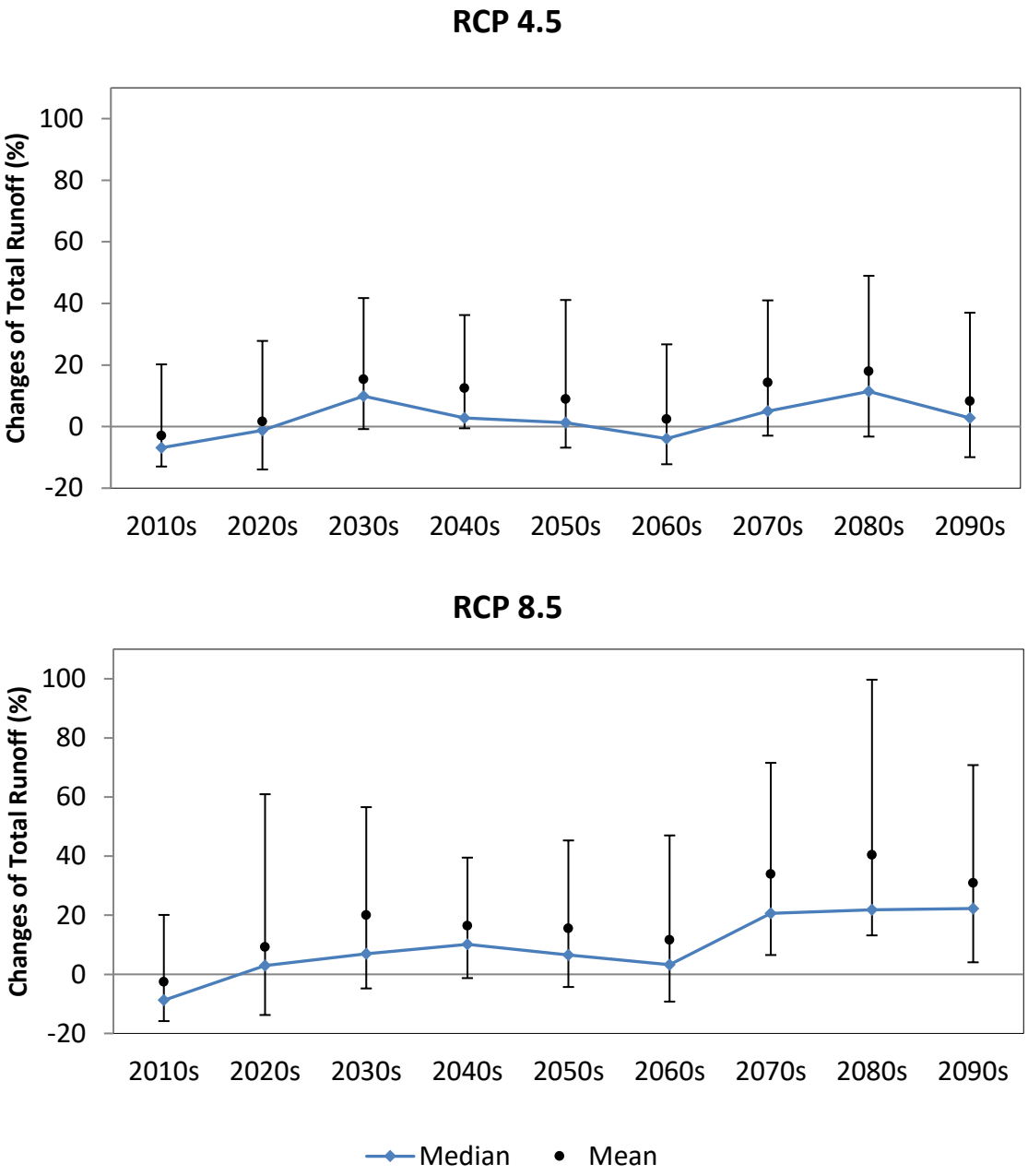

Figure 7.14 Uncertainty in future predicted runoff based on 8 CMIP5 GCMs under RCPs 4.5 and 8.5

The monthly distribution of future runoff, compared to the baseline period's data, was investigated and the results for each RCP scenario are shown in Figure 7.15. While the changes in runoff in terms of percentage are higher during winter (Nov-Apr), the amounts of runoff are low during this season, so these changes didn't create much difference. During the Early Future (2020s) and Mid Future (2050s) periods, the runoff might decrease slightly in some months from January to May but there is likely to be an overall increase in runoff.

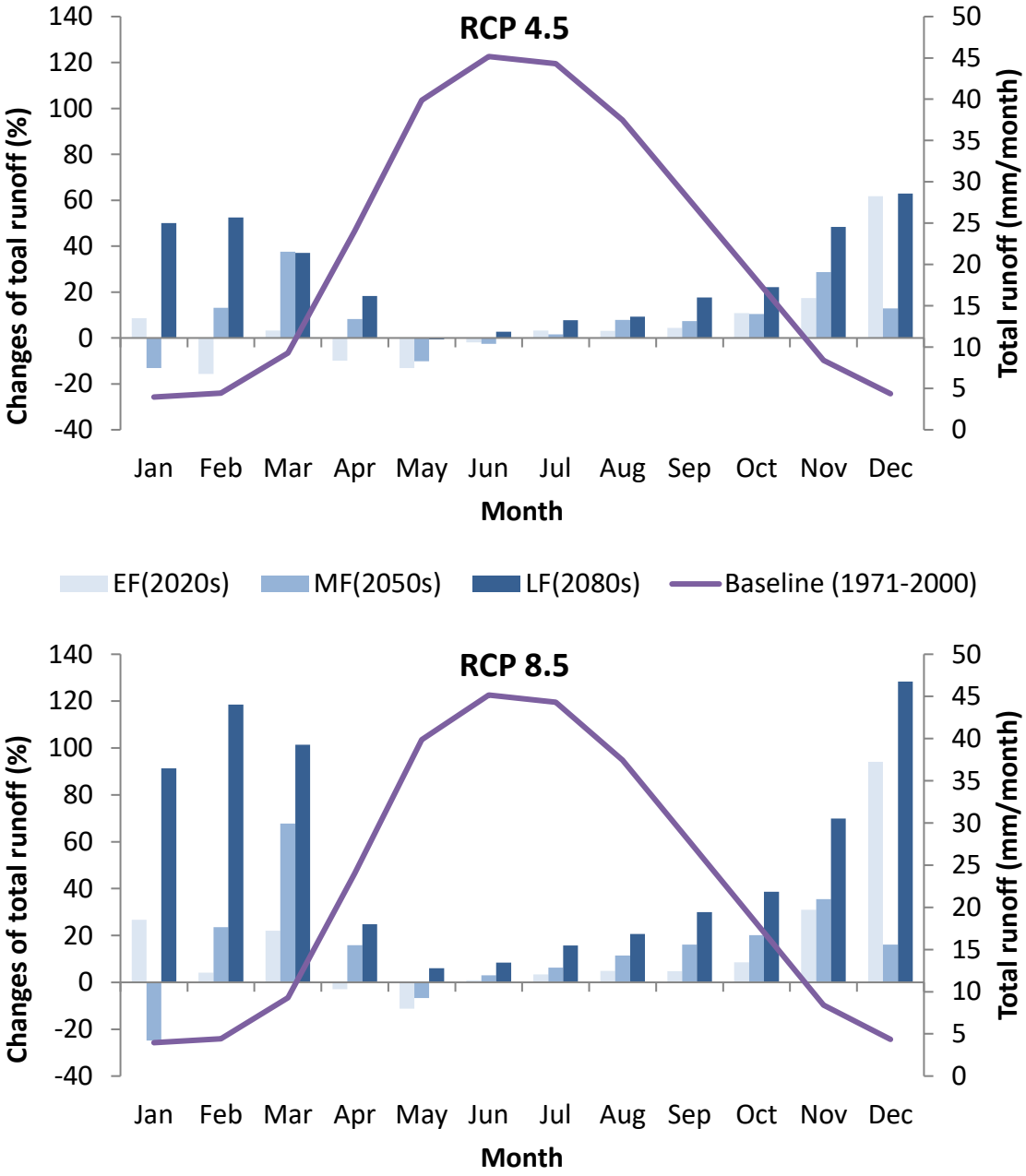

Figure 7.15 Monthly distribution of future runoff under RCPs 4.5 and 8.5

Figure 7.16 shows the changes in predicted surface runoff and baseflow for the future as well as actual evapotranspiration in the Kabul basin, as compared to the baseline period. The trend shows that though future runoff is increasing, this increase is mainly happening in surface runoff while the baseflow might actually decrease.

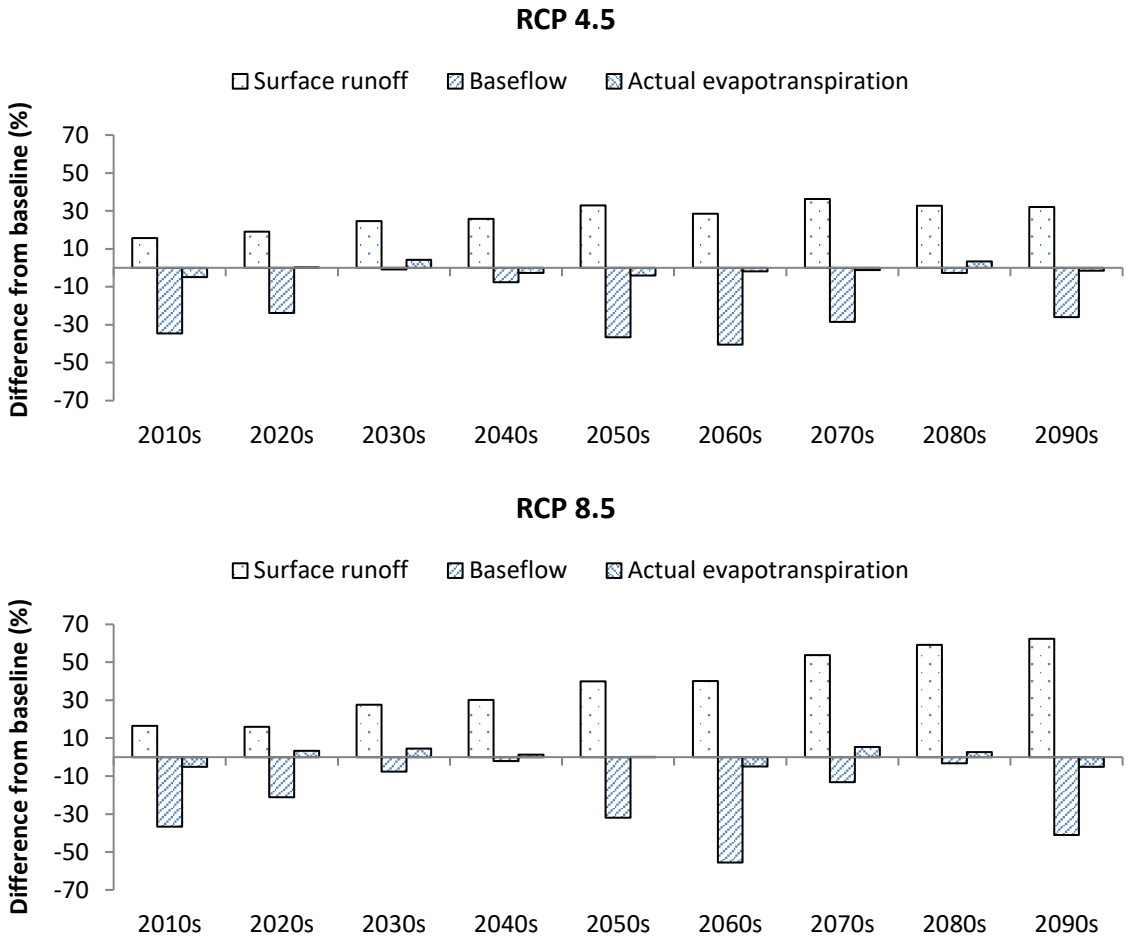

Figure 7.16 Monthly distribution of future runoff under RCPs 4.5 and 8.5

7.5 Runoff sensitivity to precipitation and temperature

Figure 7.17 is a level plot which shows the changes in runoff; the x-axis accounts for precipitation changes and the y-axis shows the changes in temperature. This plot was created by populating the annual values of all the model runs under different climatic scenarios. This plot represents, in brief, what would be the possible changes in runoff if changes in precipitation and temperature are known. Figure 7.18 shows the correlation between precipitation and temperature with runoff, each one separately.

The increases in temperature may respectively lead to a loss of snow and glacier area. Nepal et al. (2012) analyzed that increasing temperature will shift the snowline up to areas of higher altitudes and thereby reduce the snow storage capacity in the Dudh Koshi Basin, Himalays. This will influence runoff in the basin and water availability during the dry seasons. Therefore, it is important to consider varying projections from multiple GCMs and RCP scenarios for climate impact studies in order to prepare suitable adaptation strategies.

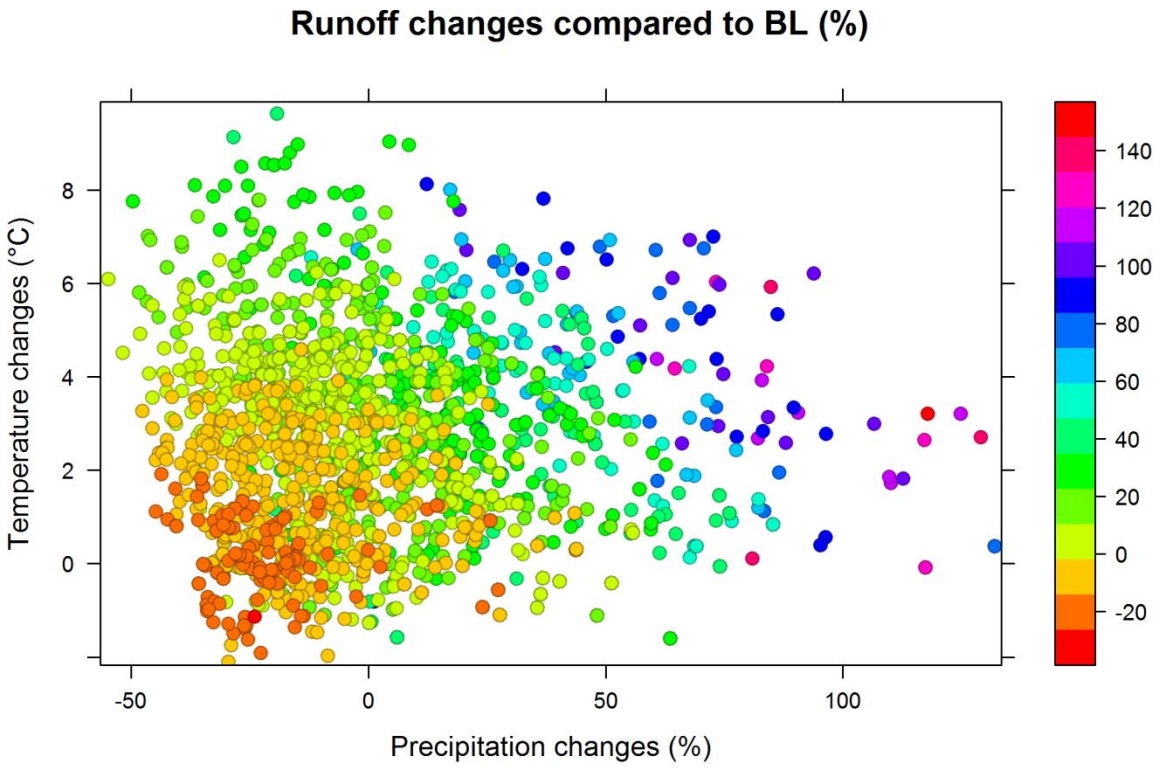

Figure 7.17 Level plot to simultaneously show the relation of precipitation and temperature changes, as compared to runoff changes

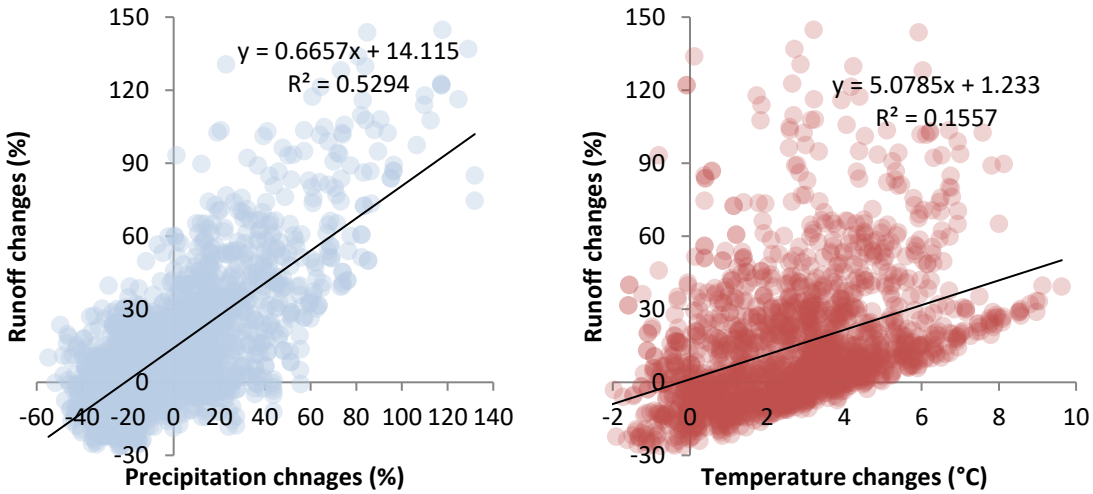

Figure 7.18 Correlation between changes in precipitation and temperature, as compared to runoff changes

7.6 Summary of the results

The J2000 hydrological model was used to reproduce the hydrological dynamics of the study basin. The model's results of the calibration and validation periods suggest that the model performed well and can be used to reproduce the hydrological dynamics of the basin. The contribution of snow- and ice-melt to the outlet runoff is estimated to be around 85% during the simulation period (1969 to 1979). The highest portion of the runoff components is for surface runoff (71.7%) while the baseflow accounts for 8.6% of the total runoff.

For the assessment of future climate predictions on water resources, bias corrected precipitation and temperature were used as inputs for the hydrological model. As per the predictions, future runoff ranges between -14% and +49% under RCP 4.5 and between -16% and +100% under RCP 8.5 during the 21st century. The median values varying between -9% and +22%. Overall, the results suggest that future runoff is more likely to increase. This is mainly due to the increase in temperature, which will cause more snow- and ice-melt. To better understand these results, the median of changes in precipitation and temperature for crosschecking with their respective generated runoff are also shown.

The results of the seasonal distribution of monthly future runoff under RCP 4.5 and RCP 8.5 show an increasing trend in runoff during the next decades under both RCP scenarios in both seasons (winter and summer).

The results of monthly changes in future runoff suggest that the percentage of change is higher during winter (Nov-Apr) but as the amount of runoff is low during this season, these changes won't create much difference. During the Early Future period (2020s) and the Mid Future period (2050s), the runoff might decrease slightly in some months from January to May but there will, overall, be an increase in runoff.

Sensitivity and uncertainty analysis of the model's parameters were also carried out. The sensitivity of the model to precipitation and temperature input data was also examined.

CHAPTER 8
FARMERS' PERCEPTIONS ABOUT CLIMATE CHANGE AND THEIR ADAPTATION MEASURES

In the last two chapters, the changes in historical and future temperature, precipitation, and runoff have been described; these changes were investigated using a set of 8 CMIP5 GCMs and historical surface observations. In this chapter, the focus is on how the changes in the historical period are being perceived by the local people in the study area, and to investigate this, two districts were selected for conducting field surveys.

Agriculture is the most important water related sector in Afghanistan and is facing climate change related problems. Climate change events have put pressure on farming activities, crop patterns, and other resources in the area. Therefore, the surveys aimed to understand the farmers' perceptions about climate change and the measures taken by them as adaptation strategies.

8.1 Selected districts for field surveys

To conduct the field surveys, two districts were selected (Figure 8.1 and Table 8.1). These districts were selected based on the importance of their agricultural activities to the country and their differences in terms of agro-climatic zones. A random sampling approach was used for interviewing farmers at both sites.

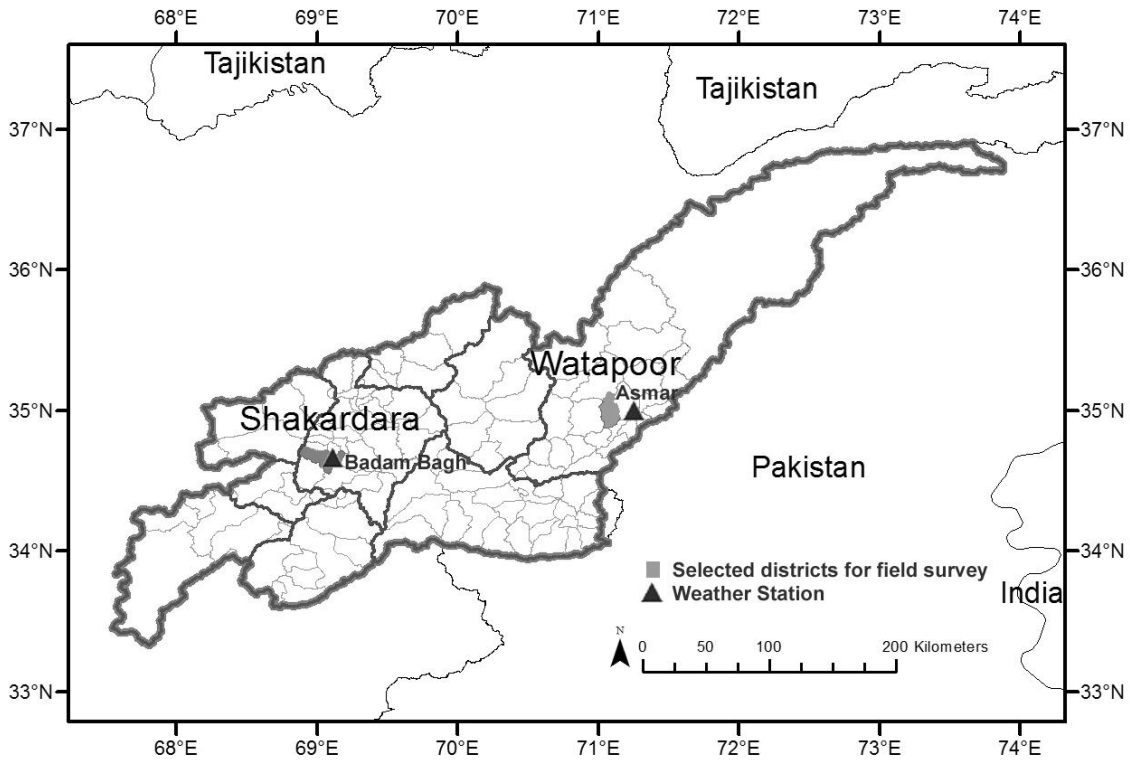

Figure 8.1 Location map of sample districts and their corresponding weather stations

Table 8.1 Climate characteristics of sample districts

District Name	Province	Area (km^2)	Weather Station				
			Name	Location	Mean Elevation (m)	Mean Temperature (℃)	Annual Mean Precipitation (mm)
Shakar Dara	Kabul	318	Badam Bagh	Inside	2427	9.6	273
Watapoor	Kunar	252	Asmar	Outside (14 km away)	1168	19.1	686

8.1.1 The Shakar Dara district

Shakar Dara is located in the central part of the Kabul Province in Afghanistan. 80% of people in Shakar Dara are farmers. The main crops traditionally were wheat, barely, and rice but in recent years, most farmers have shifted to tree planting and rice cultivation has almost vanished in the area. Urbanization is another issue which has halted agriculture development in this district. Water for irrigation and domestic use is mainly abstracted from wells and Karez as well as canals. Due to the lack of water in this area, much arable land has to be left uncultivated. This water shortage is due to drought in recent years as well as increased use of water resources as a result of increased population.

8.1.2 The Watapoor district

The Watapoor district is located in the central part of the Kunar Province in Afghanistan, and consists of 120 villages. A river coming from Chapa Dara crosses this district. Most of the villages here are situated in the valleys and some in the mountains. Water for domestic purposes and irrigation is obtained from springs, shallow wells, and river. The main crops for Watapoor include wheat, corn, rice, barely, and sugarcane. Most of the farmers also have goats and cows, which is an extra source of income for them. Apart from farming and animal husbandry, remittances from abroad are the next main source of income for people in Watapoor.

8.2 Climate extreme indices for the selected districts

In this section is shown the trend analysis that was done for climatic parameters and a few extreme indices. Comparisons were also made with climatic changes as perceived by the farmers of the regions.

Figure 8.2 shows the linear regression for trend analysis of maximum and minimum temperature for the weather stations in the two districts selected for field surveys. The temperature here shows an increasing trend during the last 40 years.

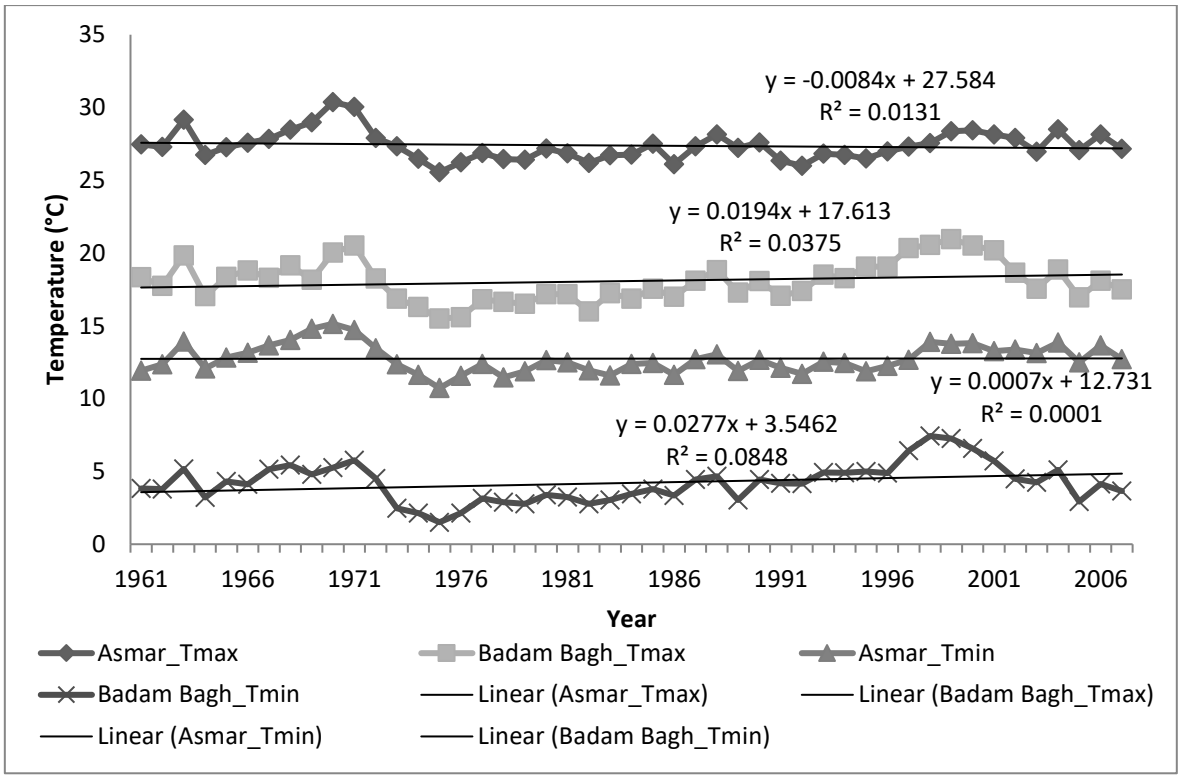

Figure 8.2 Maximum/minimum temperature of the sample districts

Figure 8.3 shows linear regression for the trend analysis of precipitation for both selected districts. In general, the trend of precipitation at Asmar showed an increasing rate while for Badam Bagh, the rate was almost constant. However, if only the years after 1990 are considered, both stations would show a decreasing trend.

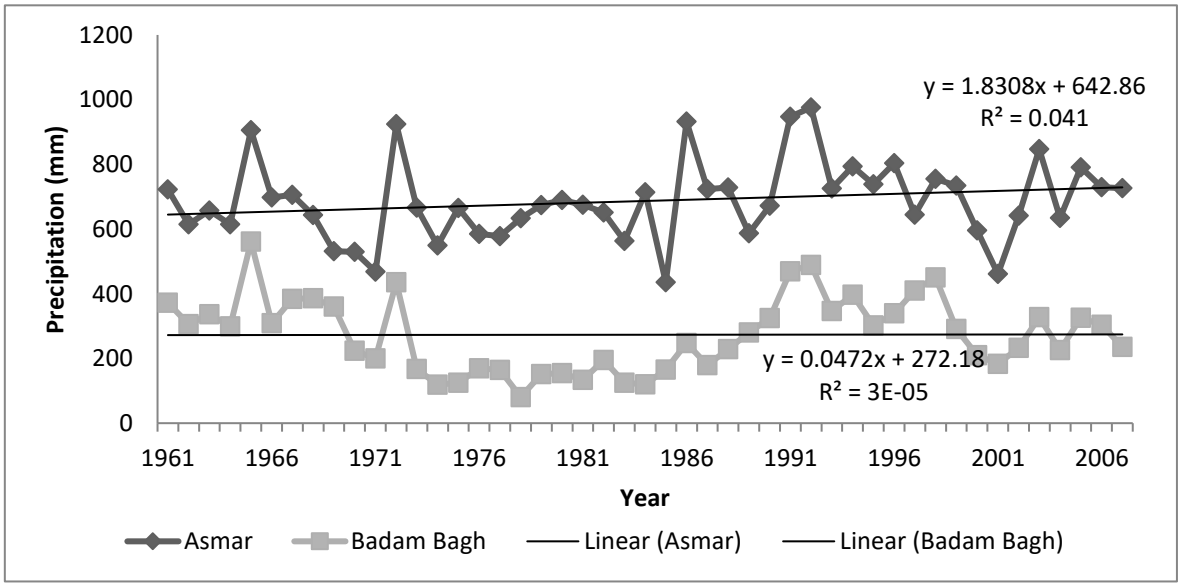

Figure 8.3 Annual precipitations of the sample districts

The climate extreme indices were then calculated for the weather stations located in the selected districts using historical data. These indices are as follows:

- SU: Number of summer days: Annual count of days when TX (daily maximum temperature) > 25°C

- ID: Number of icing days: Annual count of days when TX (daily maximum temperature) < 0°C

- FD: Number of frost days: Annual count of days when TN (daily minimum temperature) < 0°C

- SDII: Simple precipitation intensity index: $SDII_j = \frac{\sum_{w=1}^{W} RR_{wj}}{W}$

  where RR_{wj} is the daily precipitation amount on wet days during the year or season, w ($RR \geq 1mm$) in period j, and W represents the number of wet days in j.

Figure 8.4 shows linear regression for the trend analysis of the number of summer days. The values after the 1970s show an increasing trend of the number of summer days for both selected districts. This is an indicator that hot days during summer have increased.

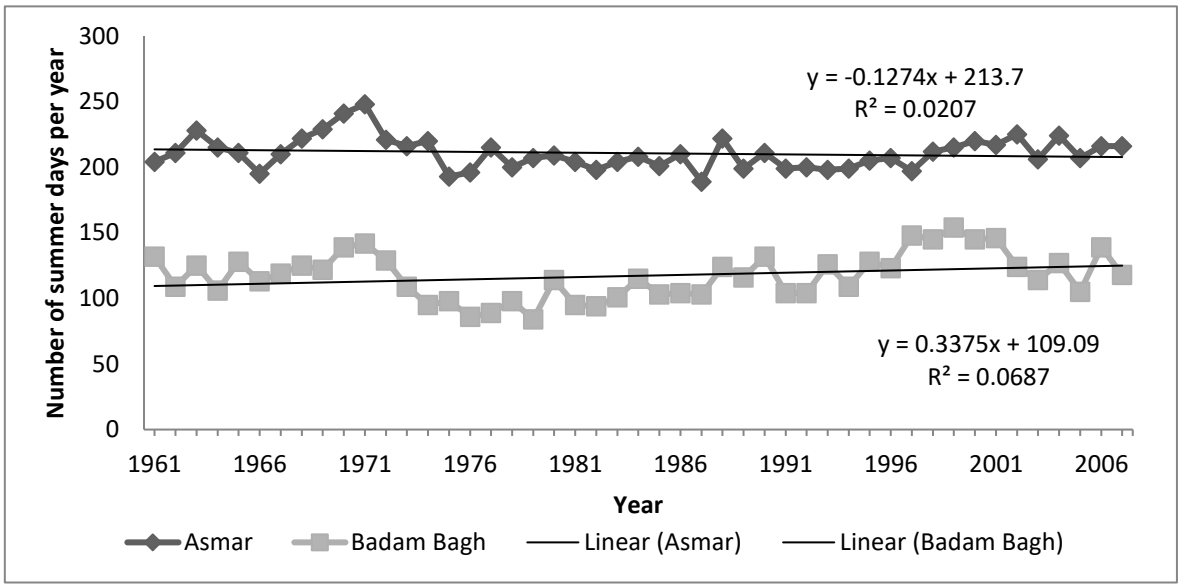

Figure 8.4 Number of summer days of the sample districts

Figure 8.5 shows linear regression for the trend analysis of the number of icing days. The values show, overall, a decreasing trend for the number of icing days for Badam Bagh. For the Asmar station, the values indicate that there was no icing day. The number of icing days indicates extreme cold during winter.

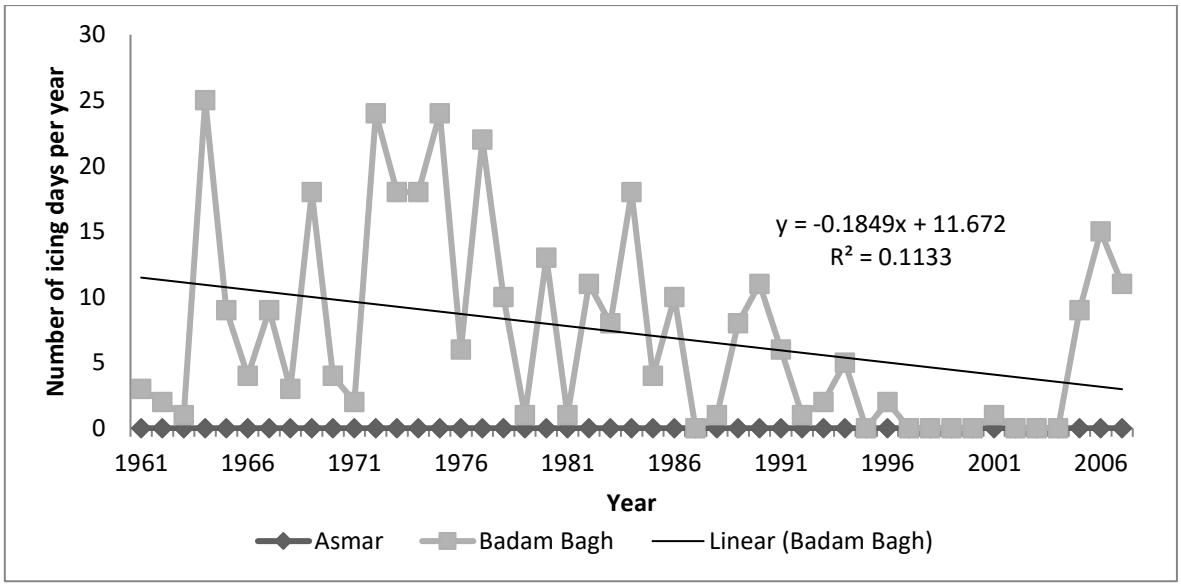

Figure 8.5 Number of icing days of the sample districts

Figure 8.6 shows linear regression for the trend analysis of the number of frost days. Similar to the values for the number of icing days, the number of frost days shows, overall, a decreasing trend in both selected districts. The number of frost days indicates cold days during winter.

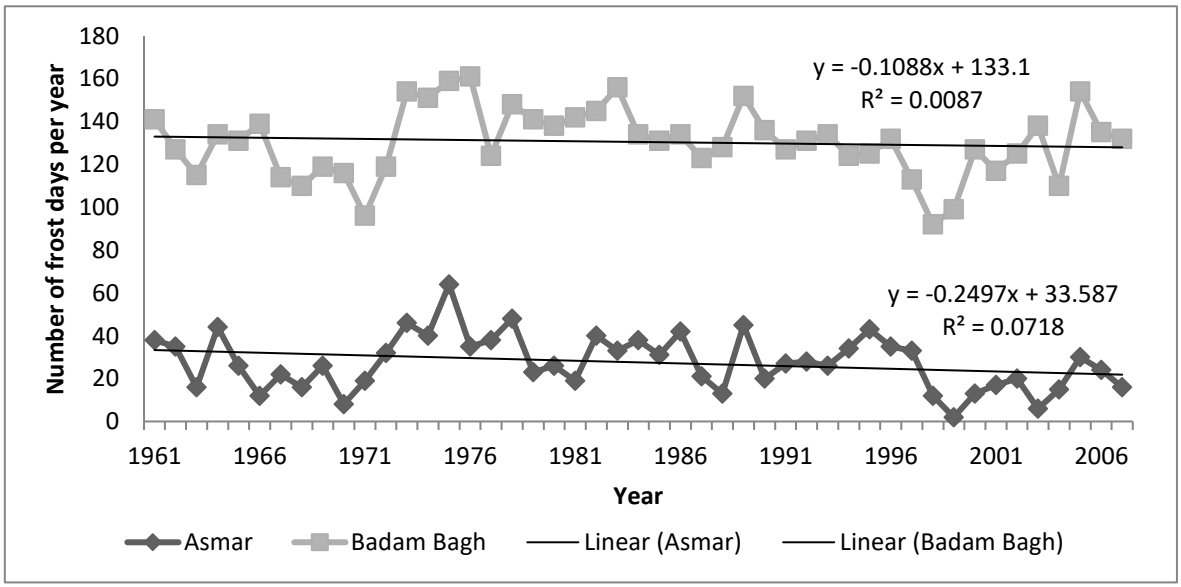

Figure 8.6 Number of frost days of the sample districts

Figure 8.7 shows linear regression for the trend analysis of the simple precipitation intensity index for both selected districts. Here, the trend shows an increase in precipitation intensity. These results suggest that more precipitation during a shorter period of time was seen in both selected districts.

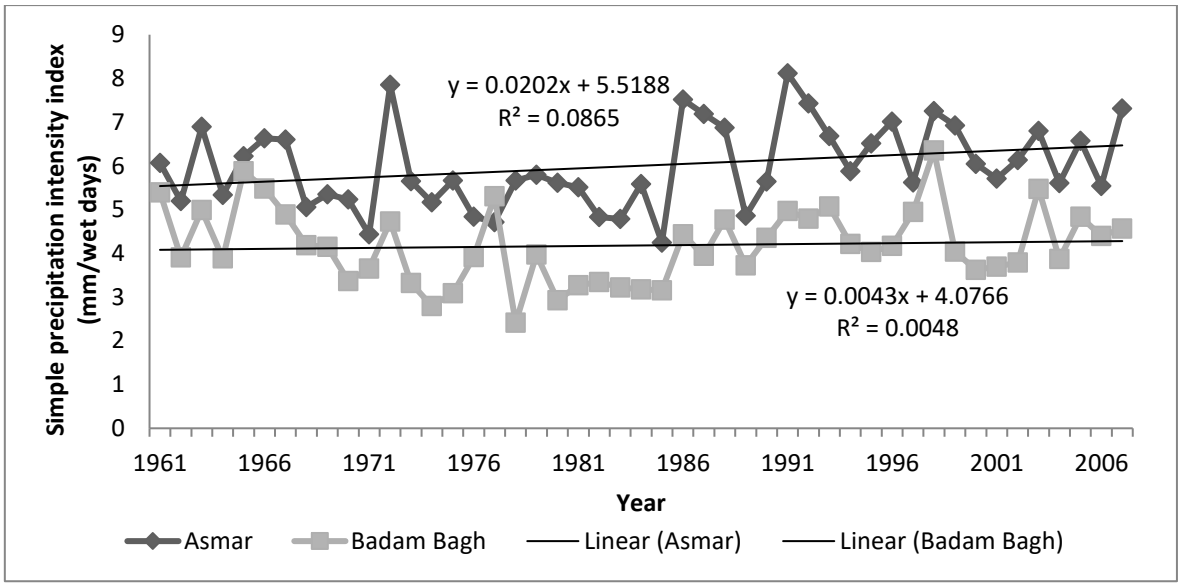

Figure 8.7 Simple precipitation intensity index of the sample districts

8.3 Field surveys using detailed questionnaires

During the field surveys, 60 farmers' households from Shakar Dara in Kabul and 60 farmers' household from Watapoor in Kunar were interviewed. The study was done during the first two weeks of October 2013.

A detailed questionnaire was prepared based on literature review and the specific characteristics of the selected districts (Annex 2). The questionnaire was made to gather information about the following items:

- Identification
- Land Information
- Irrigation system (Karez, canal, well, etc.)
- Crop information and crop calendar and its changes during the last ten years
- Livestock and associated changes during the last ten years
- Climate change indicators and causes
- Climate change impacts (with a focus on agriculture)
- Adaptation measures
- Farmers' needs and expectations from the government/other relevant agencies

8.4 Descriptive statistics based on the survey's results

The descriptive statistics approach, consisting of frequency and percentage, was used to analyze the qualitative and quantitative data obtained from the household questionnaire surveys. The results for each district were summarized separately but then the comparison was carried out between the two selected districts in order to understand the similarities and differences in responses. Comparison also was done between climate data (trends and values) and the farmers' perceptions. Field observations and other secondary data were used to understand, in greater detail, the farmers' perceptions and the adaptation measures taken by them.

Table 8.2 summarizes general information about the selected districts. All the respondents were male and most of them were illiterate (the head of the family was interviewed). It is

important to mention that most of the studies have shown a direct relation between the education level of the household head and the application of improved adaptation strategies (for example, Deressa et al., 2009). The dominant crop for both areas is wheat. Farmers in Shakar Dara had seen a greater increase in their income as compared to the Watapoor farmers, and this is because the former had shifted towards planting fruit trees, which are more beneficial based on the market price. Some of the farmers had a second job while being involved in farm activities. These secondary occupations were mainly shop keeping, taxi driving, government jobs, and other small businesses.

Table 8.2 General information on the sample districts

District	Respondents			Crop pattern in sample districts		
	Average Age (years)	Gender	Literacy rate of head of the family	Dominant Crops	Dominant Fruit Trees	Key changes during the last 10 years
Shakar Dara	53	Male	Negligible	Wheat, Barley, and Maize	Apple, Peach, and Grape	Rice has vanished, Wheat has decreased, Fruit trees have increased
Watapoor	47	Male	Negligible	Wheat, Maize, and Rice	Mulberry and Apricot	No significant change in the main crops

Table 8.3 presents the land information for both selected districts. The interviewed farmers in Shakar Dara had bigger land size compared to the ones in Watapoor. Most of the farmers owned their land. Farmers in Shakar Dara left some arable land uncultivated mainly due to lack of water. Watapoor had two crops per year planted in some parts of the land but in Shakar Dara, all the cultivated land had only one crop per year. Most of the farmers in Shakar Dara had access to canals as irrigation system but some of them, due to lack of access to the canal, were abstracting groundwater for irrigation. In Watapoor, all the farmers had access to canals.

Table 8.3 Land holding information

District	Land owned by household (%)	Average land size (ha)	Irrigated land (%)
Shakar Dara	83	3	100
Watapoor	57	1.1	79

Table 8.4 presents crop information for the current period and its changes, as compared to 10 years back. The results indicate that rice has completely vanished in Shakar Dara while there is not much change in Watapoor's crops. Wheat, barley, and maize are the main crops for both selected districts.

Table 8.4 Crop information in the sample districts

District	Current	10 years back
Shakar Dara	Wheat = 52% Maize = 14% Barely = 12% Others = 22%	Wheat = 42% Barely = 14% Rice = 12 Maize = 8% Others = 24%
Watapoor	Wheat = 54% Maize = 34% Rice = 10% Others = 2%	Wheat = 52% Maize = 32% Rice = 12% Others = 4%

To make policies for adapting to climate change, it is important to assess how farmers perceive long term changes in climate (Wheeler et al., 2013). Table 8.5 presents the changes in climatic parameters as they were perceived by the farmers in both selected districts. Most of the respondents said that temperature had increased. However, in Shakar Dara, a majority of the respondents claimed that the extreme heat of summer had decreased. To better understand their responses, another question was also added for each part: if they had any reasons/indicators for their response. For example, most people in Shakar Dara mentioned that the reason why they thought temperature had increased, compared to the past, was that snow was melting earlier than before on the close by mountains. From the trend analysis of climatic parameters and indices which have already been described, linkages were investigated using farmers' perceptions. These results are shown in Table 8.5. Wherever there is a difference between the farmers' perceptions with those trends, using indicators which were related by farmers, a possible reason has been added. For example, for Shakar Dara, the extreme hot during the summer is perceived to have decreased by the farmers but the trend of the number of summer days shows an increase. The farmers' perception might be due to having more shadow as a result of tree planting in the area, as was observed during the field survey.

The main impacts of climate change on water resources and agriculture from farmers' points of view in both selected districts are listed in Table 8.6. However, it needs to be mentioned that it is very difficult to differentiate other factors which might have influenced their responses, such as socio-economic factors. Heavy rains and increased floods were the main outcomes of climate change in Shakar Dara. The district also faced water loss/shortages but that could also be due to increased water usage in upstream areas. For Watapoor, farmers mentioned that they needed more water for irrigation as compared to the past and this could be due to increased evapotranspiration as a result of increased temperature.

Table 8.5 Perception of change in climate indicators (%)

District	Type	Indicator	Increased	Decreased	No change	Trend analysis of observations	Comment
Shakar Dara	Temperature	Extreme hot in summer	12	80	8	increased	Planting trees and more shadow
		Extreme cold in winter	8	85	7	decreased	
		Overall Temperature	92	2	7	increased	
	Precipitation	Precipitation intensity	18	72	10	increased	Planting trees and increased interception storage
		Precipitation quantity	0	90	10	increased	If consider only last 20 years it is decreased
	Water Resources	Groundwater level (Well)	0	100	0		
		Streamflow	0	100	0		
Watapoor	Temperature	Extreme hot in summer	60	3	37	decreased	
		Extreme cold in winter	58	0	42	no change	
		Overall Temperature	67	17	17	increased	
	Precipitation	Precipitation intensity	52	0	48	increased	
		Precipitation quantity	41	11	48	increased	
	Water Resources	Groundwater level (Well)	8	8	83		
		Streamflow	20	73	7		

Table 8.6 Perception of climate change impacts (%)

Major impact in Shakar Dara	**Total* (n = 60)**
Heavy rain and Flood	77
Water loss	67
Disease	55
Reduced soil fertility	43
Income loss	43
Less production/yield	42
Crop failure	35
Need more water for irrigation	33
Major impacts in Watapoor	**Total* (n = 60)**
Need more water for irrigation	92
Disease	78
Income loss	78
Water loss	68
Reduced soil fertility	68
Less production/yield	52
Heavy rain and Flood	43
Crop failure	25

* Multiple responses recorded

The adaptation measures taken by farmers in both areas are listed in Table 8.7. Among them, for the Watapoor district, the main adaptation measures are changing the crop calendar and also changing the type of crop planted. On the other hand, in Shakar Dara, the main adaptation strategies were shifting to tree planting along with changing the type of crop. Fosu-Mensah et al. (2012) found that most of the farmers are aware of climate change related issues but not all of them adopt adaptation strategies due to different reasons such as lack of funds to implement any adaptation measure. The suggestion for policymaking made then was to train more extension officers and provide more education on climate change and adaptation strategies. It was noted that farmers' perceptions about climate change and their responses take place in the context of various factors influencing agriculture and food security, such as current and past biophysical, socio-economic, and agronomic conditions (Thornton et al., 2011). Therefore, separating the responses to all these factors is difficult.

Table 8.7 Adaptation to changes in climate (%)

Shakar Dara district	**Applied**	**Other possible reasons rather than CC**
Tree planting	80	Market demand
Change in type of crop	73	Market demand
Irrigation during the night	60	
Increased use of groundwater	30	Population growth
Agroforestry	18	
deep tillage	18	
Decrease the irrigated lands	18	
Change in time of cropping	10	
Early harvesting	10	
Soil conservation activities	8	
Better irrigation system	7	
Watapoor district	**Applied**	
Change in time of cropping	88	
Change in type of crop	77	Market demand
Construction of dikes (or growing trees) along the field boundaries	55	
Deep tillage	25	
Increased use of groundwater	22	
Plantation in your home garden	10	
Construction of reservoirs and channels for ex-situ RWH	5	
Soil conservation activities	5	
Improved cook stove	2	
Agroforestry	2	

Farmers in both selected districts had many urgent needs and requests to the government, mainly to help them with providing farming input, machineries, and building more water related infrastructure (Table 8.8).

Table 8.8 Farming needs (%)

Shakar Dara district	Asked
Plants for gardening	50
Construction of dams and reservoirs	48
Seed and Fertilizer	37
Reconstruction of Canal	32
Pesticides and Medicines	32
Water Pumps	22
Modern Tools and Technologies	18
Watapoor district	**Asked**
Seed and Fertilizer	100
Reconstruction of Canal	85
Modern Tools and Technologies	63
Plants for gardening	52
Pesticides and Medicines	45
Better irrigation system	37
Water Pumps	3

8.5 Summary of the results

- Climate change has already been sensed by many farmers in the selected districts. To better understand the changes in historical climate that could then be compared with the farmers' perceptions of climate change, trend analysis of a few extreme climate indices was done. The results suggest that farmers' perceptions about climate change might not always be the same as the results of trend analysis. However, based on field observations, an effort has been made to explain the possible reasons/explanations for the differences.

- In general, as was expected from climate trend analysis, most of the farmers agree that temperature has increased but there is no equally clear trend for precipitation.

- While the amount of precipitation might not change significantly, water resources have decreased. This might be due to the changes in precipitation and runoff distribution. Broadly, the changes in the water resources in the study areas might be due to climate change or/and increase of water usage as a result of increased population.

- The main adaptation measure taken by farmers in Shakar Dara is tree planting while in Watapoor, farmers changed the crop type and crop calendar. Here, the main reason might not be only climate change but also market demands.

- The farmers have requested the government and/or other agencies to help them by providing farming inputs as well as constructing dikes, canals, and storage dams.

- Wheat is the most important crop in both selected districts.

CHAPTER 9
WHEAT YIELD UNDER FUTURE CLIMATE CONDITIONS

9.1 The AquaCrop model for wheat production

To simulate crop yield under future climate scenarios, the FAO AquaCrop model was used. AquaCrop is a useful tool to predict crop production under different water management scenarios such as rain-fed, deficit, or full irrigation conditions. Management strategies can also be investigated under present and future climatic scenarios using this model.

Wheat is a staple food grain for Afghans and it is culturally also very significant. It is cultivated in all the provinces, mainly for self-consumption. Wheat accounts for almost 2.7 to 3 million hectares of arable land, which is 80% of the planted areas under cereal cultivation in Afghanistan. The other main cereals are barley, maize, and rice. About 90% of wheat is planted during winter (October or November) and almost 80% of the total planted wheat is from irrigated land. The seeding rates range between 110-175 kg/ha for irrigated wheat, and 80-100 kg/ha for rain-fed wheat. The harvesting method is mostly by hand. Straw and grain have equal value since straw is very important as animal feed.

9.2 Data collection

The meteorological data were collected from the Afghanistan Meteorological Authority for the recent years (2008-2013). Bias corrected temperature and precipitation data from APHRODITE were also used for the baseline period of 1971 to 2000 for identifying the impacts of climate change on wheat yield. Three future time slices were used to compare with the baseline data (same as those used for the analysis of climate change described in Chapter 6).

The details of the agricultural practices in the selected districts were obtained from the Afghanistan Central Statistics Organization (CSO), the Afghanistan Ministry of Agriculture, Irrigation, and Livestock (MAIL) as well as the results of field surveys done during October 2013 for the current research.

Table 9.1 Dry yield for irrigated winter wheat in the sample districts

	Shakar Dara district	**Watapoor district**
Calendar	**Yield (ton/ha)**	**Yield (ton/ha)**
2005-2006	2.55	2.00
2006-2007	2.27	1.67
2007-2008	2.73	2.63
2008-2009	3.45	NA
2009-2010	3.29	2.25
2010-2011	2.97	NA
2011-2012	NA	2.39
2012-2013	3.20	2.25

Source: (Afghanistan Central Statistics Organization)

Figure 9.1 shows the crop calendar for winter wheat in Afghanistan. The selected districts for the field surveys are Shakar Dara and Watapoor, which are , respectively, in the central and eastern agro-climatic zones of the country.

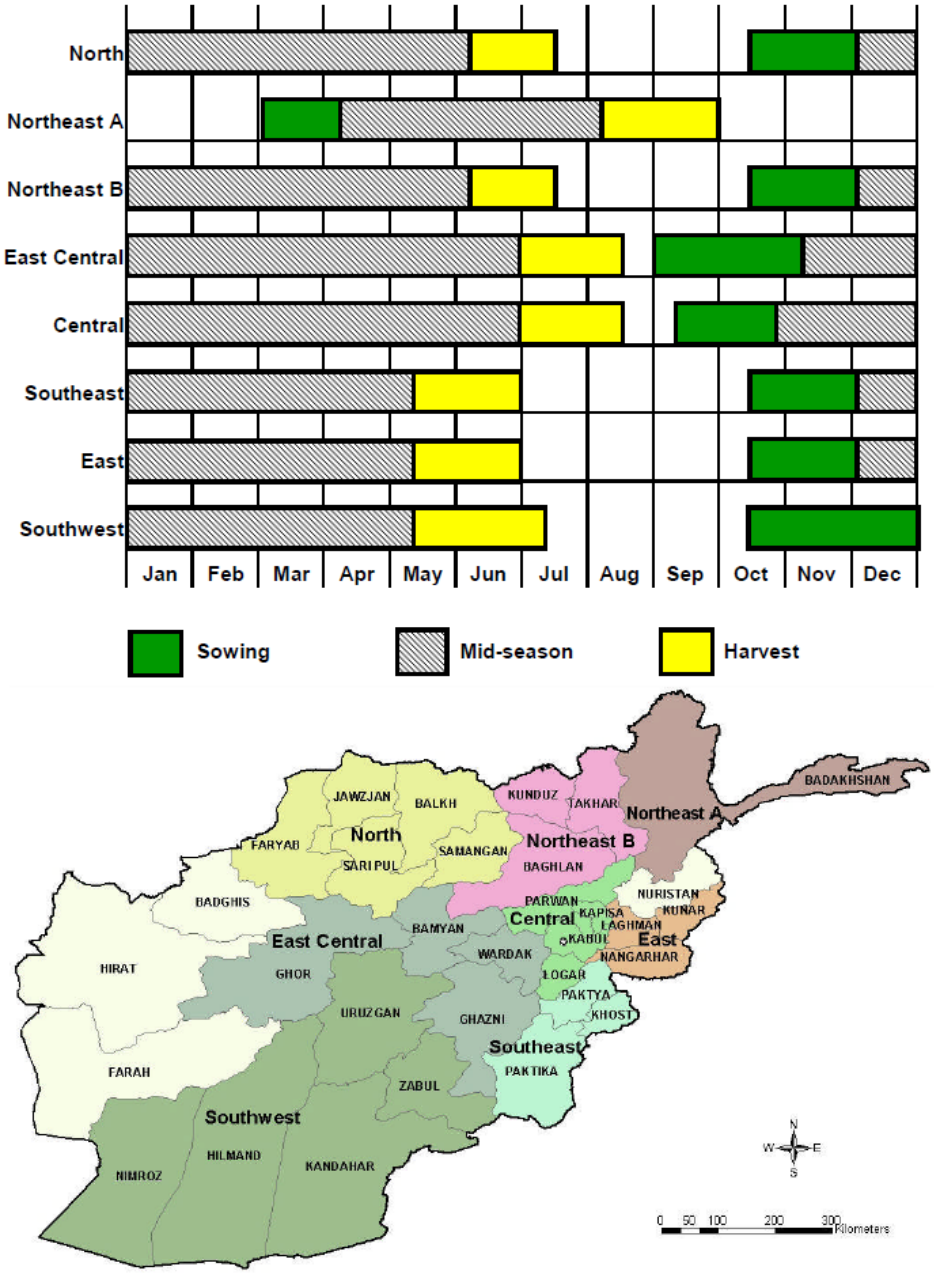

Figure 9.1 Regional crop calendars for winter wheat in Afghanistan and the reference map
Source: FEWS NET Afghanistan, USAID

For the crop model parameters, the default AquaCrop model for wheat was chosen as a starting point but the following key parameters were then modified to fit the local planting practices: planting density, sowing date, and the number of days to crop maturity. Two winter wheat varieties were selected for this study (Bezostaya for the Shakar Dara district and Solh-02 for the Watapoor district) and their details are shown in Table 9.2 (Hussain et al., 2008). The furrow irrigation method with 20 mm net application of water at 70 day intervals since the beginning of transplanting was selected as the irrigation type for the

calibration period for both districts. The transplanting date of winter wheat was selected to be October 15 for Shakar Dara and November 15 for Watapoor. The soil type in both study areas is loam, and this information is based on the USDA 2001 soil map for Afghanistan.

Table 9.2 Winter wheat varieties used in this study

Name	days to heading	days to maturity	heigh t (cm)	TKW (g)	potential yield (ton/ha)	planting date	harvesting date
Bezostaya	183	241	125	51	7.6	15-Oct	12-Jun
Solh-02	163	215	92	47	7.4	15-Nov	17-Jun

9.3 Calibration and validation of the crop model

The AquaCrop model was calibrated and validated based on 8 years of field data from 2005 to 2013 (Table 9.1). The model's performance criteria are presented in Table 9.3 for both calibration and validation periods (calibration: 2009 to 2013, and validation: 2005 to 2009).

Table 9.3 Model error statistics during calibration and validation of AquaCrop

	Selected districts	r^2	RMSE (ton/ha)
Calibration	Shakar Dara	0.92	0.12
	Watapoor	0.97	0.28
Validation	Shakar Dara	0.51	0.66
	Watapoor	0.88	0.50

Table 9.4 AquaCrop calibration parameters for winter wheat

Parameter	Shakar Dara	Watapoor	Units
Time to emergence	15	15	Day
Time to maximum canopy cover	161	137	Day
Time to maximum rooting depth	140	140	Day
Time to start of canopy senescence	183	161	Day
Time to maturity	241	215	Day
Time to flowering	170	161	Day
Length building up HI	68	42	Day
Duration of flowering	12	12	Day
Number of plants per ha	2,000,000	1,000,000	-
Initial canopy cover (CCo)	3	5	%
Maximum canopy cover (CCx)	90	54	%
Minimum effective root depth	0.3	0.3	m
Maximum effective root depth	1	1	m
Reference harvest index (HI_0)	45	36	%
Water productivity	15	15	gr/m^2
Base temperature	0	0	°C
Upper temperature	26	26	°C
Minimum T below which pollination starts to fail	5	5	°C
Maximum T below which pollination starts to fail	35	35	°C
Tmax and Tmin	daily data	daily data	°C
Rain	daily data	daily data	mm

9.4 Yield projections under future climate conditions

Description of the model's output

Climate-Crop-Soil water presented the most useful results of the model (Figure 9.1). It shows three graphs plotted as a function of time:

- The first (bottom of the figure) is the depletion of root zone soil water (Dr) with the three water stress thresholds (below the green line affecting canopy expansion; below the threshold for stomata, the red line, affecting Tr; and below the threshold, the yellow line, causing canopy senescence).

- The second is the corresponding expansion of green canopy cover (CC) and the potential CC under no stresses conditions.

- The third one shows the transpiration (Tr) of the canopy for the simulated CC and also the potential Tr.

In the menu, on the top corner, the biomass and yield are shown. The stresses due to water (both less or extra water use), temperature, soil fertility, and salinity are the other main outputs.

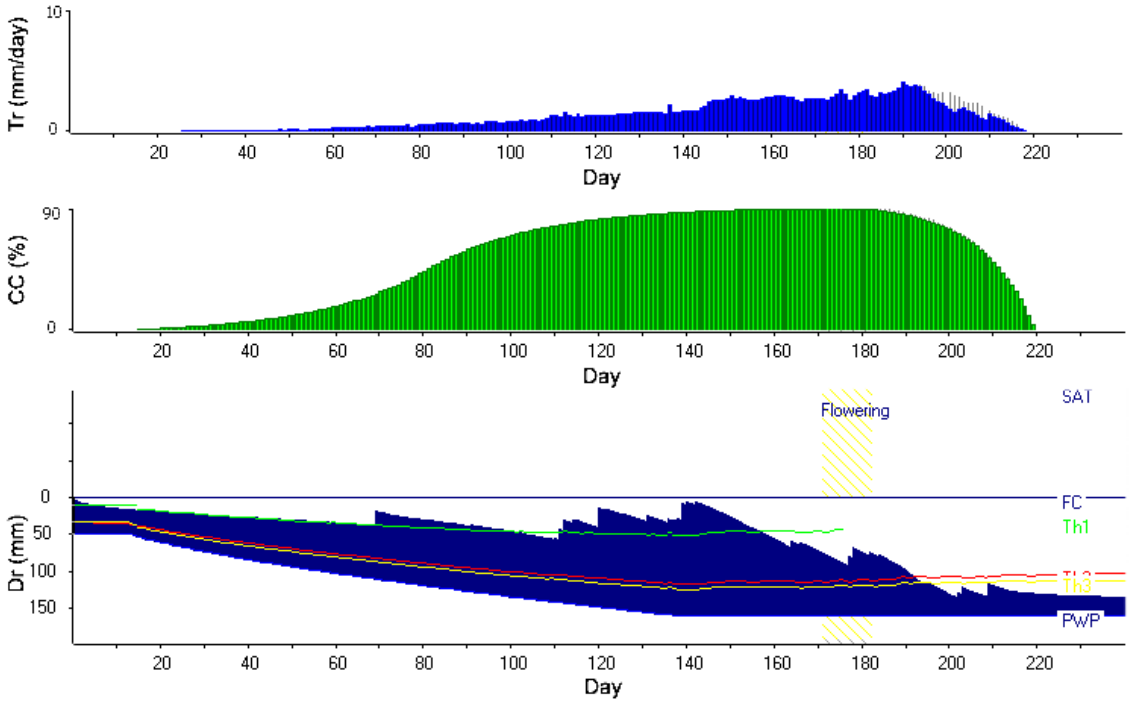

Figure 9.1 Main output from AquaCrop model

The results of the model are summarized in Table 9.5 for different climatic scenarios for both districts.

Table 9.5 Simulation results of winter wheat planted in irrigated lands

District	Time frame		Dry Yield (ton/ha)	Changes of yield (%)	Stresses (%)			ET_o (mm)	Rain (mm)	CO_2 (ppm)
					Temperature	Canopy Expansion	Stomatal closure			
Shakar Dara	Baseline		3.01		45	none	5	607	165	391
	RCP 4.5	2020s	3.24	7.5	43	none	5	612	161	424
		2050s	3.9	29.3	36	1	7	631	146	500
		2080s	4.33	43.6	31	1	8	643	147	532
	RCP 8.5	2020s	3.31	9.7	43	none	5	610	161	433
		2050s	4.4	45.9	34	1	6	637	153	574
		2080s	5.88	95.1	24	2	8	670	132	806
Watapoor	Baseline		2.15		10	none	none	671	582	391
	RCP 4.5	2020s	2.34	8.6	8	none	none	680	572	424
		2050s	2.69	24.7	4	none	1	698	532	500
		2080s	2.78	29	2	none	1	709	541	532
	RCP 8.5	2020s	2.39	10.7	7	none	none	679	572	433
		2050s	2.87	33.1	3	none	1	703	552	574
		2080s	3.38	57	1	none	1	734	477	806

The results of the model suggest that the future yield of winter wheat is more likely to increase as the stresses due to low temperature decrease.

In case of Shakar Dara, the future yield of winter wheat would increase between 7.5% to 43.6% over the 21st century under RCP 4.5 while these changes are predicted to be within 9.7% to 95.1 % under RCP 8.5 for the same period. For Watapoor, the future yield of winter wheat would increase between 8.6% to 29.0% over the 21st century under RCP 4.5 while these changes are predicted to be within 10.7% to 57.0 % under RCP 8.5 for the same period.

9.5 Optimizing the planting date and net application of water for irrigation

Figures 9.2 and 9.3 show, respectively, the results of applying different agro-adaptation measures, namely shifting the planting date and applying different levels of irrigation, to winter wheat in the Shakar Dara district. However, supplying more irrigation can be a questionable move since population in the future will increase but as the results of hydrological modeling showed, there will be an increase in future water availability, therefore this measure was also tested and might be a realistic scenario for the future. The changes in wheat yield were obtained from the calibrated AquaCrop model. The results suggest that after the application of a certain level of net irrigation water, the increase in wheat yield would be constant. Shifting the planting date can either increase or decrease the yield, which would mainly be due to changes in the level of temperature stresses. In the case of Shakar Dara, under future climatic conditions, early planting might have positive impacts on yield in some cases but overall, it appears that the current planting date is the best.

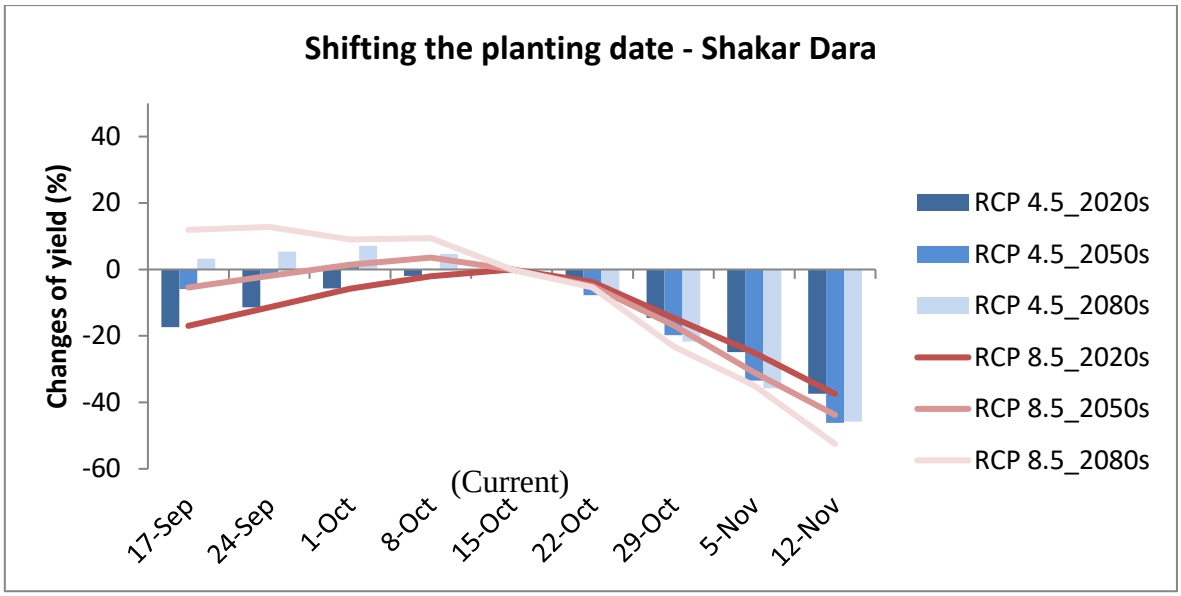

Figure 9.2 Changes in wheat yield by shifting the planting date as an adaptation measure

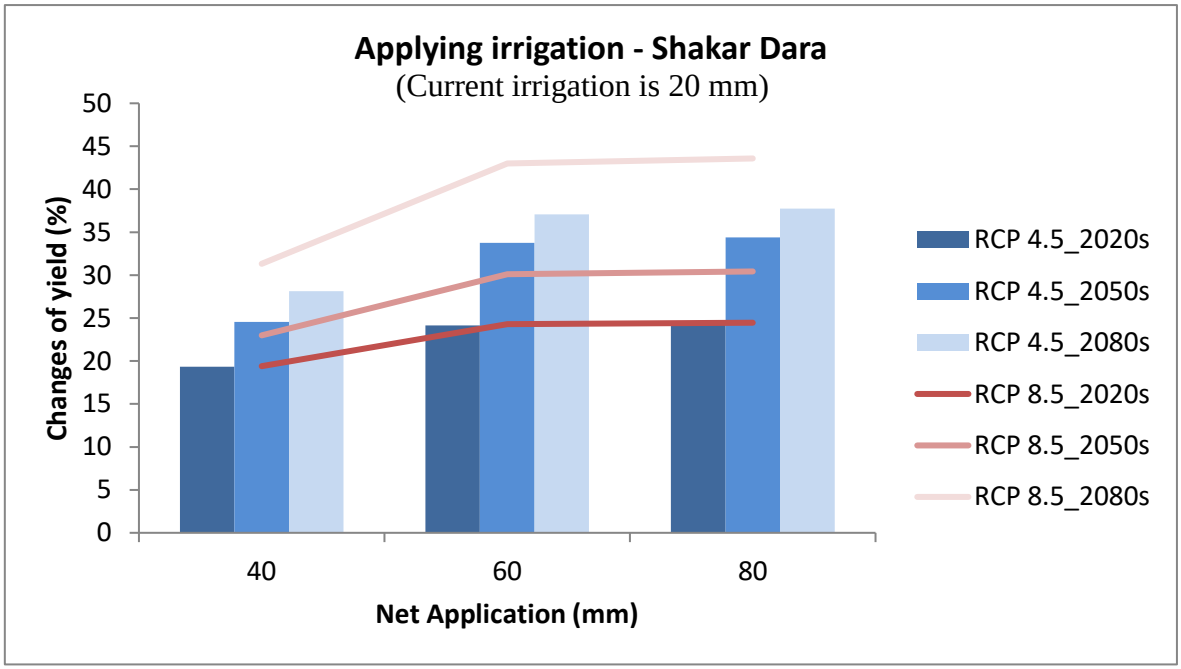

Figure 9.3 Changes in wheat yield by applying different irrigation levels as an adaptation measure

Similar to the Shakar Dara district, two adaptation measures were investigated for the Watapoor district to investigate the impacts of these measures on the yield of winter wheat. As is shown in Figure 9.4, early planting does not have much impact on yield while late planting might significantly decrease the yield. The results of applying different irrigation levels are also shown in Figure 9.5. Compared to the Shakar Dara district, in Watapoor, supplying more water for irrigation has a much lesser impact on increasing the wheat yield.

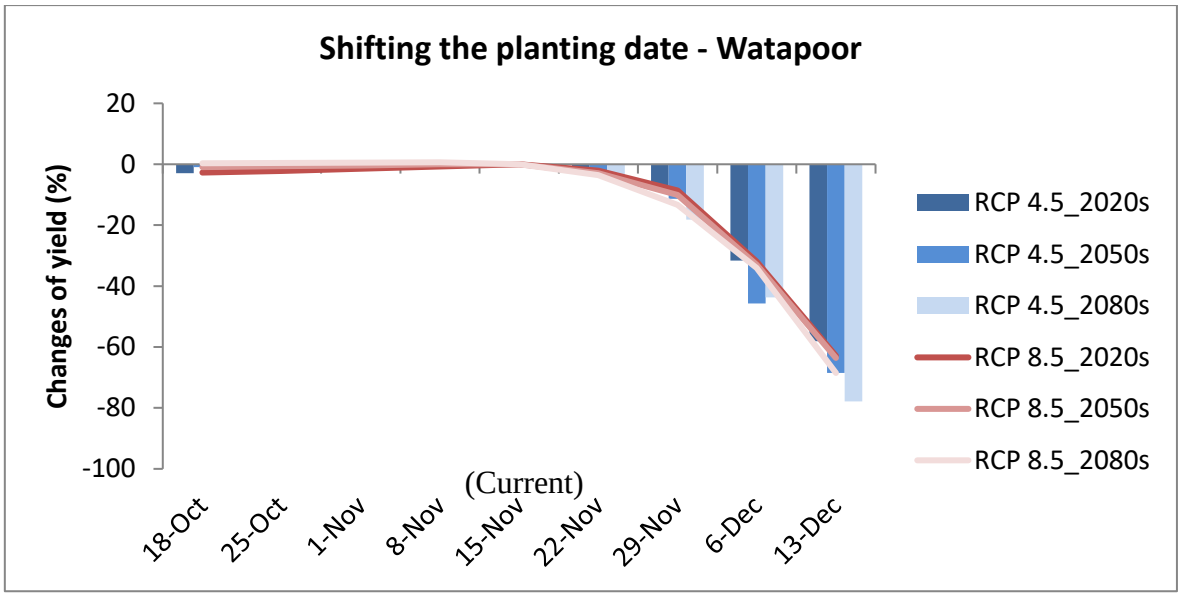

Figure 9.4 Changes in wheat yield by shifting the planting date as an adaptation measure

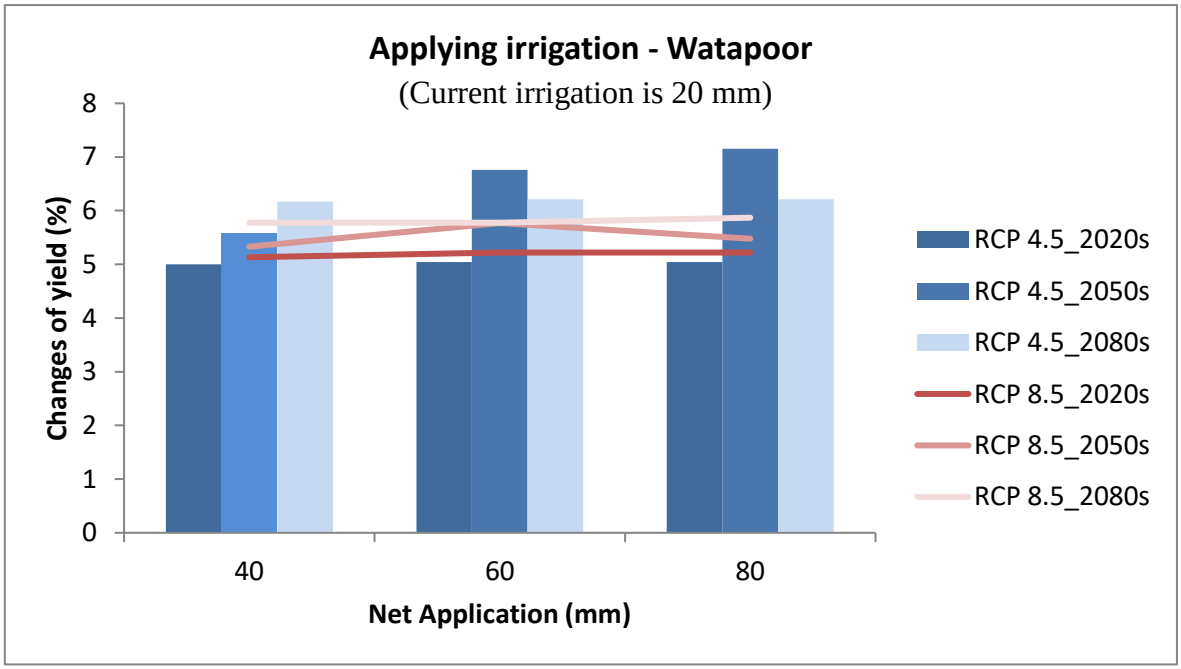

Figure 9.5 Changes in wheat yield by applying different irrigation levels as an adaptation measure

9.6 Summary of the results

- AquaCrop modeling results for winter wheat show that under future climate change scenarios, the yield will increase. The main reason for this increase is the decrease in the stresses related to cold temperature.

- In case of Shakar Dara, the future yield of winter wheat would increase between 7.5% to 43.6% over the 21st century under RCP 4.5 while these changes are predicted to be within 9.7% to 95.1 % under RCP 8.5 for the same period. For Watapoor, the future yield of winter wheat would increase between 8.6% to 29.0% over the 21st

century under RCP 4.5 while these changes are predicted to be within 10.7% to 57.0 % under RCP 8.5 for the same period.

- Shifting the planting date and applying different levels of irrigation were examined by the AquaCrop model and the results show that these measures can be effective in maximizing the yield.

- The results suggest that after the application of a certain level of net irrigation water, the increase in wheat yield would be constant. Shifting the planting date can either increase or decrease the yield, which would mainly be due to changes in the level of temperature stresses.

CHAPTER 10
SUMMARY, CONCLUSIONS AND RECOMMENDATIONS

10.1 Summary

Climate change affects the patterns of temperature and precipitation. As a result, other variables, such as water availability and its spatial and temporal distributions also get affected. Climate change is also likely to intensify the global hydrological cycle, which can increase the risk of floods and droughts. Climate change also affects the function, operation, and management practices of existing water infrastructure. Adverse impacts of climate change on water resources systems intensify the effects of other factors such as increased population, heightened economic activities, and land use changes. Afghanistan is a semi-arid and mountainous country which faced three decades of conflict. It is one of the most vulnerable countries in the world to climate change due to very limited capacity to address the impacts of climate change. It has been also considered as a data-scarce region both temporally and spatially with limited capability to measure hydro-meteorological parameters with in situ gauges. This research focused on Kabul basin which lies in the northeast quarter of Afghanistan. Kabul basin covers only twelve percent of the national territory, but it single-handedly drains one-fourth of the total annual water flow in Afghanistan and accounts for thirty five percent of the population's sustenance.

The main objective of this study was to analyze the impacts of climate change on water resources and agriculture in the data-scarce Kabul basin.

First of all the suitability of high-resolution gridded temperature and precipitation datasets was investigated to supplement the climatic parameters for Kabul basin. The gridded precipitation time series data in CPC-RFE, GSMaP-MVK, TRMM 3B42, and APHRODITE were validated using the data from recently established rain gauges over the Kabul basin in Afghanistan from 2004 to 2007. These products were evaluated at different spatial and temporal resolutions (daily, monthly, and annual). The validation approach used here includes continuous (mean absolute error [MAE], root mean square error [RMSE], correlation [r], and multiplicative bias [Mbias]) and categorical (probability of detection [POD] and false alarm ratio [FAR]) verification statistics. Furthermore, the spatial performance is evaluated by mapping the data and analyzing the distribution of precipitation as a function of elevation. The results of continuous and categorical verification statistics suggest that the APHRODITE dataset performs better than other gridded datasets for the basin. APHRODITE temperature data is also found very suitable for the study area after comparison with the observations.

The results of trend analysis suggest that the temperature has been increased over last five decades while such a clear trend for precipitation is not detected for the study area.

Predictions of precipitation and temperature for the future under different RCP (Representative Concentration Pathways) scenarios were investigated using data from 8 recent CMIP5-GCMs (Coupled Model Intercomparison Project Phase 5-General Circulation Models) after bias correction and downscaling. The GCMs' outputs were extracted from the grids based on their corresponding stations (same as those in the previous chapter). These values were downscaled and bias corrected to the stations using the linear downscaling method. At the end, the values of all the stations were averaged over the Kabul basin for each month and the changes calculated were compared to the baseline values. The values were also averaged over the seasons, winter and summer. Winter starts in November and

ends by April. Summer is also a period of six months, from May to October. Based on its better performance, the linear method was selected for bias correction. The baseline period of 1971 to 2000 was selected for this study. Three periods—Early Future (2011-2040), Mid Future (2041-2070), and Late Future (2071-2100)—were selected as future periods to be compared with the baseline values and to summarize the results. To show variability in the future, the results were also calculated on yearly and decadal bases. The median of the results from all 8 GCMs suggests an increasing trend in maximum and minimum temperature in the future, as compared to the baseline. The increases for maximum temperature range from +1.7°C to +4.1°C under RCP 4.5 and +1.7°C to +6.3°C under RCP 8.5. The increases for minimum temperature range from +1.5°C to +3.8°C under RCP 4.5 and +1.4°C to +6.0°C under RCP 8.5. The projections for precipitation mainly show a decreasing trend under both RCPs, with variations ranging from -19% to -6% under RCP 4.5 and -18% to 3% under RCP 8.5. Results suggest that the mean annual values of precipitation under RCP 4.5 range from 366 to 400 mm/yr and from 378 to 412 mm/yr under RCP 8.5. The mean values of maximum temperature in the future are predicted to be between 24.3 to 26.5°C under RCP 4.5 and 24.3 to 28.8°C under RCP 8.5 while the minimum temperature range is predicted to vary from 9.7 to 11.5°C under RCP 4.5 and 9.7 to 13.9°C under RCP 8.5. Based on the baseline observations (of 1971 to 2000), most of the precipitation occurs during winter. March is the wettest month, followed by April. The warmest month is July. All GCM ensembles show almost the same trend as the baseline values. However, it is predicted a slight decrease in precipitation during winter and an increase in precipitation during summer under both RCPs.

The J2000 hydrological model was used to reproduce the hydrological dynamics of the study basin. The model's results of the calibration and validation periods suggest that the model performed well and can be used to reproduce the hydrological dynamics of the basin. The contribution of snow- and ice-melt to the outlet runoff is estimated to be around 85% during the simulation period (1969 to 1979). The highest portion of the runoff components is for surface runoff (71.7%) while the baseflow accounts for 8.6% of the total runoff.

For the assessment of future climate predictions on water resources, bias corrected precipitation and temperature were used as inputs for the hydrological model. As per the predictions, future runoff ranges between -14% and +49% under RCP 4.5 and between -16% and +100% under RCP 8.5 during the 21st century. The median values varying between -9% and +22%. Overall, the results suggest that future runoff is more likely to increase. This is mainly due to the increase in temperature, which will cause more snow- and ice-melt. The results of the seasonal distribution of monthly future runoff under RCP 4.5 and RCP 8.5 show an increasing trend in runoff during the next decades under both RCP scenarios in both seasons (winter and summer). The results of monthly changes in future runoff suggest that the percentage of change is higher during winter (Nov-Apr) but as the amount of runoff is low during this season, these changes won't create much difference. During the Early Future period (2020s) and the Mid Future period (2050s), the runoff might decrease slightly in some months from January to May but there will, overall, be an increase in runoff.

The impacts of climate change on agriculture sector were investigated through a field survey and crop modeling approach to identify the problems and opportunities. Two field surveys using questionnaire were done to understand the farmers' perception to climate change and their adaptation measures. Based on the surveys, climate change has already been sensed by many farmers in the selected districts. To better understand the changes in historical climate that could then be compared with the farmers' perceptions of climate change, trend analysis of a few extreme climate indices was done. The results suggest that farmers' perceptions about climate change might not always be the same as the results of trend analysis. However,

based on field observations, an effort has been made to explain the possible reasons/explanations for the differences. The main adaptation measures taken by farmers were tree planting and changing the crop type and crop calendar.

The AquaCrop model was used to determine the impacts of climate change on wheat yield. Wheat is the most dominant crop in the region and accounts for 80% of planted areas of cereals in Afghanistan. The results showed an increase in wheat production under future scenarios. Shifting the planting date and applying different levels of irrigation were examined by the AquaCrop model and the results show that these measures can be effective in maximizing the yield. After the application of a certain level of net irrigation water, the increase in wheat yield would be constant. Shifting the planting date can either increase or decrease the yield, which would mainly be due to changes in the level of temperature stresses.

10.2 Conclusions

The main conclusions based on the results of this study are as follows:

- APHRODITE precipitation and temperature datasets performed better than other gridded datasets examined in this study, based on the results of categorical and continuous verification statistics, and can be used with high confidence to supplement the data for Kabul basin.

- The results of trend analysis showed that the temperature in the region has increased over last five decades. However a clear trend for precipitation was not detected for Kabul basin.

- The median of the results from all 8 GCMs suggests an increasing trend in maximum and minimum temperature in the future, as compared to the baseline. The increases for maximum temperature range from +1.7°C to +4.1°C under RCP 4.5 and +1.7°C to +6.3°C under RCP 8.5. The increases for minimum temperature range from +1.5°C to +3.8°C under RCP 4.5 and +1.4°C to +6.0°C under RCP 8.5. The projections for precipitation mainly show a decreasing trend under both RCPs, with variations ranging from -19% to -6% under RCP 4.5 and -18% to 3% under RCP 8.5.

- The results of J2000 hydrological model during the calibration and validation periods suggest that the model performed well and can be used to reproduce the hydrological response of the basin.

- As per the predictions, future runoff ranges between -14% and +49% under RCP 4.5 and between -16% and +100% under RCP 8.5 during the 21st century. The median values varying between -9% and +22%.

- Based on the surveys, climate change has already been sensed by many farmers in the selected districts. Farmers' perceptions about climate change were not always the same as the results of trend analysis. The main adaptation measures taken by farmers were tree planting and changing the crop type and crop calendar.

- Based on the results of AquaCrop model for winter wheat, which is the most dominant crop in the study area, the yield would be increased under future scenarios mainly due to decreasing the temperature stresses. Moreover, the impacts of shifting

the planting date and using full or deficit irrigation also were investigated and the results showed that those methods can be effective to maximize the yield.

10.3 Contribution of this study

- This is the first study which analyzed the suitability of gridded temperature and precipitation data (from global datasets/remote sensed products) for Kabul basin which is sparsely observed part of the world. The results lead to better understand the performance of such gridded datasets for mountainous regions. The methodology framework developed here can be followed for other data-scarce regions.

- The assessment of impacts of climate change on water resources for the study area was done for the first time using multi GCMs which cover a wide range of uncertainty in future projections of temperature and precipitation and thus on water availability.

- Linkage of field surveys with the results of modeling and trend analysis was done for the first time on study area.

10.4 Recommendations

Based on the results of this study the following recommendations were made:

10.4.1 Recommendations based on the study results

- The future projections of climatic parameters are highly uncertain. Therefore, policy makers should include a range of projections while making the decisions for adaptation plans and strategies.

- Temperature is projected to increase in future for the study area but the results suggest that it might create further opportunities due to increase in the water availability and decrease in the cold temperature stress for the crops. However lack of infrastructures might lead to further problems due to the possibility of more frequent and extreme floods and droughts.

- This study can be used as an outline for other river basins in Afghanistan.

10.4.2 Recommendations for further research

- Hydro-climatic data collection activities have recently resumed in Afghanistan after three decades of conflict. Therefore more focus should be given towards data quality and updating the study by latest available observations especially for higher altitudes of the region where there is no gauging station at the moment.

- The impacts of other changing factors such as land use, sediment transport as well as socio-economic should be incorporated along with the impacts of climate change to make the study more comprehensive.

- It is projected to have more water availability due to the increased snow- and glacier-melt in the study area. But after a certain period, as the extent of glaciers and permanent snow might shrink which leads to a decrease in water availability.

Therefore, more studies considering the dynamics of glaciers should be done for the region.

- To use the crop modeling and investigating the adaptation measures, field experiments should be done to check the validity of suggested arguments.

REFERENCES

Abadzadesahraei, S., & Sui, J. (2016). Potential Impacts of Climate Change on Water Resources in British Columbia Communities. *MDPI*, (26), 1–24. http://doi.org/10.3390/w8010023

Agarwal, A., Babel, M. S., Maskey, S., Shrestha, S., Kawasaki, A., & Tripathi, N. K. (2015). Analysis of temperature projections in the Koshi River Basin, Nepal. *International Journal of Climatology*, *279*(April 2015), n/a-n/a. http://doi.org/10.1002/joc.4342

Angus, J. E. (1994). The probability integral transform and related results. *SIAM Review*, *36*(4), 652–654.

Arnell, N. W., van Vuuren, D. P., & Isaac, M. (2011). The implications of climate policy for the impacts of climate change on global water resources. *Global Environmental Change*, *21*(2), 592–603.

Artan, G., Gadain, H., Smith, J. L., Asante, K., Bandaragoda, C. J., & Verdin, J. P. (2007). Adequacy of satellite derived rainfall data for stream flow modeling. *Natural Hazards*, *43*(2), 167–185. http://doi.org/10.1007/s11069-007-9121-6

Azizi, P. M. (2002). Special lecture on water resources in Afghanistan. *Ministry of Irrigation, Water Resources and Environment, Kabul, Afghanistan*.

Bajracharya, S. R., Palash, W., Shrestha, M. S., Khadgi, V. R., Duo, C., Das, P. J., & Dorji, C. (2014). Systematic Evaluation of Satellite-Based Rainfall Products over the Brahmaputra Basin for Hydrological Applications. *Advances in Meteorology*.

Basistha, A., Arya, D. S., & Goel, N. K. (2008). Spatial distribution of rainfall in Indian Himalayas - A case study of Uttarakhand Region. *Water Resources Management*, *22*, 1325–1346. http://doi.org/10.1007/s11269-007-9228-2

Bates, B. C., Kundzewicz, Z. W., Wu, S., & Palutikof, J.P., E. (2008). *Climate Change and Water*. *Technical Paper of the Intergovernmental Panel on Climate Change*. Geneva.

Beekma, J., & Fiddes, J. (2011). Afghanistan human development report.

Beven, K., & Binley, A. (1992). The future of distributed models : model calibration and uncertainty prediction. *Hydrological Processes*, *6*(May 1991), 279–298.

Bhatt, B. C., & Nakamura, K. (2005). Characteristics of Monsoon Rainfall around the Himalayas Revealed by TRMM Precipitation Radar. *Monthly Weather Review*, *133*(1), 149–165. http://doi.org/10.1175/MWR-2846.1

Bird, D. N., Benabdallah, S., Gouda, N., Hummel, F., Koeberl, J., La Jeunesse, I., … Woess-Gallasch, S. (2015). Modelling climate change impacts on and adaptation strategies for agriculture in Sardinia and Tunisia using AquaCrop and value-at-risk. *Science of The Total Environment*, *543*, 1019–1027. http://doi.org/10.1016/j.scitotenv.2015.07.035

Boé, J., Terray, L., Habets, F., & Martin, E. (2007). Statistical and dynamical downscaling of the Seine basin climate for hydro-meteorological studies. *International Journal of Climatology*, *27*(12), 1643–1655.

Brekke, L. D. (2009). Climate change and water resources management: A federal perspective. *DIANE Publishing*.

Brown, I., Towers, W., Rivington, M., & Black, H. (2008). Influence of climate change on agricultural land-use potential: adapting and updating the land capability system for

Scotland. *Climate Research*, *37*, 43–57. http://doi.org/10.3354/cr00753

Burton, I. (1996). The Growth of Adaptation Capacity: Practice and Policy. In J. Smith, N. Bhatti, G. Menzhulin, R. Benioff, M. Campos, B. Jallow, … R. K. Dixon (Eds.), *Adapting to Climate Change SE - 6* (pp. 55–67). Springer New York. http://doi.org/10.1007/978-1-4613-8471-7_6

Burton, I., Diringer, E., & Smith, J. (2006). *Adaptation to Climate Change: international policy options*. Pew Center on Global Climate Change Arlington, VA.

Candela, L., Tamoh, K., Olivares, G., & Gomez, M. (2012). Modelling impacts of climate change on water resources in ungauged and data-scarce watersheds. Application to the Siurana catchment (NE Spain). *The Science of the Total Environment*, *440*, 253–60. http://doi.org/10.1016/j.scitotenv.2012.06.062

Cibin, R., Athira, P., Sudheer, K. P., & Chaubey, I. (2013). Application of distributed hydrological models for predictions in ungauged basins : a method to quantify predictive uncertainty. *Hydrological Processes*. http://doi.org/10.1002/hyp

Cohn, T. a., & Lins, H. F. (2005). Nature's style: Naturally trendy. *Geophysical Research Letters*, *32*(23), L23402. http://doi.org/10.1029/2005GL024476

CSO. (2014). *Statistical Yearbook*. Kabul. Retrieved from http://cso.gov.af/

Davies, E. G. R., & Simonovic, S. P. (2011). Global water resources modeling with an integrated model of the social–economic–environmental system. *Advances in Water Resources*, *34*(6), 684–700. http://doi.org/10.1016/j.advwatres.2011.02.010

De Lavenne, A., Boudhraâ, H., & Cudennec, C. (2015). Streamflow prediction in ungauged basins through geomorphology-based hydrograph transposition. *Hydrology Research*, *46*(2), 291–302.

Deb, P., Shrestha, S., & Babel, M. S. (2015). Forecasting climate change impacts and evaluation of adaptation options for maize cropping in the hilly terrain of Himalayas: Sikkim, India. *Theoretical and Applied Climatology*, *121*(3–4), 649–667. http://doi.org/10.1007/s00704-014-1262-4

Deressa, T. T., Hassan, R. M., Ringler, C., Alemu, T., & Yesuf, M. (2009). Determinants of farmers' choice of adaptation methods to climate change in the Nile Basin of Ethiopia. *Global Environmental Change*, *19*(2), 248–255.

Dinku, T., Chidzambwa, S., Ceccato, P., Connor, S. J., & Ropelewski, C. F. (2008). Validation of high-resolution satellite rainfall products over complex terrain. *International Journal of Remote Sensing*, *29*(14), 4097–4110.

Dinku, T., Ruiz, F., Connor, S. J., & Ceccato, P. (2010). Validation and intercomparison of satellite rainfall estimates over Colombia. *Journal of Applied Meteorology and Climatology*, *49*(5), 1004–1014. http://doi.org/10.1175/2009JAMC2260.1

Ebert, E. E., Janowiak, J. E., & Kidd, C. (2007). Comparison of Near-Real-Time Precipitation Estimates from Satellite Observations and Numerical Models. *Bulletin of the American Meteorological Society*, *88*(1), 47–64. http://doi.org/10.1175/BAMS-88-1-47

Favre, R., & Kamal, G. M. (2004). Watershed atlas of Afghanistan. *Kabul: Ministry of Irriga*.

Flato, G., Marotzke, J., Abiodun, B., Braconnot, P., Chou, S. C., Collins, W., …

Rummukainen, M. (2013). Evaluation of Climate Models. *In: Climate Change 2013: The Physical Science Basis. Contribution of Working Group I to the Fifth Assess- Ment Report of the Intergovernmental Panel on Climate Change [Stocker, T.F., D. Qin, G.-K. Plattner, M. Tignor, S.K. Allen, J. Boschung, A. Nauels, Y.*

Flugel, W. (1995). Delineating hydrological response units by geographical information system analyses for regional hydrological modelling using prms / mms in the drainage basin of the river brol, Germany. *Hydrological Processes*, *9*(January 1994), 423–436.

Fosu-Mensah, B. Y., Vlek, P. L. G., & Vlek, P. L. G. (2012). Farmers ' perception and adaptation to climate change : a case study of Sekyedumase district in Ghana. *Environment, Development and Sustainability*, 495–505. http://doi.org/10.1007/s10668-012-9339-7

Frenierre, J. L., & Mark, B. G. (2014). A review of methods for estimating the contribution of glacial meltwater to total watershed discharge. *Progress in Physical Geography*, *38*(2), 173–200. http://doi.org/10.1177/0309133313516161

Geerts, S., Raes, D., Garcia, M., Miranda, R., Cusicanqui, J. A., Taboada, C., … Condori, O. (2009). Simulating yield response of quinoa to water availability with AquaCrop. *Agronomy Journal*, *101*(3), 499–508.

Gitau, M. W., & Chaubey, I. (2010). Regionalization of SWAT Model Parameters for Use in Ungauged Watersheds. *Water*, *2*(4), 849–871. http://doi.org/10.3390/w2040849

Gleckler, P. J., Taylor, K. E., & Doutriaux, C. (2008). Performance metrics for climate models. *Journal of Geophysical Research: Atmospheres*, *113*(D6).

Gleick, P. H. (1986). Methods for evaluating the regional hydrologic impacts of global climatic changes. *Journal of Hydrology*, *88*(1), 97–116.

Gudmundsson, L., Bremnes, J. B., Haugen, J. E., & Engen-Skaugen, T. (2012). Technical Note: Downscaling RCM precipitation to the station scale using statistical transformations-a comparison of methods. *Hydrology & Earth System Sciences*, *16*(9).

Habib, H. (2014). Water related problems in Afghanistan. *International Journal of Educational Studies*, *1*(3), 137–144.

Hay, L. E., Wilby, R. L., & Leavesley, G. H. (2000). A comparison of delta change and downscaled GCM scenarios for three mounfainous basins in the United States. *Journal of the American Water Resources Association*, *36*(2), 387–397.

Helfer, F., Lemckert, C., & Zhang, H. (2012). Impacts of climate change on temperature and evaporation from a large reservoir in Australia. *Journal of Hydrology*, *475*, 365–378.

Hrachowitz, M., Savenije, H. H. G., Blöschl, G., McDonnell, J. J., Sivapalan, M., Pomeroy, J. W., … Cudennec, C. (2013). A decade of Predictions in Ungauged Basins (PUB)—a review. *Hydrological Sciences Journal*, *58*(6), 1–58. http://doi.org/10.1080/02626667.2013.803183

Huntington, T. G. (2006). Evidence for intensification of the global water cycle: Review and synthesis. *Journal of Hydrology*, *319*(1–4), 83–95. http://doi.org/10.1016/j.jhydrol.2005.07.003

Hussain, M., Khan, S. B., Anwar, J., Iqbal, M. M., Muhammad, F., Hussain, F., & Qayyuam, A. (2008). A new high yielding disease resistant wheat variety Seher 06. *Pakistan Journal of Phytopathology (Pakistan)*.

Iglesias, A., Avis, K., Benzie, M., Fisher, P., Harley, M., Hodgson, N., … Webb, J. (2007). *AEA Energy & Environment - Adaptation to climate change in the agricultural sector*.

Iglesias, A., Garrote, L., Diz, A., Schlickenrieder, J., & Martin-Carrasco, F. (2011). Re-thinking water policy priorities in the Mediterranean region in view of climate change. *Environmental Science & Policy*, *14*(7), 744–757. http://doi.org/10.1016/j.envsci.2011.02.007

Kamal-Heikman, S., Derry, L. a., Stedinger, J. R., & Duncan, C. C. (2007). A Simple Predictive Tool for Lower Brahmaputra River Basin Monsoon Flooding. *Earth Interactions*, *11*(21), 1–11. http://doi.org/10.1175/EI226.1

Kawasaki, S., Watanabe, F., Suzuki, S., Nishimaki, R., & Takahashi, S. (2012). Current Situation and Issues on Agriculture of Afghanistan. *Journal of Arid Land Studies*, *348*, 345–348.

Keskinen, M., Chinvanno, S., Kummu, M., Nuorteva, P., Snidvongs, a., Varis, O., & Västilä, K. (2010). Climate change and water resources in the Lower Mekong River Basin: putting adaptation into the context. *Journal of Water and Climate Change*, *1*(2), 103. http://doi.org/10.2166/wcc.2010.009

Kour, R., Patel, N., & Krishna, A. P. (2016). Climate and hydrological models to assess the impact of climate change on hydrological regime: a review. *Arabian Journal of Geosciences*, *9*(9), 1–31.

Krause, P., Bende-Michl, U., Fink, M., Helmschrot, J., Kralisch, S., & Künne, A. (2009). Parameter sensitivity analysis of the JAMS / J2000-S model to improve water and nutrient transport process simulation - a case study for the Duck catchment in Tasmania. *18th World IMACS / MODSIM Congress*, (July), 3179–3186.

Kumar, V., & Jain, S. K. (2010). Trends in seasonal and annual rainfall and rainy days in Kashmir Valley in the last century. *Quaternary International*, *212*(1), 64–69.

Lashkaripour, G. R., & Hussaini, S. a. (2007). Water resource management in Kabul river basin, eastern Afghanistan. *The Environmentalist*, *28*(3), 253–260. http://doi.org/10.1007/s10669-007-9136-2

Lee, R. (2011). *Presentation on Extratropical storm tracks in some of the CMIP5 Models*.

Lioubimtseva, E., & Henebry, G. M. (2009). Climate and environmental change in arid Central Asia: Impacts, vulnerability, and adaptations. *Journal of Arid Environments*, *73*(11), 963–977. http://doi.org/10.1016/j.jaridenv.2009.04.022

Maxino, C. C., McAvaney, B. J., Pitman, A. J., & Perkins, S. E. (2008). Ranking the AR4 climate models over the Murray-Darling Basin using simulated maximum temperature, minimum temperature and precipitation. *International Journal of Climatology*, *28*(8), 1097–1112.

Mcsweeney, C., New, M., & Lizcano, G. (2007). *UNDP Climate Change Country Profiles - Afghanistan*.

Meinshausen, M., Smith, S. J., Calvin, K., Daniel, J. S., Kainuma, M. L. T., Lamarque, J.-F., … Vuuren, D. P. P. (2011). The RCP greenhouse gas concentrations and their extensions from 1765 to 2300. *Climatic Change*, *109*(1–2), 213–241. http://doi.org/10.1007/s10584-011-0156-z

Montanari, A., & Toth, E. (2007). Calibration of hydrological models in the spectral domain:

An opportunity for scarcely gauged basins? *Water Resources Research*, *43*(5), n/a-n/a. http://doi.org/10.1029/2006WR005184

Moretti, G., & Montanari, A. (2008). Inferring the flood frequency distribution for an ungauged basin using a spatially distributed rainfall-runoff model. *Hydrology and Earth System Sciences*, *12*(4), 1141–1152.

Mukherjee, S., Joshi, R., Prasad, R. C., Vishvakarma, S. C. R., & Kumar, K. (2015). Summer monsoon rainfall trends in the Indian Himalayan region. *Theoretical and Applied Climatology*, *121*(3–4), 789–802.

Nasrabadi, E., Masoodian, S. A., & Asakereh, H. (2013). Comparison of Gridded Precipitation Time Series Data in APHRODITE and Asfazari Databases within Iran ' s Territory, *2013*(April), 235–248.

Nastos, P. T., Kapsomenakis, J., & Douvis, K. C. (2013). Analysis of precipitation extremes based on satellite and high-resolution gridded data set over Mediterranean basin. *Atmospheric Research*, *131*, 46–59. http://doi.org/10.1016/j.atmosres.2013.04.009

Nepal, S. (2012). *Evaluating Upstream-Downstream Linkages of Hydrological Dynamics in the Himalayan Region*. *Thesis*.

Nepal, S., Krause, P., Flügel, W., Fink, M., & Fischer, C. (2012). Understanding the hydrological system dynamics of a glaciated alpine catchment in the Himalayan region using the J2000 hydrological model. *Hydrological Processes*. http://doi.org/10.1002/hyp

NRC. (2006). *Surface Temperature Reconstructions for the Last 2,000 Years*. Washington, D.C.

Onyutha, C., Tabari, H., Rutkowska, A., Nyeko-Ogiramoi, P., & Willems, P. (2016). Comparison of different statistical downscaling methods for climate change rainfall projections over the Lake Victoria basin considering CMIP3 and CMIP5. *Journal of Hydro-Environment Research*, *12*, 31–45. http://doi.org/10.1016/j.jher.2016.03.001

Palazzi, E., Hardenberg, J., & Provenzale, A. (2013). Precipitation in the Hindu-Kush Karakoram Himalaya: Observations and future scenarios. *Journal of Geophysical Research: Atmospheres*, *118*(1), 85–100.

Parry, M. L., Rosenzweig, C., Iglesias, A., Livermore, M., & Fischer, G. (2004). Effects of climate change on global food production under SRES emissions and socio-economic scenarios. *Global Environmental Change*, *14*(1), 53–67. http://doi.org/10.1016/j.gloenvcha.2003.10.008

Pedersen, F. S. (2009). Sustainable agricultural production: Providing an alternative to opium in Afghanistan. *Agricultural Water Management*, *80*, 87–99.

Pfennig, B., & Wolf, M. (2007). Extraction of process-based topographic model units using SRTM elevation data for Prediction in Ungauged Basins (PUB) in different landscapes. *International Congress on Modelling and Simulation*, 685–691.

Pinto, J. G., Neuhaus, C. P., Leckebusch, G. C., Reyers, M., & Kerschgens, M. (2010). Estimation of wind storm impacts over Western Germany under future climate conditions using a statistical-dynamical downscaling approach. *Tellus A*, *62*(2), 188–201. http://doi.org/10.1111/j.1600-0870.2009.00424.x

Prudhomme, C., & Davies, H. (2008). Assessing uncertainties in climate change impact

analyses on the river flow regimes in the UK. Part 2: future climate. *Climatic Change*, *93*(1–2), 197–222. http://doi.org/10.1007/s10584-008-9461-6

Qin, W., Wang, D., Guo, X., Yang, T., & Oenema, O. (2015). Productivity and sustainability of rainfed wheat-soybean system in the North China Plain: results from a long-term experiment and crop modelling. *Scientific Reports*, *5*(October), 17514. http://doi.org/10.1038/srep17514

Reichler, T., & Kim, J. (2008). How well do coupled models simulate today's climate? *Bulletin of the American Meteorological Society*, *89*(3), 303.

Renard, B., Kavetski, D., Kuczera, G., Thyer, M., & Franks, S. W. (2010). Understanding predictive uncertainty in hydrologic modeling: The challenge of identifying input and structural errors. *Water Resources Research*, *46*(5), W05521. http://doi.org/10.1029/2009WR008328

Samuel, J., Coulibaly, P., & Metcalfe, R. a. (2012). Evaluation of future flow variability in ungauged basins: Validation of combined methods. *Advances in Water Resources*, *35*, 121–140. http://doi.org/10.1016/j.advwatres.2011.09.015

SDSM. (2004). Using SDSM Version 3.1 — A decision support tool for the assessment of regional climate change impacts.

Seibert, J., & McDonnell, J. J. (2002). On the dialog between experimentalist and modeler in catchment hydrology: Use of soft data for multicriteria model calibration. *Water Resources Research*, *38*(11).

Shrestha, M. S., Artan, G. a., Bajracharya, S. R., & Sharma, R. R. (2008). Using satellite-based rainfall estimates for streamflow modelling: Bagmati Basin. *Journal of Flood Risk Management*, *1*(2), 89–99. http://doi.org/10.1111/j.1753-318X.2008.00011.x

Shrestha, S., Shrestha, M., & Babel, M. S. (2016). Modelling the potential impacts of climate change on hydrology and water resources in the Indrawati River Basin, Nepal. *Environmental Earth Sciences*, *75*(2016), 1–13. http://doi.org/10.1007/s12665-015-5150-8

Singh, R. B., & Sen Roy, S. (2002). Climate variability and hydrological extremes in a Himalayan catchment. In *ERB and Northern European FRIEND Project 5 Conf., Slovakia*.

Sivapalan, M., Takeuchi, K., Franks, S. W., Gupta, V. K., Karambiri, H., Lakshmi, V., … O'connell, P. E. (2003). IAHS Decade on Predictions in Ungauged Basins (PUB), 2003–2012: Shaping an exciting future for the hydrological sciences. *Hydrological Sciences Journal*, *48*(6), 857–880.

Solomon, S. (2007). *Climate change 2007-the physical science basis: Working group I contribution to the fourth assessment report of the IPCC* (Vol. 4). Cambridge University Press.

Steduto, P., Hsiao, T. C., Fereres, E., & Raes, D. (2012). *Crop yield response to water*. FAO Roma.

Steduto, P., Hsiao, T. C., Raes, D., & Fereres, E. (2009). AquaCrop—The FAO crop model to simulate yield response to water: I. Concepts and underlying principles. *Agronomy Journal*, *101*(3), 426–437.

Stott, P. A., Kettleborough, J. A., & Allen, M. R. (2006). Uncertainty in continenta-scale

temperature predictions. *Geophysical Research Letters*, *33*(2).

Sun, W., Ishidaira, H., & Bastola, S. (2012). Calibration of hydrological models in ungauged basins based on satellite radar altimetry observations of river water level. *Hydrological Processes*, *26*(23), 3524–3537. http://doi.org/10.1002/hyp.8429

Taylor, K. E., Stouffer, R. J., & Meehl, G. A. (2012). An overview of CMIP5 and the experiment design. *Bulletin of the American Meteorological Society*, *93*(4), 485.

te Linde, a. H., Aerts, J. C. J. H., Bakker, a. M. R., & Kwadijk, J. C. J. (2010). Simulating low-probability peak discharges for the Rhine basin using resampled climate modeling data. *Water Resources Research*, *46*(3), n/a-n/a. http://doi.org/10.1029/2009WR007707

Thornton, P. K., Jones, P. G., Ericksen, P. J., & Challinor, A. J. (2011). Agriculture and food systems in sub-Saharan Africa in a 4 C+ world. *Philosophical Transactions of the Royal Society of London A: Mathematical, Physical and Engineering Sciences*, *369*(1934), 117–136.

Trzaska, S., & Schnarr, E. (2014). A Review of Downscaling Methods for Climate Change Projections. *United States Agency for International Development by Tetra Tech ARD*, (September), 1–42.

Tsanis, I. K., Koutroulis, A. G., Daliakopoulos, I. N., & Jacob, D. (2011). Severe climate-induced water shortage and extremes in Crete. *Climatic Change*, *106*(4), 667–677.

Tunnemeier, T., & Houben, G. (2005). *Hydrogeology of the Kabul river basin, Part 1, Geology, aquifer characteristics, climate and hydrology*. 30655 Hannover, Germany.

UNEP. (2007). UNEP Annual Report.

Vancutsem, C., Ceccato, P., Dinku, T., & Connor, S. J. (2010). Evaluation of MODIS land surface temperature data to estimate air temperature in different ecosystems over Africa. *Remote Sensing of Environment*, *114*(2), 449–465. http://doi.org/10.1016/j.rse.2009.10.002

Veerakachen, W., Raksapatcharawong, M., & Seto, S. (2014). Performance evaluation of Global Satellite Mapping of Precipitation (GSMaP) products over the Chaophraya River basin, Thailand. *Hydrological Research Letters*, *8*(1), 39–44. http://doi.org/10.3178/hrl.8.39

Wagener, T., & Montanari, A. (2011). Convergence of approaches toward reducing uncertainty in predictions in ungauged basins. *Water Resources Research*, *47*(6), W06301. http://doi.org/10.1029/2010WR009469

Walker, W. E., Harremoës, P., Rotmans, J., van der Sluijs, J. P., van Asselt, M. B. A., Janssen, P., & Krayer von Krauss, M. P. (2003). Defining uncertainty: a conceptual basis for uncertainty management in model-based decision support. *Integrated Assessment*, *4*(1), 5–17.

Wheeler, S., Zuo, a., & Bjornlund, H. (2013). Farmers' climate change beliefs and adaptation strategies for a water scarce future in Australia. *Global Environmental Change*, *23*(2), 537–547. http://doi.org/10.1016/j.gloenvcha.2012.11.008

Wilby, R. L., Beven, K. J., & Reynard, N. S. (2008). Climate change and fluvial flood risk in the UK : more of the same ? *Hydrological Processes*, *2523*(December 2007), 2511–2523. http://doi.org/10.1002/hyp

Winiger, M., Gumpert, M., & Yamout, H. (2005). Karakorum-Hindukush-western Himalaya: Assessing high-altitude water resources. *Hydrological Processes*, *19*(12), 2329–2338. http://doi.org/10.1002/hyp.5887

Xie, P., Chen, M., Yang, S., Yatagai, A., Hayasaka, T., Fukushima, Y., & Liu, C. (2007). A Gauge-Based Analysis of Daily Precipitation over East Asia. *Journal of Hydrometeorology*, *8*(3), 607–626. http://doi.org/10.1175/JHM583.1

Xie, P., Yarosh, Y., Love, T., Janowiak, J. E., & Arkin, P. A. (2002). A real-time daily precipitation analysis over South Asia. In *Preprints of the 16th Conference of Hydrology: 2002; Orlando*.

Zhang, X., & Srinivasan, R. (2010). GIS-based spatial precipitation estimation using next generation radar and raingauge data. *Environmental Modelling & Software*, *25*(12), 1781–1788. http://doi.org/10.1016/j.envsoft.2010.05.012

Zong-ci, Z., Yong, L. U. O., & Jian-bin, H. (2013). A Review on Evaluation Methods of Climate Modeling. *Advances in Climate Change Research*, *4*(3), 137–144. http://doi.org/10.3724/SP.J.1248.2013.137

APPENDICES

APPENDIX A - DATA AVAILABILITY

The available hydro-meteorological data for Kabul basin

The following table shows a summary of all available hydro-meteorological data for Kabul basin. Based on these data, for each objective of the study, the following periods are selected for the analysis: (more details are shown in the next tables)

- Performance evaluation of precipitation products: 2004-2007
- Performance evaluation of Aphrodite temperature product: 1973-1980
- Developing J2000 hydrological modeling: 1968-1979 (calibration and validation)
- Baseline for comparison of GCMs output (1971-2000)

Surface observations			
Type	**Resolution**	**Availability**	**Source**
River Discharge	daily	1968-1979 2008-2011	USGS, Afghanistan Ministry of Energy and Water
Precipitation	daily	2003-2012	USGS (AgroMET project), Afghanistan Meteorological Authority
Temperature	daily	1973-1980 2008-2012	Afghanistan Meteorological Authority
Relative humidity, Sunshine hours, Wind speed	daily	2003-2007	Afghanistan Meteorological Authority
Precipitation data from remote sensed and interpolated global datasets			
Name	**Resolution**	**Availability**	**Source**
CPC-RFE	daily	2001-present	Climate Prediction Centre (CPC), NOAA
GSMaP MVK	hourly	2003-2010	Japan Aerospace Exploration Agency
TRMM	3-hourly	1998-present	National Aeronautics and Space Administration (NASA)
APHRODITE	daily	1951-2007	Research Institute for Humanity and Nature (RIHN), Meteorological Research Institute of Japan Meteorological Agency (MRI/JMA)
Temperature data from remote sensed and interpolated global datasets			
Name	**Resolution**	**Availability**	**Source**
APHRODITE	daily	1961-2007	Research Institute for Humanity and Nature (RIHN), Meteorological Research Institute of Japan Meteorological Agency (MRI/JMA)

- Hydrological Stations of Kabul basin with the number of days with recorded data before 1980

Station Name	River	Y	X	1959	1960	1961	1962	1963	1964	1965	1966	1967	1968	1969	1970	1971	1972	1973	1974	1975	1976	1977	1978	1979	1980
PIRKOTI	URGUN	32.92	69.25												141	365	366	365	365	365	366	365	273		
URGUN	DAHANE LEGAD	32.97	69.15														267	365	365	365	366	365	273		
DOMANDI	SHUMAL	33.28	69.58					328	366	205															
SPERA	SPERA	33.28	69.6									259	366	365	365	365	366	365	365	365	366	365	365	46	
TORA TIGHA	SHUMAL	33.37	70.17											265	365	365	366	365	365	365	366	365	66		
MATUN	MATUN	33.38	69.88				9	365	366	365	365	365	366	365	365	365	366	365	365	365	366	365	365	140	
KHARWAR DAM INFLOW	CHARKH	33.72	68.87														92	365	365	365	366	365	365	79	
KHARWAR DAM OUTFLOW	CHARKH	33.73	68.87														92	365	365	365	366	365	365	79	
CHAMKANI	GABER	33.75	69.8									92	366	365	181		92	365	365	365	366	365	365	273	
DODA	KHURRAM	33.8	69.67														70	365	365	365	366	365	365	273	
CHAMKANI2	KHURRAM	33.8	69.8				29	365	366	365	365	365	366	365	365	365	366	365	365	365	366	365	365	273	
PUL-I-BANGAKH	KHURRAM	33.8	69.88				31	365	366	365	365	365	366	365	365	365	366	365	365	365	366	365	365	96	
AHMADKHEL	KHURRAM	33.83	69.65									140	366	365	365	365	366	365	365	365	366	365	365	365	274
SHEKHABAD	LOGAR	34.08	68.75			92	365	365	366	365	365	365	366	365	365	365	366	365	365	365	366	365	273	92	274
BAND-I-CHAK WARDHAK	LOGAR	34.1	68.57																	241	366	365	365	365	274
SABAY	HAZARNAW	34.1	70.37																	6	366	365	365	273	
KAJAB	LOGAR	34.23	68.5					320	366	365	365	365	366	365	365	365	366	365	365	365	366	365	365	273	
DAKAH	KABUL	34.23	71.03										315	365	365	365	366	365	365	365	366	365	365	365	204
MAIDAN	KABUL	34.32	68.85			92	365	365	366	365	365	365	366	365	365	365	366	365	365	365	366	365	365	365	274
TANGI SAIDAN	KABUL	34.4	69.08			92	365	365	366	365	365	365	366	365	365	365	366	365	365	365	366	365	365	365	274
BAND-I-AMIR GHAZI	CHAKARI	34.42	69.38							220	365	365	366	365	365	365	366	365	365	365	366	365	365	365	274
SULTANPUR	SURKHRUD	34.42	70.3										299	365	365	365	366	365	365	273	352	365	365	365	91
SANG-I-NAWESHTA	LOGAR	34.43	69.2			92	365	365	366	365	365	365	366	365	365	365	366	365	365	365	366	365	365	365	274
DARONTA	KABUL	34.47	70.37	92	366	365	365	365	274																
PUL-I-KAMA	KONAR	34.47	70.55								4	365	366	365	365	365	366	365	365	365	366	365	365	273	
PUL-I-SOKHTA	PAGHMAN	34.5	69.13					306	366	365	365	365	366	365	365	365	366	365	365	365	366	365	365	365	274
Below QARGHA RES.	QARGHA	34.55	69.03						92	365	365	365	366	365	365	365	366	365	365	365	366	365	365	365	274
PUL-I-QARGHAI	LAGHMAN	34.55	70.23		92	365	365	365	366	365	365	365	366	365	365	365	366	365	365	365	366	365	365	273	
Above QARGHA RES.	QARGHA	34.57	69.02					260	366	365	273				289	365	366	365	365	365	366	365	365	365	274
TANG-I-GHARU	KABUL	34.57	69.4	92	366	365	365	365	366	365	365	365	366	365	365	365	366	365	365	365	366	365	365	365	274
NAGHLU	KABUL	34.62	69.72	92	366	365	365	365	366	365	365	365	366	365	365	365	366	365	365	365	366	365	365	365	274
KONARI	KONAR	34.63	70.82	92	366	365	365	365	366	365	365	273													
TAGAB	TAGAB	34.67	69.68										147	365	365	365	366	365	365	365	366	365	365	120	
NAWABAD	KONAR	34.82	71.12																		275	365	365	273	
ASMAR	KONAR	34.88	71.17		313	365	365	365	366	365	365	365	366	365	365	273									
CHAGHASARAI	PECH	34.9	71.13		313	365	365	365	366	365	365	365	366	365	365	365	366	365	365	365	366	365	365	59	
SHUKHI	PANJSHER	34.93	69.48								92	365	366	365	365	365	366	365	365	365	366	365	365	365	274
PUL-I-ASHAWA	GHORBAND	35.08	69.13	92	366	365	365	365	366	365	365	365	366	365	365	365	366	365	365	365	366	365	365	365	35
BAGH-I-LALA	SALANG	35.15	69.22			92	365	365	113	365	365	365	366	365	365	365	366	365	365	365	366	365	365	365	60
GULBAHAR	SHATUL	35.15	69.28									216	366	365	365	365	366	365	365	365	366	365	365	365	66
GULBAHAR2	PANJSHER	35.17	69.28	92	366	365	365	365	366	365	365	365	366	365	365	365	366	365	365	365	366	365	365	365	274
OMARZ	PANJSHER	35.37	69.63				92	241	366	365	365	365	366	365	365	365	366	365	365	365	366	365	365	365	274
GAWARDESH	LANDAISIN	35.38	71.53																	245	366	365	203		

- Hydrological Stations of Kabul basin with the number of days with recorded data after 2005

Station Name	River	Y	X	2005	2006	2007	2008	2009	2010	2011	2012
Above Qargha	Paghman	34.57	69.02			275	366	365	365	365	274
Bagh-i-Lala	Salang	35.15	69.22				92	365	365	365	273
Below Qargha	Paghman	34.55	69.03	223	365	365	366	365	365	363	274
Chaghasarai	Pech	34.9	71.13			286	366	365	365	365	274
Dakah	Kabul	34.23	71.03			275	366	365	365	365	274
Doabi	Dara Hazara	35.33	69.62					226	365	365	274
Gulbahar - Panjshir	Panjshir	35.17	69.28			92	366	365	365	365	274
Gulbahar - Shatul	Shatul	35.15	69.28				283	365	365	365	274
Keraman	Hazara	35.28	69.65					229	365	365	274
Khawak	Panjshir	34.93	69.48					214	365	365	274
Lolenj	Ghorband	34.95	68.65					184	365	365	274
Maidan (Pul_i_Surkh)	Kabul	34.32	68.85			193	366	365	365	365	
Naghlu	Kabul	34.62	69.72				143	365	365	365	274
Nawabad	Konar	34.82	71.12			286	365	365	365	365	274
Near Chardehi (Parsa)	Parsa	34.98	69.03					92	365	365	274
Near Stalif	Stalif	34.82	69.07					14	365	365	274
Omarz	Panjshir	35.37	69.63					232	365	365	105
Paryan (Near Khawak)	Panjshir	35.57	69.9					92	365	365	274
Pul-i-Ashawa	Ghorband	35.08	69.13				239	365	365	365	274
Pul-i-Behsud	Kabul	34.43	70.45					190	365	365	274
Pul-i-Islam Abad	Alishing	34.75	71					214	365	365	274
Pul-i-Kama	Konar	34.47	70.55			176	366	365	363	365	274
Pul-i-Nalyar	Alinigar	34.9	70.37					214	273		
Pul-i-Qarghai	Laghman	34.55	70.23			286	365	365	365	365	274
Qala-e-Malik	Paghman	34.57	68.95				92	365	365	365	147
Sabay	Hazarnow	34.1	70.37		61	365	366	365	365	365	274
Sang-i-Nawashta	Logar	34.43	69.2	160	365	365	366	365	365	365	274
Shakardara	Shakardara	34.68	69					221	365	365	274
Shukhi	Panjshir	34.93	69.48				92	365	365	365	274
Sultanpur	Surkhrood	34.42	70.3					92	365	365	274
Tangi Saidan	Kabul	34.4	69.08			286	366	365	365	365	274
Tang-i-Gharu	Kabul	34.57	69.4	220	365	365	366	365	365	365	220

- Weather Stations of Afghanistan with the number of days with recorded data after 2003 (Tmax, Tmean, Tmin, RH, Precipitation, Evaporation, Wind Speed)

Station Name	Y	X	Altitude (m)	2003	2004	2005	2006	2007
Logar	34.1	69.05	1935	92	366	365	334	120
Kabul	34.55	69.21	1791	91	366	365	334	243
Jalalabad	34.43	70.46	580	92	365	353	304	151
Mazar	36.7	67.2	378	92	366	334	334	212
Laghman	34.65	70.21	770	92	366	365	334	151
Faizabad	37.11	70.51	1200	84	335	337	303	89
Bamyan	34.81	67.81	2550	92	366	304	274	150
Sheberghan	36.66	65.71	360	92	366	365	334	90
Serdey				92	366	365	334	181
Ghazni	33.53	68.41	2183	92	366	365	304	212
Kandahar	31.5	65.85	1010	92	366	364	304	150
Farah	32.36	62.18	700	92	366	335	274	122
Herat	34.21	62.21	964	92	366	365	304	181
Gardiz	33.61	69.23	2350	92	366	365	334	181
Jabul Seraj	35.13	69.25	1630	92	366	365	334	150

APPENDIX B - HOUSEHOLD QUESTIONNAIRE

Questionnaire to conduct a field survey on "farmer's perception about climate change and their adaptation measures" in Kabul basin, Afghanistan:

1. Identification

    1.1. Province_____

    1.2. District_____

    1.3. Village_____

    1.4. Date of the survey_____/_____/_____

    1.5. Name of farmer_____

    1.6. Gender: Male☐ Female☐

    1.7. Age of the farmer_____

    1.8. Number of people in the household (Male/Female)_____/_____

    1.9. Education level (Head/Other members)_____/_____

    1.10. Major occupation _____ Secondary Occupation _____

    1.11. Is your income from agriculture increased? Yes☐ No☐

2. Land Information

    2.1. Land owned by household? Yes☐ No☐ Comment_____

    2.2. How much land you have (Jerib)? _____

    2.3. How much Irrigated/Rainfed land you have (Jerib)? _____/_____

    2.4. How much irrigated land with one crop per year? _____

    2.5. How much irrigated land with two crops per year? _____

    2.6. Did you leave some arable land uncultivated? Yes☐ No☐ If yes, what are the reasons? Lack of water☐ Lack of seed☐ Lack of labour☐ Other reason (specify)_____

3. Irrigation System

    3.1. If you have access to irrigation: irrigation system used? Canal☐ Karez☐ Well☐ Other (specify)_____

4. Crop Information

    4.1. Major crops you grow:

Name	Wheat	Irrigated Barely	Rainfed Barely	Maize	Rice	Oilseeds	Potato	Melon /Watermelon	Cotton	Opium	Alfalfa	Clover
Area (Jerib)												
Production (seer)												
Date of planting												
Date of harvest												
Frequency of Irrigation (how many times)												

4.2. Major crops you grew 10 years back?

Name	Wheat	Irrigated Barely	Rainfed Barely	Maize	Rice	Oilseeds	Potato	Melon /Watermelon	Cotton	Opium	Alfalfa	Clover
Area (Jerib)												
Production (seer)												
Date of planting												
Date of harvest												

4.3. Major crops you planned for next year?

Name	Wheat	Irrigated Barely	Rainfed Barely	Maize	Rice	Oilseeds	Potato	Melon /Watermelon	Cotton	Opium	Alfalfa	Clover
Area (Jerib)												

4.4. Which fruit trees do you grow?

Name	Apricot	Peach	Vineyards	Apple	Mulberry	Pomegranate	Plum	Almond	Pistachio	Walnuts	Citrus

Number Trees											
Area (Jerib)											

4.5. Which fruit trees did you grow before (10 years back)?

Name	Apricot	Peach	Vineyards	Apple	Mulberry	Pomegranate	Plum	Almond	Pistachio	Walnuts	Citrus
Number Trees											
Area (Jerib)											

4.6. Do you have a vegetable garden for consumption at home? Yes☐ No☐

4.7. Did you receive farming inputs from any organizations? Yes☐ No☐ If yes, which one: Seed ☐ Fertilizer☐ Tools☐ Other (specify) _____

5. Livestock

5.1. Total animals owned (now/10 years back)? Cattle_____/_____ Sheep_____/_____ Goats_____/_____ Donkeys_____/_____ Horses_____/_____ Camels_____/_____

5.2. Total number of poultry animals you have/had (now/10 years back)? _____/_____

6. Climate Change Causes

6.1. Have you realized any changes in extreme hot in summer? Increased☐ Decreased ☐ I don't know☐ If yes one specific indicator: _____

6.2. Have you realized any changes in less cold in winter? Increased☐ Decreased☐ I don't know☐ If yes one specific indicator: _____

6.3. Is precipitation changing (intensity, quantity, time)? Yes☐ No☐ I don't know☐ If yes, which one you agree: Intensity: increased ☐ decreased☐, Quantity: increased ☐ decreased☐, Time: earlier ☐ later☐

6.4. Have you ever observed any changes of water resources in your area? Yes☐ No ☐ I don't know☐ If yes, which one you agree for water availability: Depth of well: increased

☐ decreased☐, Stream flow: increased ☐ decreased☐ any other indicator (specify): _____

6.5. Is there any increase in dry period? Yes☐ No☐ I don't know☐

6.6. Are climatic hazards increasing? Yes☐ No☐ I don't know☐ if yes, what are they? Floods☐ Drought☐ Thunderstorms☐ Landslides☐

6.7. Did you get any warning about these hazards before it happened? Yes☐ No☐

6.8. In your experience, is climate warming over the last 10 years? Yes☐ No☐ I don't know☐ If yes why do you think so _____

7. Climate Change Impacts

7.1. What are the major risks/shocks you had due to climate change? Heavy rain and Flood☐ crop failure☐ Disease☐ Water loss☐ Income loss☐ Other (specify) _____

7.2. How do you think these changes have impacted your agricultural system? Less production/yield ☐ need more water for irrigation ☐ reduced soil fertility ☐ Other (specify) _____

8. Adaptation

8.1. Have you/your family members changed/planned to change your profession (non-agriculture) from agriculture or vice versa? If yes, why and what? _____

_____

8.2. Mention how do you cope with the changes? Change in time of cropping☐ change in type of crop☐ improved cook stove☐ plantation in your home garden☐ construction of reservoirs and channels for ex-situ RWH☐ Agroforestry☐ soil conservation activities☐ deep tillage☐ Mulching☐ Increased use of groundwater☐ construction of dikes (or growing trees) along the field boundaries☐ high efficiency irrigation schemes☐ others (specify) _____

In your opinion, what type of assistances can help your family/society to minimize the negative impact of climate change?

APPENDIX C - PHOTOS FROM FIELD VISITS

Photos taken during the field visit to Shakar Dara and Watapoor districts

Main channel line and recent flood's impact, Shakar Dara, Afghanistan (Field survey 2013)

Flooded areas, Shakar Dara, Afghanistan (Field survey 2013)

Abandoned arable lands due to lack of water in downstream areas, Shakar Dara, Afghanistan (Field survey 2013)

Karez, a popular traditional way to abstract and convey the water, Shakar Dara, Afghanistan (Field survey 2013)

Cultivated lands, Watapoor, Afghanistan (Field survey 2013)

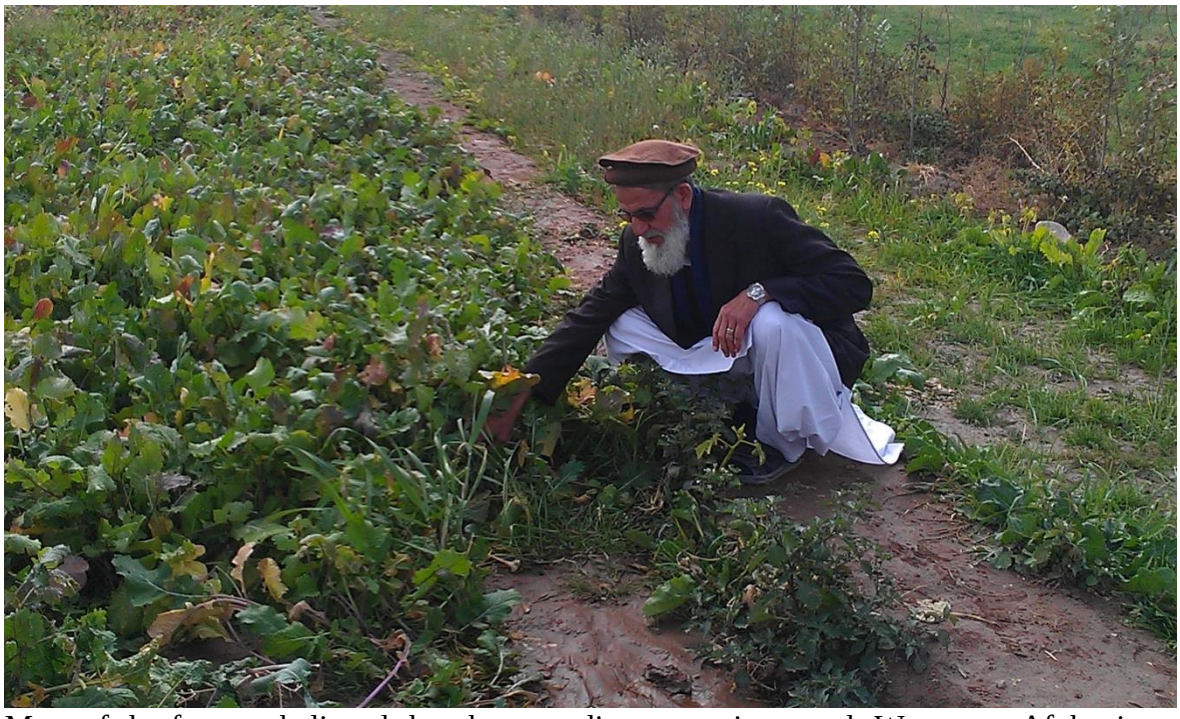

Most of the farmers believed that the crop disease are increased, Watapoor, Afghanistan (Field survey 2013)